

# **Proteomic analysis of TRIF interactome and functional characterisation of novel TRIF interacting proteins**

**Suaad M. Ahmed, MSc.  
Institute of Immunology**



**NUI MAYNOOTH**  
Ollscoil na hÉireann Má Nuad

**Thesis submitted for the degree of Doctor of Philosophy  
National University of Ireland Maynooth  
June 2012**

**Head of the department: Prof. Kay Ohlendieck  
Supervisor: Dr. Sinead Miggin**

# Table of contents

	<b>Page</b>
<b>Declaration</b>	viii
<b>Acknowledgement</b>	ix
<b>Dedication</b>	x
<b>Publications</b>	xi
<b>Abstract</b>	xii
<b>Abbreviations</b>	xiv
<b>Chapter 1 General introduction</b>	
1.1 The Innate immune system	1
1.2 Pathogen Recognition Receptors	1
1.3 Toll-like Receptors	3
1.3.1 TLR1, TLR2 and TLR6	4
1.3.2 TLR3	6
1.3.3 TLR4	7
1.3.4 TLR5	8
1.3.5 TLR7 and TLR8	9
1.3.6 TLR9	9
1.3.7 TLR10	10
1.3.8 TLR11, TLR12 and TLR13	10
1.4 TLRs signalling pathway	11
1.5 TLR adaptors	11
1.5.1 MyD88	13
1.5.2 MAL	17
1.5.3.1 TRIF	18
1.5.3.2 TLR3-independent TRIF-dependent pathways	22
1.5.4 TRAM	22
1.5.5 SARM	24
1.6 Negative regulation of TLR signalling	25

1.7	Role of TLRs in human diseases	28
1.8	Project Aims	30

## **Chapter 2 General Materials and Methods**

2.1	General Materials	31
2.2	Methods	31
2.2.1	Cell culture techniques	31
2.2.2	Cell stock freezing and resuscitation	31
2.2.3	Transfection of cells with plasmid and esiRNA	31
2.2.4	Transformation of competent cells	32
2.2.5	Preparation of plasmid DNA	32
2.2.6	Glycerol stocks	32
2.2.7	Sodium dodecyl sulphate polyacrylamide gel electrophoresis (SDS-PAGE)	32
2.2.8	Western blot	33
2.2.9	Immunoprecipitation of HA-TRIF	34
2.2.10	Immunoprecipitation of endogenous TRIF	34
2.2.11	Silver staining	35
2.2.12	Gel de-staining and sample preparation for Mass Spectrometry (MS)	35
2.2.13	Ion Trap Mass Spectrometry	36
2.2.14	RNA isolation using TRIZOL reagent.	37
2.2.15	First-strand cDNA synthesis	37
2.2.16	PCR	38
2.2.17	Real time PCR	38
2.2.18	Agarose gel electrophoreses	38
2.2.19	Reporter assays	39
2.2.20	Enzyme-Linked Immunosorbent Assay (ELISA)	40
2.2.21	Meso Scale Human 7-Plex / MMP 3-Plex / IFN- $\beta$ / RANTES Assay	40
2.2.22	Immunofluorescence	41
2.2.23	Statistics	42

## **Chapter 3 Proteomic analysis of the TRIF interactome**

3.1	Introduction	43
3.2	Results	46
3.2.1	Immunoprecipitation of HA-TRIF	46
3.2.2	Identification of HA-TRIF interactors	48
3.2.3	TRIF protein interaction networks	48
3.2.3.1	poly(I:C)-independent TRIF interactors	49
3.2.3.2	TRIF interactors following 20 min poly(I:C) stimulation	53
3.2.3.3	TRIF interactors following 40 min poly(I:C) stimulation	56
3.2.3.4	TRIF interactors following 60 min poly(I:C) stimulation	61
3.2.3.5	LPS-independent TRIF interactors	67
3.2.3.6	TRIF interactors 20 min following LPS stimulation	70
3.2.3.7	TRIF interactors 40 min following LPS stimulation	74
3.2.3.8	TRIF interactors 60 min following LPS stimulation	79
	3.2.4 Co-immunoprecipitation of TRIF and novel interactors	85
3.3	Discussion	87

## **Chapter 4 Investigating the novel role of human ADAM15 in TLR3 and TLR4 signalling**

4.1	Introduction	90
4.1.1	Background	90
4.1.2	ADAM Domain structure and function	90
4.1.2.1	The Prodomain	90
4.1.2.2	The metalloprotease domain	92
4.1.2.3	The disintegrin domain	93
4.1.2.4	The cysteine-rich and EGF-like domains	93
4.1.2.5	The cytoplasmic tail	93
4.1.3	Subcellular localisation of ADAM	94
4.1.4	ADAM-mediated shedding	94
4.1.5	ADAMs and human diseases	95
4.1.6	The ADAM15 gene	95
4.2	Results	98

4.2.1	ADAM15 interact with TRIF	98
4.2.2	ADAM15 inhibited TRIF-dependent reporter gene assay	98
4.2.3	ADAM15 inhibited TLR3 and TLR4-mediated reporter gene activity	100
4.2.4	Poly(I:C) increased ADAM15 transcription	100
4.2.5	Downregulation of ADAM15 by esiRNA	103
4.2.6	Suppression of ADAM15 expression enhanced IFN $\beta$ , TNF $\alpha$ and Rantes mRNA expression	103
4.2.7	Downregulation of ADAM15 increased cytokine and chemokine secretion	107
4.2.8	Knockdown of ADAM15 increased the phosphorylation of p65	109
4.2.9	ADAM15 mediates TRIF degradation	109
4.2.10	Cellular localization of ADAM15	112
4.2.11	Interaction network	112
4.3	Discussion	117

## **Chapter 5 Dishevelled and Toll-like receptors cross-talk**

5.1	Introduction	119
5.1.1	Wnt signalling pathway	119
5.1.2	Canonical Wnt Signalling	119
5.1.3	Non-canonical WNT signalling	121
5.1.4	Wnt signalling in immune system	123
5.1.5	Dishevelled	123
5.2	Results	126
5.2.1	DVLs interact with TRIF	126
5.2.2	DVLs inhibited TRIF-dependent reporter gene assays	126
5.2.3	DVLs Inhibited TLR3-dependent signalling in reporter assays	130
5.2.4	Effect of DVLs on MyD88-dependent reporter activity	130
5.2.5	Inhibition of DVLs attenuates TLR3 and TLR4 signalling	134
5.2.6	Inhibition of DVLs decreased I $\kappa$ B $\alpha$ degradation and phosphorylation of IRF3	136
5.2.7	Effect of $\beta$ -catenin activation on TLR3 and TLR4 signalling	136
5.2.8	Activation of $\beta$ -catenin decreased I $\kappa$ B $\alpha$ degradation and increased phosphorylation of IRF3 and p38	138

5.2.9	Regulation of DVLs by the TLRs	142
5.2.10	TRIF and Myd88 inhibit $\beta$ -catenin-induced Lef Transcription	142
5.2.11	poly(I:C) and LPS inhibited $\beta$ -catenin expression	145
5.3	Discussion	147

## **Chapter 6 Proteomic analysis of endogenous TRIF interaction and the negative regulation of TRIF signalling by Optineurin**

6.1	Introduction	150
6.2	Results	151
6.2.1	Characterisation of commercially available TRIF antibodies	151
6.2.2	Examination of TLR3 and TLR4 responsiveness in U373-CD14 cells	153
6.2.3	Immunoprecipitation of endogenous TRIF	153
6.2.4	Identification of endogenous TRIF interactors	156
6.3	Optineurin negatively regulates TRIF signalling	161
6.3.1	Introduction	161
6.3.2	Results	163
6.3.2.1	OPTN interacts with TRIF	163
6.3.2.2	Poly(I:C) and LPS induce OPTN expression	163
6.3.2.3	OPTN inhibits TRIF- and TLR3-dependent reporter gene activity	166
6.3.2.4	Suppression of OPTN by esiRNA	166
6.3.2.5	Downregulation of OPTN expression enhanced IFN $\beta$ , and Rantes mRNA expression	169
6.3.2.6	Effect of OPTN suppression on cytokine and chemokine secretion	169
6.4	Discussion	172

## **Chapter 7 General discussion** 175

## **Bibliography** 181

## **Appendices** 222

## **Declaration**

I hereby declare that the contents of this thesis are entirely my own work and that it has not been previously submitted as an exercise for a degree to this or any other university. The work and information of others have been acknowledged and cited in the text.

Signed:

Date:

## **Acknowledgements**

First of all, I would like to address especial thanks to my supervisor, Dr. Sinead Miggin for her kindness, support, advice, time she made available for me and patience in improving my writing.

I would like also to thank my colleagues in the Immune Signalling lab, Aisha, Ashwini and Enda for their help and good cooperation. Many thanks to the undergraduate students in the lab for their help.

The thanks are due to Edel and Caroline for their help with running the MS samples and to Ica for her technical assistance regarding usage of the confocal microscope.

Further, I am grateful to my small and extended families for their unlimited support. I sincerely thank my husband Mohamed for his advice, moral and practical support and my wonderful children; Ahmed, Aya and Awab for their moral support, patience and interest in my work even when they do not fully understand it. Their tolerant support gave me the confidence that I could do it! I am also grateful to my father Haj Mohamed, all my sisters and Aunt Fatima who their continuous prayers, encouragement and moral support are playing a great role in my success.

Last but not least, I would like to thanks my best friend Ezdehar for her support, encouragement and her nice words.

## **Dedication**

I dedicate this study to the soul of my Mother who taught and inspired me to work hard without tiredness and successfully achieve my goals.

I ask Allah to forgive her and enter her into paradise with the Prophets and Martyrs.

## **Publications**

**Suaad Ahmed**, Ashwini Maratha, Aisha Qasim Butt, Enda Shevlin and Sinead Miggin.  
The metalloprotease ADAM15 interact with TRIF and negatively regulates TRIF-mediated  
TLR signalling. 2012. JI, under review.

Aisha Qasim Butt, **Suaad Ahmed**, Ashwini Maratha and Sinead M. Miggin. 14-3-3 $\epsilon$  and  
14-3-3 $\sigma$  inhibit TLR3 and TLR4 mediated pro-inflammatory cytokine induction. J Biol  
Chem. 2012. In Press.

## Abstract

Toll-like receptors (TLRs) are germline-encoded pattern-recognition receptors that initiate innate immune responses by recognising molecular structures shared by a wide range of pathogens, known as pathogen-associated molecular patterns (PAMPs). TIR domain-containing adaptor inducing IFN- $\beta$  (TRIF) is an important adaptor protein in TLR3 and TLR4 signalling pathways that mediate proinflammatory cytokine and IFN responses following their activation by double-stranded RNA and LPS, respectively.

In the present study, we sought to investigate the novel proteins and pathways that serve to modulate the functionality of TRIF. To this end, immunoprecipitation and LC-MS analyses of the overexpressed and endogenous TRIF immunocomplexes were performed. A disintegrin and metalloproteinase domain-containing protein 15 (ADAM15), Segment polarity protein dishevelled homolog DVL3 (DVL3) and Optineurin (OPTN) were identified as TRIF-interacting partners. Their interactions with TRIF were also confirmed by direct immunoprecipitation experiments of overexpressed and endogenous TRIF.

More specifically, ADAM15 was found to interact with TRIF at 60 and 20 min. upon poly(I:C) and LPS stimulation, respectively. Overexpression of ADAM15 in HEK293, HEK293-TLR3 and HEK293-TLR4 inhibited TRIF, TLR3 and TLR4-dependent activation of NF- $\kappa$ B, IFN $\beta$  and Rantes promoter activation, respectively. Moreover, downregulation of ADAM15 by esiRNA enhanced poly(I:C) and LPS-induced cytokine/chemokine secretion in the U373-CD14 cell line.

This study also demonstrated that all of the three DVLS isoforms (DVL1, DVL2 and DVL3) interacted constitutively with TRIF when overexpressed in HEK293-TLR4. However, immunoprecipitation of endogenous TRIF in U373-CD14 cell line showed that DVL3 associated with TRIF at 20-40 min upon LPS, but not poly(I:C) stimulation. Overexpression of all DVLS isoforms in HEK293 and HEK293-TLR3 decreased TRIF and TLR3-induced NF- $\kappa$ B, IFN $\beta$  and Rantes, respectively. Nevertheless, DVLS inhibition using a chemical inhibitor attenuated poly(I:C) and LPS-dependent upregulation of TNF $\alpha$ ,

IFN $\beta$  and Rantes mRNA, as well as LPS-induced phosphorylation of IRF3 in wild-type murine BMDMs.

Furthermore, the study also showed that OPTN interacted constitutively with TRIF when overexpressed in HEK293-TLR3. Immunoprecipitation of endogenous TRIF revealed that OPTN interacted with TRIF in a ligand-dependent manner only. Poly(I:C) and LPS stimulation in U373-CD14 increased OPTN protein expression levels after 24 h. Overexpression of OPTN negatively regulates TRIF and TLR3-dependent reporter gene activation. In addition, suppression of OPTN expression using esiRNA increased poly(I:C)-induced IFN $\beta$  mRNA expression as well as TNF $\alpha$ , and Rantes secretion in U373-CD14. However, suppression of OPTN decreased/increased LPS-induced TNF $\alpha$ /Rantes, respectively.

In conclusion, this study analysed, for the first time, TRIF immunocomplex and identified ADAM15, DVL3 and OPTN as novel TRIF interacting proteins and showed their role in TRIF-mediated TLR signalling. This study has advanced our understanding of the complexities of TRIF signalling in the context of TLR and we proposed that TRIF could be a key modulator of alternate signalling pathways.

## Abbreviations

ACN	Acetonitrile
ADAMs	A disintegrin and metalloproteinase
AIFM	Apoptosis-inducing factor 1, mitochondrial
AIM2	Absent in melanoma 2
APC	Adenomatous polyposis coli
ATP	Adenosine-5'-triphosphate
BCL-2	B-cell lymphoma 2
BMDM	Bone marrow derived macrophages
BSA	Bovine serum albumin
CANX	Calnexin
CALR	Calreticulin
CamK2	Calcium-calmodulin kinase2
CARD11	Caspase recruitment domain 11
CCL5	Chemokine (C-C motif) ligand 5
cDNA	Complementary DNA
cGMP	Cyclic guanosine monophosphate
CKI	Casein kinase I
CLIP1	CAP-Gly domain-containing linker protein 1
CLRs	C-type lectin receptors
CMV	Cytomegalovirus
Co-IP	(co-) immunoprecipitation
CSF1	Colony stimulating factor 1
Da	Dalton
DAG	Diacyl glycerol
DAI	DNA-dependent activator of IFN-regulatory factors
DAPI	4',6-diamidino-2-phenylindole
DCs	Dendritic Cells
DDT	Dithiothreitol
DEP	Dishevelled-EGL10-Pleckstrin

DIX	Dishevelled-Axin
DMEM	Dulbecco's Modified Eagle's Medium
DMSO	Dimethylsulfoxide
DNA	Deoxyribonucleic acid
dNTP	Deoxyribonucleotide triphosphate
dsRNA	Double-stranded RNA
dToll	Drosophila Toll
DVLs	Dishevelled
ECM	Extracellular matrix
E. coli	Escherichia coli
EDTA	Ethylenediaminetetraacetic acid
EGF	Epidermal growth factor
EGFR	Epidermal growth factor receptor
EGTA	Ethylene glycol tetraacetic acid
EIF2AK	Eukaryotic translation initiation factor 2-alpha kinase 2
ELISA	Enzyme-Linked Immunosorbent Assay
ERK	Extracellular-signal-regulated kinases
ESI	Electrospray ionisation
ESR1	Estrogen receptor 1
EV	Empty vector
FADD	FAS-associated death domain protein
FGFR2	fibroblast growth factor receptors
FLS2	Flagellin-sensing 2
Fzd	Frizzled
GAPDH	Glyceraldehyde-3-phosphate dehydrogenase
GSK3 $\beta$	Glycogen synthase kinase beta
h	Hour
HA	Hemagglutinin
HCV	Hepatitis C virus
HEK	Human embryonic kidney
HIV-1	Human immunodeficiency virus

HRP	Horseradish peroxidase
HSV	Herpes simplex virus
hToll	Human Toll
IBD	Inflammatory bowel disease
IF	Immunofluorescence
IFI16	Interferon, gamma-inducible protein 16
IFN $\beta$	Interferon beta
IgG	Immunoglobulin G
I $\kappa$ B	Inhibitor of NF $\kappa$ B
IKBKB	Inhibitor of nuclear factor kappa-B kinase subunit beta
IKK	I $\kappa$ B kinase
IL-1	Interleukin-1
IL-1R	Interleukin-1 receptor
IP	Immunoprecipitation
IP3	Inositol 1,4,5-trisphosphate
IQGAP1	IQ motif containing GTPase activating protein1
IRAK	Interleukin-1 receptor-associated kinase
IRF	Interferon regulatory factor
JUN	c-Jun N-terminal kinase
kDa	Kilo Dalton
L	litre
LB	Luria Broth
LC-MS	Liquid chromatography and mass spectrometry
LEF	lymphoid enhancer factor
LPS	Lipopolysaccharide
LRP	low density lipoprotein receptor-related protein
LRR	Leucine-rich repeats
LRRFIP1	Leucine-rich repeat (LRR) flightless-interacting protein 1
M	Molar
MAL	MyD88 adaptor-like
MALP2	Macrophage-activating lipopeptide 2

MAPK	Mitogen activated protein kinase
MCM	Minichromosome maintenance complex
mDC(s)	Myeloid dendritic cell(s)
MDA5	Melanoma differentiation-associated gene 5
MDDCs	Monocytes-derived dendritic cells
MEN	Multiple endocrine neoplasia I
mg	Milli gram
MIF	Macrophage migration inhibitory factor
min	Minute
ml	Milli-litre
mM	Milli-molar
MMPs	Matrix metalloproteinases
mRNA	Messenger RNA
MS	Mass spectrometry
MS	Multiple sclerosis
MW	Molecular weight
MyD88	Myeloid differentiation primary response gene (88)
NBS	Nijmegen breakage syndrome
NEMO	NF $\kappa$ B essential modulator
NFAT	Nuclear factor of activated T-cells
NFKBIA	NF-kappa-B inhibitor alpha
NF- $\kappa$ B	Nuclear factor- $\kappa$ B
NFR	NF- $\kappa$ B repression factor
ng	Nano gram
Nibrin	NBN
NLK	Nemo-like kinase
NLRs	NOD-like receptors
NLRP1	NACHT, LRR and PYD domains-containing protein 1
nM	Nano molar
NOD	Nucleotide oligomerization domain
NP	Nucleoprotein

NRE	Negative regulatory element
OA	Osteoarthritis
PAMPs	Pathogen-associated molecular patterns
PBS	Phosphate-buffered saline
PCP	Planar cell polarity
PCR	Polymerase chain reaction
pDCs	Plasmacytoid dendritic cells
PDE	Phosphodiesterase
PDZ	post synaptic density-95, disc large and zonular occludens-1
PGK1	phosphoglycerate kinase 1
PHB	Prohibitin
PI3K	Phosphatidylinositol-3 kinase
PL C	Phospholipase C
PMSF	Phenylmethanesulfonyl fluoride
Poly:(I:C)	Polyinosinic-polycytidylic acid
PTBP1	Polypyrimidine tract binding protein 1
PRD	Positive regulatory domain
PRRs	Pathogen recognition receptors
Q-RT-PCR	Quantitative -reverse transcriptase- polymerase chain reaction
RA	Rheumatoid arthritis
Rantes	Regulated on activation normal T cell expressed and secreted
RHIM	RIP homotypic interaction motif
RIG-I	Retinoic acid-inducible protein
RIP	Receptor-interacting protein
RLA	Relative luciferase activity
RLRs	Retinoic acid-inducible gene (RIG)-I-like
RNA	Ribonucleic acid
rpm	Rotations per minute
RSV	Respiratory Syncytial virus
R.T.	Room temperature
RT-PCR	Reverse transcriptase- polymerase chain reaction

S	Second
SARM	sterile $\alpha$ - and armadillo-motif-containing protein
SDS	Sodium dodecyl sulphate
SDS-PAGE	SDS-polyacrylamide gel electrophoresis
SH	Src homology
siRNA	Small interfering RNA
SLE	Systemic lupus erythematosus
ssRNA	Single-stranded RNA
TAB	TAK-1 binding protein
TACE	TNF converting enzyme
TAE	Tris-acetate-EDTA
TAG	TRAM adaptor with GOLD domain
TAK-1	TGF- $\beta$ -activated protein kinase 1
TANK	TRAF family-member-associated NF $\kappa$ B activator
TB	Tuberculosis
TBK-1	TANK binding kinase 1
TBKBP1	TBK1-binding protein 1
TBST	Tris buffered saline containing Tween 20
TCR	T cell receptor
TCF	T cell factor
TE	Tris-EDTA
TFA	Trifluoroacetic acid
TGF- $\beta$	Transforming growth factor $\beta$
TICAM	Toll/IL-1 receptor domain-containing adaptor molecule
TIR	Toll/IL-1 receptor
TLR	Toll like receptor
TNF- $\alpha$	Tumour necrosis factor alpha
TRAF	TNF receptor associated factor
TRAM	TRIF related adaptor molecule
TRIF	TIR domain-containing adaptor inducing IFN- $\beta$
TRIO	Triple functional domain

TPI1	Triosephosphate isomerase 1 (TPI1)
V	Volts
VEGF	Vascular endothelial growth factor
v/v	Volume per volume
VSV	Vesicular stomatitis virus
WB	Western blot
WNV	West Nile Virus
Wt	Wild type
w/v	Weight per volume

# **Chapter 1**

## **General Introduction**

## **1.1 The Innate immune system**

The immune system is the host defence against invading microbial pathogens. It eliminates microorganisms by discriminating between self and non-self. In mammals the immune system can be divided into two branches: innate immunity, and adaptive immunity (Takeda et al., 2005; Kanzler et al., 2007). The innate immune system is responsible for the early detection and destruction of invading pathogens and relies on a set of germ line-encoded pattern recognition receptors (PRRs) for detection (Lee and Kim, 2007). In contrast, the adaptive immune response detects non-self through recognition of peptide antigens using antigen receptors expressed on the surface of B and T cells and provides the host with immunological memory (Tauszig-Delamasure et al., 2002). To initiate immune responses, PRRs recognize pathogen associated molecular pattern (PAMPs) and induce activation of various intracellular signalling pathways leading to inflammation. Once invading pathogens cross the epithelial barrier they are recognized by resident tissue macrophages. Activated macrophages release a host of cytokines and chemokines, which promote the recruitment of neutrophils to site of infection and initially invading microorganisms. Mediators of the innate immune system also induce upregulation of co-stimulatory molecules on dendritic cells (DCs), resulting in recruitment of cells of the adaptive immune system (Janeway and Medzhitov, 2002; Lee and Kim, 2007; Mogensen, 2009).

## **1.2 Pathogen Recognition Receptors**

The innate immune system utilizes PRRs in three different compartments including cell membranes, body fluids and cytoplasm (Lee and Kim, 2007). PRRs are expressed as the first line of defense against infection by macrophages, monocytes, dendritic cells, neutrophils and epithelial cells, as well as, cells of the adaptive immune system (Mogenson, 2009; Takeuchi and Akira, 2010). Several classes of PRRs have been identified: Toll-like receptors (TLRs), retinoic acid inducible gene-I (RIG-I)-like receptors (RLRs), NOD-like receptors (NLRs), C-type lectins receptors (CLRs) and DNA sensors (Keating et al., 2011, Marsili et al., 2012) (Figure 1.1). Upon recognition of the microbial components, PRRs activates a cascade of signalling pathways leading to the induction of a range of specific inflammatory and antiviral genes and cytokines that orchestrate innate immunity and chemokines and co-stimulatory molecules that promote T cell activation and specific



immunity (Marsili et al., 2012) (Figure 1.1). TLRs are the best characterised signalling receptors among the PRRs (Iwasaki and Medzhitov, 2004) and will be discussed in more detail below. The cytosolic receptors RIG-I and melanoma-differentiation-associated gene 5 (MDA5) are RNA-sensing helicases. They detect dsRNA of many replicating viruses (Kato et al., 2008). Recent reports show that RIG-I can also trigger IL-1 $\beta$  and/or IL-18 production typically induced by inflammasome (poeck et al., 2010). NLRs are a further set of intracellular PRRs distinct from RLRs that have emerged as central regulators of immunity and inflammation with demonstrated relevance to human diseases. NLRs recognize PAMPs, as well as, host-derived danger signals or DAMPs (danger associated molecular patterns) and much attention has been focused on the ability of several NLRs to activate the inflammasome complex and drive proteolytic processing of inflammatory cytokines (Schroder et al., 2010). The C-type lectin family of proteins encompasses upwards of 1000 members with diverse functions including cell adhesion, regulation of natural killer function, complement activation, tissue remodeling, platelet activation, endocytosis, phagocytosis and innate immunity. Many C-type lectins recognize carbohydrate structures on viruses, bacteria, parasites and fungi and have been shown to play a role in host defense, exerting functions independent of other PRRs (Osorio et al., 2011). Cytosolic dsDNA produced during DNA-virus infection is also a potent activator of innate immune responses. Several cytosolic DNA sensors have recently been described, all of which contribute to recognition of infecting viral DNA. These DNA sensors include DAI (DNA-dependent activator of IRF) IFN-inducible IFI16 protein (IFI16), Stimulator of interferon genes, STING RNA polymerase-III (Pol-III), absent in melanoma 2 (AIM2) extra chromosomal histone H2B, leucine rich repeat (in FLII) interacting protein (LRRFIP1) Ku70 ( Keating et al., 2011; Marsili et al., 2012).

### **1.3 Toll-like Receptors**

It was initially thought that the innate immune system largely functioned in a non- specific manner. However, in 1989, Janeway found that the innate immune system specifically detect pathogens via germ line-encoded receptors termed pattern recognition receptors (PRR). PRRs recognize highly conserved microbial structure and thereby initiate an immune response (Janeway, 1989). The first proof of specificity in innate immunity came

with the discovery of the *Drosophila* protein Toll (dToll), which was critical for effective immune response to fungus *Aspergillus fumigatus* in the adult fly (Lemaitre et al., 1996). Soon after that a human homologue of Toll (hToll, later called Toll-like receptor 4) was discovered (Medzhitov et al., 1997). At least 13 TLRs have been identified in mammals so far (Brikos and O'Neill, 2008). Both humans and mice express TLR1-9 (Figure 1.2). In addition humans, but not mice, express TLR10. However, mice, but not humans, express TLR11, 12, and 13 (Lee and Kim, 2007; Carpentier et al., 2008). The TLRs are type I transmembrane receptors, consisting of an N-terminal leucine-rich repeats (LRR) in the extracellular domain, a Toll-interleukin (IL)-1R (TIR) homologous region in the cytoplasmic domain and a transmembrane domain (O'Neill et al., 2000, Takeda et al., 2005). The TLRs differ from one another in terms of the cell types in which they are expressed, their ligand specificity, the signalling adaptors that they utilise and the cellular responses they induce (Iwasaki and Medzhitov, 2004). The most characterised TLRs are TLRs 1-9, which can be broadly divided into two groups on the basis of their PAMP specificity. The first group are expressed on the cell surface and recognise PAMPs in cell wall components and flagellin from both Gram-positive and Gram-negative bacteria, yeast, and fungi. This group includes TLR2 that forms a heterodimer with TLR1 or TLR6 and recognises bacterial lipoproteins and lipopeptides, TLR4 which recognises lipopoly-saccharides (LPS) and TLR5 which recognises flagellin (Mogensen 2009; Boo et al., 2010). The second group of TLRs, which reside in intracellular compartments, detects PAMPs in nucleic acids derived from bacterial and viral pathogens. This includes TLR3 which recognises double-stranded RNA, a product of viral replication in host cells, TLR7 and TLR8, which recognises single-stranded RNA derived from RNA viruses and small interfering RNA (siRNA), and TLR9 which recognises unmethylated CpG-containing DNA of bacterial and viral origin (Chaturvedi et al., 2008; Mogensen 2009; Boo et al., 2010).

### **1.3.1 TLR1, TLR2 and TLR6**

TLR2 is located on the cell surface and recognises extracellular ligands. It forms heterodimers with either TLR1 or TLR6 and recognises many different microbial and synthetic components. These include lipoproteins/lipopeptides from various pathogens, peptidoglycan and lipoteichoic acid from Gram-positive bacteria. TLR1/2 heterodimers

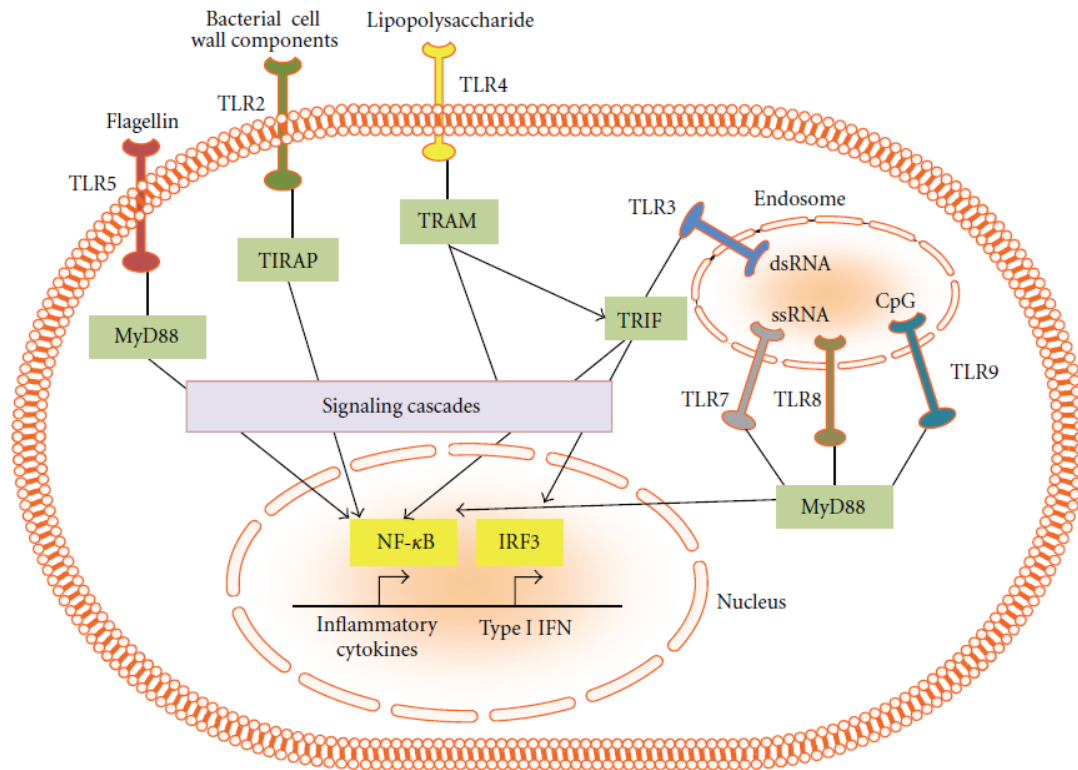


**Figure 1.2: An overview of human Toll-like receptors and their ligands.** TLR2 is essential in the recognition of microbial lipopeptides. TLR2 heterodimerises with TLR1 to facilitate recognition of triacyl lipopeptides and with TLR6 to facilitate recognition of diacyl lipopeptides. TLR3 is implicated in the recognition of viral dsRNA. TLR4 is the receptor for LPS. TLR5 recognises flagellin, whereas TLR7 is implicated in viral-derived ssRNA recognition. TLR9 is essential in CpG DNA recognition. TLR signalling may originate from either the cytoplasmic TIR domain of plasma membrane localised TLRs (TLR1/2, TLR2/6, TLR4, TLR5) or from the endosomally localised intracellular TLRs (TLR3, TLR7, TLR8, TLR9). (Adapted from Muccioli, et al., 2012).

recognize triacyl lipopeptides such as Pam<sub>3</sub>CSK<sub>4</sub> (a synthetic bacterial lipopeptide), and TLR2/6 heterodimers recognize diacyl lipopeptides such as the Mycoplasma-derived macrophage-activating lipopeptide 2 (MALP2) (Janeway and Medzhitov, 2002). Moreover several viruses, such as Herpes simplex virus (HSV), Cytomegalovirus (CMV), Hepatitis C virus (HCV) and Measles virus induce type I IFNs and proinflammatory cytokines via TLR2 signalling (Boo and Yang, 2010). In support of these findings is the fact that macrophages from TLR6-deficient mice do not show any production of inflammatory cytokines in response to mycoplasma-derived diacyl lipopeptides. However, these cells showed normal production of inflammatory cytokines in response to triacyl lipopeptides derived from Gram-negative bacteria (Takeuchi et al., 2001). In contrast, macrophages from TLR1-deficient mice showed a normal response to mycoplasma-derived diacyl lipopeptides, but an impaired response to triacyl lipopeptides (Takeuchi et al., 2002). Thus, TLR1 and TLR6 functionally associate with TLR2 and discriminate between diacyl or triacyl lipopeptides. TLR2 has been shown to functionally collaborate with distinct types of receptors such as dectin-1, a lectin family receptor for the fungal cell wall component  $\beta$ -glucan recognition (Gantner et al., 2003). Thus, TLR2 recognises a wide range of microbial product through functional cooperation with several proteins that are either structurally related or unrelated and this facilitates the emanation of various signalling cascades (Takeda and Akira, 2005).

### **1.3.2 TLR 3**

Double-stranded RNA (dsRNA), is a replication intermediate of several viruses, is detected by the innate immune system through TLR3. TLR3 expression is predominantly observed in the intracellular compartments of dendritic cells (DCs) and macrophages, while some fibroblasts also express TLR3 on their cell surface (Yoneyama and Fujita, 2010). Notably, dsRNA is produced during the replication of most RNA viruses, including the enveloped Respiratory Syncytial virus (RSV), Influenza A virus and the West Nile virus (WNV) (Groskreutz et al., 2006; Le Goffic et al., 2006; Kong et al., 2008; Boo and Yang 2010). TLR3 also plays an important role in the detection of DNA viruses including mouse CMV and HSV (Tabeta et al., 2004; Zhang et al 2007).

The role of TLR3 in antiviral immune responses was experimentally proved using an artificial dsRNA ligand and TLR3 knockout mice (Alexopoulou et al., 2001). The synthetic dsRNA ligand, polyinosinic:polycytidylic acid (poly(I:C) has immunostimulatory activity similar to dsRNA and TLR3-deficient mice have been found to have their response to dsRNA impaired (Alexopoulou et al., 2001). However, the function of TLR3 in antiviral immunity is controversial. It has been shown that the expression of Type 1 interferon (IFN) and inflammatory cytokines were reduced but not abolished in cells such myeloid DCs derived from TLR3 deficient mice in response to dsRNA and poly(I:C) (Takeda et al., 2003; Alexopoulou et al., 2001). Moreover, reports have suggested that TLR3 is involved in the support of viral growth or pathogenesis rather than protection (Wang et al., 2004; Le Goffic et al., 2006). TLR3-independent mechanisms of dsRNA recognition have been reported. Studies have shown that the Retinoic acid-inducible gene I-like helicases such as RIG-I and MDA-5 can also sense viral RNA in the cytoplasm of infected cells (Andrejeva et al., 2004; Yoneyama et al., 2004). Although TLR3 was reported to play a key role in sensing poly(I:C) by epithelial cells (Guillot et al., 2005; Rudd et al., 2006; Matsukura et al., 2007), it played only a moderate or minor role in sensing poly(I:C) in macrophages or conventional DCs (Alexopoulou et al., 2001; Yamamoto et al., 2003). In contrast, RIG-I and MDA5 were found to play a more important role than TLR3 in sensing poly(I:C) in fibroblasts and DCs (Kato et al., 2005, Kato et al., 2006).

### **1.3.3 TLR4**

TLR4 was the first cloned mammalian TLR and has been the most extensively studied. It has been identified in many cell types, such as endothelial cells, monocytes, thyroid cells, endometrial cells, mesangial cells, adipocytes and human  $\beta$ -cells (Garay-Malpartida et al., 2011). TLR4, together with the co-receptors MD2 and CD14, form a signalling complex that responds to lipopolysaccharide (LPS), the endotoxin component of Gram-negative bacteria outer membrane (Janeway and Medzhitov, 2002; Lee and Kim, 2007). It has been suggested that the co-receptor CD14 may facilitate diversification of the TLR4 ligand repertoire and also aids towards the full activation of the downstream signalling pathways (Godowski, 2005)

In addition to LPS, TLR4 recognizes other ligands such as taxol, heat shock proteins 60 and 70, oligosaccharides of hyaluronic acid, heparan sulfate and fibrinogen (Takeda and Akira, 2005). However, all these endogenous ligands require very high concentrations to activate TLR4 which is in contrast to the low concentrations of LPS that are required to mediate TLR4 activation (Takeda and Akira, 2005). TLR4-deficient mice generated by gene targeting are hypo-responsive to LPS, confirming that TLR4 is the essential receptor for LPS recognition (Hoshino et al., 1999). It has been reported that TLR4 was also involved in the recognition of certain group of viruses including mouse mammary tumor virus, molony murine leukemia virus and RSV (Takeda and Akira, 2003). TLR4 has been established as an essential component in the recognition of LPS. However, several reports indicated that LPS can also be recognized independently of TLR4. The NOD family, NOD1 and NOD2 confer intracellular recognition to LPS and mutant NOD2 protein was defective in LPS-induce-NF- $\kappa$ B activation (Inohara et al., 2001; Ogura et al., 2001).

#### **1.3.4 TLR5**

TLR5 recognizes an evolutionarily conserved site on bacterial flagellin that is required for flagellar filament assembly and motility (Andersen-Nissen et al., 2005). It is responsible for flagellin-induced responses in epithelial cells, endothelial cells, macrophages, DCs and T cells (Steiner, 2007). In addition, flagellin activates TLR5 on CD4 and CD25 T-regulatory cells, leading to increased suppressive activity, suggesting that flagellin has a complex role in bridging innate immunity and adaptive immunity (Crellin et al., 2005). Flagellin was shown to have TLR5-independent proinflammatory activity that depends on two related intracellular pattern recognition receptors, Neuronal apoptosis inhibitory protein 5 (Naip5) and Ice protease-activating factor (Ipaf), which are members of the NACHT-leucine-rich repeat-containing receptor (NLR) family (Steiner, 2007). Flagellin acts as a PAMP in plants as well, whereby flagellin is sensed through the Flagellin-sensing 2 gene (FLS2). This gene encodes a LRR transmembrane receptor-like kinase with similarities to TLRs in mammals (Akira and Hemmi, 2003). Evidence indicates that the LRR domain of FLS physically interacts with flagellin. However, there is no significant homology between the LRR domains of TLR5 and FLS2 (Akira and Hemmi 2003; Takeda and Akira 2003).

### **1.3.4 TLR7 and TLR8**

TLR7 and TLR8, which are localised to endolysosomal compartments, are structurally highly conserved proteins that recognise the same ligand in some cases (Akira and Hemmi 2003; Larange´ et al., 2009). More specifically, they recognize viral infections in the form of foreign nucleic acids. TLR7 can recognize synthetic RNA homologs such as resiquimod (R848) and ssRNA derived from ssRNA viruses such as vesicular stomatitis virus (VSV) (Gorden et al., 2006). However, studies have demonstrated that non-rodent (human, bovine, and porcine) TLR8 signalling can be activated by synthetic ligands such as imiquimod (R837), resiquimod and some guanine nucleotide analogs. In contrast, rodent (mouse and rat) TLR8s, whose primary sequences and structures are identical to non-rodent TLR8s, were not activated by non-rodent ligands (Akira and Hemmi 2003; Govindaraj et al., 2011). TLR7 is expressed in plasmacytoid DCs (pDCs) and in response to TLR7 stimulation, pDCs produce large amounts of IFN $\alpha$ . TLR7 activation also leads to DC maturation and expression of CD40, CD80, and CD86 (Gorden et al., 2006). TLR8 is expressed in myeloid DCs (mDCs), and monocytes. It's activation in mDCs leads to IL-12 and TNF $\alpha$  production as well as upregulation of CD8, CD40 and CD80 (Larange et al., 2009).

### **1.3.5 TLR9**

TLR9 is essential for recognition of synthetic CpG oligonucleotides and unmethylated CpG motifs in bacterial and viral DNA. It is highly expressed in pDCs and, most likely, recognises its ligand intracellularly, perhaps in the endosome or lysosomes (Ahmad-Nejad et al., 2002). The critical involvement of TLR9 in the recognition of bacterial DNA was demonstrated using TLR9-deficient mice. Hemmi and colleagues showed that TLR9 deficient mice do not show any response to CpG DNA, in terms of splenocyte proliferation, inflammatory cytokine production from macrophages and maturation of DCs (Hemmi et al., 2000; Akira and Hemmi, 2003). Recently, it has been reported that Hepatitis B virus (HBV) impaired TLR9 expression and function in pDCs and B lymphocytes, which may in turn contribute to the establishment and/or persistence of chronic infection (Vincent et al., 2011). Activation of the TLR9 pathway by CpG motifs is also impaired severely in human keratinocytes expressing human papilloma virus (HPV) or E6 and E7 the major oncoproteins from this dsDNA virus (Hasan et al., 2007). It has been discovered that the full-

length TLR9 has to be cleaved from the N-terminal to generate a functional (processed) TLR9 C-terminal. Interestingly, though both the full-length and cleaved forms of TLR9 are capable of binding ligand, only the processed form recruits MyD88 upon activation, arguing that this truncated receptor, rather than the full-length form, is functional (Ewald et al., 2008, Balashov et al., 2010).

### **1.3.6 TLR10**

Like other TLRs, TLR10 has multiple leucine-rich repeats and TIR domain. It shares the highest homology with TLR1 and TLR6. TLR10 can form either a homodimer or a heterodimer with TLR1 or TLR2. TLR10 expression has been detected in pDCs, monocytes and B cells (Lazarus et al., 2004). The ligand for TLR10 has not yet been identified. However, a study investigating TLR10 polymorphisms in asthmatic patients suggested that TLR10 may be involved in the recognition of airborne pathogens or airborne allergens (Lazarus et al., 2004; Nyman et al., 2008). It has been reported that hypoxia or reactive oxygen species (ROS) increased TLR10 expression in human monocytes (Kim et al., 2010).

### **1.3.7 TLR11, TLR12 and TLR13**

TLR11, TLR12 and TLR13 are present in mice but not in human. Protozoan profilin-like protein from *Toxoplasma* has been reported to activate DCs through TLR11 and is the first defined ligand for this TLR. Moreover, TLR11 is required for in vivo parasite-induced IL-12 production and optimal resistance to infection, thereby establishing a role for TLR11 receptor in host recognition of protozoan pathogens (Lauw et al., 2005; Yarovinsky et al., 2005). Little is known about ligand recognition by TLR12 and TLR13. However, Mishra et al. (2008) studied the expression and distribution of TLR11-13 in the murine brain. It was found that parasite infection caused an increase of both mRNAs and protein levels of all three TLRs. All three TLR proteins were present in both CNS and immune cell types. Among them TLR13 was expressed the most, followed by TLR11 then TLR12 (Mishra et al., 2008). Recently TLR13 has been shown to be involved in the recognition of the vesicular stomatitis virus and bacteria RNA (Shi et al., 2010, Oldenburg et al., 2012, Hidmarket et al., 2012). In addition, small interfering RNA against TLR13 reduced cytokine

induction by bacteria RNA in DCs. Moreover, Chinese hamster ovary cells transfected with TLR13, but not with TLR7 or 8, could activate NF- $\kappa$ B in response to bacteria RNA or *Streptococcus pyogenes* in an RNA-specific manner (Hidmarket et al., 2012).

#### **1.4 TLRs signalling pathway**

Stimulation of TLRs by microbial components triggers the expression of several genes that are involved in immune responses. Microbial recognition of TLRs facilitates dimerization of TLRs. Whilst TLR2 has been shown to form a heterodimer with TLR1 or TLR6, in other cases, TLRs are believed to form homodimers (Akira and Takeda, 2004). Ligand engagement with their respective TLRs leads to a conformational change within the TLR which facilitates the interaction of their cytoplasmic TIR domains with downstream TIR domain-containing adaptor molecules. Upon recognition of their cognate ligand, TLRs induce the expression of a variety of host defense genes. These include inflammatory cytokines, chemokine and upregulation of the immune cells (Janeway and Medzhitov, 2002). TLR signalling is mediated by adaptor proteins and protein kinases, ultimately leading to the activation of IFN regulatory factors (IRF), IRF3, 5 and 7, or nuclear factor- $\kappa$ B (NF- $\kappa$ B) family and release of pro-inflammatory cytokine including tumor necrosis factor  $\alpha$  (TNF- $\alpha$ ), IL-1 $\beta$ , IL-6, IL-12 and IL-18 (Sirén et al., 2005; Häcker et al., 2006). As a major transcription factor for anti-viral activity, NF- $\kappa$ B is thought to play an important role in the induction of pro-inflammatory molecules, such as IL-1 $\beta$  and TNF- $\alpha$ , upon cellular responses against viral infections (Schoenemeyer et al., 2005). Moreover, activation of the IRF pathway leads to the secretion of type I IFNs such as IFN- $\alpha$  and IFN- $\beta$ . Whilst IRF5 is a strong transcription activator for IFN- $\alpha$  production, IRF7 can induce both IFN- $\alpha$  and IFN- $\beta$  (Romieu-Mourez et al., 2006; Yang and Seki, 2012). The TLRs signalling pathways are illustrated in Figure 1.3.

#### **1.5 TLR adaptors**

All TLRs have a TIR domain that initiates the signalling cascade through TIR adaptors. The TLR adaptors serve as platforms that organise downstream signalling cascades leading to a specific cellular response. To date, five adaptor proteins have been discovered, Myeloid differentiation protein-88 (MyD88), MyD88 adaptor-like (Mal, also referred to as

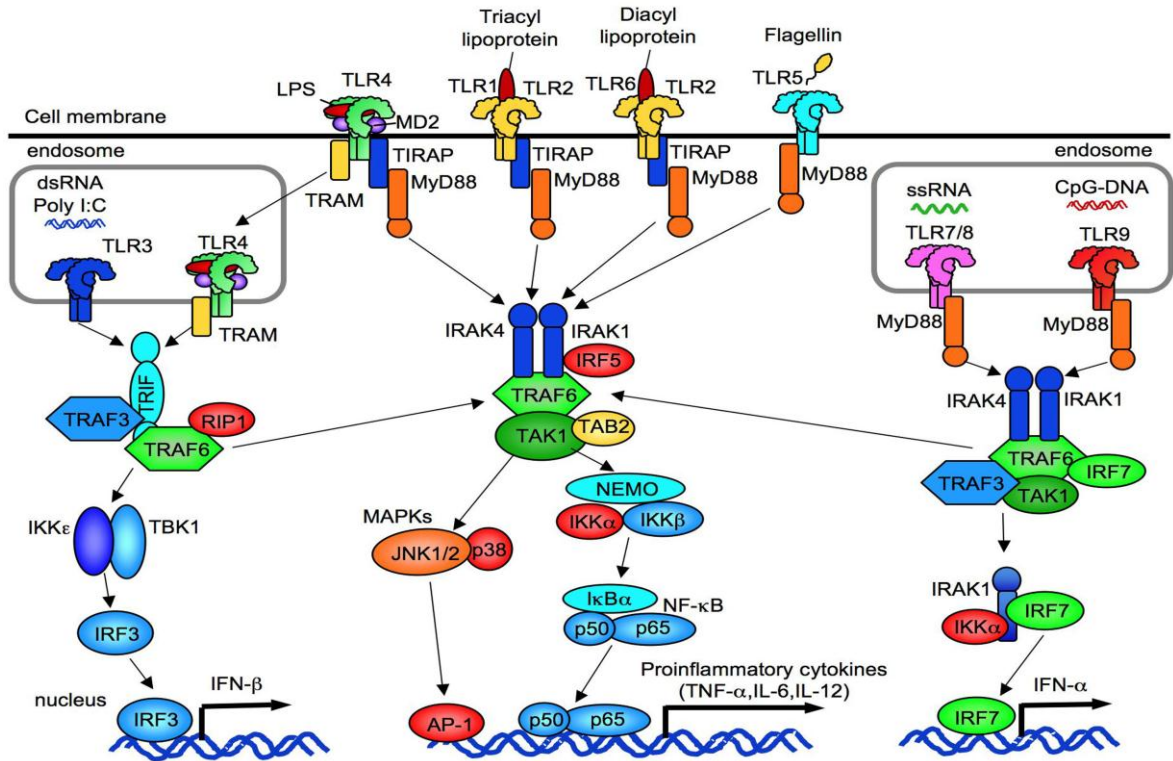


**Figure 1.3: Overview of TLR signalling.** All TLRs recruit either MyD88 and/or TRIF and these in turn, recruit IRAKs to the receptor upon ligand binding. IRAK then activates TRAF6, leading to the activation of the I $\kappa$ B kinase (IKK) complex consisting of IKK $\alpha$ , IKK $\beta$  and NEMO/IKK $\gamma$ . The IKK complex phosphorylates I $\kappa$ B, result in nuclear translocation of NF- $\kappa$ B which induces expression of inflammatory cytokines. TIRAP, a second TIR domain-containing adaptor, is involved in the MyD88-dependent signalling pathway via TLR2 and TLR4. In TLR3 and TLR4-mediated signalling pathways, activation of IRF3 and induction of IFN- $\beta$  are observed in a MyD88-independent manner. A third TIR domain-containing adaptor, TRIF, is essential for the MyD88-independent pathway. TRIF mediates IRF-3 activation through IKK $\epsilon$  and TANK-binding kinase 1 (TBK1). A fourth TIR domain-containing adaptor, TRAM, is specific to the TLR4-mediated MyD88-independent/TRIF-dependent pathway (Adapted from Yang and Seki, 2012).

TIR-domain containing adaptor protein (TIRAP)), TIR-domain-containing adaptor inducing interferon (TRIF also known as TIR-containing adaptor molecule (TICAM-1)), TRIF-related adaptor molecule (TRAM also called TIR-containing adaptor molecule-2 (TICAM-2)) and Sterile alpha and Armadillo repeat protein (SARM) (Takeda et al., 2004; O'Neill and Bowie, 2007) (Figure 1.4). MyD88, which was the first adaptor molecule to be identified, is involved in signalling triggered by all TLRs, with the exception of TLR3, and plays a major role in TLR-induced signal transduction. Despite the prominent role of MyD88 in TLR signalling, studies using MyD88-deficient mice revealed the existence of both MyD88-dependent and -independent pathways. (Takeda and Akira, 2005; Mogenson, 2009).

### **1.5.1 MyD88**

Whilst MyD88 was discovered in 1990 (Lord et al., 1990), its role in TLR signalling was not known until 1998 (Medzhitov et al., 1998). Prior to being implicated in TLR signalling, MyD88 was found to be an adaptor molecule that functions to recruit the Interleukin-1 receptor (IL-1R) associated protein kinase (IRAK-1) to the Interleukin-1 receptor complex following IL-1 stimulation resulting in the activation of NF- $\kappa$ B (Wesche et al., 1997). MyD88 is 296 amino acids and contains three domains, a N-terminal death domain which enables interactions with the IRAKs, an interdomain and a C-terminal TIR domain which facilitates homotypic interaction with other TIR-containing proteins (Medzhitov et al., 1998; O'Neill and Bowie, 2007). MyD88 functions as a universal adaptor and is shared by all TLRs, except TLR3 which exclusively recruits TRIF. MyD88 deficient mice and macrophages failed to secrete the proinflammatory cytokines IL-6 and TNF- $\alpha$  in response to LPS stimulation. Furthermore, MyD88 deficient mice were found to be more resistant to LPS-induced death than wild type mice (Kawai et al., 1999). However, mitogen activated protein kinases (MAPK) and NF- $\kappa$ B activation was still present, albeit delayed in the MyD88 deficient mice in response to LPS. This was the first indication of the presence of a MyD88-independent pathway in LPS signalling (Kawai et al., 1999). Further studies using MyD88-deficient macrophages found that they were completely unresponsive to TLR2, TLR7 and TLR9 ligands (Takeuchi et al. 2000; Alexopoulou et al., 2000). In terms of signalling upon stimulation, MyD88 recruits members of the IRAK family through

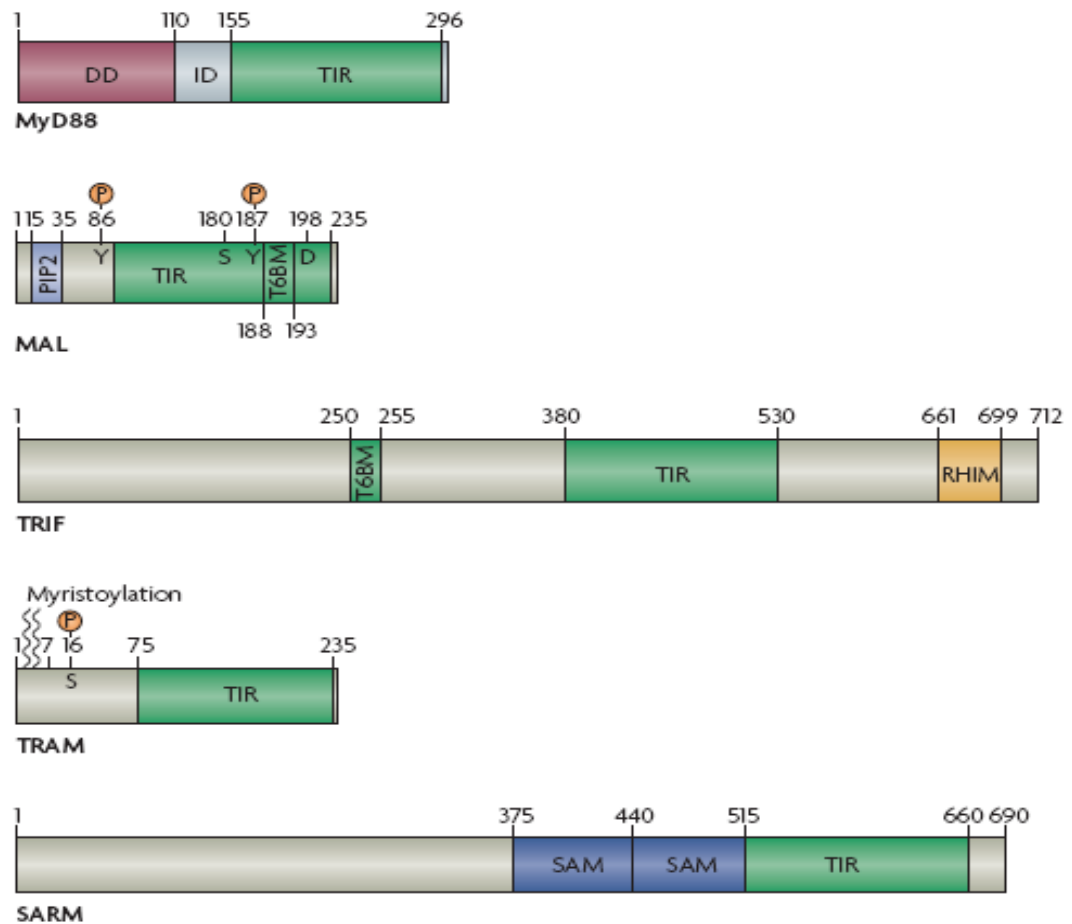


**Figure 1.4: Domain structure of the TIR-domain-containing adaptor proteins.** MyD88 contains a C-terminal death domain (DD), intermediate domain (ID) and an N-terminal TIR domain. MAL contains at the N-terminus a PIP2 binding domain followed by the TIR domain and TRAF6 binding motif (T6BM). It also contains two phosphorylation sites for Bruton’s tyrosine kinase at positions 86 and 187. Located at position 180 is the serine/leucine site linked to the genetic susceptibility to several diseases including tuberculosis (TB) and malaria. At position 198 is the aspartic acid indicating the presence of the caspase-1 cleavage site. TRIF is 712 amino acid long. It consists of a TRAF6 binding motif (T6BM), the TIR domain and a receptor-interacting protein (RIP) homotypic interaction motif (RHIM). TRAM consists of 235 amino acid. It contains a myristoylation site at the N terminus, followed by serine at position 16 which is phosphorylated by protein kinase C- $\epsilon$  and the TIR domain between amino acid 75 and 235. SARM consist of two sterile  $\alpha$ -motif (SAM) domains followed by the TIR domain. (Adapted from O’Neill and Bowie, 2007).

homotypic interaction of the death domain of both molecules. IRAK-1 was the first IRAK shown to be important in the ability of LPS to induce NF- $\kappa$ B activation. Other studies demonstrated that IRAK-4 is crucial in NF- $\kappa$ B activation in response to TLR ligands and is responsible for both the recruitment and phosphorylation of IRAK-1 (Wesche et al., 1997; Li et al., 2002; Swantek et al., 2000). Data suggested that IRAK-2 may play a prominent role in NF- $\kappa$ B activation, particularly during the late phase of TLR signalling (Chen, 2005; Mogenson, 2009). The phosphorylation of IRAK-1 leads to the recruitment TNF-receptor associated factor 6 (TRAF6) which is an ubiquitin E3 ligase that works in conjunction with a ubiquitin conjugating enzyme complex to polyubiquitinate target proteins, including itself (Chen, 2005). IRAK-1 and TRAF 6 association lead to the activation of two distinct signalling pathways. One pathway leads to activation of transcription factor activator protein 1 (AP-1) through activation MAPK (Change and Karin, 2001). Another pathway activates the transforming growth factor activated kinase1 TAK1 and TAK1 binding protein 2 (TAB2) complex, which enhances activity of the I $\kappa$ B kinase (IKK) complex (Takeda and Akira, 2004; Jenkins and Mansell, 2010). Once activated, the IKK complex induces phosphorylation and subsequent degradation of I $\kappa$ B, which leads to nuclear translocation of the transcription factor NF- $\kappa$ B and subsequent activation of NF- $\kappa$ B dependent genes, including the pro-inflammatory cytokines IL-1, IL-6 and TNF $\alpha$  (Feng and Chao et al., 2011) (Figure 1.4).

In 2010 Lin et al., showed the crystal structure of the MyD88: IRAK4: IRAK2 death domain (DD) complex, which reveals a left-handed helical oligomer that consists of 6 MyD88, 4 IRAK4 and 4 IRAK2 DDs. Assembly of this helical signalling tower is hierarchical, in which MyD88 recruits IRAK4 and the MyD88: IRAK4 complex recruits the IRAK4 substrates IRAK2 or the related IRAK1. Formation of these Myddosome complexes brings the kinase domains of IRAKs into proximity for phosphorylation and activation (Lin et al., 2010). In addition to the MyD88 pathway, which results in NF- $\kappa$ B translocation, there is a cell specific pathway which activated by TLR7, TLR8 and TLR9. In pDCs, the activation of these TLRs results in IFN $\alpha$  production. This pathway is MyD88 dependent and involves the nuclear translocation of IRF-7 (Honda et al., 2004). In pDCs it has been shown that the DEAD/H-box helicases DHX9 and DHX36 directly bound to the

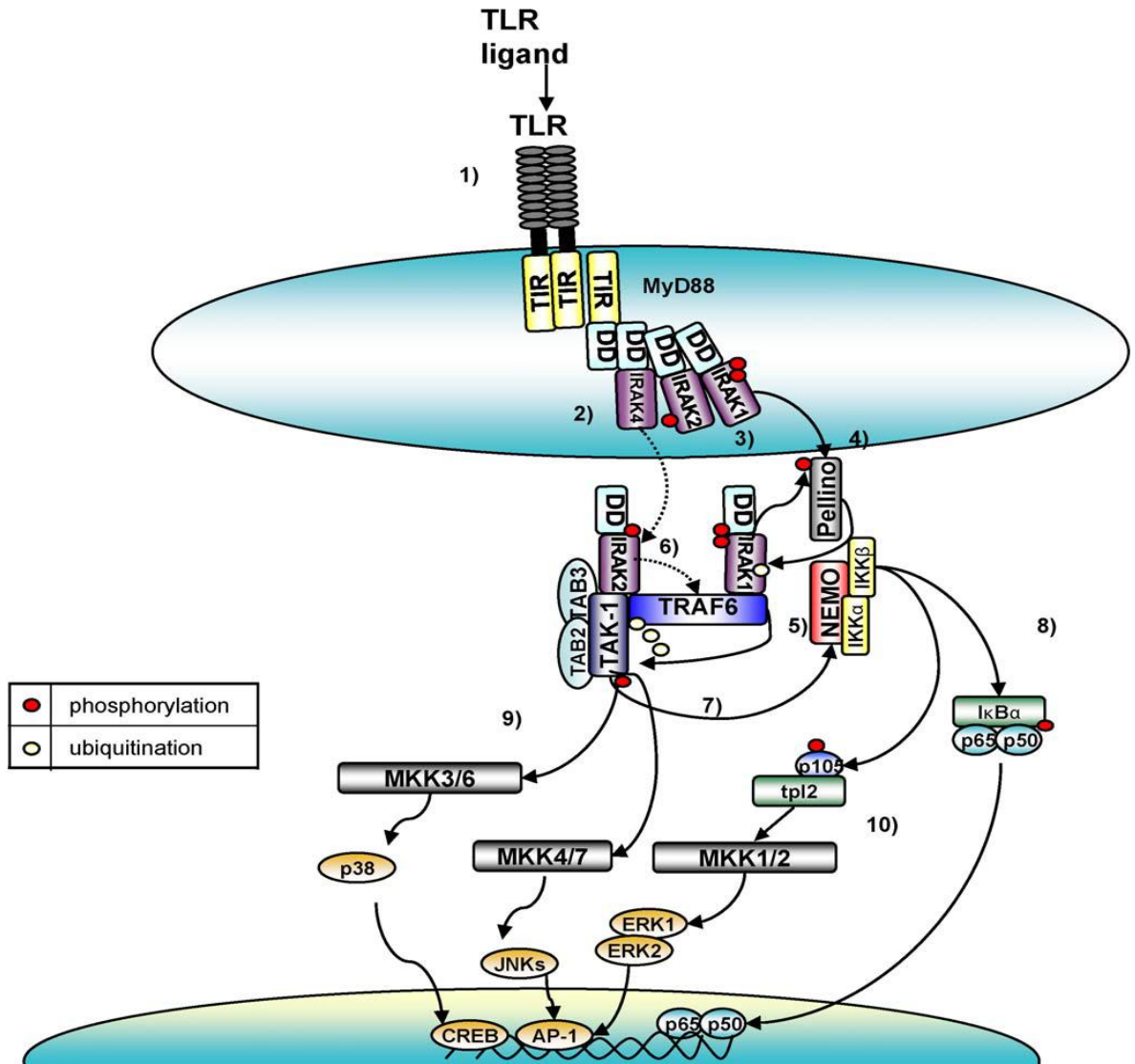


**Figure 1.4: MyD88-dependent pathway.** (1) Stimulation of TLR, by TLR ligand MyD88-dependent activation of NF $\kappa$ B and MAPK. IRAK4 interacts with MyD88 through death domain interactions. (2) IRAK-4 is thought to phosphorylate both IRAK-1 and IRAK-2 which induces their autophosphorylation activity. (3) Phosphorylated IRAK-1 is released from the receptor complex and subsequently associate with TRAF6. (4) IRAK-1 phosphorylates Pellino which can ubiquitinate IRAK-1. IRAK-1 and Pellino form a complex with TRAF6. (5) NEMO binds to ubiquitinated IRAK-1. (6) IRAK-2 induces the poly-ubiquitination of TRAF6. The polyubiquitination of TRAF6 results in the recruitment of the TAK-1/TAB2 complex and activation of TAK-1. (7) TAK-1 activates the IKK complex. (8) The IKK complex phosphorylates I $\kappa$ B $\alpha$  which allows p65/p50 to translocate in the nucleus. (9) For MAP kinase activation, TAK-1 activates MKK3/6 and MKK4/7 for p38 and JNK activation, respectively. (10) The IKK complex phosphorylates the inhibitory protein p105. Upon phosphorylation and degradation of p105, tpl2 is activated and subsequently activates MKK1/MKK2. MKK1/MKK2 activates ERK1 and ERK2. (Adapted from Flannery and Bowie, 2010).

TIR domain of MyD88, showing a TLR9-independent, MyD88 depending DNA sensing in pCDs (Kim et al., 2010). Moreover, the DHX36 governs a pathway specific for IRF7 activation and IFN- $\alpha$  induction whilst the DHX9 triggers nuclear translocation of the NF $\kappa$ B subunit p50 and subsequent upregulation of genes such as TNF $\alpha$  and IL-6 (Kim et al., 2010, Keating et al., 2011). Furthermore, recently new MyD88-dependent signalling mechanism has been identified. This signalling pathway proceeds via IFN $\gamma$  receptor/C-C chemokine receptor type 2 and governs the mobilization and activation of monocytes in response to challenge with a systemic intracellular bacterium (Pietras et al., 2011).

The MyD88 pathway is negatively regulated by three proteins, MyD88 short (MyD88s), transforming growth factor- $\beta$  (TGF- $\beta$ ) and IRAK-M (Janssens et al., 2002; Kobayashi et al., 2002; Naiki et al 2005). MyD88s is a splice variant of MyD88 and missing the interdomain located between the DD and TIR (amino acids 110-157) and its expression is induced in response to continuous stimulation with bacterial products or pro-inflammatory cytokines (Janssens et al., 2002). Naiki et al. (2005) showed that TGF- $\beta$  blocked NF- $\kappa$ B activation and cytokine production in response to TLR2, TLR4 and TLR5 ligands by decreasing MyD88 protein but not mRNA levels. Another negative regulator of MyD88 signalling is IRAK-M. IRAK-M prevents the dissociation of IRAK-1 and IRAK-4, which results in IRAK-1 being unable to interact with TRAF6 and is therefore unable to induce a signalling cascade (Kobayashi et al., 2002).

### **1.5.2 Mal**

Mal was the second TLR adaptor protein to be described (Fitzgerald et al., 2001; Horng et al., 2001). Mal is 235 amino acids in size and contains an N-terminal phosphatidylinositol-4,5-bisphosphate (PIP<sub>2</sub>) binding domain and a C-terminal TIR domain (Nunez Miguel et al., 2007; O'Neill and Bowie, 2007). Initially, Mal was characterised as a protein that specifically associates with TLR4 and found to interact with MyD88 in co-immunoprecipitation assays as well as in a yeast two-hybrid screen. Overexpression of Mal was found to activate NF- $\kappa$ B and JNK (Fitzgerald et al., 2001; Horng et al., 2001) and Mal-deficient mice were found to respond normally to the ligands for TLR5, TLR7 and TLR9 (Horng et al., 2002). However, as well as having defects in cytokine production and activation of NF- $\kappa$ B and MAP kinases in response to the TLR4 ligand, they were shown to have impaired response to TLR2 ligands (Yamamoto et

al., 2002). Similar to MyD88-deficient mice, Mal-deficient mice were found to be completely resistant to LPS-induced shock and were shown to have delayed activation of NF- $\kappa$ B and MAP kinases in response to LPS (Horng et al., 2002). The ability of Mal to act as a bridging adaptor for MyD88 is dependent on its localisation to the plasma membrane. The localisation of Mal to the plasma membrane is facilitated by its PIP2 binding domain (Nunez Miguel et al., 2007). At the plasma membrane, Mal acts as a bridging adaptor for MyD88, bringing it to the activated TLR4, to initiate signal transduction. A role of Mal distinct from that of MyD88 was identified when a putative TRAF6 binding motif was identified in Mal but not in MyD88. Mal was found to co-immunoprecipitate with TRAF6 and a mutation within the TRAF6 binding motif of Mal abolishes NF- $\kappa$ B activation by TLR2 and TLR4 (Mansell et al., 2004). Mal like many components of the TLR signalling pathway is subject to negative regulation. It has been shown that suppression of cytokine signalling 1 (SOCS1) mediates polyubiquitination of Mal on two N-terminal lysine residues, thereby mediating Mal degradation via the 26S proteasome (Mansell et al., 2006).

#### **1.5.3.1 TRIF**

TRIF was identified following the analysis of databases for TIR domain containing proteins and following a two hybrid screen (Yamamoto et al., 2002; Oshiumi et al., 2003). TRIF, 712 amino acids in length, is much larger than the other TLR adaptors. It contains three TRAF6-binding sites in its N terminal domain, a TIR domain and a receptor-interacting protein (RIP) homotypic interaction motif (RHIM) in its C-terminal domain (Oshiumi et al., 2003). Although TRIF contains a TIR domain, its amino acid sequence is very divergent from other TIR domain-containing adapter protein sequences (Han et al., 2004). Oshiumi and his colleagues showed that TRIF interacted with TLR3 in both co-immunoprecipitation assays and yeast two-hybrid screen. No interaction was found with either TLR2 or TLR4. In contrast to MyD88 and Mal, TRIF dramatically induce IFN- $\beta$  promoter activity. Overexpression of TRIF also induced activation of NF- $\kappa$ B promoter but at low level compared with MyD88 or Mal. A dominant negative version of TRIF, but not MyD88 or Mal, inhibited TLR3 activation of NF- $\kappa$ B and IFN- $\beta$  indicating a unique role for TRIF in TLR3 signalling (Yamamoto et al., 2002; Oshiumi et al., 2003). Moreover, TRIF deficient mice were impaired in TLR3 and TLR4-induced IFN- $\beta$  production and activation of IRF3.

Furthermore, inflammatory cytokine production in response to TLR4 ligands was severely impaired, whilst responses to TLR2, TLR7 and TLR9 ligands in TRIF-deficient macrophages were not impaired (Yamamoto et al., 2003). Mice deficient in both MyD88 and TRIF showed complete loss of NF- $\kappa$ B activation in response to TLR4 stimulation. These findings demonstrate that TRIF is essential for TLR3 and TLR4-mediated signalling pathways (Yamamoto et al., 2003). In contrast to MyD88 and Mal-deficient mice, TRIF-deficient mice displayed normal LPS-induced MyD88-dependent activation of IRAK-1, NF- $\kappa$ B and MAPK indicating that TRIF is not involved in LPS-induced activation of the MyD88-dependent pathway. However, the production of pro-inflammatory cytokines in response to LPS, but not other TLR ligands was impaired in these mice. This led to the suggestion that in the case of TLR4, both the MyD88-dependent and MyD88-independent pathways need to be intact to enable the production of pro-inflammatory cytokines (Yamamoto et al., 2003). When the response to LPS was examined in embryonic fibroblasts from MyD88 and TRIF double knockout mice, activation of NF- $\kappa$ B and JNK was completely abolished, confirming that TRIF was responsible for the delayed activation of NF- $\kappa$ B previously found in MyD88-deficient mice (Yamamoto et al., 2003).

During TLR3 and TLR4 signalling, TRIF (associated with TRAM in the case of TLR4) (Fitzgerald et al., 2003) is responsible for initiating a signalling pathway through TRAF3, TBK1 and IKK $\epsilon$  (Hacker et al., 2006; Guo et al., 2007) which mediate direct phosphorylation of IRF3 and IRF7. As a consequence of phosphorylation, IRF3 and IRF7 form hetero- or homodimers, translocate to the nucleus, in association with transcriptional coactivators such as CBP and p300 and bind to target sequences in DNA, such as IFN-stimulated response elements (Fitzgerald et al., 2003). IRFs, together with NF- $\kappa$ B and AP1, can form a multiprotein complex termed the 'enhanceosome', which induces transcription of the IFN- $\beta$  gene (Sharma et al., 2003). TRIF-dependent activation of NF- $\kappa$ B occurs through binding of TRAF6 to TRIF and subsequent ubiquitination-dependent recruitment and activation of TAK1 (Sato et al., 2003). In order to obtain robust NF- $\kappa$ B activation, a second molecule, receptor interacting protein 1 (RIP1), involved in TNF-receptor mediated NF- $\kappa$ B activation, is also recruited to TRIF (Meylan et al., 2004). RIP1 is polyubiquitinated to form a complex with TRAF6, and these two molecules appear to cooperate in facilitating TAK1 activation, resulting in IKK-mediated activation of NF- $\kappa$ B as well as activation of

the MAPK pathway (Cusson-Hermance et al., 2005). Recently, using yeast two-hybrid screening, it was found that three TRAF proteins TRAF1, 2 and 6, interacted with the N-terminal region of TRIF. Further, it was suggested that the binding of TRAF2 and TRAF6 to TRIF cooperatively activates the IFN-inducing pathway through ubiquitination of TRIF, a modification which occurs unrelated to TRAF3 recruitment in the TRIF signalling complex (Sasai et al., 2010). A simplified TRIF signalling pathway is predicted in figure 1.5. In addition to NF- $\kappa$ B and IRF3 activation, TRIF is the only TLRs adaptor that induces apoptosis upon overexpression in human embryonic kidney (HEK) 293 cells. Domain mapping experiments indicate that the N-terminal and middle TIR domains did not induce apoptosis, whereas the C-terminal 181 amino acids (positions 532-712) were sufficient to induce apoptosis (Han et al., 2004). Moreover, TRIF-induced apoptosis was not inhibited by I $\kappa$ B $\alpha$ , a dominant negative of IRF3, or IRF7 or by various combinations of these molecules. TRIF-induced apoptosis was also not inhibited by kinase inactive mutants of TBK1, IKK $\beta$ , and IKK $\epsilon$ . It was found that TRIF induced apoptosis through a RIP/Fas-associated death domain (FADD)/caspase-8-dependent pathway (Han et al., 2004).

Han et al. (2010) reported the identification of a splice variant of TRIF lacking the TIR domain and is therefore designated as TRIS. TRIS form heterocomplex with TRIF through their C-terminal RHIM motifs. Overexpression of TRIS activates NF- $\kappa$ B and IRF3, while knockdown of TRIS inhibited TLR3-mediated NF- $\kappa$ B and IRF3 activation (Han et al., 2010).

The TRIF pathway is negatively regulated by a number of molecules, however in most cases they do not target TRIF specifically, but affect downstream components of the TRIF pathway such as TBK1 or IRF (O'Neill and Bowie, 2007). It has been reported that SRC homology 2 (SH2) domain containing protein tyrosine phosphatase2 (SHP2) negatively regulates TRIF signalling by binding to the kinase domain of TBK1 thereby preventing its activation (An et al., 2006). SHP2 was found to negative regulate TLR3 and TLR4 activated IFN- $\beta$  production as well as pro-inflammatory cytokine production in response to TLR3 but not TLR2, TLR7 or TLR9 ligands. Knockdown of SHP2 was found to increase TLR3 and TLR4 induced IFN- $\beta$  production (An et al., 2006). SARM, the fifth TLR adaptor has also been shown to negatively regulate the TRIF but not the MyD88 pathway (Carty et al., 2006) and will be discussed below. A splice variant of TRAM called

TRAM adaptor with GOLD domain (TAG) was also shown to inhibit IRF3 activation upon LPS stimulation probably by displacing TRIF from TRAM (Palsson-McDermott et al., 2009). Knockdown of TAG was shown to enhance induction of the chemokine CCL5 (RANTES), but not IL-8 upon LPS stimulation in human peripheral blood mononuclear cells (Palsson-McDermott et al., 2009).

Su et al. (2006) showed that overexpression of TRAF1 inhibited TRIF and TLR3-mediated activation of NF- $\kappa$ B, IFN-stimulated response element and the IFN- $\beta$  promoter. Overexpression of TRIF caused caspase-dependent cleavage of TRAF1 and the cleaved N-terminal, but not C-terminal, fragment of TRAF1 was responsible for inhibiting TRIF signalling. Further, mutation of the caspase cleavage site of TRAF1, or addition of the caspase inhibitor cram, inhibited TRAF1 cleavage and abolished the ability of TRAF1 to inhibit TRIF signalling (Su et al., 2006).

In some cases, virally encoded proteases directly target components of the innate immune system to abolish anti-viral signalling. Targeted proteolysis of adaptor molecules serves as a powerful means to eliminate anti-viral signalling by suppressing common downstream targets of key innate immune signalling pathways (Mukherjee et al., 2011). Hepatitis C virus contains a serine protease NS3-4A that causes the proteolysis of TRIF (Li et al., 2005). The cleavage of TRIF by NS3-4A inhibits TLR3 mediated activation of NF- $\kappa$ B and IRF3, thus inhibiting the innate immune response to the virus (Li et al., 2005). Moreover the vaccinia virus protein A46R contains a TIR domain which facilitates its interaction with all the TLR adaptors, except SARM. The interaction of A46R with TRIF leads to the inhibition of IRF3 activation and concomitant gene induction (Stack et al., 2005). Also, Coxsackievirus B3 (CVB3) mediates TRIF cleavage through the virally-encoded protein, termed 3C<sup>pro</sup>. Mukherjee et al. (2010) demonstrated that 3C<sup>pro</sup> cleaves both the N and C-terminal domains of TRIF, localises with TRIF in the cytoplasm and inhibits TRIF mediated type I IFN and apoptotic signalling. Recently, Qu and colleagues showed that a 3CD protease-polymerase from Hepatitis A Virus (HAV), disrupted TLR3 signalling by targeting TRIF for degradation, thus inhibiting poly(I:C)-mediated dimerization of IRF3, IRF3 translocation to the nucleus and IFN- $\beta$  promoter activation (Qu et al., 2011).

### **1.5.3.2 TLR3-independent TRIF-dependent pathways**

Recently, it was demonstrated the presence of a TLR3-independent, TRIF-dependent poly(I:C) sensor in dendritic cells. It was shown that three new members of the DExD/H-box helicase family, DDX1, DDX21, and DDX36 use TRIF to activate the NF- $\kappa$ B pathway and type I IFN responses (Zhang et al., 2011). Moreover, it was shown that TRIF also mediates TLR5 signalling in intestinal epithelial cells (Choi et al., 2010). Choi et al. (2010) demonstrated that stimulation of cells with flagellin induces a physical interaction between TLR5 and TRIF in a time dependent manner. In fact, suppressed TRIF expression reduces TLR5-induced NF- $\kappa$ B and MAPK activation in response to flagellin, and TRIF deficiency inhibited flagellin-induced cytokine expression (Choi et al., 2010). However, the same group reported that TRIF plays an inhibitory role in TLR5-elicited responses by inducing proteolytic degradation of TLR5 (Choi et al., 2010). TRIF overexpression in human HEKT293 and human colonic epithelial (NCM460) cells abolishes the cellular protein level of TLR5, whereas it does not alter TLR5 mRNA level. Also, TRIF overexpression dramatically suppresses flagellin-TLR5-driven NF- $\kappa$ B activation in normal human colon mucosal epithelium NCM460 cells. Also, TRIF-induced TLR5 protein degradation is completely inhibited in the presence of a caspase inhibitor, indicating that TRIF induced caspase activity mediates TLR5 protein degradation (Choi et al., 2010). In addition, it was shown that the C-terminus of TRIF and the extracellular domain of TLR5 are required for TRIF-induced TLR5 degradation. Furthermore, TRIF-induced proteolytic degradation is extended to TLR3, TLR6, TLR7, TLR8, TLR9, and TLR10, whereas the cellular level of TLR1, TLR2, and TLR4 was not affected by TRIF overexpression. These results suggest that, in addition to mediating TLR3- or TLR4-induced signalling as an adaptor molecule, TRIF can participate in proteolytic modification of certain members of TLRs to modulate the functionality of TLRs at the post-translational level (Choi et al., 2010).

### **1.5.4 TRAM**

TRAM was identified following a database screening in 2003 (Oshiumi et al., 2003). It consists of 235 amino acids and is the smallest TLR adaptor protein. It contains a putative myristoylation site at the N-terminus and undergoes phosphorylation by protein kinase C $\epsilon$  (PKC $\epsilon$ ) at the serine residue at position 16 and a TIR domain in its C-terminus (Rowe et al.,

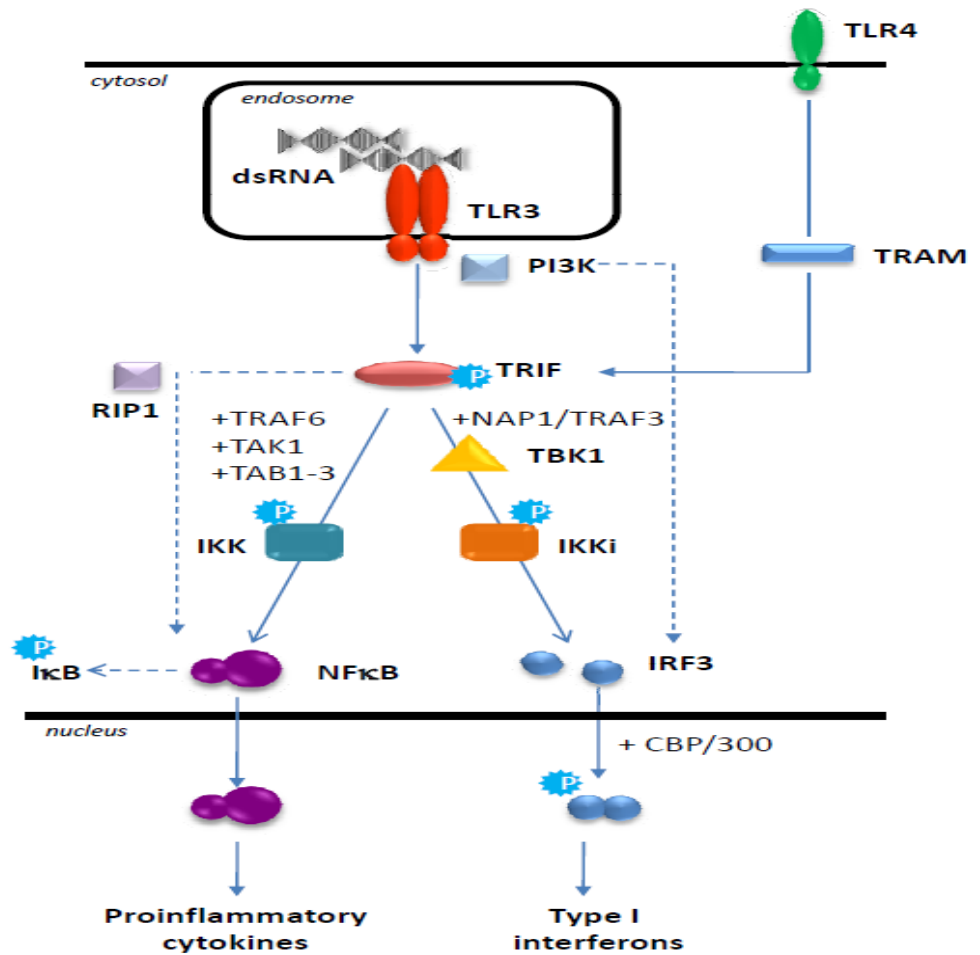


**Figure 1.5: TRIF signalling pathway:** DsRNA binds to TLR3 in the endosome activating TRIF. TLR4 can also activate TRIF via TRAM adaptor protein. TRIF interacts with TBK1 via NAP1 and TRAF3 and the signal transduced to the IKKi leading to the phosphorylation of IRF3. PI3K is also required to complete IRF activation. IRFs dimerise then translocate to the nucleus where they bind to the DNA and transactivate type 1 IFN genes expression in conjunction with the co-activator CBP/p300. TLR3 also activates NFκB by a TRAF-6 mediated interaction with TRIF involving the TAK1/TAB1/TAB2/TAB3 complex which activate TAK1 causing it to phosphorylate and activate IKK. This phosphorylate IκB and targets it for degradation causing NFκB nuclear translocation. Signalling via RIP1 is required for full activation of NFκB and transcriptional of target genes. (Adapted from Dunlevy et al., 2010)

2006; O'Neill and Bowie, 2007). TRAM physically interacts with TLR4, TRIF and Mal, but not with TLR3, and acts as bridging adaptor between TLR4 and TRIF in the MyD88-independent pathway (Fitzgerald et al., 2003; Oshiumi et al., 2003; Yamamoto et al., 2003). Using RNAi knockdown, both TRIF and TRAM were shown to be required for LPS induced IFN- $\beta$  production (Oshiumi et al., 2003). Overexpression of TRAM barely activates AP-1 and only weakly activates NF- $\kappa$ B and the IFN- $\beta$  promoter. Unlike the other TIR-containing adaptors, TRAM has been implicated in the TLR4 signalling pathway. Originally, TRAM was thought to be localised to the plasma membrane which facilitated its ability to signal (Rowe et al., 2006). However, it has been shown that TRAM contains a sorting signal that controls its trafficking between the plasma membrane and endosomes and that TRAM does not induce TRIF-dependent signalling from the plasma membrane. It has been demonstrated that TLR4 and TRAM must be delivered to the endosomes to facilitate the activation of IRF3 signalling (Kagan et al., 2008). Another modification of TRAM, which has been shown to be essential for its signalling ability, is the phosphorylation of the serine at position 16 by PKC $\epsilon$ . Mutation of this phosphorylation site (Serine16Alanine) results in loss of phosphorylation and the ability of TRAM to signal in response to LPS (McGettrick et al., 2006). TRAM-deficient cells were found to have impaired TLR4 mediated cytokine production and B cell activation, while other TLR were not affected (Yamamoto et al., 2003).

### **1.5.5 SARM**

SARM was the last TIR-containing adaptor protein to be characterised. It was originally identified as an orthologue of Drosophila protein CG7915 (Mink et al, 2001). SARM is a 690 amino acid long and contains two sterile  $\alpha$  motifs (SAMs) domains, a C-terminal TIR domain and N-terminal heat Armadillo repeat motif (ARM) (O'Neill et al., 2003). It was found that overexpression of SARM did not activate NF- $\kappa$ B or IRF3 (Liberati et al., 2004). In contrast to the other TLR adaptors, SARM was found to act as a negative regulator of TRIF-dependent TLR signalling. It blocked gene induction downstream of TRIF, but not MyD88, and suppression of endogenous SARM expression led to enhanced TRIF-dependent cytokine production (Liberati et al., 2004; Carty et al., 2006). Carty et al. (2006) showed that association between TRIF and SARM was strongly enhanced following LPS

or poly(I:C) treatment. It was hypothesised that SARM mediated its inhibitory effects by preventing the interaction of TRIF with upstream or downstream signalling molecules. However, Peng et al. (2010) demonstrated that human SARM is capable of blocking the LPS-induced MyD88- and TRIF-mediated AP-1 activation. Suppression of endogenous SARM with siRNA increased AP-1 basal level. In addition, Belinda et al. (2008) showed that the horseshoe crab orthologue SARM (CrSARM) downregulated TRIF dependent TLR signalling in response to infection. The CrSARM expression was upregulated within 3 h and strongly repressed at 6 h of infection. This suggested that SARM negatively regulating TRIF signalling is evolutionary conserved from horseshoe crab to human (Belinda et al., 2008). Surprisingly in contrast to its role in human cells, murine SARM in the CNS appears to positively regulate TNF- $\alpha$  induction, which affects microglia activation and accumulation and protects critical neuron subsets from virus-induced pathology. Mice lacking SARM were reported to be more susceptible to lethal West Nile virus (WNV) disease. This phenotype was also associated with region-specific differences in WNV replication, with higher levels of viral RNA observed in the brainstem of SARM knockout mice (Szretter et al., 2009). Recently, *Drosophila* SARM has been shown to be involved in axonal degradation. SARM knockout neurons in slice cultures exhibit reduced cell death in response to oxygen/glucose deprivation (Osterloh et al., 2012).

### **1.6 Negative regulation of TLR signalling**

Defects in TLR signalling make the host susceptible to various pathogens. However, stimulation of TLRs by microbial components can triggers excess production of inflammatory cytokines such as TNF- $\alpha$ , IL-6 and IL-12, which may lead to systemic disorders with a high mortality rate in the host (Takeda and Akira, 2005). To control TLR signalling, a number of negative regulators are upregulated and serve to modulate the TLR immune response through negative feedback mechanisms (Figure 1.6). Others negative modulators of TLR signalling are constitutively expressed and control primary TLR signalling events. Together these molecules serve to prevent potentially harmful immune responses (Janssens et al., 2002). In addition, anti-inflammatory factors produced indirectly during immune responses can also negatively regulate TLR signalling. Such potent anti-

inflammatory factors include TGF $\beta$ , IL-10 and steroid hormones (Janssens et al., 2002; Lee and Kim, 2007).

Negishi et al. (2005) showed that IRF4 inhibited the expression of MyD88-dependent and IRF5-dependent genes following TLR stimulation. Moreover, it was found that TLR activation induced IRF4 mRNA, which competes with IRF5, for interaction with MyD88. In addition, TLR-dependent induction of proinflammatory cytokines is markedly enhanced in peritoneal macrophages derived from IRF4-deficient mice, whereas the proinflammatory cytokine induction is inhibited by ectopic expression of IRF4 in a macrophage cell line (Negishi et al., 2005). Dok1 and Dok2, downstream adaptors of protein tyrosine kinases, are constitutively expressed and activated within minutes following TLR4 stimulation (Shinohara et al., 2005). These proteins specifically inhibit the extracellular-signal-regulated kinases (ERK) pathway, but not the pathways involving p38, JNK, and NF- $\kappa$ B. The inhibition seems to be specific for TLR4 (Shinohara et al., 2005). Other TLRs regulators include  $\beta$ -arrestin 1 and  $\beta$ -arrestin 2. It has been demonstrated that  $\beta$ -arrestin 1 and  $\beta$ -arrestin 2 interact with TRAF6 after TLR activation in macrophages. This interaction inhibits TRAF6 autoubiquitination and concomitant NF- $\kappa$ B and AP-1 activation. Endotoxin treated  $\beta$ -arrestin 2 deficient mice had higher expression of proinflammatory cytokines and were more susceptible to endotoxic shock (Wang et al., 2006). Recently, Xia et al. (2011) showed that Nucleotide-binding oligomerization domain protein 26 (NLRX1), a NOD-like receptor family member, negatively regulates TLR-mediated NF- $\kappa$ B activation. NLRX1 interacts with TRAF6 or I $\kappa$ B kinase (IKK) upon LPS stimulation resulting in inhibition of IKK $\alpha$  and IKK $\beta$  phosphorylation and NF- $\kappa$ B activation. In addition, knockdown of NLRX1 in various cell types enhances IKK phosphorylation and production of NF- $\kappa$ B-responsive cytokines after LPS stimulation. Knockdown of NLRX1 in mice markedly enhanced their susceptibility to LPS-induced septic shock and levels of plasma IL-6 (Xia et al., 2011). In addition to the negative regulators of the MyD88 and TRIF pathways that have been mentioned described herein, TLRs can be negatively regulated by nuclear receptors, including the glucocorticoid receptor (GR), liver X receptors (LXRs) and peroxisome proliferator-activated receptor  $\gamma$  (PPAR $\gamma$ ) (lee and Kim, 2007).

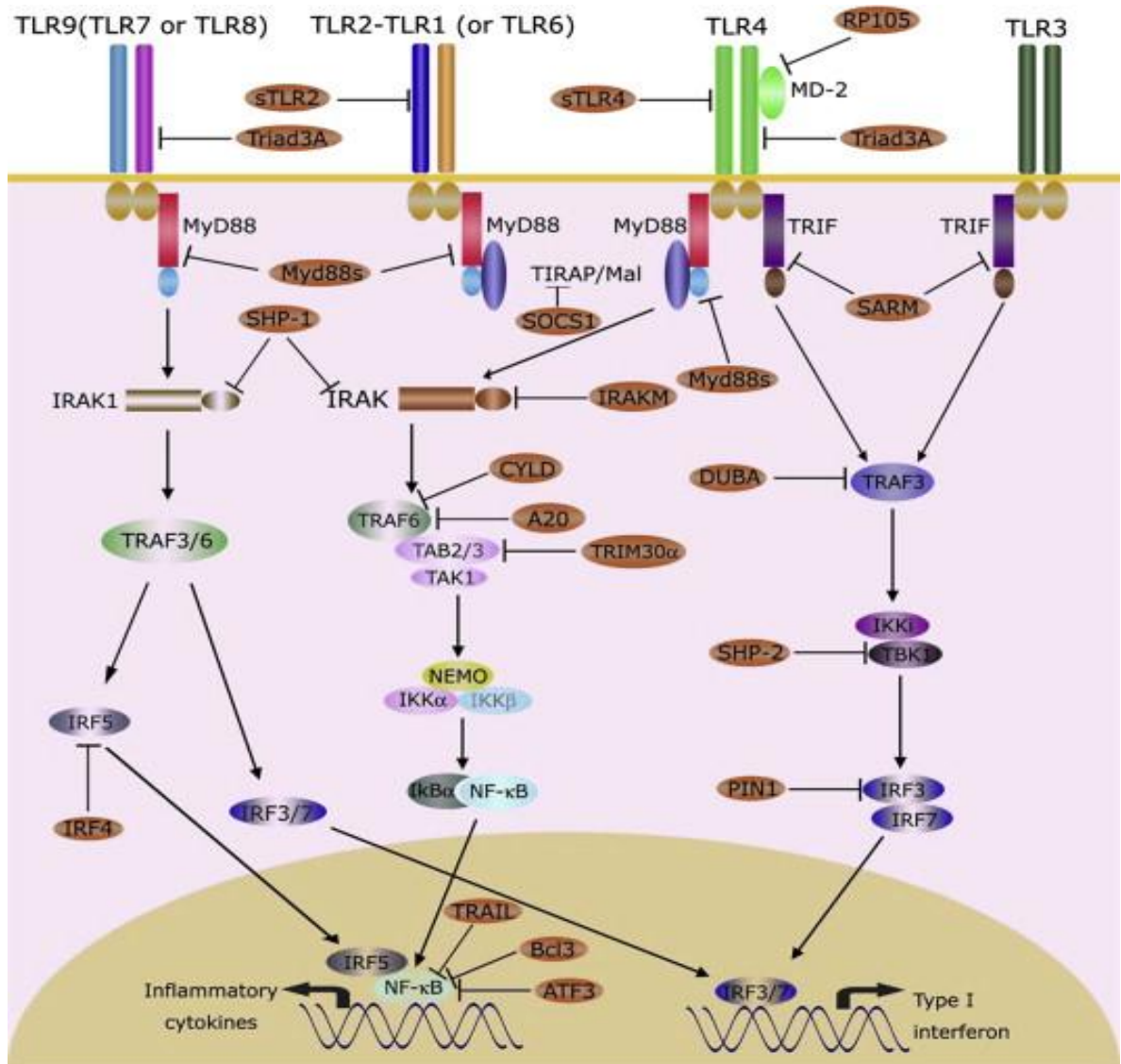


**Figure 1.6: The negative regulators of TLR signalling pathways.** The negative regulators were marked in brown near to their targets proteins. Triad3A, acts as an E3 ubiquitin-protein ligase and enhances ubiquitination and proteolytic degradation of certain TLRs. Suppressor of cytokine signalling (SOCS)-1 interacts with Mal and induces its polyubiquitination and subsequent proteasomal degradation and their by act as negative regulator of TLR2 and TLR4 signalling. The Tripartite-motif protein (Trim) 30 $\alpha$  act as a negative regulator of TLR-mediated NF- $\kappa$ B activation by targeting TAB2 and TAB3 for degradation. Radioprotective 105 (RP 105) and its helper molecule, MD-1, have a physical association with TLR4/MD2, and this association inhibits LPS-TLR4/MD2 complex formation. Other negative regulators such as IRF4, MyD88s, IRAKM, SARM and SHP2 were discussed in more details in the text (Adapted from Wang et al., 2009).

## **1.7 Role of TLRs in human disease**

Different mutation of the TLRs and many experimental models have revealed the significance of TLRs in susceptibility to infection and their involvement in the pathogenesis of a number of non-infective inflammatory disorders such as cancer, allergy, autoimmunity, inflammatory bowel disease and atherosclerosis (Montero and Martin, 2009). For example, a clear role for TLR4 in sepsis, rheumatoid arthritis (RA) and allergy is documented (O'Neill et al., 2009; Shotorbaniet al., 2011). TLR2 has been implicated in similar pathologic conditions and also in systemic lupus erythematosus (SLE) and tumor metastasis. Also, TLR7 has also been implicated in SLE (O'Neill et al., 2009; Shotorbaniet al., 2011).

Atherosclerosis is considered as a disease whereby excessive inflammation of endothelium and smooth muscle cells of the artery wall is evident. The TLRs have been reported to participate in the initiation and development of atherosclerosis (Schoneveld et al., 2008). Specifically, increased TLR2 and TLR4 mRNA expression in atherosclerotic plaques and on circulating blood cells during atherosclerotic lesion development was reported (Curtiss and Tobias, 2009; Schoneveld et al., 2008). Moreover, other reports have suggested that polymorphisms in the human TLR4 gene are associated with the development and progression of atherosclerosis (Kiechl et al., 2002). TLR dysregulation has been reported in patients with inflammatory bowel disease (IBD). Pathophysiological features of IBD include uncontrolled excessive inflammation in the gastrointestinal mucosa and the upregulation of proinflammatory and T cell cytokines. While TLR3 expression was reported to be downregulated, TLR4 expression was upregulated during the IBD (Cario and Podolsky, 2006). Results have also suggested that TLR2 and its co-receptors TLR1 and TLR6 are involved in the initial immune response to bacteria in the pathogenesis of IBD (Pierik et al., 2006).

Functional TLRs are expressed in a wide variety of tumours and evidence suggests that TLR signalling pathways in tumours may be associated with subversion of host defense in favour of the neoplastic process (Huang et al., 2008). It is suggested that activation of tumoral TLRs induces the synthesis of proinflammatory factors and immunosuppressive molecules. These enhance the resistance of tumour cells to cytotoxic lymphocyte attack and facilitate their evasion or, may promote proliferation and survival of

tumour cells by inducing the release of cytokines such as IL-6, IL-13, TNF- $\alpha$  and other growth factors (Huang et al., 2005). Moreover, it has been reported that TLRs induce resistance to apoptosis, increase angiogenesis and vascular permeability, and enhance tumour cell invasion by regulating metalloproteases and integrins. (Huang et al., 2008; Wang et al., 2003). Other studies have directly demonstrated that NF- $\kappa$ B plays a pivotal role in TLRs-induced tumourgenesis when TLRs are activated by their ligand, as constitutively active NF- $\kappa$ B is often found in a number of human malignancies ((Palayoor et al., 1999; Pikarsky et al., 2004). However, there are studies suggesting that TLR3 triggers apoptosis of human prostate cells and breast cancer cells. Because apoptosis may be a potent mechanism of eliminating tumor cells, these results suggest that TLR3 or TLR3 ligands may be very useful tool for cancer therapy (Salaun et al., 2006; Paone et al., 2008). SLE is a complex chronic inflammatory disease that arises spontaneously and can affect the skin, joints, kidneys, lungs, nervous system, and other organs (Marshak-Rothstein, 2006). Nucleic acid-sensing TLRs (TLR3, 7, 8 and 9), particularly TLR7, have been implicated in SLE and are thought to exacerbate the disease pathology. Single nucleotide polymorphism analyses as well as experimental mouse models have shown that TLRs are involved in SLE. Regarding the role of TLRs in SLE, it has been proposed that TLRs may be stimulated by exogenous antigens, like viral ssRNA, which then stimulate resident immune cells, or the TLRs may recognise endogenous self-antigens, thus initiating and propagating inflammation and autoimmunity (Montero and Martin, 2009; Horton et al., 2010). The involvement of the TLRs in such disease makes them important targets for the development of new vaccines and innovative therapies to prevent and treat human diseases.

RA is a chronic autoimmune disease that is characterised by inflammation of the synovial joints, which leads to joint destruction (McCormack et al., 2009; Shotorbaniet al., 2011). Roelofs et al. (2005) showed that TLR2, TLR3, TLR4 and TLR7 expression was markedly increased in synovial tissue from RA patients, compared with synovial tissue from healthy controls. Moreover, DCs from RA patients have been shown to produce increased levels of the pro-inflammatory cytokines TNF- $\alpha$  and IL-6 upon engagement of TLR2 or TLR4, but not TLR3 and TLR7 (Roelofs et al., 2005). Other studies have shown that inhibition of TLR4 suppresses the severity of experimental arthritis and results in lower IL-1 expression in arthritic joints (Abdollahi-Roodsaz et al., 2007). In addition, clinical and

histopathological evaluation of IL-1/TLR2 deficient mice revealed that they presented with a more severe arthritis when compared to wild-type counterparts. In contrast, IL-1/TLR4 deficient mice were protected against severe arthritis and had markedly lower numbers of Th17 cells and a reduced capacity (Abdollahi-Roodsaz et al., 2008).

## **1.8 Project Aims**

The present available knowledge regarding how TRIF activate and transmit TLR signalling pathways is much less compared to MyD88-dependent signalling pathways. As mention earlier, TLRs activation has been linked to the pathogenesis of infectious disease, tumor growth and rheumatoid arthritis. Specifically the TRIF pathways have been shown to have a close tie with these diseases (Ouyang et al., 2007, Shotorbaniet al., 2011). Nevertheless, better understanding of the TRIF signalling pathways would be therapeutically useful for the development of vaccines and treatments that could control disease associated inflammations and anti-viral responses. Therefore, the main objectives of this project were:

1. To characterise the time dependent association of known/unidentified proteins with TRIF.
2. To identify possible differential association of proteins with TRIF following TLR3 versus TLR4 ligand engagement.
3. To functionally characterise selected novel TRIF interacting molecules towards a greater understanding of TRIF signalling following TLR3/4 ligand engagement.

## **Chapter 2**

### **General Materials and Methods**

## **2.1 General Materials**

See Appendix 2.

## **2.2 Methods**

### **2.2.1 Cell culture techniques**

All mammalian cells were grown at 37 °C in a humid environment with 5 % CO<sub>2</sub> in the appropriate complete growth culture medium, DMEM or RPMI supplemented with 10 % (v/v) FBS 1 % (v/v) penicillin/streptomycin, 1 % (v/v) fungzone, and 1 % (v/v) Sodium Pyruvate. Specifically HEK293-TLR3 cells were cultured in complete DMEM containing 10 mg/ml blasticidin. HEK293-TLR4 cells were cultured in complete DMEM containing 10 mg/ml blasticidin and 100 mg/ml hygrogold. Human Astrocytoma U373-CD14 cell line was cultured in complete RPMI containing 250 µg/ml G418. Adherent cell monolayers were detached from tissue culture flasks using trypsin/EDTA, and split every 3-4 days at a ratio 1:5 or 1:10 depending on cell growth.

### **2.2.2 Cell stock freezing and resuscitation**

Adherent cells were trypsinised, re-suspended in full growth medium, and centrifuged at 380 g for 5 min. Pelleted cells were re-suspended in freezing medium (90 % (v/v) FBS, 10 % (v/v) DMSO) and aliquoted into cryovials. Cell stocks were frozen at -80 °C for 4 hours before long-term storage in liquid nitrogen. For resuscitation of the cells, cryovials were thawed at 37 °C, and cells were re-suspended in full growth medium before centrifugation at 380 g for 5 min. Medium was removed and cell pellet was then re-suspended and grown in complete growth medium (DMEM, 10 % (v/v) FBS, 1 % (v/v) penicillin/streptomycin, 1 % (v/v) fungzone and 1 % (v/v) Sodium pyruvate) at 37 °C in a humidified atmosphere of 5 % CO<sub>2</sub>. Cells were selected after becoming confluent in appropriate selection medium as mentioned earlier.

### **2.2.3 Transfection of cells with plasmid and esiRNA**

Transfection of cells with plasmid DNA was carried out using Lipofectamine 2000 transfection reagent (Invitrogen) according to the manufacturer's instructions. Transfection

of esiRNA was performed using DreamFect™ Gold (OZ Bioscience) according to the manufacturer's instructions.

#### **2.2.4 Transformation of competent cells**

Plasmid DNA (5 µl; ~100 ng) was added directly to 100 µl of thawed, *E. coli* DH5α competent cells (Invitrogen) and incubated on ice for 30 min. Thereafter, cells were transferred to a 40 °C heat block for 30 s before being immediately returned to ice for a further 2 min. Cells were re-suspended in 0.5 ml LB broth and incubated at 37 °C with gentle shaking for 1 hour. The microfuge tube was briefly centrifuged and the upper medium was removed. Approximately 100 µl of the transformed bacteria were plated out onto LB-agar plates supplemented with 100 µg/ml ampicillin. Plates were inverted and incubated at 37 °C overnight.

#### **2.2.5 Preparation of plasmid DNA**

Single colonies were inoculated into 5 ml of LB broth containing 100 µg/ml ampicillin at 37 °C with gentle shaking for 4-5 h. Thereafter, the inoculum was transferred to a conical flask containing 95 ml of LB broth and 100 µg/ml ampicillin and incubated overnight at 37 °C with gentle shaking. Bacterial cells were pelleted by centrifugation (380 g, 30 min at 4 °C). DNA was extracted from the cells using the High Speed Midi Kit as described by the manufacturer (QIAGEN). The DNA concentration determined using the NanoDrop ND-1000 spectro-photometer (Thermo Scientific).

#### **2.2.6 Glycerol stocks**

The transformed cells (600 µl) were mixed with 800 µl of 50 % glycerol in a cryovial and stored at -80 °C. The stocks were used to inoculate 100 ml liquid cultures as necessary.

#### **2.2.7 Sodium dodecyl sulphate polyacrylamide gel electrophoresis (SDS-PAGE)**

SDS-PAGE was performed based on Laemmli method and carried out using the mini-gel system (Biorad). Plates were first arranged in the relevant casting rig and the system was checked for leaks. 10 % acrylamide resolving gels were prepared based on the recipe given (Table 2.2.1) and topped with dH<sub>2</sub>O to ensure a flat surface, prevent drying and air bubbles

forming. The resolving gel was poured such that adequate provision was made to allow for the stacking gel to be poured. The resolving gel was let set for between 5-30 minutes. The 5 % stacking gel was prepared as described (Table 2.2.2). The dH<sub>2</sub>O was decanted from the gel. The stacking gel was then poured followed by placing the appropriate spacer comb in the gel to form the loading well and the stacking gel was allowed to polymerise for between 5-30 minutes. The comb was then removed from the gel and the gel was transferred from the casting rig to the electrophoresis chamber (Biorad). The chamber was then filled with 1x running buffer (Table 2.2.4). The samples to be analysed were then mixed with 5x loading buffer (Table 2.2.5), followed by boiling at 100 °C for 5 min prior to the loading in the wells. Routinely, precision plus dual colour standards protein marker (Bio-Rad) was loaded and served as molecular weight reference. Electrophoresis was performed at 100 V for 2-3 h. Gels were then carefully removed from electrophoresis chamber and casting rig and the 5 % stacking gel was cut away and discarded. The gels were then stained or subjected to western blot.

### **2.2.8 Western blot**

Proteins were transferred to polyvinylidene difluoride membrane (PVDF; Millipore), using a wet transfer apparatus. Briefly, PVDF membranes were first activated by soaking them in methanol for 1 min followed by washing in 1x transfer buffer (Table 2.2.7). The gels and the membranes were sandwiched between wet sponge and papers, (sponge, papers, gel, membrane, papers, sponge). All sandwiches were clamped tightly after ensuring that there is no air bubbles between the gel and the membrane. The sandwiches were then placed in the transfer chamber (Fisher Scientific), and the chamber was filled with 1x transfer buffer (Table 2.2.7). Transfer was carried out at 200 mA for 1.5 h or overnight at 30 mA. The PVDF membrane were then blocked in 5 % (w/v) fat free dry milk in TBST for at least 1 h at RT, and then washed with TBST (Table 2.2.9). Primary antibodies were diluted in 5 % (w/v) fat free dry milk in TBST or 5 % (w/v) BSA in TBST. Membranes were then incubated overnight at 4 °C with primary antibody at an appropriate dilution on a roller. After multiple washes with TBST, the membrane was incubating with a horseradish peroxidase (HRP)-conjugated secondary antibody raised against the appropriate species, diluted (1:2000) in 5% (w/v) fat free dry milk in TBST for 1 h. Unbound antibody was

washed away with TBST and specific polypeptide bands were visualized using supersignal westdura (Fisher) and then images were captured using the GeneSnap acquisition and GeneTools analysis software, (GeneGenius Gel Documentation and Analysis System; Syngene).

### **2.2.9 Immunoprecipitation of HA-TRIF**

HEK293-TLR3 and HEK293-TLR4 were plated into 6 well plates. After 24 h, cells were co-transfected with the indicated plasmid using Lipofectamine 2000 (Invitrogen) according to the manufacturer's instructions. The total amount of DNA (3 µg/well) was kept constant by the addition of empty vector. After 20 h, the transfected cells were stimulated with the TLR ligands (20 µg/ml poly(I:C) HEK293-TLR3 or 1 µg/ml LPS HEK293-TLR4) for the indicated time. The cells were lysed in 600 µl of lysis buffer (50 mM HEPES, pH 7.5, 150 mM NaCl, 2 mM EDTA, pH 8.0, 1 % NP-40, 0.5 % sodium deoxycholate supplemented with 1 mM PMSF, 1 mM DDT, 1 mM NaVO<sub>3</sub>, (5mM EGTA for co-IP TRIF and ADAM15) and protease inhibitor cocktail) and left on ice for 20 min. The lysates were subjected to centrifugation for 5 min (15620 g at 4 °C) to remove cell debris. Next, 1 µg of mouse monoclonal anti-HA antibody (Covance) was incubated with 50 µl A/G Plus-agarose beads (Santa Cruz) overnight at 4 °C with gentle shaking. Cleared cell lysates were mixed with the beads and incubated for 2 h at 4 °C with gentle shaking. Immunoprecipitated complexes were washed at least 4 times with lysis buffer followed by centrifugation for 2 min at 220 g. Proteins were resolved from the beads by the addition of 40 µl of loading buffer, followed by boiling for 5 min. Thereafter, samples were separated by SDS-PAGE gel electrophoresis followed by staining or immunoblot analysis.

### **2.2.10 Immunoprecipitation of endogenous TRIF**

Human astrocytoma U373-CD14 cells were plated onto T175 flasks. When the cells become confluent (90-95 %), cells were stimulated with 20 µg/ml poly(I: C) or 1 µg/ml LPS for different time points as indicated. After that the medium was removed from the cells and cells were scraped in 10 ml of ice-cold PBS and centrifuged for 10 minutes (220 g at 4 °C). Cells were lysed in 600 µl of lysis buffer (50 mM HEPES, pH 7.5, 150 mM NaCl, 2 mM EDTA, pH8.0, 1 % NP-40, 0.5 % sodium deoxycholate supplemented with 1 mM

PMSF, 1 mM DDT, 1 mM NaVO<sub>3</sub>, (5 mM EGTA for co-IP TRIF and ADAM15) and protease inhibitor cocktail) and left on ice for 20 min. The lysates were subjected to centrifugation for 5 min at 15620 g at 4 °C to remove cell debris. Next, precoupling of the antibody to beads was performed by incubating 2 µg of anti-TRIF polyclonal antibody (Exalpa) with 50 µl slurry of Protein A/G Plus–agarose (Santa Cruz) overnight at 4 °C with gentle shaking. Next, 500 µl of the cleared cell lysates was added to the precoupled beads and incubated at 4 °C for 2 h with gentle shaking. The beads were washed 4 times with lysis buffer. Immunoprecipitated complexes were separated by SDS-PAGE and subjected to immunoblotting.

### **2.2.11 Silver staining**

After electrophoresis, gels were placed into fixing solution (30 % (v/v) ethanol, 10 % (v/v) acetic acid) for a minimum of 30 min. The gels were then rinsed in 20 % (v/v) ethanol twice for 10 min, which was followed by washing twice in milliQ dH<sub>2</sub>O (10 min per wash). The water was removed and sensitising solution (0.8 mM sodium thiosulfate) was poured onto the gels for one min after which the gels were once again washed twice in milliQ dH<sub>2</sub>O (2 min per wash). The gels were then stained with staining solution (12 mM silver nitrate) for 20 min to 1 h. After the staining solution was removed, the gels were washed in milliQ dH<sub>2</sub>O for 10 s. Next, the developing solution (0.04 % (v/v) formaldehyde in 3 % (w/v) sodium potassium carbonate) was added to the gel. Once the protein bands were visualised, the gels were placed in stop solution (2 % (v/v) acetic acid in 0.3 M TRIS) for storing.

### **2.2.12 Gel de-staining and sample preparation for Mass Spectrometry (MS)**

Bands from a 1D gel protein gel were excised from the control and experimental lanes and placed into siliconised 1.5 ml Eppendorf tubes (Sigma-Aldrich). Silver-stained proteins were destained with chemical reducers to remove the silver. The reactive substances of the chemical reducers were potassium ferricyanide and sodium thiosulfate. These chemical agents were prepared prior to digestion as two stock solutions of 30 mM potassium ferricyanide and 100 mM sodium thiosulfate, both dissolved in water. A working solution was prepared by mixing a 1:1 ratio of the above stock solutions. This working solution was

unstable, and therefore had to be prepared fresh for each reaction. Working solution (50  $\mu$ l) was added to cover the gel plugs and occasionally vortexed. The stain intensity was monitored until the brownish colour disappeared, then the gel plugs were rinsed a few times with water to stop the reaction. Cysteine residues were reduced and alkylated using DTT and Iodoacetamide (IAA) as follows. Briefly, 50  $\mu$ l 10 mM DTT (in 100 mM  $\text{NH}_4\text{HCO}_3$ ) was added to each tube followed by shaking at 56  $^\circ\text{C}$  for 1 h. The tubes were centrifuged briefly and the solution was removed and 50  $\mu$ l of 50 mM IAA (in 100 mM  $\text{NH}_4\text{HCO}_3$ ) was added and incubated for 30 min in the dark at RT with gentle agitation. After brief spinning the solution was removed and gel plugs were washed with sequential additions of ammonium bicarbonate ( $\text{NH}_4\text{HCO}_3$ ) and acetonitrile (ACN). First, 300  $\mu$ l of 100 mM  $\text{NH}_4\text{HCO}_3$  was added to each tube and incubated for 15 minutes at 37  $^\circ\text{C}$  with gentle agitation, followed by addition 1:1 of 20 mM  $\text{NH}_4\text{HCO}_3$ /ACN for 15 min at 37  $^\circ\text{C}$  with gentle agitation. Finally, the gel pieces were dehydrated in 100 % ACN for 10 min at 37  $^\circ\text{C}$  with gentle agitation. Samples were digested with 4 ng/ $\mu$ l trypsin (Promega) at 37  $^\circ\text{C}$  overnight. Peptide were extracted using 2:1 ACN: 5 % (v/v) trifluoroacetic acid (TFA) for 15 min at 37  $^\circ\text{C}$  with gentle agitation, dried by vacuum centrifugation overnight at RT and stored -20  $^\circ\text{C}$  for subsequent MS analysis. On the day of MS analysis, samples were re-suspended in 20  $\mu$ l of 0.1 % TFA and centrifuged at 13680 g at 4  $^\circ\text{C}$  for 15 min, then filtered and centrifuged at 13680 g for 5 min at 4  $^\circ\text{C}$ . From each sample, 10  $\mu$ l was pipetted into MS vials (Agilent) for subsequent protein identification.

### **2.2.13 Ion Trap Mass Spectrometry**

The mass spectrometric analysis of peptides was performed at the Proteomics Suite of the Department of Biology, National University of Ireland Maynooth, using a Model 6340 Ion Trap LC/MS apparatus (Agilent Technologies). Peptides were separated using a nanoflow Agilent 1200 series system, equipped with a Zorbax 300SB C18 5  $\mu\text{m}$ , 4 mm 40 nl pre-column and an Zorbax 300SB C18 5  $\mu\text{m}$ , 43 mm x 75  $\mu\text{m}$  analytical reversed phase column using HPLC-Chip technology. The mobile phases utilised were A: 0.1 % formic acid, B: 50 % acetonitrile and 0.1 % formic acid. Samples (5  $\mu$ l) were loaded into the enrichment column at a capillary flow rate set to 4 ml/min with a mix of A and B at a ratio 19:1 (v/v). Tryptic peptides were eluted with a linear gradient of 10-90 % solvent B over 15 min with a

constant nano pump flow rate of 0.60 ml/min. The capillary voltage was set to 1900 V and the flow and the temperature of the drying gas were 4 l/min and 300 °C, respectively. A 1 min post time of solvent (A) was used to remove sample carry over. For protein identification, database searches were performed using the Mascot MS/MS Ion search (Matrix Science, London, UK). All searches used *Homo sapiens* (human) as taxonomic category and the following parameters: (i) two missed cleavages by trypsin, (ii) mass tolerance of precursor ion 1.2 Da and product ions 1 Da, (iii) carboxymethylated cysteine fixed modification, and (iv) oxidation of methionine as variable modification. Pathway studio software (Ariadne genomics) was used to visualize the interconnectivity between the identified protein hits and to make network interaction maps.

#### **2.2.14 RNA isolation using TRIZOL reagent**

Cells were seeded into 6 well plates and treated/transfected as required for the experiments. Thereafter, the medium were removed and cells were lysed in 1 ml of TRIZOL (Invitrogen) then 0.2 ml of chloroform (5:1 v/v chloroform) was added followed by mixing and incubation for 10 min at RT. The mixture was subjected to centrifugation at 15620 g for 15 min at 4 °C. After centrifugation, the mixture was separated into lower phenol-chloroform phase (red) and upper aqueous phase (colourless). RNA remained exclusively in the aqueous phase. Next, 500 µl of the upper aqueous phase was transferred into fresh tube, and RNA was precipitated by addition of 500 µl isopropyl alcohol. The mixture was incubated for 10 min at RT, followed by centrifugation at 15620 g for 15 min at 4 °C. The supernatant was removed and the RNA pellet was washed once with 500 µl 75 % ethanol and centrifuged at 13680 g for 5 min at 4 °C. The ethanol was removed and the pellet was air dried for 5 min at RT. The RNA was dissolved in 30 µl RNAase free water (Sigma), and the RNA concentration was measured using a NanoDrop ND-1000 spectrophotometer (Thermo Scientific). Samples were stored at -20 °C until required for first strand cDNA synthesis.

#### **2.2.15 First-strand cDNA synthesis**

Total cellular RNA (1 µg) was mixed with 1 µl of random hexamers primers (500 µg/ml) (Fisher scientific) and water to make a final volume of 17 µl. The mixture was incubated at 70 °C for 5 min. The mixture was then briefly centrifuged and chilled on ice for 2 min.

Next, 5  $\mu$ l of 5x reaction buffer, 1.3  $\mu$ l deoxynucleotides (10 mM dNTP), 0.7  $\mu$ l Rnase inhibitor and 1  $\mu$ l MMLV reverse transcriptase were then added to give a final reaction mix of 25  $\mu$ l. The cDNA synthesis was performed by incubation the reaction mixture in a thermocycler at 37 °C for 40 min followed by incubation at 42 °C for 40 min. Reactions were heat inactivated at 80 °C for 10 min then held at 4 °C. The samples were stored at -20 °C until required for PCR.

#### **2.2.16 PCR**

The first strand cDNA samples were diluted 1:5, then 3.5  $\mu$ l was used per PCR reaction. Next, 5  $\mu$ l of 5x reaction buffer, 2  $\mu$ l of 2.5 mM dNTP, 2  $\mu$ l of 25 mM MgCl<sub>2</sub>, 2.1  $\mu$ l H<sub>2</sub>O, 1.5  $\mu$ l of 20  $\mu$ M forward and reverse primers, 7.5  $\mu$ l of 50 % glycerol and 0.4  $\mu$ l of Taq DNA polymerase were then added to give a final reaction mixture of 25  $\mu$ l. The samples were placed in a Thermocycler (Eppendorf) and the samples were subjected to the following cycling conditions: (1) 95 °C, 3 min, (2) 94 °C, 1 min, (3) 60 °C, 30 s (4) 72 °C, 1 min (5) repeat 2 to 4 for 35 cycles, (6) 72 °C, 7 min (8) 80 °C, 10 min (9) hold at 4 °C. Samples were subjected to agarose gel electrophoresis.

#### **2.2.17 Real time PCR**

The cDNA samples were used as template and diluted 1:25, then 2.5  $\mu$ l was used per each reaction. Next, 2.5  $\mu$ l of 4  $\mu$ M of both forward and reverse primers, 2.5  $\mu$ l H<sub>2</sub>O and 10  $\mu$ l of Sybr green mater mix (2x) were added to give a final reaction mixture of 20  $\mu$ l. The reactions were performed in duplicate using an Opticon 2 Thermocycler (MJ Research), and the samples were subjected to the following cycling conditions: 15 min at 95 °C to denature the cDNA, followed by 37 cycles of (1 min at 94 °C, 15 s at 60 °C to permit primer annealing, followed by 30 s at 72 °C for elongation). The melting curve from 65 °C to 95 °C was recorded every 1 °C.

#### **2.2.18 Agarose gel electrophoreses**

Agarose gels were prepared by adding appropriate amount of agarose (depending on the required concentration) to TAE (0.04 M Tris-acetate, 1 mM EDTA, pH 8.0) and microwaving until the agarose melted. The molten agarose was allowed to cool down, then

mixed with 1:10000 dilution of Sybr safe DNA gel Stain (Invitrogen). The agarose was poured into a casting tray and a plastic comb was inserted to create the wells and then allowed to solidify. The plastic comb was removed and the agarose gel was placed into the electrophoresis unit (Hoefer Scientific Instruments). The gel was then covered with TAE running buffer. Next, 15  $\mu$ l of the RT-PCR product was loaded into the well. A voltage of 100 V was applied to the gel apparatus until sufficient separation was obtained. The DNA gel bands were visualized and photographed using the G:box documentation system (Syngene).

### **2.2.19 Reporter assays**

HEK293-TLR3 and HEK293-TLR4 cells were seeded into 96 well plates ( $5 \times 10^4$  cells/well). After 24 h, cells were co-transfected with vectors encoding either a reporter gene for the IFN $\beta$  promoter (p125), IFN $\beta$  PRDII, IFN $\beta$  PRDIII, NF- $\kappa$ B, or Rantes promoter (80 ng/well) and either empty vector or increasing amounts of an expression vector encoding full length V5-ADAM15, Myc-DVL1 Myc-DVL2, Myc-DVL3, and Optineurin as indicated using lipofectamine 2000 (Invitrogen) according to the manufacturer's instructions. A total of 40 ng/well Renilla-luciferase reporter gene was transfected simultaneously as an internal control. After 24 h, HEK293-TLR3 were stimulated with 20  $\mu$ g/ml poly(I:C) and HEK293-TLR4 were stimulated with 1  $\mu$ g/ml LPS for additional 24 h. Thereafter, cell lysates were prepared and reporter gene activity was measured using the Dual-Luciferase Assay system (Promega). Data were expressed as the mean fold induction relative to the control. HEK-293T cells were seeded into 96 well plates ( $5 \times 10^4$  cells/well). After 24 h, cells were co-transfected with vectors encoding either a reporter gene for the IFN- $\beta$  promoter (p125), IFN $\beta$  PRDII, IFN $\beta$  PRDIII, NF- $\kappa$ B, or Rantes (80 ng/well) and either empty vector or vector encoding full length HA-TRIF or, vector encoding full length Myc-MyD88 (20 ng/well) and increasing amounts of an expression vector encoding V5-ADAM15, Myc-DVL1, Myc-DVL2, Myc-DVL3, and Optineurin as indicated using lipofectamine 2000 (Invitrogen) according to the manufacturer's instructions. A total of 40 ng/well Renilla-luciferase reporter gene was transfected simultaneously as internal control. After 24 h, cells were harvested and cell lysates were prepared followed by assessment of

reporter gene activity using the Dual-Luciferase Assay system. (Promega) Data were expressed as the mean fold induction relative to the control.

### **2.2.20 Enzyme-Linked Immunosorbent Assay (ELISA)**

Microtitre plates (Fisher Scientific) were coated with appropriate capture antibody (1 µg/ml for TNFα and Rantes, 2 µg/ml for IL-6) overnight at RT. The following day, the plates were washed three times with wash buffer (PBS containing 0.05 % (v/v) Tween-20) followed by blocking with blocking buffer (PBS containing 1 % BSA) for at least 2 h. The plates were then washed three times with wash buffer. Next, serial dilutions of the standards (ranging from 0 to 4000 pg/ml; 100 µl/well) and the samples were added (100 µl/well) followed by incubation at 4 °C overnight. Next day, the plates were washed three times with the wash buffer followed by the addition of the appropriate detection antibody (0.2 µg/ml for IL-6, 0.25 µg/ml for Rantes and 0.5 µg/ml for TNFα) for 2 h at RT. The plates were washed three times with the wash buffer followed by the addition of the streptavidin-HRP conjugate antibody (1:2000 for Rantes and TNFα; 1:200 for human IL-6) for 30 min. Thereafter, the plates were washed three times with the wash buffer followed by the addition of the substrate. Plates were incubated at RT for 5 min with gentle shaking. The absorbance was measured at 450 nm using a BioTek plate reader.

### **2.2.21 Meso Scale Human 7-Plex / MMP 3-Plex / IFN-β / RANTES Assay**

Levels of IFN-γ, IL-10, IL-12 p70, IL-1β, IL-6, IL-8, and TNFα in cell free supernatants were measured using a Meso Scale 96-Well plate Human 7-Plex ultra-sensitive assay kit or a Meso Scale MMP 1, MMP 3, and MMP 9 96-Well MMP 3-plex ultra-sensitive assay kit (Meso Scale Discovery (MSD)). Levels of IFN-β and RANTES were measured using a Single Plex assay kit (Meso Scale Discovery). The human single/multiplex assay detected the respective cytokine/chemokines/MMPs in a sandwich immunoassay format. MSD supplied a 96 well ultra-sensitive plate precoated with the respective cytokine /chemokine/MMP capture antibodies on spatially distinct spots on the plate. First, the pre-coated single/multiplex plate was incubated for 30 min at RT with 25 µl/well of Diluent 2 with vigorous shaking. Next, the cell free supernatants or appropriate dilution of the calibrator (highest calibrator point was obtained by diluting the stock calibrator 10-fold in

Diluent 2 and from this an 8 point standard curve with a 4-fold serial dilution was prepared- assay range 500,000 to 0 pg/ml (MMP3-multiplex), 2500 to 0 pg/ml (7 multi plex and Rantes), 25000 to 1.5 pg/ml for IFN $\beta$ ) were added to the appropriate wells of the MSD plate in duplicate. The plate was sealed with an adhesive seal and incubated for 2 h with vigorous shaking at RT. Next, the plate was washed three times with wash buffer (PBS, 0.05 % Tween 20 (PBST)) and was pat dry. Next, the working concentration of Sulfo-tag detection antibody was prepared as followed. Briefly, the 50x stock sulfo-tag was diluted to a final working concentration of 1x by adding 60  $\mu$ l of the stock to 2.94 ml of Diluent 3 supplied with the kit. Next, 25  $\mu$ l of the 1x working concentration of Sulfo-tag detection antibody was added to each well of the MSD plates followed by sealing of the plates and incubation for 2 h at RT with vigorous shaking. Next, the plates were washed three times with PBST followed by the addition of 150  $\mu$ l/well of 2x Read Buffer T to each well of the MSD plates. Analysis of the plates was performed using a SECTOR Imager and data analysis was performed using the MSD Discovery Workbench analysis software.

#### **2.2.22 Immunofluorescence**

Cells were cultured on Collagen precotaed glass coverslip into 6-well plates. After 24 h, cells were transfected with the indicated plasmids. After 24 h, cells were stimulated as indicated or left untreated (control). Thereafter, cells were washed with PBS and fixed in 4 % para- formaldehyde for 10 min. Cells were permeabilised using 0.5 % Triton X-100 in PBS for 5 min followed by blocking for at least 1 h in blocking buffer (1 % BSA in PBS with 0.05 % (v/v) Tween-20). Next, primary antibodies were diluted (1:50) in the blocking buffer and vortexed well followed by centrifugation for 3 min at 15620 g. Next, 200  $\mu$ l of the primary antibody was added to each coverslip followed by incubation for 2 h at RT. Thereafter, cells were washed three times (10 min/wash) with wash buffer (PBS containing 0.05 % (v/v) Tween 20). The Alexa fluor secondary antibodies were diluted 1:200 in the blocking buffer, vortexed and centrifuged for 3 min at 15620 g. Then, 200  $\mu$ l of the diluted secondary antibody mix was added to the coverslip followed by incubation for 1 h at RT in the dark. Unbound antibodies were removed by washing the coverslips with wash buffer. Next, the nuclei was stained with DAPI dye (10  $\mu$ g/ml) in PBS for 5 min at RT in the dark. Coverslips were then washed with PBS, mounted on glass slides using Vectashield

mounting solution (Vector laboratories) and stored in the fridge until analysed. Images were captured using an Olympus 1000 confocal microscope and analysed using fluoview software.

### **2.2.23 Statistics**

Statistical analyses were performed using Graphpad Prism 4 software. Differences were analysed using one-way and two-way ANOVAs and t-test.

## **Chapter 3**

### **Proteomic analysis of the TRIF interactome**

### 3.1 Introduction

Proteins interact with each other in a highly specific manner, and protein interactions play a key role in many cellular processes. Identifying and characterising protein-protein interactions and their networks is essential for understanding the mechanisms of biological processes on a molecular level and is also a useful tool for identifying novel disease markers (Schoemaker et al., 2007). There are many approaches that allow the identification of interacting partners including, the yeast two hybrid system, immunoprecipitation pull down assay (IP), chromatin immunoprecipitation (ChIP), in vivo fluorescence resonance energy transfer (FRET) and antibody arrays or protein chips (Yan and Chen, 2005; Byrum et al., 2011; Bailey et al; 2012).

Proteomics has emerged as a field for studying global gene expression profiles at the protein level. In general, proteomics involves the identification of protein components and the measurement of protein abundance in biological systems such as cultured cells or tissue samples. The most popular use of the proteomic technology is the identification of protein complexes (Zhou and Veenstra, 2007). Currently, mass spectrometry (MS) has been overwhelmingly applied as the technology base for proteomics analysis. Proteins have been identified and quantified by characterisation of their derived peptides using either electrospray ionisation (ESI) or matrix assisted laser desorption/ionisation (MALDI)-based MS (Yan and Chen, 2005; Chakravarti et al., 2002).

Isolating the protein complex is the most critical step in determining the success of the downstream proteomic analysis. While advances in technology have had a huge impact, sample preparation issues related to isolation of protein complexes remain a critical factor in determining the success of these studies (Zhou and Veenstra, 2007). IP of protein complexes followed by liquid chromatography and mass spectrometry (LC-MS) is a widely used method in proteomics research to identify proteins and to study protein-protein interactions. IP techniques allow purification of proteins of interest and reduce sample complexity before introduction to the mass spectrometer (Lin et al., 2003; Zhou and Veenstra, 2007). The effectiveness of IP experiments is an important factor for identification of proteins and protein-protein interactions (Yang et al., 2009; Li et al., 2011).

As mentioned in Section 1.5.3, TRIF plays an important role in TLR3 and TLR4 signalling pathways. Recent studies revealed that TRIF also involved in TLR2 and TLR5. However, the knowledge about how TRIF mediated TLR signalling and whether TRIF play another role in other signalling pathways is not fully understood. Analysis of TRIF intercome could lead to identification of novel TRIF interacting partners which will improve our knowledge about TRIF signalling. Therefore, it is of interest in this Chapter to use different strategies (Figure 3.1) to (1) characterise time dependent association of known-unknown proteins with TRIF and to (2) identify possible differential association of proteins following TLR3 and TLR4 ligand engagement.

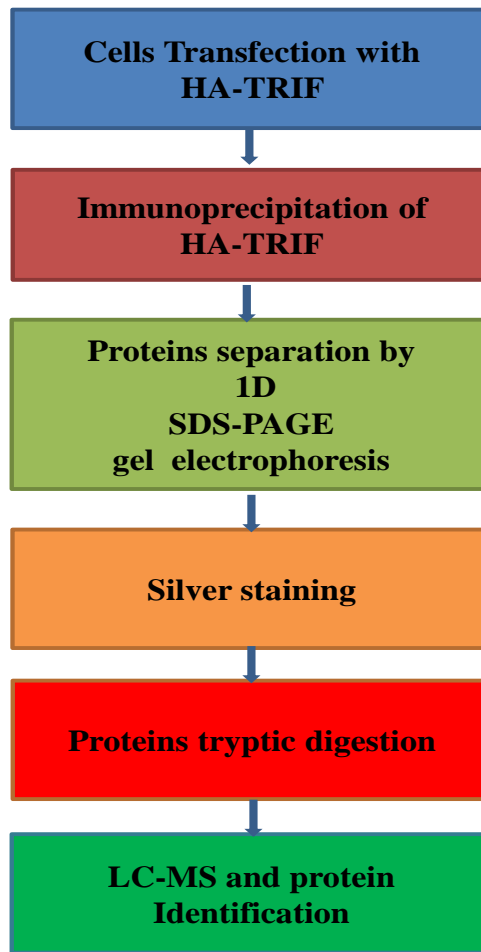


**Figure 3.1: Strategy adopted to identify TRIF binding partners.** HEK293-TLR3 and HEK293-TLR4 cells were transfected with TRIF-HA for 20 h. Next, cells were stimulated with 20  $\mu\text{g/ml}$  poly(I:C) (HEK293-TLR3) or 1  $\mu\text{g/ml}$  LPS (HEK293-TLR4). Thereafter, cells were collected and immunoprecipitation of HA-TRIF was performed using 1  $\mu\text{g/ml}$  of anti-HA antibody. Proteins were separated by SDS-PAGE and then the gels were silver stained. Visualized proteins band were cut in small pieces, destained and tryptic digested followed by protein identification using LC-MS analysis.

## 3.2 Results

### 3.2.1 Immunoprecipitation of HA-TRIF

To identify the proteins that interact with TRIF in a ligand and time dependent manner, HEK293-TLR3 and HEK293-TLR4 cells were transfected with HA-TRIF. After 20 h, cells were stimulated with the indicated ligand for the appropriate time followed by immunoprecipitation of HA-tagged TRIF. Correlating with previous report (Han et al., 2004), TRIF overexpression caused cell death therefore experimental optimisation was required to achieve optimal TRIF expression with minimal cell death. It was found that transfection of cells in a 10 cm dish with 1-3  $\mu\text{g}$  of TRIF resulted in minimal cell death, but TRIF expression was barely detectable. In contrast, transfection of cells with 5-10  $\mu\text{g}$  of TRIF resulted in massive cell death. It was consistently found that the optimal expression of TRIF with minimal cell death was achieved by overexpressing 3  $\mu\text{g}$  of HA-TRIF into one well of a 6-well plate followed by cell harvesting 20 h after transfection. Thus, HEK293-TLR3 and HEK293-TLR4 were transfected with 3  $\mu\text{g}$  of HA-TRIF or empty vector (EV) as negative control into one well of a 6-well plate. After 20 h, cells were left untreated or stimulated with 20  $\mu\text{g}/\text{ml}$  poly(I:C) (HEK293-TLR3) or 1  $\mu\text{g}/\text{ml}$  LPS (HEK293-TLR4) for 20, 40 and 60 min, in duplicate to ensure adequate protein recovery. Thereafter, the cells were collected and TRIF IP was performed as described (Materials and methods, Section 2.2.9). It was evident that HA-TRIF expression was achieved in both cell types (Figure 3.2, panels A and C) at all-time points. It must be noted that whilst the predicted molecular weight of TRIF is 76-78 kDa, routinely, in the current study, HA-TRIF was detected at approximately 100 kDa. This finding concurs with Dansako et al. (2009) who showed that overexpressed TRIF was detected at 102 kDa. Alterations in electrophoretic mobility may be attributed to post translational modification of TRIF, such as phosphorylation. An aliquot of the protein sample was subjected to SDS-PAGE followed by silver staining to visualise the protein bands (Figure 3.2, panels B and D). Each gel lane was cut into 24 gel pieces, followed by in-gel tryptic digestion and LC-MS analysis as described (Materials and methods, section 2.2.12). It is clear that many of the proteins detected were nonspecific since they also appeared in the control (EV). Further optimisation of the experimental procedure may be required to reduce nonspecific binding. However, this was beyond the scope of the current project. Herein, we opted to exclude any proteins that were identified by LC-MS in the EV lane.

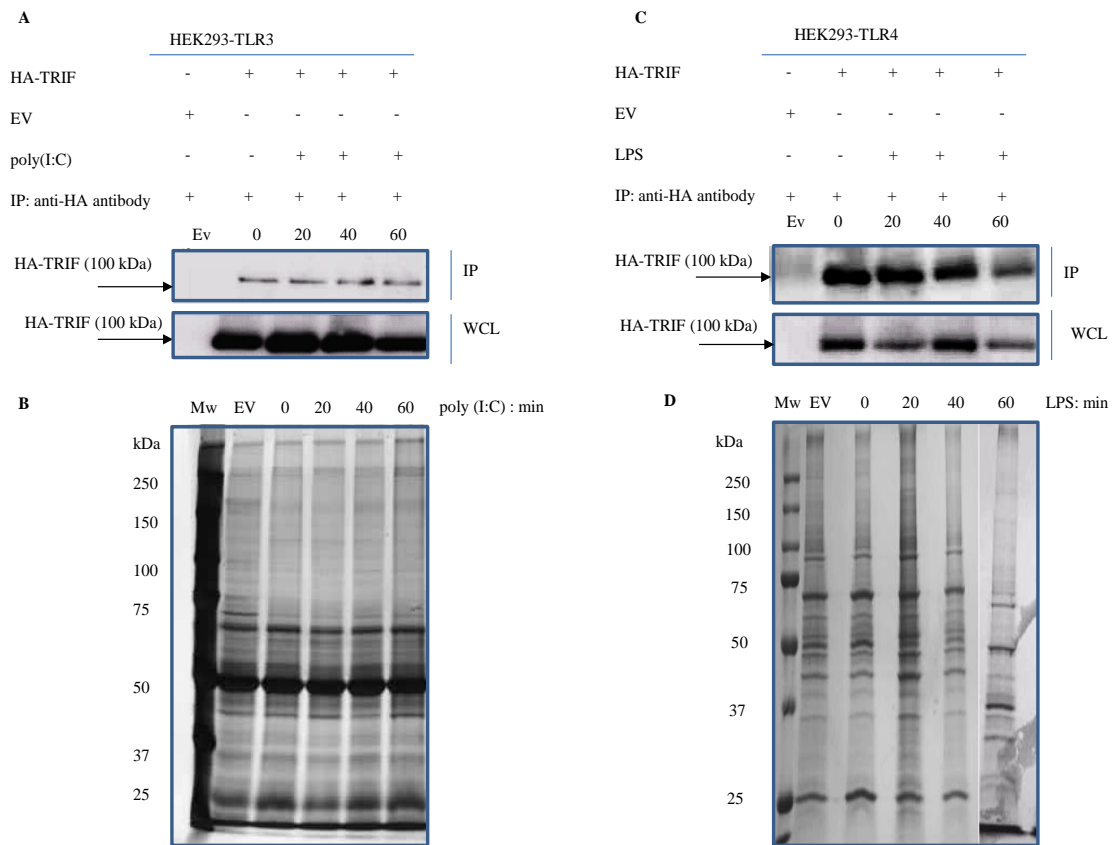


**Figure 3.2: Immunoprecipitation of HA-TRIF in HEK293-TLR3 and HEK293-TLR4.** (A, B) HEK293-TLR3 (C, D) HEK293-TLR4 were seeded into 6-well plates. When the cells were 80 % confluent, cells were transfected with 3  $\mu\text{g}/\text{well}$  of EV or 3  $\mu\text{g}/\text{well}$  of HA-TRIF. After 20 h, cells were left untreated or stimulated with 20  $\mu\text{g}/\text{ml}$  poly(I:C) (HEK293-TLR3) or 1  $\mu\text{g}/\text{ml}$  (HEK293-TLR4) for the times indicated. Thereafter, cells were collected and lysed in lysis buffer (50 mM HEPES, pH 7.5, 150 mM NaCl, 2 mM EDTA, pH 8.0, 1 % NP-40, 0.5 % sodium deoxycholate, supplemented with 1 mM PMSF, 1 mM DDT, 1 mM  $\text{NaVO}_3$ , and protease inhibitor cocktail). Cleared cells lysates were incubated with 1  $\mu\text{g}$  of anti-HA monoclonal antibody precoupled with 50  $\mu\text{l}$  A/G Plus-Agarose beads for 2 h at 4  $^\circ\text{C}$  with gentle shaking. Immunoprecipitated complexes were washed 4 times with lysis buffer, and proteins were released from the beads with the addition of 40  $\mu\text{l}$  Laemmli loading buffer. Immunoprecipitated proteins and whole cell lysates (WCL) were separated by SDS-PAGE and subjected to immunoblot analysis using an anti-HA antibody panel (A and C). To visualize protein bands for tryptic digestion and LC-MS analysis, gels were silver stained (B and D). Images were captured using a G:Box system (Syngene).

### **3.2.2 Identification of HA-TRIF interactors**

Gel plugs were destained followed by tryptic digestion as described (Materials and methods, section 2.2.12) and analysed using Agilent 6340 Ion trap LC-MS machine. The MS spectra of the peptide ions were identified using the Mascot software programme ([www.matrixscience.com](http://www.matrixscience.com)) to search against the publicly available NCBI nonredundant protein database ([www.ncbi.nlm.nih.gov](http://www.ncbi.nlm.nih.gov)). The results generated at each time point for each cell line was compared to the control (EV). Proteins which were similar to that identified in the control were excluded from further analysis and considered as unspecific binding. Proteins that interact with TRIF in a ligand independent manner and those that interact with TRIF in a poly(I:C) and LPS dependent manner are listed in the Appendix 1, Tables 3.1- 3.4 (HEK293-TLR3 cells) and Tables 3.5- 3.8 (HEK293-TLR4 cells), respectively. In general, it was found that many interactors were unique to either TRIF-dependent TLR3 or TLR4 signalling. Many other proteins were identified as being present in the TRIF immunocomplex, regardless of the ligand used to stimulate the cell or the time of stimulation, e.g., Prohibitin, Prohibitin2, Transgelin and Menin. The proteins that interact with TRIF following time dependent poly(I:C) and LPS stimulation will be described in more detail.

### **3.2.3 TRIF protein interaction networks**

A significant number of proteins were identified as TRIF interactors. To facilitate experimental data interpretation, a software package known as Pathway Studio 9.0 was utilised ([www.ariadnegenomics.com](http://www.ariadnegenomics.com)). The software package contextualises proteins in terms of signalling pathways, gene regulation networks and protein interaction maps, and also permits the filtration of proteins that may involve in regulating TLR signalling and innate immunity. The software comes with a built-in resource termed ResNet which includes over 800,000 unique relationships derived from over 19 million PubMed abstracts as well as 61 full-text journals. The ResNet database also contains a collection of reference pathways comprise a large number of receptor signalling pathways and cellular process pathways. The proteins that were identified as TRIF interactors were selected and details (Swissprot number) of the selected proteins were uploaded to the Pathway Studio programme. Next, the relationships between the various proteins were defined using various parameters including direct interactions, common targets and cell

process menus. In all cases, TRIF (termed TICAM-1 within the Pathway Studio Software) was included in each list as it was not identified by MS.

### **3.2.3.1 poly(I:C)-independent TRIF interactors**

Following the identification of proteins that interact with TRIF in a ligand independent manner, the protein identities were uploaded to the Pathway Studio software program. A direct interaction network of the proteins that co-immunoprecipitated with TRIF independent of poly(I:C) stimulation in HEK293-TLR3 was generated (Figure 3.3). A direct regulation between phosphatidylinositol-3-kinase regulatory subunit beta (PIK3CB) and Nibrin (NBN) was found. However, the other identified proteins were not found to interact directly with each other. With regard to the identified proteins, the common targets network indicated that both TRIF and the newly identified proteins were involved in the regulation of mitogen activated protein kinases (MAPKs), inhibitor of nuclear factor kappa-B kinase subunit beta (IKBKB), NF-kappa-B inhibitor alpha (NFKBIA), caspase-3, (CASP3), caspase-1, (CASP1), transforming growth factor beta (TGFB1), the estrogen receptor 1 (ESR1) and apoptosis regulator BCL-2 (Figure 3.4). These data showed that both TRIF and PIK3CB are involved in regulation of anti-apoptotic BCL-2 protein. This finding correlates with a previous study showing that BCL-2 interacts with Beclin1, a key component of the PI3 kinase complex that initiates autophagosome and leads to autophagy inhibition (Pattingre et al., 2005). Interestingly, it has been reported that TLR signalling enhances the interaction of TRIF and MyD88 with Beclin 1, and reduces the binding of Beclin 1 to BCL-2. These findings indicate that TLR signalling via its adaptor proteins reduces the binding of Beclin 1 to BCL-2 by recruiting Beclin 1 to the TLR-signalling complex leading to autophagy (Shi and Kehrl, 2008). Moreover, it was suggested that PI3K p110-beta stimulates tumour growth by regulating BCL-2 expression, as knockdown of PI3K p110-beta by siRNA decreased BCL-2 protein expression (An et al., 2007). Furthermore, it was found that TRIF and the newly identified proteins serve to modulate various cellular processes such as the inflammatory response, immunity, innate immune response, phagocytosis, autophagy, viral reproduction and cytokine production (Figure 3.5). Notably, many of the newly identified proteins are strongly linked with the modulation of apoptosis and this is supported by previous studies showing that TRIF is critically involved in mediating apoptosis through caspase-8 (Han et al., 2004). Interestingly, caspase-8 has been shown

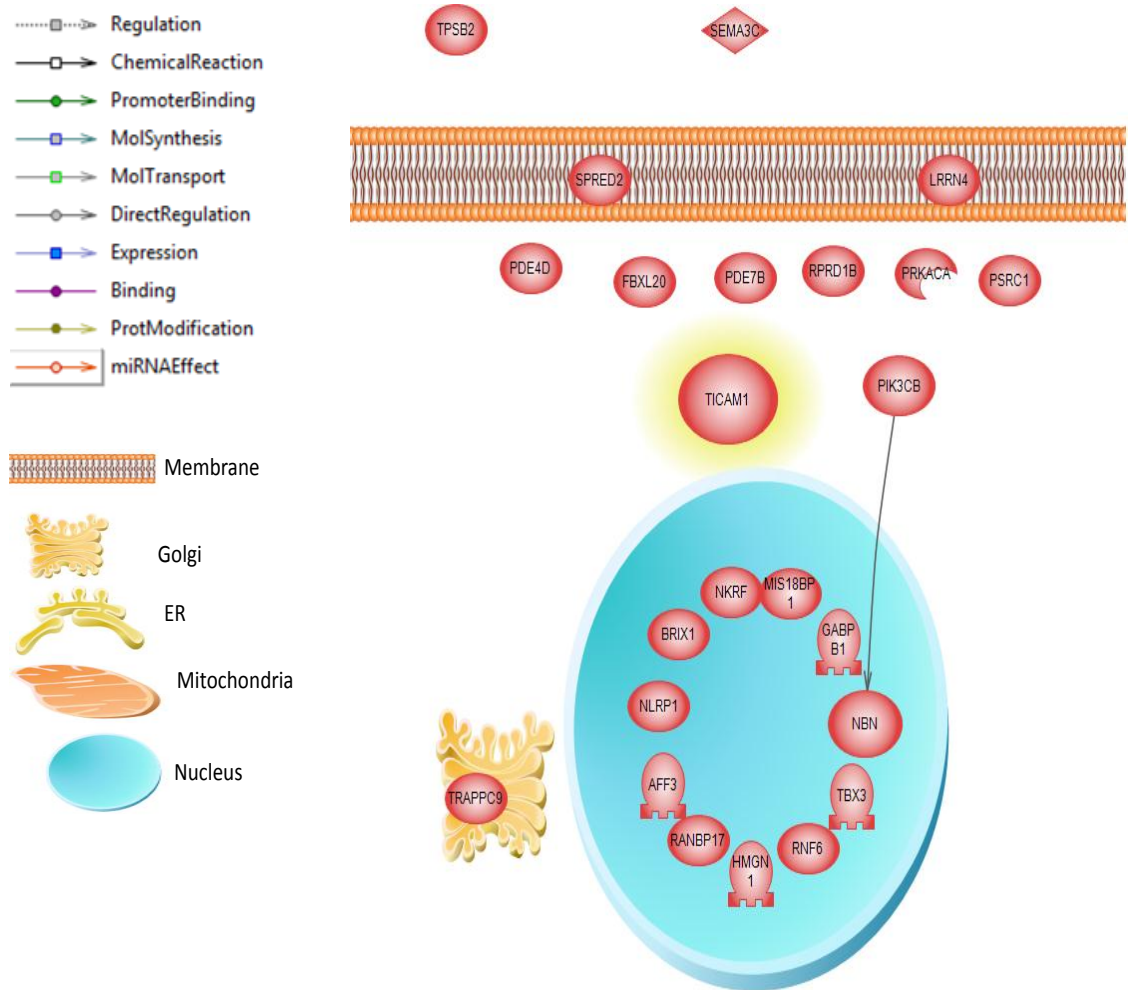


**Figure 3.3: Direct interactions network of poly(I:C)-independent TRIF interacting proteins.** HEK293-TLR3 cells were transfected with HA-TRIF. After 20 h, the cells were collected and IP of HA-TRIF was performed. Next, the TRIF IP-complex was analysed using the LC-MS. The newly identified protein interactors were uploaded to the Pathway Studio software analysis program and direct interaction network was made. Red entities indicate proteins that were identified following IP of HA-TRIF. TRIF (Ticam-1) is indicated in red with yellow surround. The grey solid line indicates the direct regulation of NBN by PIK3CB.

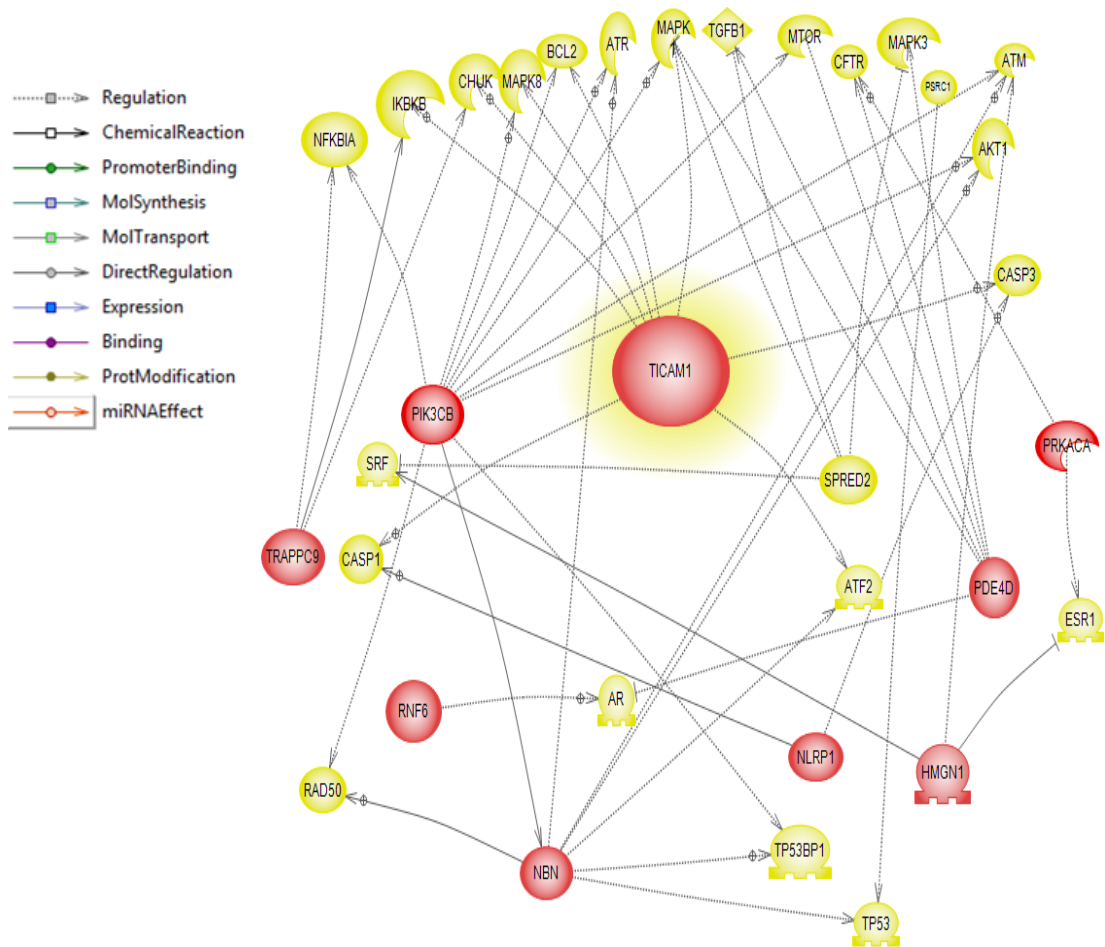


**Figure 3.4: Common targets network of poly(I:C)-independent TRIF interacting proteins.** HEK293-TLR3 cells were transfected with HA-TRIF. After 20 h, the cells were collected and IP of HA-TRIF was performed. Next, the TRIF IP-complex was analysed using the LC-MS. The newly identified protein interactors were uploaded to Pathway Studio software analysis program and common targets network was constructed. Red entities are the proteins identified following IP and LC-MS of HA-TRIF. Yellow entities indicate the proteins that are co-regulated by the newly identified proteins and TRIF. The red entity with yellow surround indicates TRIF (Ticam-1). Grey solid lines indicate direct regulation. Grey dotted lines indicate and regulation.

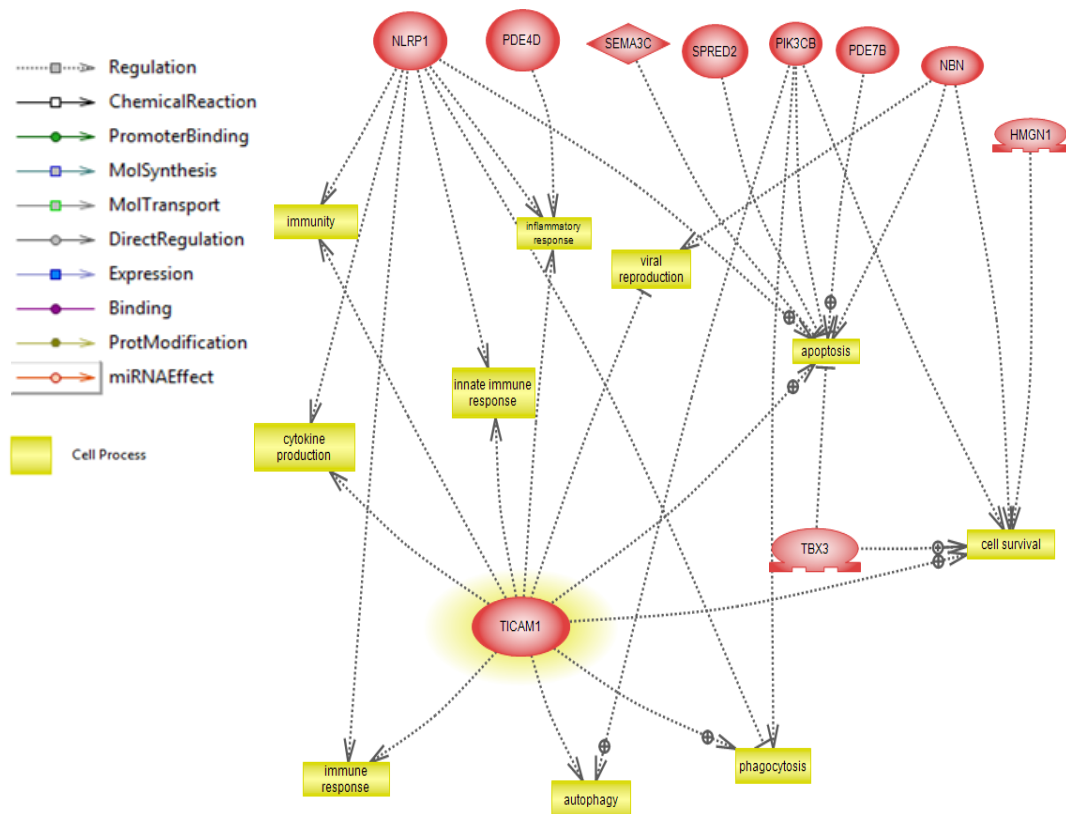


**Figure 3.5: Cell processes of poly(I:C)-independent TRIF interacting proteins.** HEK293-TLR3 cells were transfected with HA-TRIF. After 20 h, the cells were collected and IP of HA-TRIF was performed. Next, the TRIF IP-complex was analysed using the LC-MS. The newly identified protein interactors were uploaded to Pathway Studio software analysis program and the cellular processes network was constructed. Red entities are the proteins identified following IP and LC-MS of HA-TRIF. Yellow entities indicate the cellular processes that are co-regulated by the identified proteins and TRIF. The red entity with yellow surround indicates TRIF (Ticam-1). Dotted grey lines indicate regulation.

to activate caspase-3, a protein identified as being commonly modulated by TRIF and the newly identified protein, NLRP-1 (Figure 3.4).

### **3.2.3.2 TRIF interactors following 20 min poly(I:C) stimulation**

Following transfection of HEK293-TLR3 cells with HA-TRIF, cells were stimulated with poly(I:C) for 20 min followed by IP of HA-TRIF and LC-MS analysis of the TRIF-immunocomplex. A number of proteins were identified as being present in the HA-TRIF immunoprecipitated complex. Interestingly, it was found that a number of these proteins have previously been shown to interact directly with one another (Figure 3.6, purple lines). For example, the newly identified protein Calreticulin (CALR) was shown to bind directly Calnexin (CANX). CALR and CANX serve as molecular chaperones for glycoproteins in the endoplasmic reticulum of eukaryotic cells (McDonnell et al, 1996). Importantly, Molinari et al. (2004) showed that CALR depletion specifically accelerates the maturation of cellular and viral glycoproteins with a modest decrease in folding efficiency. CALX depletion prevents proper maturation of some proteins such as influenza hemagglutinin but does not interfere appreciably with the maturation of several others. Another example is the direct binding of the tumor suppressor protein Prohibitin (PHB) to the Minichromosome maintenance complex (MCM2). Rizwani et al. (2009) demonstrated that PHB physically interacted with MCM2, MCM5 and MCM7 and that PHB can function as a potent inhibitor of DNA replication by interacting with members of MCM complex.

Interestingly the common targets network showed that both TRIF and the newly identified protein Caspase recruitment domain (CARD11) are involved in the regulation of TRAF6 (Figure 3.7). CARD11 is a multidomain adapter that is required for NF- $\kappa$ B activation during T cell receptor signalling (TCR) (Gaide et al., 2002; Egawa et al., 2003). It has been demonstrated that during the TCR signalling, upon CARD11 activation, CARD11 recruits namely, TRAF6, Caspase 8, TAK1, and IKK $\gamma$  to induce NF- $\kappa$ B activity that is required for T-cell activation and proliferation in the adaptive immune response (McCully and Pomerantz, 2008). Accordingly, interaction between TRIF and TRAF6 was reported. Disruption of TRAF6-binding motifs of TRIF disabled it from associating with TRAF6, and resulted in a reduction in the TRIF-induced activation of the NF- $\kappa$ B-dependent but not IFN- $\beta$  promoter (Sato et al., 2003). These indicate involvement of TRIF and the newly identified CARD11 in NF- $\kappa$ B activation through binding to TRAF6.

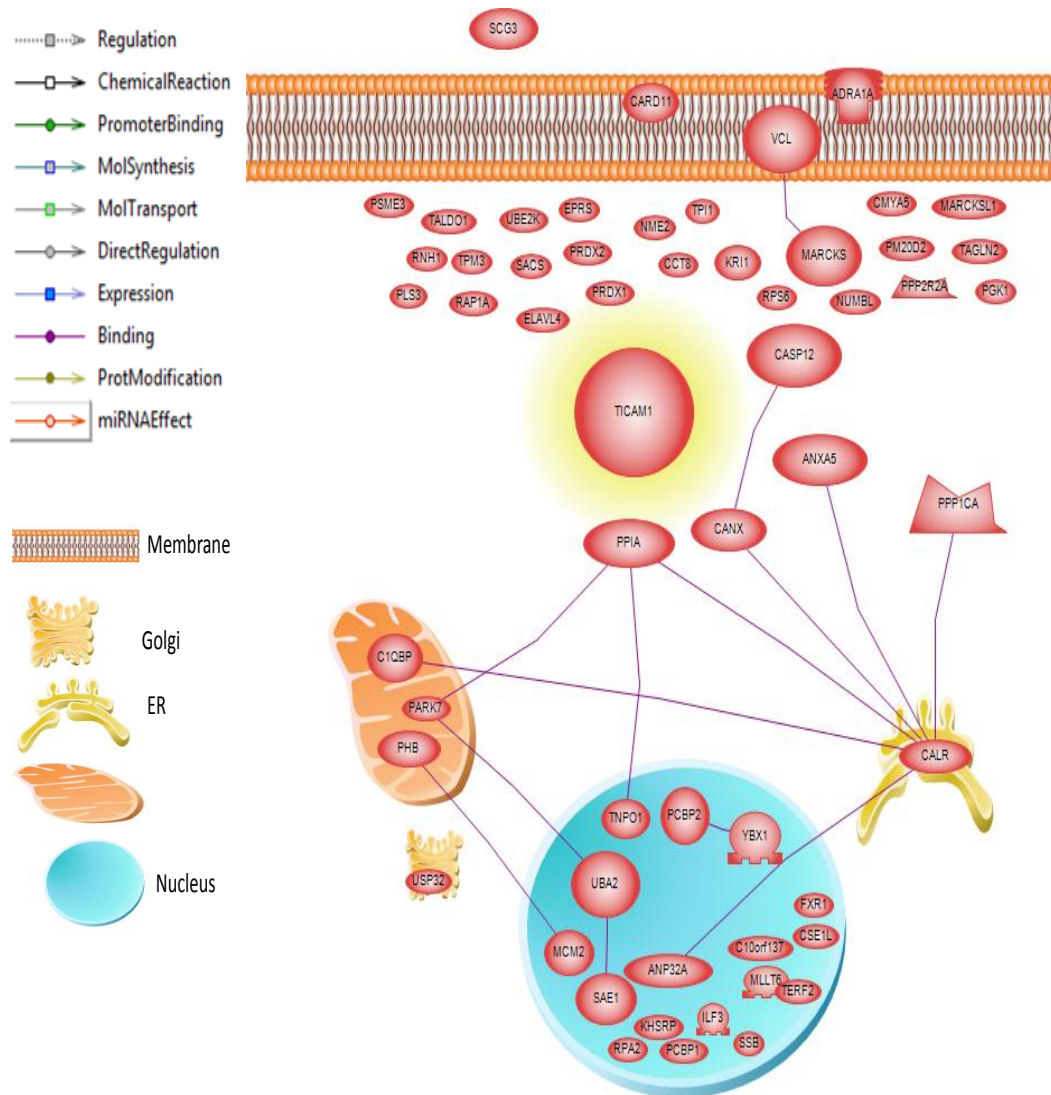


**Figure 3.6: Direct interactions network of poly(I:C)-dependent TRIF interacting proteins.** HEK293-TLR3 were transfected with HA-TRIF. After 20 h, cells were stimulated with 20  $\mu\text{g/ml}$  poly(I:C) for 20 min. Then, IP of HA-TRIF was performed and the IP-complex was analysed by LC-MS. The newly identified protein interactors were uploaded to Pathway Studio software analysis program and direct interaction network was constructed. Red entities indicate proteins that were identified in HA-TRIF IP-complex. TRIF (Ticam-1) is indicated in red with yellow surround. Purple line indicates direct binding.



Remarkably, most of newly identified proteins, concomitantly with TRIF, serve to regulate many cellular processes including immune response, apoptosis, viral replication and phagocytosis (Figure 3.8). For example, the newly identified CALR has been shown to function as pro-phagocytic and is highly expressed on the surface of several human cancers (Chao et al., 2010). Blockade or knockdown of CALR suppressed the phagocytosis of tumor cells by dendritic cells (Obeid et al., 2007). Moreover, the CALR homologue CANX plays important role in phagocytosis (Muller-Taubenberger et al., 2002) and viral reproduction. Pieren et al. (2005) showed that inactivation of the CANX affects viral replication and infectivity but not viability of mammalian cells. Notably, TRIF is also involves in phagocytosis regulation. It has been reported that MyD88-mediated phagocytosis of the Gram-negative bacteria *Borrelia burgdorferi* can be initiated by TRIF and is dependent on activation of PI3K (Shin et al., 2009). Another interesting newly identified protein is the nuclear factor 90, also known as interleukin enhancer binding factor 3 (IL3). The IL3 is a ds-RNA binding protein that has been shown to inhibit human immunodeficiency virus type 1 (HIV-1) replication in stably transfected cell line (Urcuqui-Inchima et al., 2006). Moreover, it was demonstrated that IL3 co-IPs with H5N1 viral nucleoprotein (NP) and that suppression of IL3 in Hela and A549 cell lines significantly increased viral polymerase complex activity and virus replication (Wang et al., 2009). Accordingly, TRIF is known to induce IRF3 activation and mediates induction of IFN- $\beta$  by TLR3 and TLR4 and thereby suppresses vaccine virus replication in macrophages (Stack et al., 2005). Despite the fact that these proteins have not previously shown to interact with TRIF, they share with TRIF, the ability to regulate various cellular processes which may indicate that they could regulate TRIF activity during these processes.

### **3.2.3.3 TRIF interactors following 40 min poly(I:C) stimulation**

Following transfection of HEK293-TLR3 cells with HA-TRIF, cells were stimulated with poly(I:C) for 40 min followed by IP of HA-TRIF and LC-MS analysis of the TRIF-IP-complex. A number of proteins were specifically identified as being present in the HA-TRIF-IP-complex. Direct interaction network showed that phosphoglycerate kinase 1 (PGK1) bound to glyceraldehyde 3 phosphate dehydrogenase (GAPDH) (Figure 3.9). PGK1 is an ATP-generating glycolytic enzyme that forms part of the glycolytic pathway and is directly involved in CXCL12 CXCR4 signalling. Moreover it

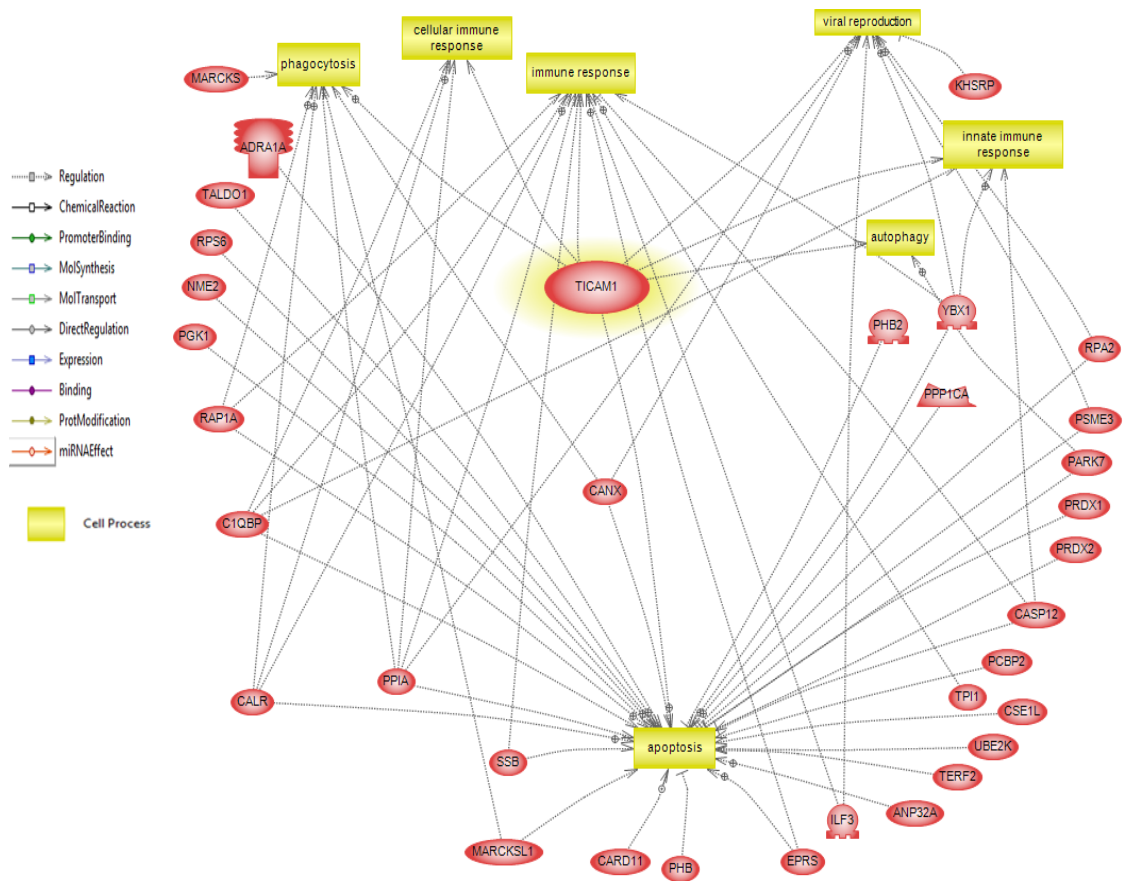


**Figure 3.8: Cell processes of poly(I:C)-dependent TRIF interacting proteins.** HEK293-TLR3 were transfected with HA-TRIF. After 20 h, cells were stimulated with 20  $\mu\text{g/ml}$  poly(I:C) for 20 min. Then, IP of HA-TRIF was performed and the IP-complex was analysed by LC-MS. The newly identified protein interactors were uploaded to Pathway Studio software analysis program and cell processes network was constructed. Red entities indicate proteins that were identified in HA-TRIF-IP-complex. Yellow entities indicate cellular processes that are co-regulated by the identified proteins and TRIF. TRIF (Ticam-1) is indicated in red with yellow surround. Grey dotted lines indicate regulation.

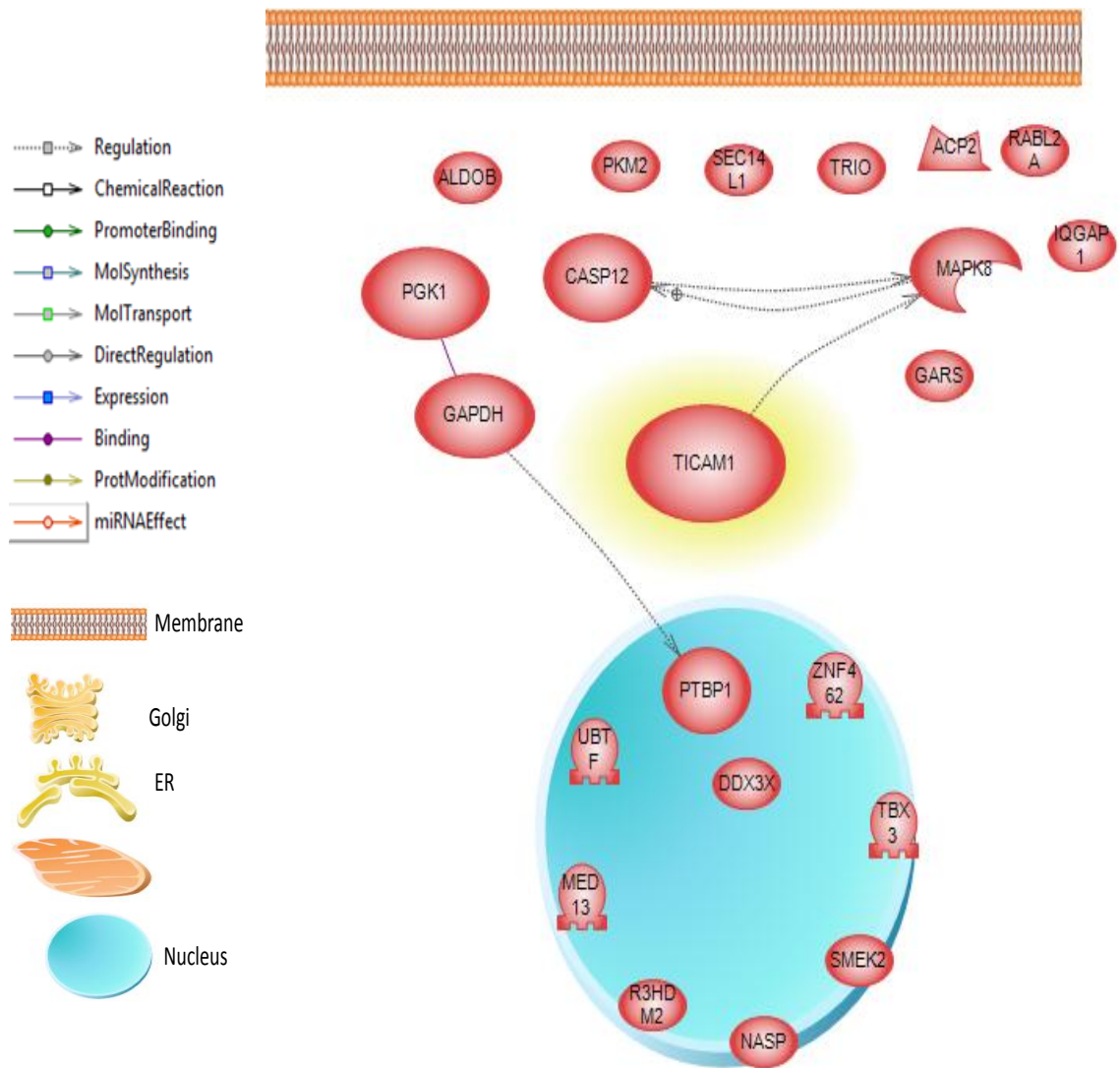


**Figure 3.9: Direct interactions network of poly(I:C)-dependent TRIF interacting proteins.** HEK293-TLR3 were transfected with HA-TRIF. After 20 h, cells were stimulated with 20  $\mu\text{g/ml}$  poly(I:C) for 40 min. Then, IP of HA-TRIF was performed and IP-complex was analysed by LC-MS. The newly identified protein interactors were uploaded to Pathway Studio software analysis program and direct interaction network was constructed. Red entities indicate proteins that were identified in HA-TRIF IP-complex. TRIF (Ticam-1) is indicated in red with yellow surround. Purple line indicates direct binding. Grey dotted lines indicate regulation.

was found that fibroblasts that overexpress PGK1 displayed a higher proliferative index and contributed to the invasion of prostate cancer cells, possibly through expression of MMP2, MMP3 and activation of the AKT and ERK pathways (Wang et al., 2010). Also, the interaction network showed that both TRIF and Caspase 12 (CASP12) regulated Mitogen-activated protein kinase 8 (MAPK8) which in turn regulated Caspase 12 (Figure 3.9). These data are in agreement with a previous study that showed TLR3 activation, which exclusively uses TRIF, results in activation of NF- $\kappa$ B, IRF-3 and MAP kinase (p38 and JNK) signalling (Johnson et al., 2008). CASP12 is also known to be essential for endoplasmic reticulum (ER) stress-induced apoptosis (Nakagawa et al., 2000) and studies reported activation of CASP12 and JNK during ER stress-induced apoptosis (Yoneda et al., 2001)

Interestingly, the common targets network showed that the newly identified proteins are involved in regulation of many different proteins including, IRF3, TBK1, IRF7, MAPK1, and 9 Caspase1, 2, 3 and 8 and NOTCH (Figure 3.10). For example, the newly identified DEAD-box helicase (DDX3X) was reported to bind TBK1 and that TBK1 and DDX3X acted synergistically in their ability to stimulate the IFN promoter. RNAi-mediated reduction of DDX3X expression led to an impairment of IFN production in macrophages (Soulat et al., 2008). Schröder et al. (2008) also showed that DDX3X is involved in TBK1/IKK $\epsilon$ -mediated IRF activation and IFN- $\beta$  promoter induction. The identification of the DDX3X in the TRIF immunocomplex support the recent finding that DDX1, DDX21, and DHX36 utilise the TRIF pathway independent of TLR3 to activate type I IFN responses in dendritic cells (Zhang et al., 2011). Importantly, two newly identified proteins namely polypyrimidine tract binding protein 1 (PTBP1) and triple functional domain (TRIO) were shown to be involved in Notch regulation (Figure 3.10). Notch signalling is an ancient process that regulates cell fate, stem cell maintenance and initiation of differentiation in embryonic and postnatal tissues (Grego-Bessa et al., 2004). PTBP1 is a multi-functional RNA-binding protein and different functions have been identified for vertebrate PTBP1, including translational control, mRNA stability, mRNA localization and may also act as a transcriptional activator (Dansereau et al., 2002; Cheung et al., 2006). It has been shown that in developing *Drosophila*, the absence of the PTBP1 homolog, hephaestus, resulted in increased Notch activity (Dansereau et al., 2002). The presence of these two proteins that they involved in Notch regulation in the TRIF IP complex may suggest a functional

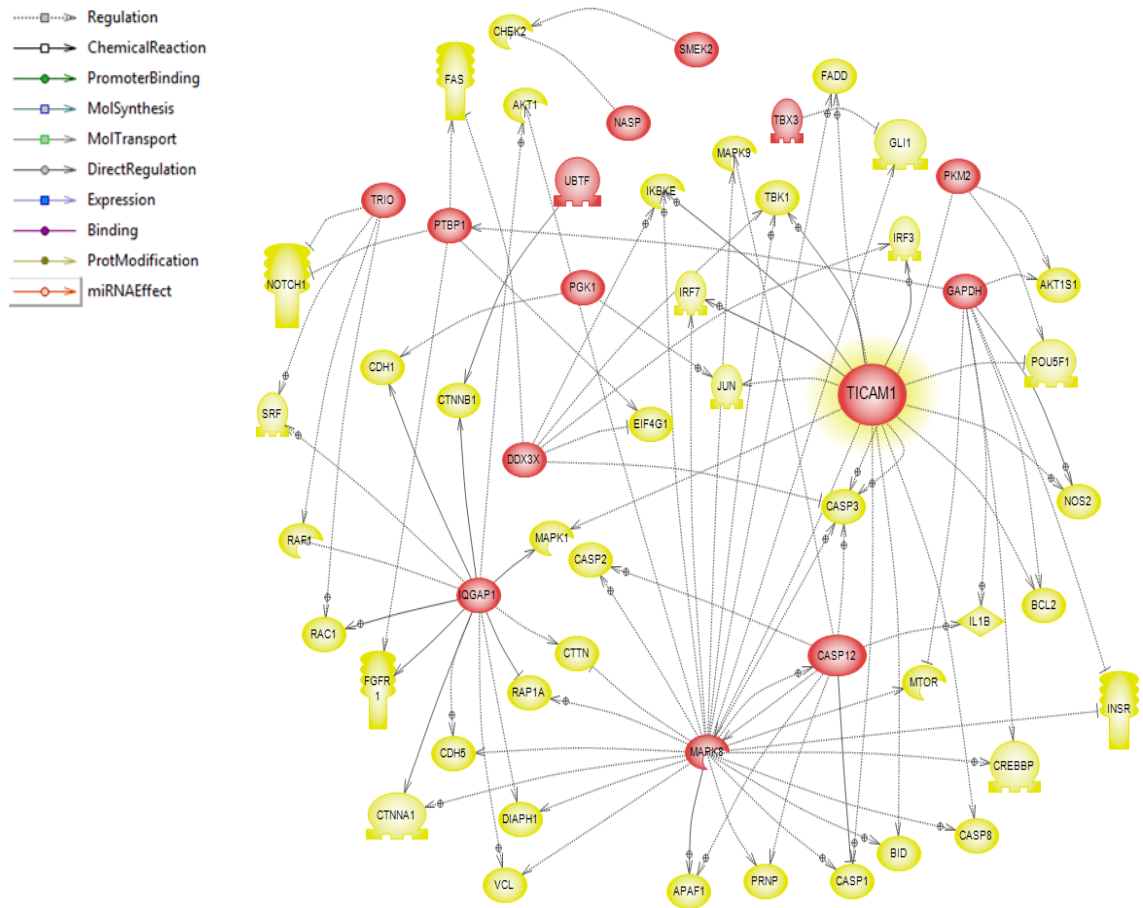


**Figure 3.10: Common targets network of poly(I:C)-dependent TRIF interacting proteins.** HEK293-TLR3 were transfected with HA-TRIF. After 20 h, cells were stimulated with 20  $\mu\text{g/ml}$  poly(I:C) for 40 min. Then, IP of HA-TRIF was performed and the IP-complex was analysed by LC-MS. The newly identified protein interactors were uploaded to Pathway Studio software analysis program and common targets network was constructed. Red entities indicate proteins that were identified in HA-TRIF IP-complex. Yellow entities indicate the proteins that are co-regulated by the newly identified proteins and TRIF. TRIF (Ticam-1) is indicated in red with yellow surround. Grey solid and dotted lines indicate direct regulation and regulation respectively.

role for TRIF in Notch signalling. Interestingly, links between TLR and Notch signalling have been previously reported whereby TLR agonists such as bacterial lipopeptide, poly(I:C), lipopolysaccharide and unmethylated CpG DNA serve to up-regulate Notch1 in primary and macrophage-like cell lines (Amsen et al. 2004; Palaga et al., 2008). Moreover, stimulation of macrophages with TLRs ligands triggered activation of Notch signalling, which in turn regulated gene expression patterns involved in pro-inflammatory responses, through activation of NF- $\kappa$ B (Palaga et al., 2008). Furthermore, most of these identified proteins and TRIF are involved in apoptosis inflammatory response, innate immune response, phagocytosis, autophagy, viral transcription and viral reproduction regulation (Figure 3.11). This correlates with a previous study showing that CASP12 blocks the inflammatory response initiated by NF- $\kappa$ B and Caspase-1 (Scott and Saleh, 2007). The PTBP1 protein, as discussed earlier, has been previously shown to modulate Notch signalling, apoptosis, viral replication and viral transcription (Figure 3.11). Li et al. (1999) demonstrated that PTBP1 binds to the leader RNA of mouse hepatitis virus and serves as a regulator of viral transcription. As TRIF known to be involves in viral recognition and typ1 IFN activation (Riad et al., 2011), it may be of interest to investigate the role of PTBP1in TRIF-mediated signalling.

#### **3.2.3.4 TRIF interactors following 60 min poly(I:C) stimulation**

Following transfection of HEK293-TLR3 cells with HA-TRIF, cells were stimulated with poly(I:C) for 60 min followed by IP of HA-TRIF and LC-MS of the TRIF immunocomplex. Proteins including ADAM metallopeptidase domain 15 (ADAM15), multiple endocrine neoplasia I (MEN) adenomatous polyposis coli (APC), IQ motif - containing GTPase activating protein1 (IQGAP1), phosphoinositide-3-kinase, regulatory subunit 2 beta (PIK3R2), CREB regulated transcription coactivator 1(CRTC1) and Probable ATP-dependent RNA helicase DDX28 were specifically identified as TRIF interactors (Figure 3.12). Some of these proteins have been previously shown to interact with one another as illustrated in the direct interaction network (Figure 3.12). IQGAP1 binds directly to APC, CLIP and Menin (MEN1).

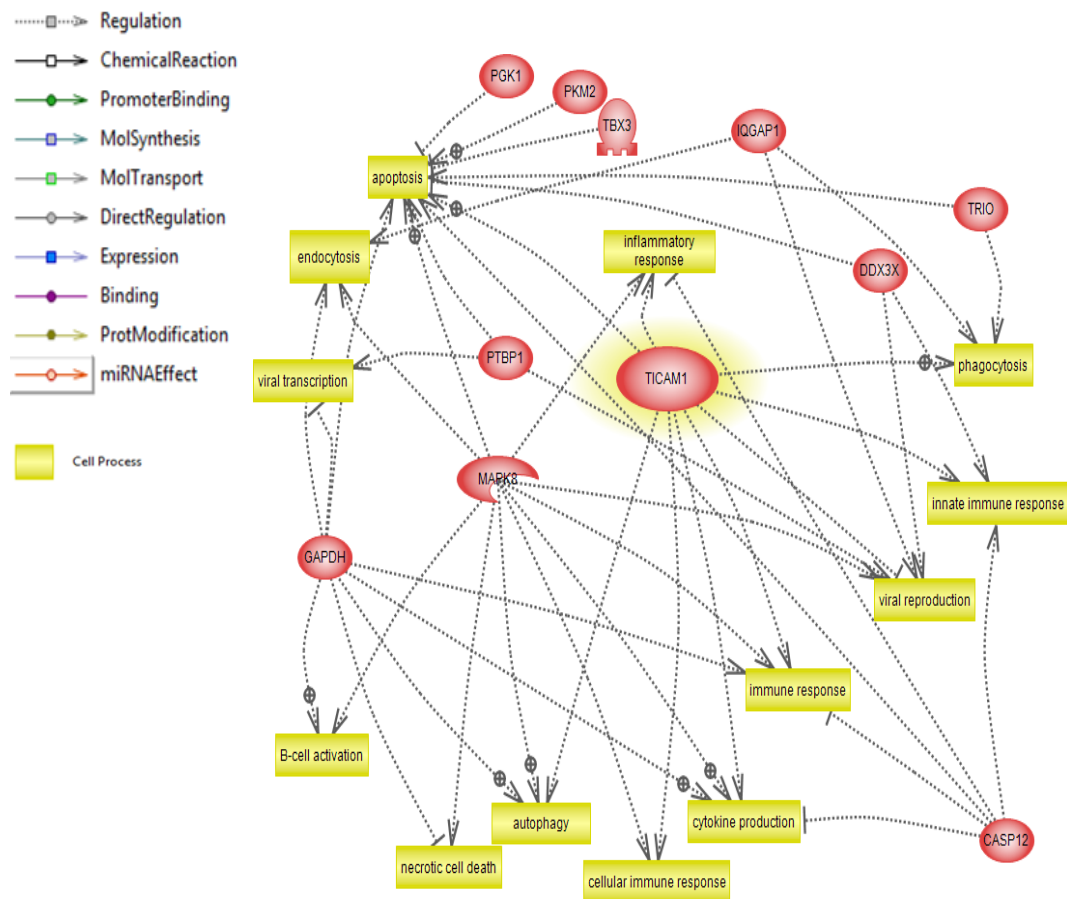


**Figure 3.11: Cell processes of poly(I:C)-dependent TRIF interacting proteins.** HEK293-TLR3 were transfected with HA-TRIF. After 20 h, cells were stimulated with 20  $\mu\text{g/ml}$  poly(I:C) for 40 min. Then, IP of HA-TRIF was performed and the IP-complex was analysed by LC-MS. The newly identified protein interactors were uploaded to Pathway Studio software analysis program and cell processes network was constructed. Red entities indicate proteins that were identified in TRIF IP-complex. Yellow entities indicate cellular processes that are co-regulated by the identified proteins and TRIF. TRIF (Ticam-1) is indicated in red with yellow surround. Grey dotted lines indicate regulation.

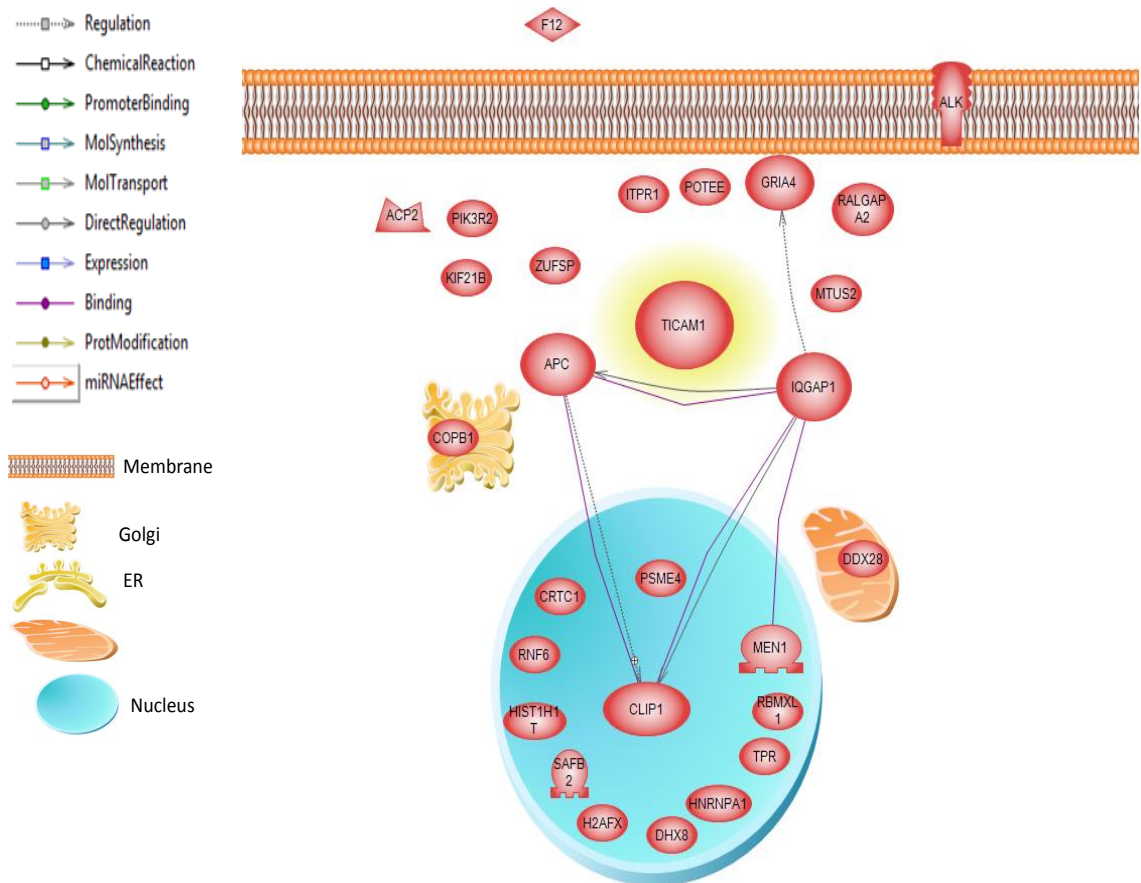


**Figure 3.12: Direct interactions network of poly(I:C)-dependent TRIF interacting proteins.** HEK293-TLR3 were transfected with HA-TRIF. After 20 h, cells were stimulated with 20  $\mu\text{g/ml}$  poly(I:C) for 60 min. Then, IP of HA-TRIF was performed and IP-complex was analysed by LC-MS. The newly identified protein interactors were uploaded to Pathway Studio software analysis program and direct interaction network was constructed. Red entities indicate proteins that were identified in TRIF IP-complex. TRIF (Ticam-1) is indicated in red with yellow surround. Purple line indicates direct binding. Grey solid lines indicate direct regulation. Grey dotted lines indicate regulation.

IQGAP1 is a scaffolding protein composed of multiple protein recognition motifs through which it interacts with a wide spectrum of binding partners, including CLIP-170, epidermal cadherin (E-cadherin),  $\beta$ -Catenin, APC, components of the mitogen-activated protein kinase pathway and RAP1 (Jeong et al., 2007). Interestingly, both  $\beta$ -Catenin and APC are key components of the canonical wnt signalling pathway, and Wnt signalling and TLRs have been shown to intersect in *Drosophila*. Also, growing evidence supports the notion that Wnt signalling may be involved in orchestrating the immune response in response to microbial stimulation of innate immune cells of vertebrate origin (Neumann et al., 2009; Schaale et al., 2011). Importantly, E-cadherin which was reported to bind IQGAP1 is known to be cleaved by the newly identified protein ADAM15 (Najy et al., 2008). E-cadherin is involved in cell-cell interaction, embryonic development, organ morphogenesis, tissue integrity, and wound healing, and disruption of E-cadherin has been observed in multiple pathophysiological conditions, including inflammation and cancer (Yasmeen et al., 2006; Wever et al., 2007). Notably, ADAM15, which belongs to the disintegrin and metalloprotease family, was also shown to be involved in different inflammation diseases such as atherosclerosis, rheumatoid arthritis (RA) and intestinal inflammation (Charrier-Hisamuddin et al. 2008).

Moreover, common targets network showed that the newly identified proteins are involved in regulation of different MAPKs, JUN, Nuclear factor NF-kappa-B p100 subunit (NFKB2), epidermal growth factor (EGF) and EGF receptor (EGFR) (Figure 3.13). More specifically, the newly identified MEN1 was shown to be involved in MAPK1, 3 and 8 and NFKB2 regulation (Figure 3.13). MEN1 is a tumor suppressor protein and was identified as the gene responsible for the disease multiple endocrine neoplasia type 1 (Yazgan and Pfarr, 2002). Heperen et al. (2001) also showed that the NF- $\kappa$ B proteins p50, p52 and p65 interact specifically and directly with Menin in vitro and in vivo. Overexpression of Menin repressed p65-mediated transcriptional activation on NF- $\kappa$ B sites and MAPK-induced phosphorylation of nuclear factors such, as c-JUN without altering ERK2 or JNK1 activity (Gallo et al., 2002). Importantly, it was found that TRIF and the newly identified proteins serve to modulate various cellular processes such as inflammatory response, immune response, immune invasion phagocytosis, T-cell activation, cell differentiation and cell proliferation (Figure 3.14). Notably, many of the newly identified proteins are strongly linked with the modulation of apoptosis, cell



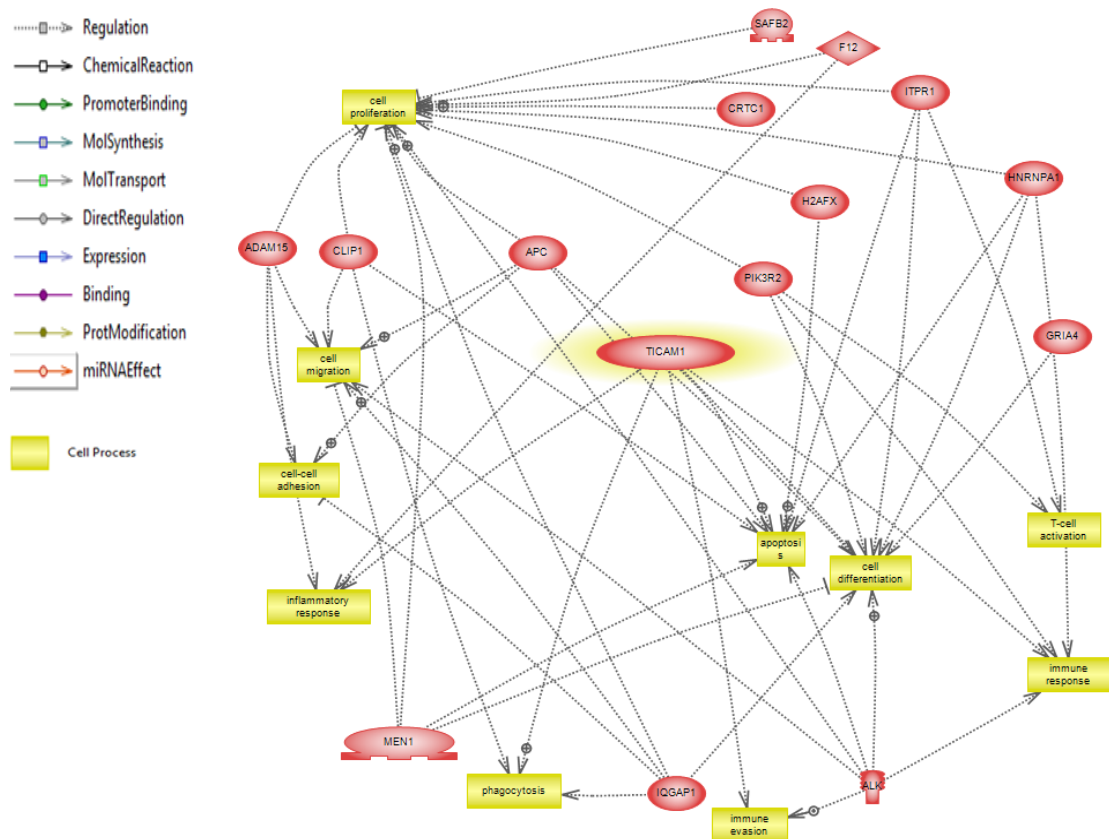


**Figure 3.14: Cell processes of poly(I:C)-dependent TRIF interacting proteins.** HEK293-TLR3 were transfected with HA-TRIF. After 20 h, cells were stimulated with 20  $\mu\text{g/ml}$  poly(I:C) for 60 min. Then, IP of HA-TRIF was performed and IP-complex was analysed by LC-MS. The newly identified protein interactors were uploaded to Pathway Studio software analysis program and cell processes network was constructed. Red entities indicate proteins that were identified in TRIF IP-complex. Yellow entities indicate cellular processes that are co-regulated by the identified proteins and TRIF. TRIF (Ticam-1) is indicated in red with yellow surround. Grey dotted lines indicate regulation.

differentiation and cell proliferation. It should be noted that TLRs are also linked to cancer. Recently, Umemura et al. (2011) investigated the role of TLR3 in metastatic progression. It was found that metastatic tumor cells were highly sensitive to TLR3-mediated apoptosis after double-stranded RNA treatment when compared to primary tumor cells. Enhanced apoptosis in metastatic cells was dependent on double-stranded RNA, TLR3 and also TRIF. Thus, interaction of these proteins with TRIF may affect TRIF activity during apoptosis or other processes regulated by TRIF (Umemura et al. 2011). Moreover, Galli et al. (2010) showed that TLR3 and TLR5 stimulation of human prostate cancer cells triggers the production of chemokines, which, in turn, favor the attraction of immune effectors, thereby representing a tool to enhance the efficacy of conventional therapies by stimulating anticancer immune responses.

### **3.2.3.5 LPS-independent TRIF interactors**

HEK293-TLR4 were transfected with HA-TRIF. After 20 h, cells were collected and IP of HA-TRIF was performed followed by LC-MS analysis of the TRIF IP-complex. A significant numbers of proteins were identified as TRIF interacting partners. As predicted following analysis of the TRIF interaction network (Figure 3.15), there is no previous report of direct binding between these identified proteins and TRIF or between each other. However, the DBF4 homolog A (DB4) protein is directly regulated by MEN1. Interestingly, MEN1 was also identified in HEK-TLR3 upon poly(I:C) stimulation for 60 min. Thus, MEN1 is associated with TRIF in HEK-TLR3 and HEK293-TLR4 cells. The DBF4 is a kinase subunit that is essential for regulating the initiation of DNA replication in *Saccharomyces cerevisiae*. The human homologue of DBF4 (HsDBF4) was shown to be directly involved in regulating the initiation of DNA replication by targeting minichromosome maintenance (MCM2) protein in mammalian cells (Jiang et al., 1999). Importantly MCM2 was also identified in HEK293-TLR3 upon poly(I:C) stimulation for 20 min. This may suggest an involvement of these proteins in TRIF-mediated apoptosis. Moreover, the common targets network for the newly identified proteins and TRIF include MAPKs, IRF3, TGFB1, EGFR, NFKB2, ESR1 and Tyrosine kinase-type cell surface receptor HER2 (ERBB2), SMAD3 and SMAD4 (Figure 3.16). Interestingly, TRIF, MEN1 and ADAM15 have been linked with MAPK1 regulation (Figure 3.16). This correlates with a study which showed that ADAM15 expression decreased the phosphorylation of ERK1/2 (Chen et al., 2008).

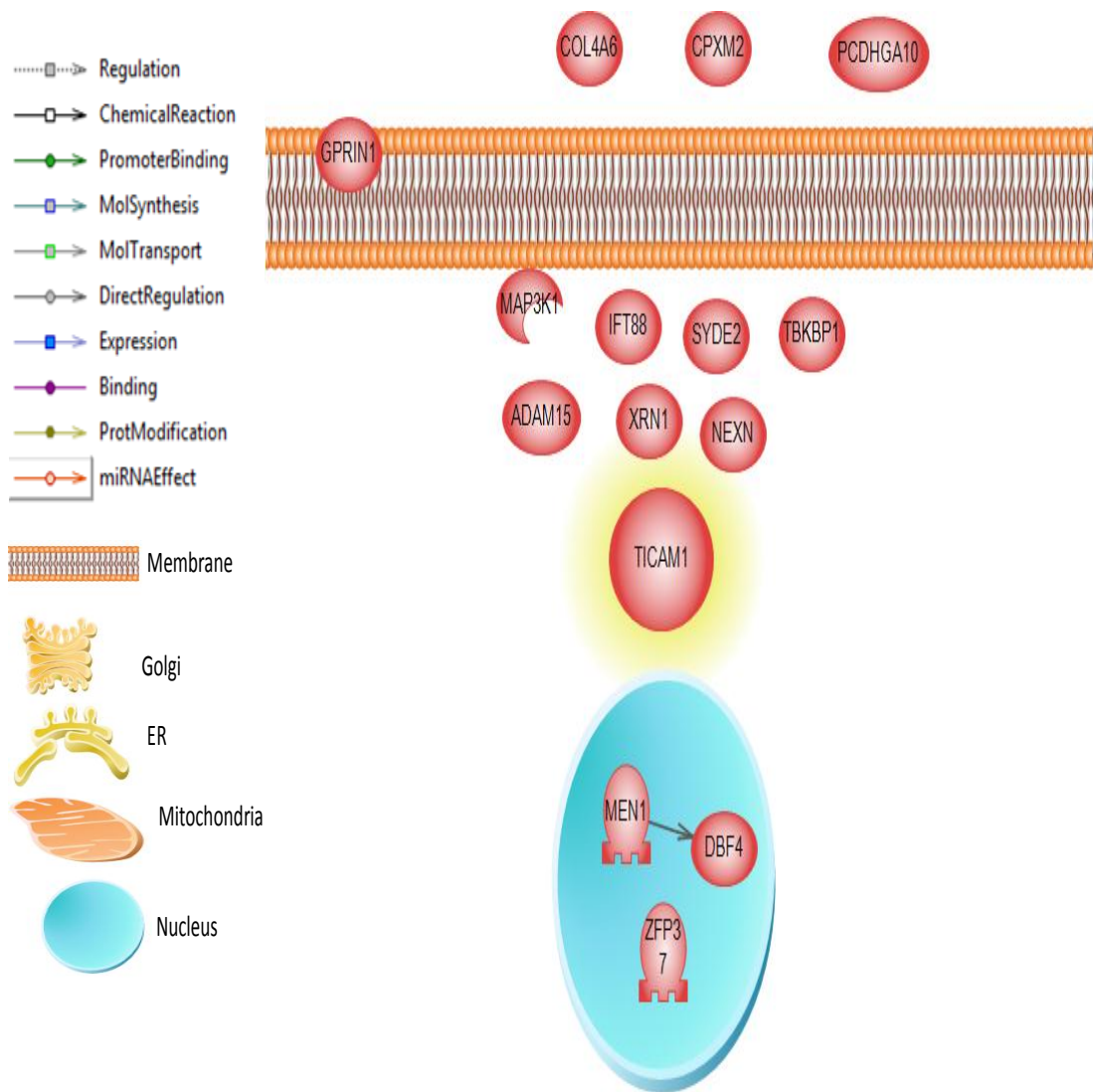


**Figure 3.15: Direct interaction network of LPS-independent TRIF interacting proteins.** HEK293-TLR4 cells were transfected with HA-TRIF. After 20 h, cells were collected and IP of HA-TRIF was performed and TRIF IP-complex was analysed by LC-MS. The newly identified protein interactors were uploaded to the Pathway Studio software analysis program and direct interaction network was constructed. Red entities indicate proteins that were identified in TRIF IP-complex. TRIF (Ticam-1) is indicated in red with yellow surround. Grey solid line indicates direct regulation.

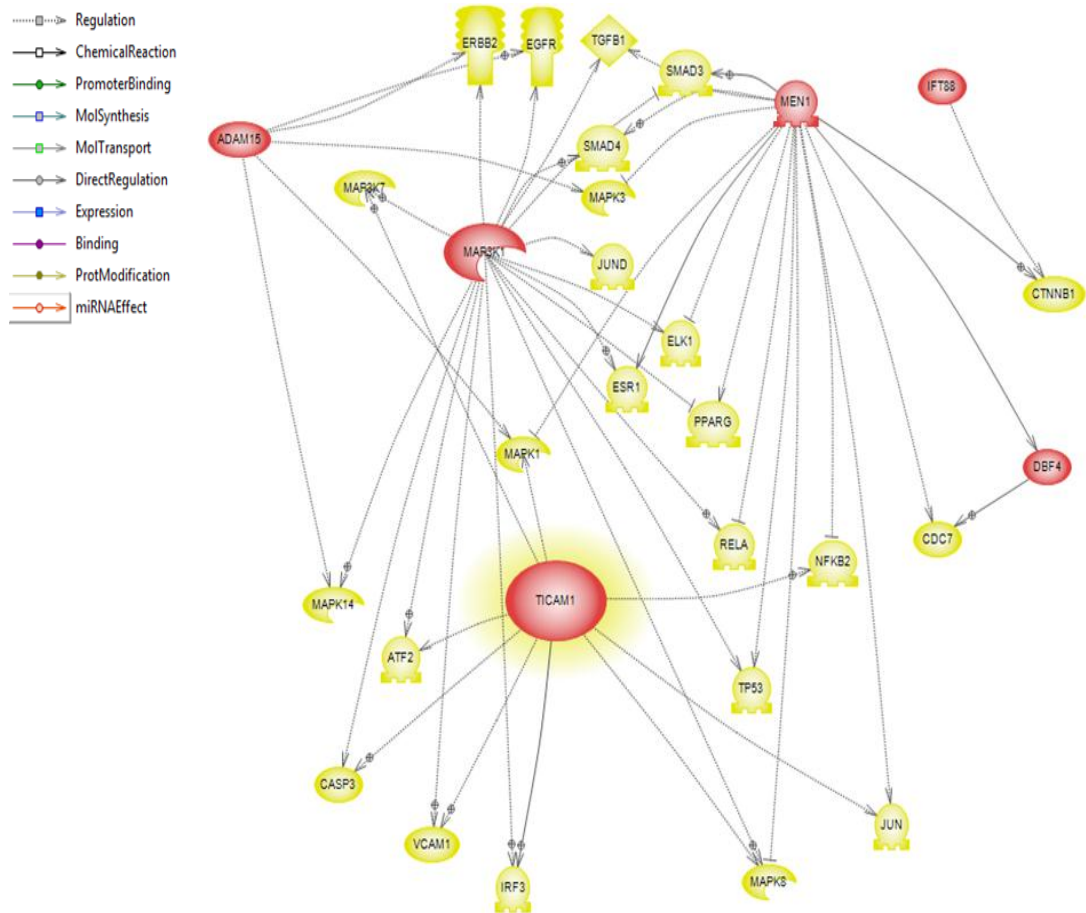


**Figure 3.16: Common targets network of LPS-independent TRIF interacting proteins.** HEK293-TLR4 cells were transfected with HA-TRIF. After 20 h, cells were collected and IP of HA-TRIF was performed followed by IP-complex analysis by LC-MS. The newly identified protein interactors were uploaded to the Pathway Studio software analysis program and common targets network was constructed. Red entities indicate proteins that were identified in TRIF IP-complex. Yellow entities indicate the proteins that are co-regulated by the newly identified proteins and TRIF. TRIF (Ticam-1) is indicated in red with yellow surround. Grey solid and dotted lines indicate direct regulation and regulation, respectively.

Interestingly, whereas MEN1 was shown also to suppress ERK phosphorylation (Gallo et al., 2002), activation of the TRIF pathway resulted in activation of p38 and ERK MAPK pathways (Qi and Shelhamer., 2005). This suggests that ADAM15 and MEN1 may regulate TRIF-mediated MAPK activation. Furthermore, the identified proteins were strongly associated with the regulation of cell differentiation, cell migration, cell proliferation, cell adhesion, apoptosis and immunity (Figure 3.17). Some of these processes were also modulated by TRIF (Figure 3.17) indicating that these proteins may cooperate with each other to modulate the cellular processes.

### **3.2.3.6 TRIF interactors 20 min following LPS stimulation**

HEK293-TLR4 were transfected with HA-TRIF. After 20 h, cells were stimulated with LPS for 20 min and IP of HA-TRIF was performed followed by LC-MS analysis of the TRIF IP-complex. A significant numbers of proteins were identified as TRIF interacting partner. Interestingly, a number of the newly identified hits previously have been reported to bind or regulate one another as illustrated in the interaction network (Figure 3.18). For example importin- $\beta$ 1 (KPNB1) binds directly to proliferating cell nuclear antigen (PCNA) and GAPDH regulates both KPNB1 and PCNA (Figure 3.18). PCNA was first identified as an autoantigen that reacts with autoantibodies in patients with systemic lupus erythematosus (SLE) (Miyachi et al., 1978). PCNA plays an essential role in DNA replication, repair and methylation, chromatin assembly, cell cycle regulation, and ribosomal DNA transcription (Kaneda et al., 2004). These findings are supported by studies showing TLR involvement, particularly the nucleic acid-sensing TLR3, 7, 8 and 9 in SLE (Montero and Martin, 2009; Horton et al., 2010).

Moreover, the common target network showed that both TRIF and the newly identified protein macrophage migration inhibitory factor (MIF) were involved in the regulation of Caspase-3 and 8, macrophage colony stimulating factor 1 (CSF1) and interleukin 18 (IL-18) (Figure 3.19). Macrophage migration inhibitory factor (MIF) is a pro-inflammatory cytokine produced by human pulmonary artery endothelial cells (HPAECs). Its expression increases in response to various death-inducing stimuli, including LPS (Damico et al., 2008; Zhang et al., 2012). Studies have showed that MIF functions as an endogenous pro-survival factor in HPAECs through regulation of the FLICE-like inhibitory protein (FLIP). FLIP modulates or blocks death receptor-

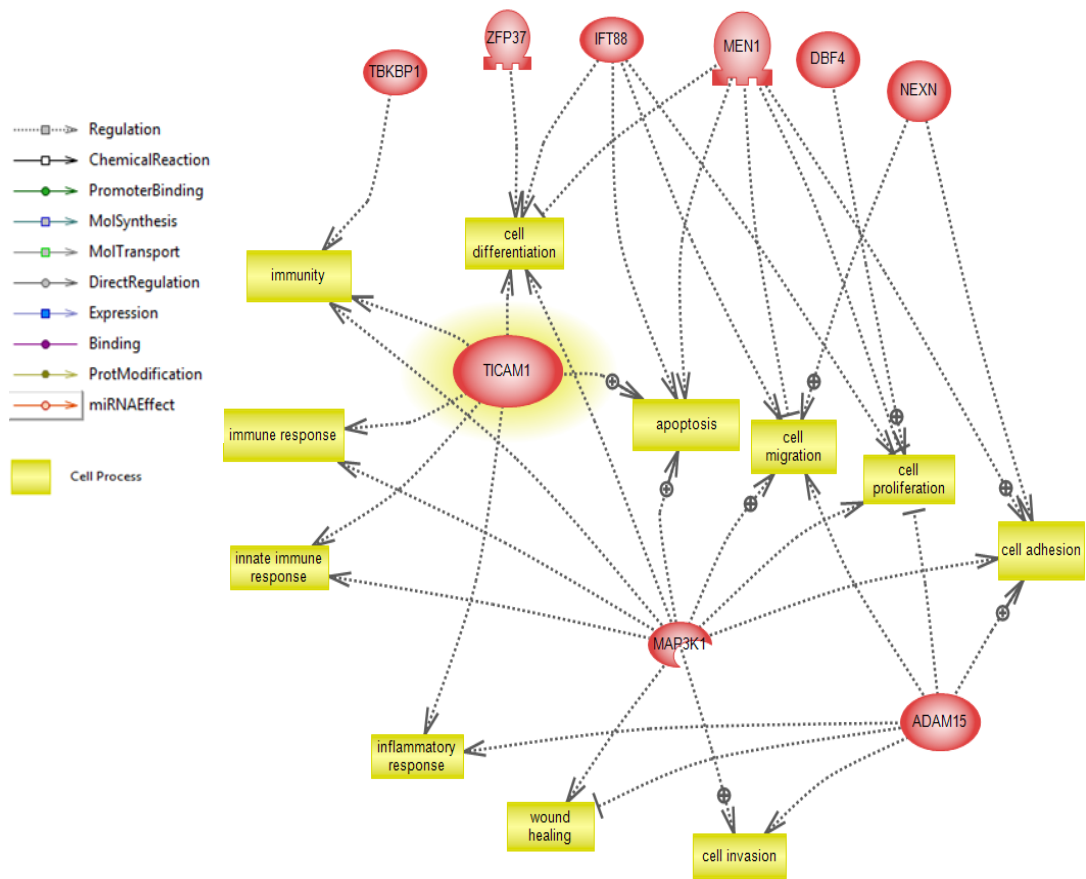


**Figure 3.17: Cell processes network of LPS-independent TRIF interacting proteins.** HEK293-TLR4 were transfected with HA-TRIF. After 20 h, cells were collected and IP of HA-TRIF was performed followed by analysis of the IP-complex by LC-MS. The newly identified protein interactors were uploaded to Pathway Studio software analysis program and cell processes network was constructed. Red entities indicate proteins that were identified in TRIF IP-complex. Yellow entities indicate cellular processes that are co-regulated by the identified proteins and TRIF. TRIF (Ticam-1) is indicated in red with yellow surround. Grey dotted lines indicate regulation.

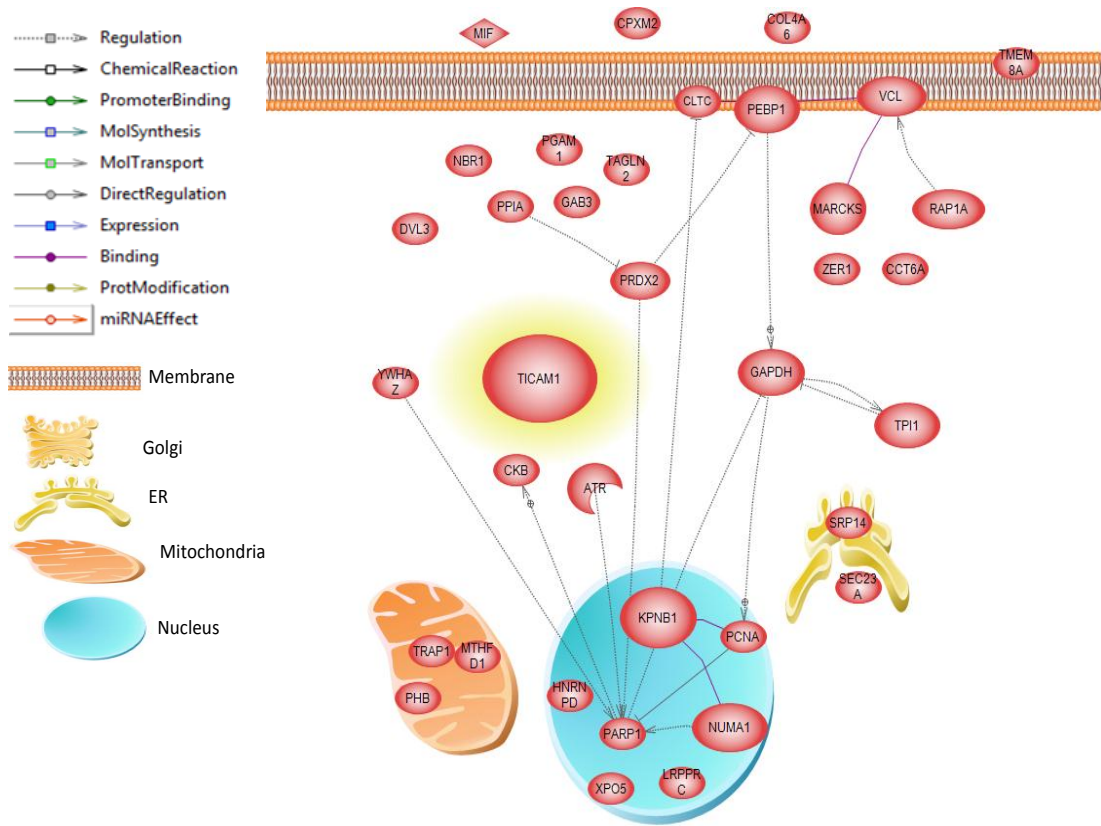


**Figure 3.18: Direct interaction network of LPS-dependent TRIF interacting proteins.** HEK293-TLR4 were transfected with HA-TRIF. After 20 h, cells were stimulated with 1  $\mu\text{g/ml}$  LPS for 20 min followed by IP of HA-TRIF and LC-MS analysis of the TRIF-IP-complex. The newly identified protein interactors were uploaded to Pathway Studio software analysis program and cell processes network was constructed. Red entities indicate proteins that were identified in TRIF IP-complex. TRIF (Ticam-1) is indicated in red with yellow surround. Purple line indicates binding Grey dotted lines indicate regulation. Grey solid line indicates direct regulation.

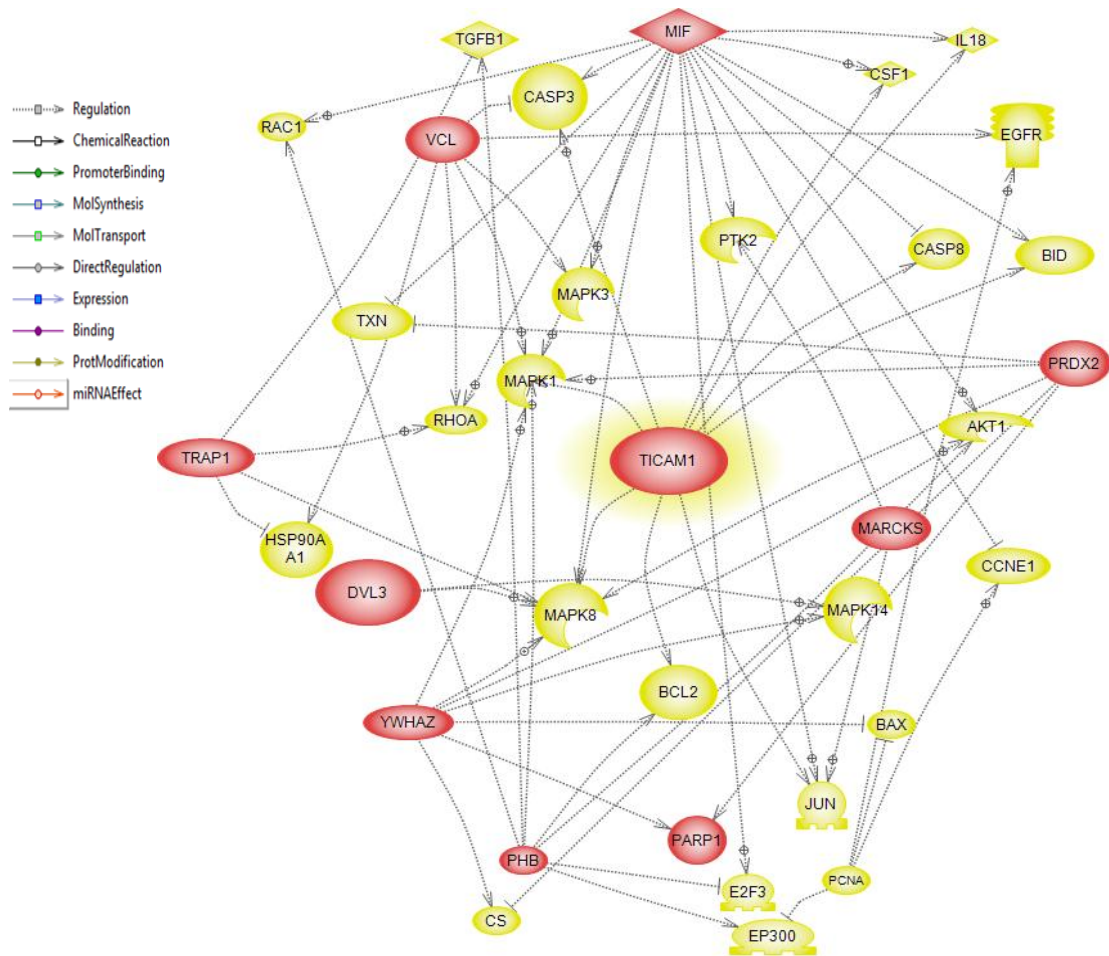


**Figure 3.19: Common targets network of LPS-dependent TRIF interacting proteins.** HEK293-TLR4 were transfected with HA-TRIF. After 20 h, cells were stimulated with 1  $\mu\text{g/ml}$  LPS for 20 min followed by IP of HA-TRIF and LC-MS analysis of the TRIF-IP-complex. The newly identified protein interactors were uploaded to Pathway Studio software analysis program and common targets network was constructed. Red entities indicate proteins that were identified in TRIF IP-complex. Yellow entities indicate proteins that are co-regulated by the identified proteins and TRIF. TRIF (Ticam-1) is indicated in red with yellow surround. Grey dotted lines indicate regulation.

stimulated cell death by competing with Caspase-8 for binding to FADD (Damico et al., 2008). Importantly, TRIF is known to mediate apoptosis through activation of caspase-8 (Han et al., 2004). This suggests that MIF may affect TRIF-mediated Caspase-8 activation and thereby affect TRIF-mediated apoptosis. Another interesting protein identified as a TRIF interactor is Segment polarity protein dishevelled homolog (DVL3), which was shown to be involved in MAPK8 and MAPK14 regulation (Figure 3.19). DVL3 play important role in both the canonical wnt- $\beta$ -catenin pathway and the planar cell polarity (PCP) pathway (Lee et al., 2008). Bikkavilli et al. (2008) demonstrated that in the canonical Wnt- $\beta$ -catenin signalling pathway, DVL3 is critical for Wnt3A-induced p38 MAPK activation. As mention earlier, the TRIF pathway induces MAPK activation, thus linking the TLR and wnt signalling pathways (Bikkavilli et al., 2008; Neumann et al., 2009). Furthermore, the cellular processes network showed that MIF was involved in the regulation of many of the cellular processes that were also regulated by TRIF including apoptosis, autophagy, immune response, phagocytosis, cytokine production, inflammatory responses and viral reproduction (Figure 3.20). It was reported that MIF acts as an important mediator of the inflammatory response in alcoholic liver disease. Moreover, it has been reported that the plasma from HIV-1-infected patients contains elevated levels of MIF and that peripheral blood mononuclear cells (PBMCs) from HIV-infected patients release a greater amount of MIF. Furthermore, HIV-1 replication in PBMCs declines when these cells were treated with anti-MIF antibodies (Regis et al., 2010). Thus, MIF may be an interesting protein to characterise in the context of TRIF signalling.

### **3.2.3.7 TRIF interactors 40 min following LPS stimulation**

HEK293-TLR4 were transfected with HA-TRIF. After 20 h, cells were stimulated with LPS for 40 min and IP of HA-TRIF was performed followed by LC-MS analysis of the TRIF IP-complex. A numbers of proteins were identified as TRIF interacting partners. A direct interaction network showed that PHB bound to apoptosis inducing factor 1 (AIFM1) and this protein directly regulates PHB2 expression (Figure 3.21). It should be mentioned that PHB was also identified in HEK-TLR3 upon poly(I:C) stimulation for 20 min. PHB is present in various cellular compartments, including mitochondria, nucleus, and plasma membrane. It function as a potential tumor suppressor, an anti-

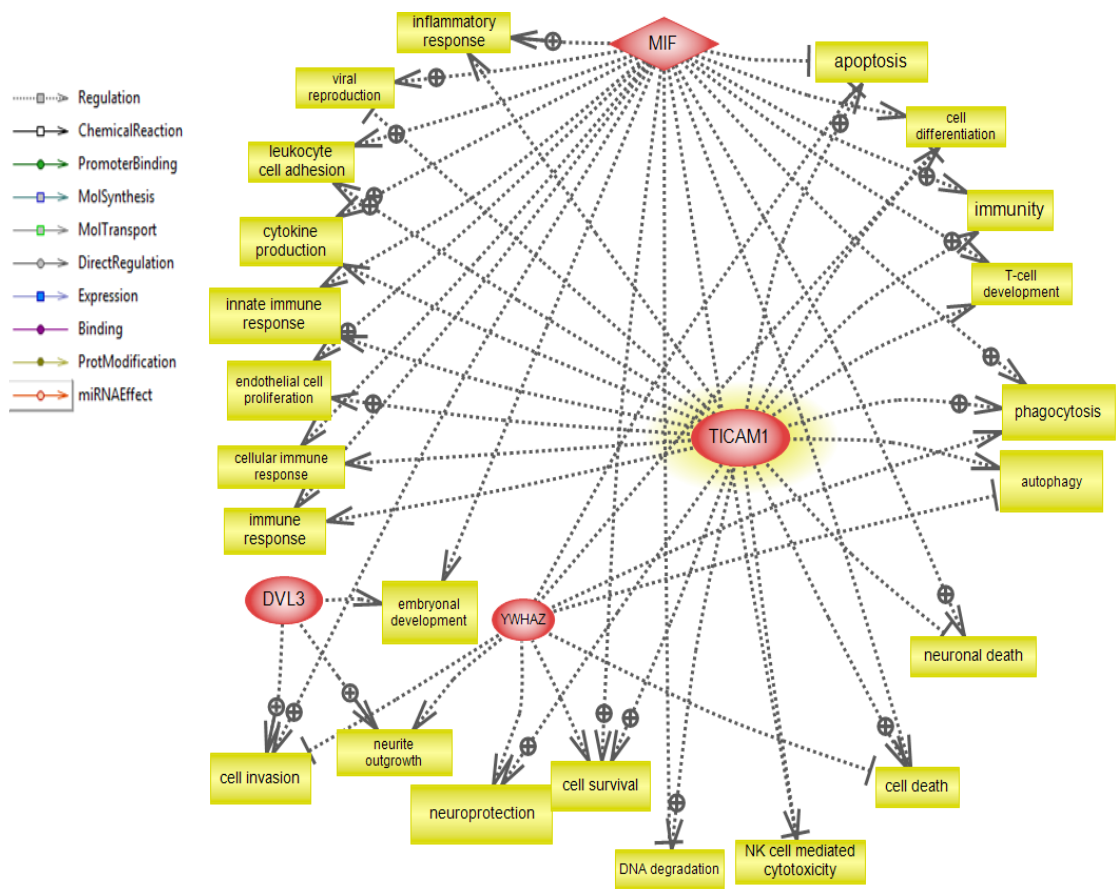


**Figure 3.20: Cell processes network of LPS-dependent TRIF interacting proteins.** HEK293-TLR4 were transfected with HA-TRIF. After 20 h, cells were stimulated with 1  $\mu\text{g/ml}$  LPS for 20 min followed by IP of HA-TRIF and LC-MS analysis of the TRIF-IP-complex. The newly identified protein interactors were uploaded to Pathway Studio software analysis program and cell processes network was constructed. Red entities indicate proteins that were identified in TRIF IP-complex. Yellow entities indicate cellular processes that are co-regulated by the identified proteins and TRIF. TRIF (Ticam-1) is indicated in red with yellow surround. Grey dotted lines indicate regulation.

proliferative protein and a regulator of cell-cycle progression and apoptosis (Theiss et al., 2007). PHB in the gastrointestinal tract has been implicated in protection against infection and inflammation and the induction of apoptosis in other tissues (Mishra et al., 2005). Furthermore, it was found that PHB overexpression decreased the accumulation of reactive oxygen metabolites, as well as increasing the permeability induced by oxidative stress in intestinal epithelial cells, suggested that PHB plays a role in the cellular defense against oxidant injury (Theiss et al., 2007). Importantly, deregulation of TLRs has been reported during intestinal inflammation and an essential role for TLR signalling in the pathogenesis of inflammatory bowel diseases (IBD) has been established through many studies (Harris, et al., 2006; Cario, 2010). Together, these data suggest that the counterregulation of PHB via TRIF (or vice versa) may modulate inflammatory condition in the bowel.

Moreover, many of the newly identified proteins and TRIF have previously been reported to be involved in the regulation of proteins such as MAPK1 and 8, BCL2, ESR1, Glycogen synthase kinase-3 beta (GSK3B) and JUN as shown in the common targets network (Figure 3.22). It should be mentioned that two of the newly identified proteins namely, PHB and AIFM1 regulates GSK3B. GSK3 is a component of many diverse signalling pathways, including insulin/insulin-like growth factor (IGF-1) signalling and the Wnt signalling pathways (Gould and Manji, 2005). Regarding the Wnt/ $\beta$ -catenin pathway, active GSK-3 phosphorylates  $\beta$ -catenin leading to its ubiquitin-dependent degradation. However, when GSK-3 is inhibited,  $\beta$ -catenin is not degraded, and this permits the interaction of  $\beta$ -catenin with T-cell-specific transcription factor (TCF) leading to transcriptional activation of target gene (Cadigan and Peifer, 2009). The link between TLRs and Wnt signalling was mentioned earlier. Another interesting finding is that both TRIF and the newly identified protein Scribbled (SCRIB) regulate MAPK1 and 8 and JUN. The cell polarity regulator, human Scribble (hSCRIB), is a potential tumour suppressor whose loss is a frequent event in late stage cancer development. In mammals, SCRIB regulates cell migration and wound healing in vivo (Dow et al., 2008). Moreover the suppression of MAPK signalling reported to be a highly conserved function of Scribble and that hSCRIB interacts with ERK and loss of hSCRIB results in elevated phospho-ERK levels (Nagasaka et al., 2010).

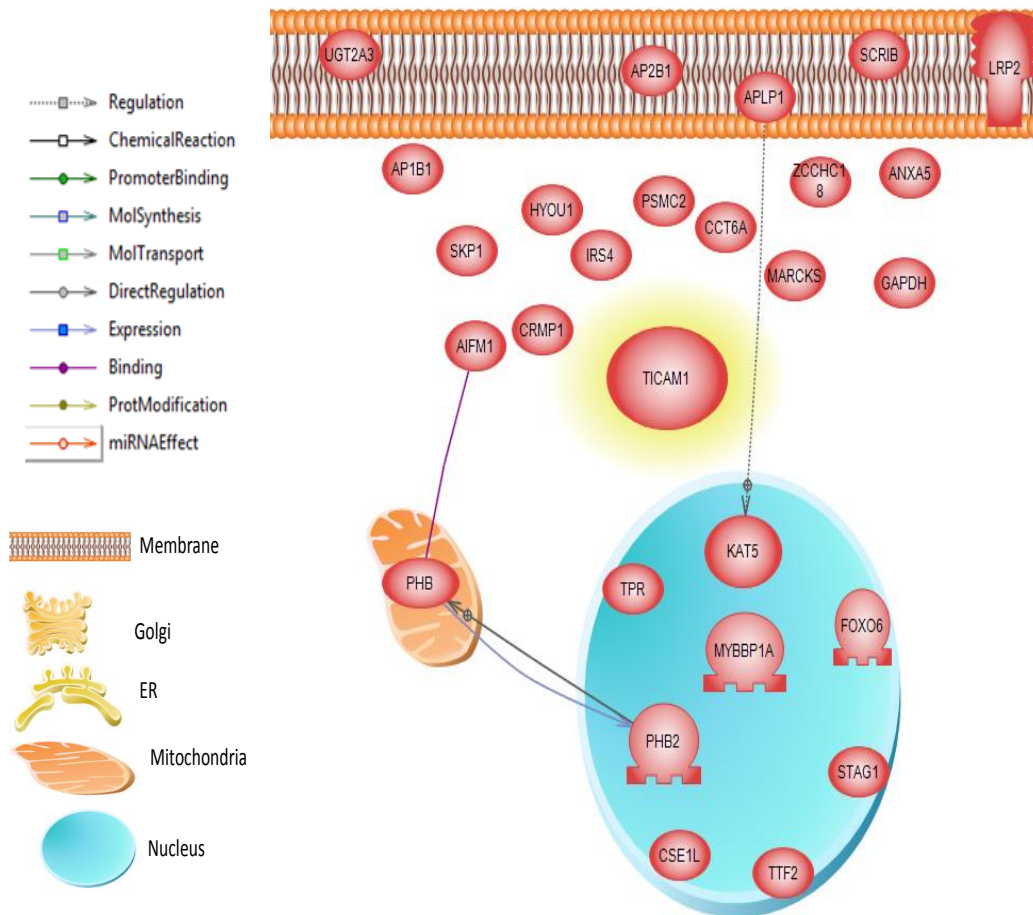


**Figure 3.21: Direct interaction network of LPS-dependent TRIF interacting proteins.** HEK293-TLR4 were transfected with HA-TRIF. After 20 h, cells were stimulated with 1  $\mu\text{g/ml}$  LPS for 40 min followed by IP of HA-TRIF and LC-MS analysis of the IP-complex. The newly identified protein interactors were uploaded to Pathway Studio software and direct interaction network was constructed. Red entities indicate proteins that were identified in TRIF IP-complex. TRIF (Ticam-1) is indicated in red with yellow surround. Purple line indicates binding, grey solid and dotted lines indicate direct regulation and regulation respectively.

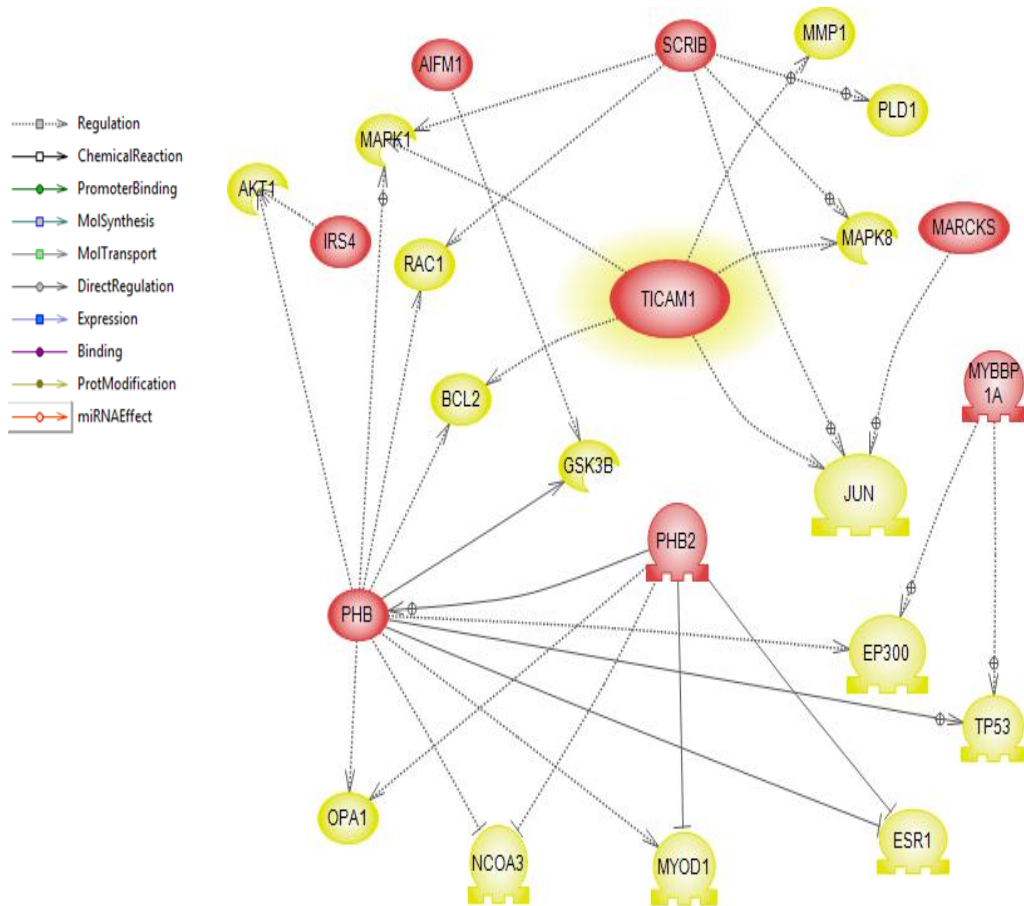


**Figure 3.22: Common targets network of LPS-dependent TRIF interacting proteins.** HEK293-TLR4 were transfected with HA-TRIF. After 20 h, cells were stimulated with 1  $\mu\text{g}/\text{ml}$  LPS for 40 min followed by IP of HA-TRIF and LC-MS analysis of the TRIF-IP complex. The newly identified protein interactors were uploaded to Pathway Studio software and common targets network was constructed. Red entities indicate proteins that were identified in TRIF IP-complex. Yellow entities indicate proteins that are co-regulated by the identified proteins and TRIF. TRIF (Ticam-1) is indicated in red with yellow surround. Grey solid and dotted lines indicate direct regulation and regulation respectively.

Furthermore, cellular processes such as apoptosis, endocytosis, complement activation, immune responses, cytokinesis and cytokine production were all regulated by TRIF and the and the newly identified proteins (Figure 3.23). Most of the identified protein hits are strongly involved in apoptosis regulation. An important protein identified is Low-density lipoprotein receptor-related protein 2 (LRP2), which showed to be involved in endocytosis, and cytokine production (figure 3.23). LRP2 is an endocytic receptor expressed on the apical surface of several epithelial cells that internalizes a variety of ligands including nutrients, hormones and their carrier proteins, signalling molecules and extracellular matrix proteins (Marzolo and Farfán, 2011). A GSK3 site was described in the intracellular cytoplasmic tail of LRP2. This site appears constitutively to be phosphorylated by GSK3 and regulates the cell membrane location of LRP2 (Bolós et al., 2010). Interestingly, as mentioned earlier GSK3 is involved in wnt/ $\beta$ -catenin pathway and was reported to be regulated by the two identified proteins namely, PHB and AIFM1.

#### **3.2.3.8 TRIF interactors 60 min following LPS stimulation**

HEK293-TLR4 were transfected with HA-TRIF. After 20 h, cells were stimulated with LPS for 60 min and IP of HA-TRIF was performed followed by LC-MS analysis of TRIF IP-complex. A significant numbers of proteins were identified as TRIF interacting proteins. Directed interaction network showed only one regulation between GAPDH and triosephosphate isomerase 1 (TPI1) (Figure 3.24). TPI and GAPDH are glycolytic enzymes essential for efficient energy production. Importantly, anti-TPI and GAPDH antibodies were found in the cerebrospinal fluid and in lesions of patients with the autoimmune disease multiple sclerosis (MS) suggested that TPI and GAPDH may be recruited into the immune cascade at different stages of the disease. (Kölln et al., 2010). Moreover, IgM antibodies against TPI were detected in the patient's serum from the acute phase of the Hepatitis A virus infection (Ritter et al., 1994). Furthermore the newly identified proteins and TRIF share regulation of proteins such as Caspase-1, 3 and 8, MAPK1 eukaryotic translation initiation factor 2-alpha kinase 2 (EIF2AK), IKBKB, IFN- $\beta$  and BCL2 as illustrated in the common targets network (Figure 3.25). For example, Absent in melanoma 2 (AIM2) share with TRIF the regulation of caspase-1 and 3 and also involved in IFN- $\beta$  regulation (Figure 3.25). AIM2 also known as Interferon-inducible protein is a member of the interferon (IFN)- inducible p200-protein

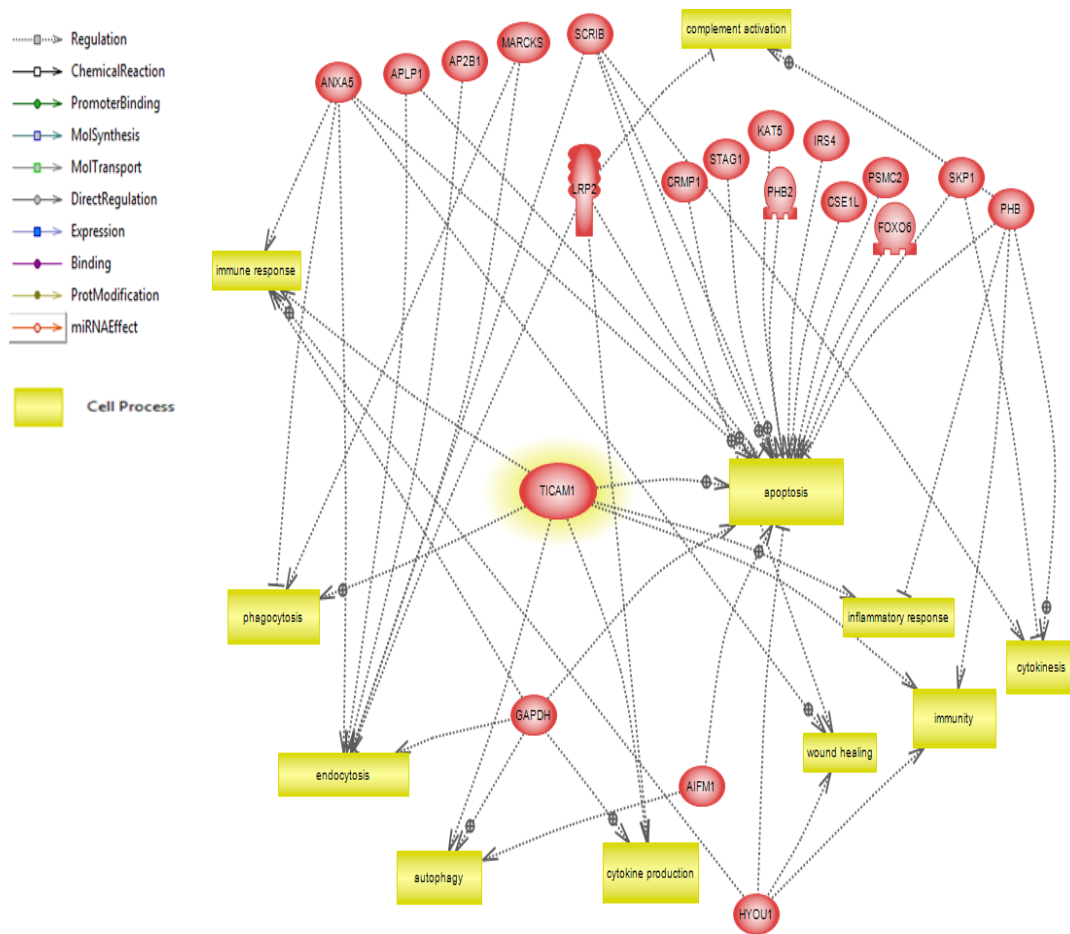


**Figure 3.23: Cell processes network of LPS-dependent TRIF interacting proteins.** HEK293-TLR4 were transfected with HA-TRIF. After 20 h, cells were stimulated with 1  $\mu\text{g/ml}$  LPS for 40 min followed by IP of HA-TRIF and LC-MS analysis of the TRIF-IP complex. The newly identified protein interactors were uploaded to Pathway Studio software analysis program and cell processes network was constructed. Red entities indicate proteins that were identified in TRIF IP-complex. Yellow entities indicate cellular processes that are co-regulated by the identified proteins and TRIF. TRIF (Ticam-1) is indicated in red with yellow surround. Grey dotted lines indicate regulation.

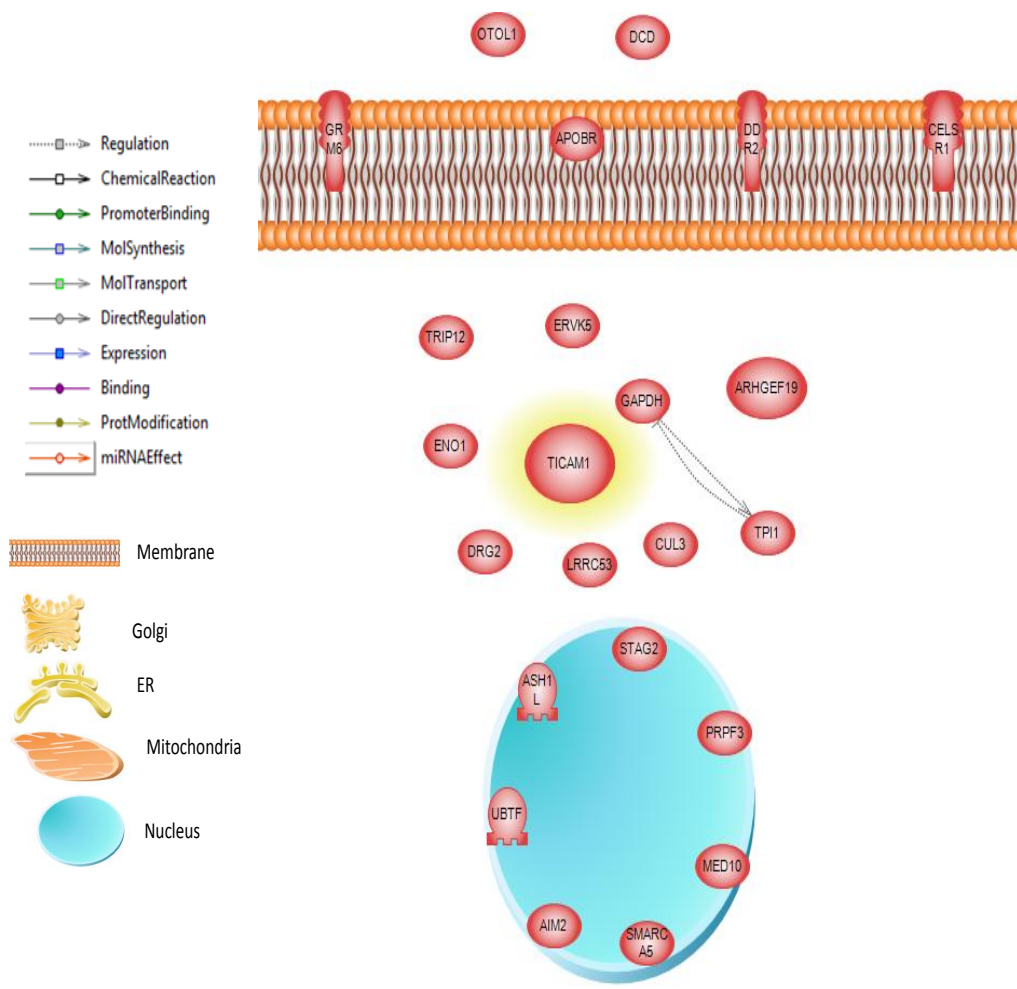


**Figure 3.24: Direct interaction network of LPS-dependent TRIF interacting proteins.** HEK293-TLR4 were transfected with HA-TRIF. After 20 h, cells were stimulated with 1  $\mu\text{g/ml}$  LPS for 60 min followed by IP of HA-TRIF and LC-MS analysis of the TRIF-IP complex. The newly identified protein interactors were uploaded to Pathway Studio software programme and direct interaction network was constructed. Red entities indicate proteins that were identified in TRIF IP-complex. TRIF (Ticam-1) is indicated in red with yellow surround. Grey dotted line indicates regulation.

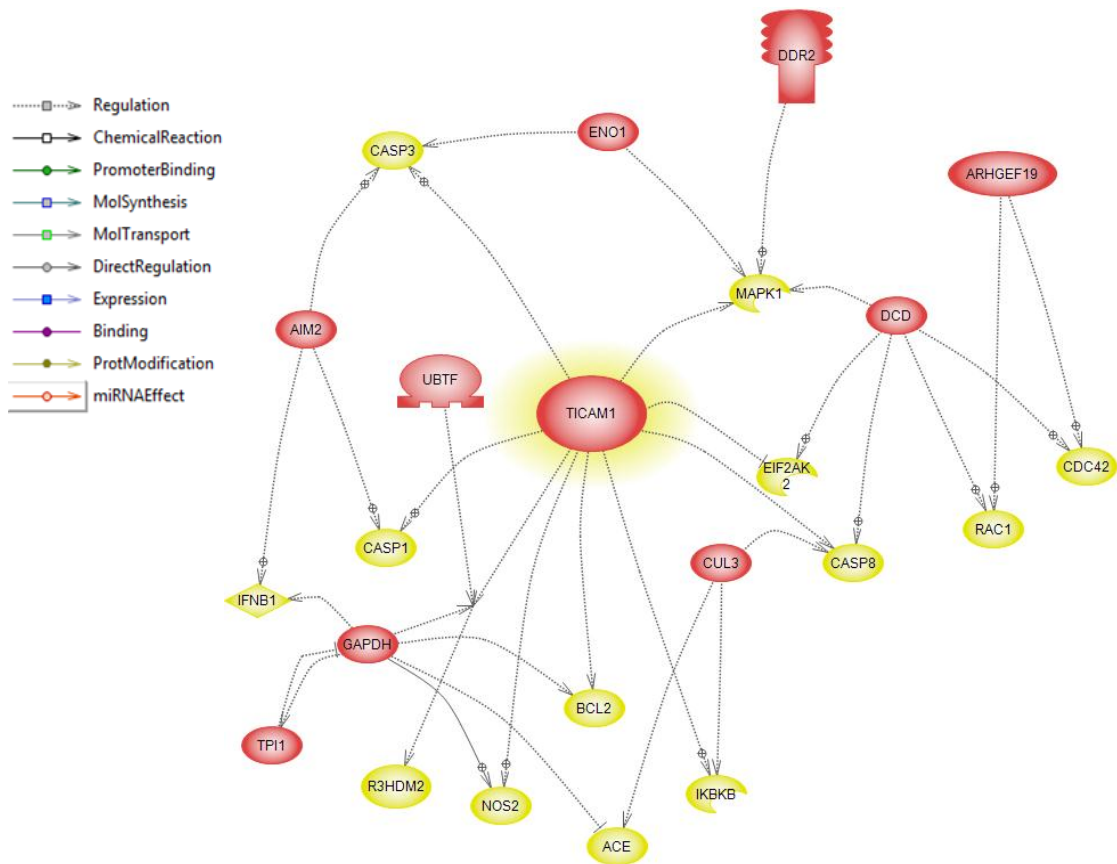


**Figure 3.25: Common targets network of LPS-dependent TRIF interacting proteins.** HEK293-TLR4 were transfected with HA-TRIF. After 20 h, cells were stimulated with 1  $\mu\text{g/ml}$  LPS for 60 min followed by IP of HA-TRIF and LC-MS analysis of the TRIF-IP complex. The newly identified protein interactors were uploaded to Pathway Studio software programme and common targets network was constructed. Red entities indicate proteins that were identified in HA-TRIF IP-complex. Yellow entities indicate proteins that are co-regulated by the identified proteins and TRIF. TRIF (Ticam-1) is indicated in red with yellow surround. Grey dotted lines indicate regulation.

family. It can sense double-stranded DNA (dsDNA) in the cytoplasm and through its pyrin domain (PYD) can form an inflammasome to activate caspase-1 and induce cell death (Hornung et al., 2009; Jones et al., 2010; Panchanathan et al., 2010). Moreover, knockdown of AIM2 abrogates caspase-1 activation in response to cytoplasmic double-stranded DNA and the double-stranded DNA vaccinia virus (Hornung et al., 2009). Interestingly, different studies showed that TRIF is involved in caspase-1 activation and the processing of IL-1 $\beta$  (Harder et al., 2009; Lamkanifi et al., 2009). AIM2 is the second inflammasome component to be identified in TRIF IP-complex. As mentioned earlier, NLRP1 was also identified in HEK-TLR3 independent of poly(I:C) stimulation. Collectively, these data suggest a potential role for TRIF in inflammasome activation. Importantly, cell processes network analysis showed that most of the newly identified proteins and TRIF were involved in regulation of apoptosis, innate immune response, cytokine production, inflammatory response, virulence, immunity and autophagy (Figure 3.26). The newly identified protein  $\alpha$ -Enolase shared with TRIF the regulation of inflammatory response, virulence, apoptosis cellular immune response (Figure 3.26). Interestingly,  $\alpha$ -Enolase and TRIF was also showed to be involved in regulation of MAPK1 and Caspase-3 (Figure 3.25).  $\alpha$ -Enolase is an abundantly expressed glycolytic enzyme that is expressed in most tissues. High level  $\alpha$ -Enolase expression has been demonstrated in the plasma of patients with lung, breast and prostate carcinomas (Georges et al., 2011). Moreover, an anti- $\alpha$ -Enolase antibody were found in in various systemic autoimmune diseases such as SLE, mixed and cryoglobulinemia (MC) and RA, suggesting that the alpha-Enolase autoantigen may drive these chronic inflammatory diseases (Andrew et al., 2005; Pratesi et al., 2000). Interestingly, it has been reported that the TLRs signalling pathways intensively contribute to the pathogenesis of RA and SLE (Montero and Martin, 2009; Roelofs et al., 2005; Wähämaa et al., 2011). In addition, immune reactivity of TLR2, TLR3, TLR4 and TLR7 was demonstrated in RA synovial lining (Takagi et al., 2011). Moreover, TLR ligands, such as PGN, CpG DNA, heat shock proteins and RNA from both infectious organisms and endogenous necrotic cells, have been identified in the joints of RA patients (Van der heijden et al., 2000; Brentano et al., 2005).

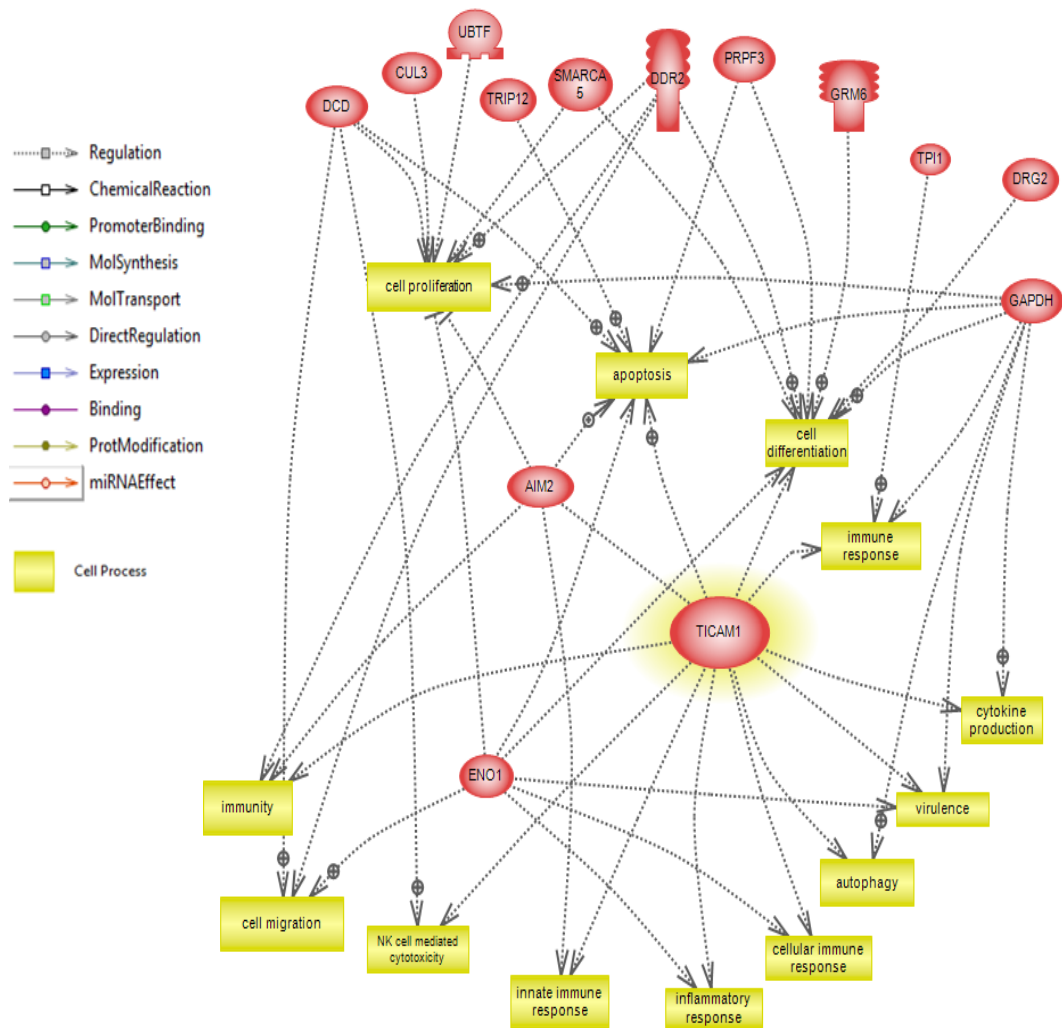


**Figure 3.26: Cell processes network of LPS-dependent TRIF interacting proteins.** HEK293-TLR4 were transfected with HA-TRIF. After 20 h, cells were stimulated with 1  $\mu$ g/ml LPS for 60 min followed by IP of HA-TRIF and LC-MS analysis of the TRIF-IP complex. The newly identified protein interactors were uploaded to Pathway Studio software analysis program and cell processes network was constructed. Red entities indicate proteins that were identified in TRIF IP-complex. Yellow entities indicate cellular processes that are co-regulated by the identified proteins and TRIF. TRIF (Ticam-1) is indicated in red with yellow surround. Grey dotted lines indicate regulation.

Collectively, these data showed that both TRIF and the newly identified proteins share the regulation and modulation of many proteins and cellular processes respectively and that these proteins may positively or negatively modulate TRIF activity during these cellular processes.

#### **3.2.4 Co-immunoprecipitation of TRIF and novel interactors**

Using proteomics, it is clear that a number of potentially interesting proteins and signalling pathways that may modulate TRIF functionality were identified. To validate whether TRIF and the newly identified protein interact, co-immunoprecipitation experiments were performed. Interactions were confirmed by co-immunoprecipitation of epitope-tagged TRIF and the selected protein of interest in HEK293-TLR3 or HEK293-TLR4 cells. Thereafter, endogenous co-immunoprecipitation experiments were performed in the human astrocytoma cell line U373-CD14. The proteins selected for further study were disintegrin and metalloproteinase domain-containing protein 15 (ADAM15) and segment polarity protein dishevelled homolog (DVL) 3. The interactions between TRIF and these two proteins were confirmed by overexpression and endogenously. ADAM15 was selected for further study as is well known as inflammatory mediator and reported to play important role in RA, Osteoarthritis (OA) and cancer (Charrier-Hisamuddin et al., 2008; Böhm et al., 2010). The link between TLRs, RA and cancer was already mentioned. Moreover, our group are interested in investigating the role of TLRs in RA and OA. Thus, it was of interest to us to further examine the role of ADAM15 in TRIF-mediated TLR signalling. As already discussed, DVL3 is important activator of Wnt signalling pathways and intersections between TLR and Wnt signalling pathways have been reported. (Blumenthal et al., 2005; Staal et al., 2008; Neumann et al., 2009). Therefore, the regulatory role of DVL3 in TLR signalling was investigated. Also, as already indicated, proteomic analysis showed that AIM2 was present in the TRIF immunocomplex following stimulation of HEK293-TLR4 cells with LPS for 60 min. Thus, co-immunoprecipitation experiments were performed to further explore whether TRIF and AIM2 interact. However, for some reason overexpression of AIM2 was not possible. Different concentrations of AIM2 were used in combination with TRIF. Also, expression of AIM2 alone did not result in its expression. Thus, further validation of the interaction between TRIF and AIM2 will be needed to establish whether they interact. Also, the ability of many of the other proteins identified using the proteomics approach, to interact with TRIF and to modulate TLR3

and TLR4 signalling requires further research. Regarding ADAM15 and DVL3, it was found that both of these proteins co-immunoprecipitate with TRIF and modulate TLR3 and TLR4 signalling. Their functional involvement in TRIF dependent signalling will be discussed in Chapters 4 and 5.

### 3.3 Discussion

In this study immunoprecipitation of overexpressed human HA-TRIF in HEK293-TLR3 and HEK293-TLR4 was performed and a multi-TRIF protein complex was analysed using LC-MS. Many novel protein hits have been identified, but unfortunately, TRIF and its known binding partners e.g. TLR3, TBK1, TRAF6, and IRFs, were not identified. However, these proteins maybe present in the IP complex but their concentrations were less than the detectable level. Another issue regarding the use of LC-MS technique is the reproducibility of sample analysis. Additionally, the complexity of this technique leads to variation in the peptides and proteins identified. Nevertheless, these variations could be due to different factors including the biological nature of the samples and minor differences in liquid- chromatography (Pelikan et al., 2007; Tabb et al., 2010). These heighlight the limitations of the LC-MS technique. It must be emphasised that whilst HA-TRIF was not detected by LC-MS, it was detected by immunoblot analysis. Regarding the detection of HA-TRIF by LC-MS, further optimisation may be required. For example, different IP conditions or digestion of the proteins using enzymes other than trypsin. Additionally, more sensitive proteomics approaches may be utilised e.g. using an OrbitRAP mass analyser. It is possible that TRIF itself may not be suitable for in-gel proteomics analysis for various reasons such as an inability to migrate through the gel at sufficient levels to permit detection by LC-MS. Thus, gel-free proteomics approaches may be used in the future. Concerning the above mentioned issues regarding the use of this approach all of the protein interactors identified in this study require additional validation by more direct experiments.

Though many of the proteins identified in the current study did not show a direct interaction with TRIF (as per Pathway Studio networks), they are commonly regulated by many proteins and many cellular processes. Recently, Zhang et al. (2011) identified DDX1, DDX21 and DHX36 as dsRNA sensors that use the TRIF pathways to activate type I IFN responses independently of TLR3 in myeloid dendritic cells (mDCs). Using a proteomics approach, DDX3X and DDX28 were identified in the current study following poly(I:C) stimulation of cells for 40 and 60 min, respectively. Phosphoinositide-3-kinase catalytic beta polypeptide (p85 $\beta$ ), a subunit of Phosphoinositide 3-kinases (PI3K), was identified in HEK293-TLR3 at time point zero and 60 min following poly(I:C) stimulation. PI3K has been shown to physically interact with TRIF. Interestingly, pharmacological inhibition of PI3K in monocyte-derived

dendritic cells (DCs) was found to enhance IFN- $\beta$  expression upon TLR3 or TLR4 engagement (Aksoy et al., 2005). However, in the same models of DCs activation, PI3K inhibition increased DNA-binding activity of NF- $\kappa$ B, but not IRF (Aksoy et al., 2005). Another interesting protein identified is the NF- $\kappa$ B repression factor (NRF), which was identified in HEK293-TLR3 independent of poly(I:C) stimulation. NRF is a nuclear inhibitor of NF- $\kappa$ B protein that can silence the IFN- $\beta$  promoter via binding to negative regulatory element (NRE) (Nourbakhsh et al., 1999). This provides a link between NRF and the NF- $\kappa$ B pathway. Identification of NLRP1 and AIM2, the core components of caspase-1-activating inflammasomes (Faustin et al., 2009), in this screening suggest that TRIF may play a role in inflammasomes activation and so, further investigation of NLRP1 and AIM2 in the context of TRIF signalling is essential.

Interestingly, in HEK293-TLR4 at time point zero, the adapter TBK1-binding protein 1 (TBKBP1) was identified in the TRIF IP-complex. TBKBP1 is an adapter protein which constitutively binds TBK1 and the inhibitor of nuclear factor kappa-B kinase subunit epsilon (IKBKE). TBKBP1 was thought to play a role in antiviral innate immunity but its exact functions are still not well known (Bouwmeester et al., 2004). Another interesting hit to look at is the Macrophage migration inhibitory factor (MIF) which was identified in HEK293-TLR4 cells following LPS stimulation for 20 min. MIF was originally identified as a T-cell-derived cytokine that inhibits the random migration of macrophages. MIF is proved to be an important pro-inflammatory cytokine secreted by most of the cells including T cells, macrophages, endothelial cells and smooth muscle cells. It induces the production of a large number of inflammatory mediators such as TNF- $\alpha$ , IL-1 $\beta$ , IL-6, and IL-8 (Calandra et al., 1994; Onodera et al., 2004). MIF was found to be involved in regulation of many and diverse immunological cellular processes as shown in Figure 3.20.

Nibrin which was identified in the TRIF immunocomplex in HEK293-TLR3 independent of poly (I:C) plays a critical role in the cellular response to DNA damage and the maintenance of chromosome integrity. Mutations in Nibrin cause the Nijmegen breakage syndrome (NBS), which is an autosomal recessive syndrome characterized by chromosomal instability, radiation sensitivity, immunodeficiency and predisposition to cancer, particularly to lymphoid malignancies (Varon et al., 1998; Kondratenko et al., 2007). This may link TRIF to diseases such as cancer.

Menin is another interesting protein to explore in the context of TRIF signalling. It is a tumour suppressor gene that its mutation causes the familial cancer syndrome

multiple endocrine neoplasia type 1 (MEN1) (Poisson et al., 2003). Heppner et al. (2001) found that NF- $\kappa$ B proteins p50, p52 and p65 were capable of directly interacting with Menin in vitro and in vivo. They suggested that Menin repressed p65-mediated transcriptional activation on NF- $\kappa$ B sites in a dose-dependent and specific manner.

In conclusion, this study has provided an insight into the TRIF interactome and to the best of my knowledge this is the first study performed to investigate the TRIF protein complex. Many of the proteins identified in the study are involved in the regulation of immunity, apoptosis, cell differentiation, viral reproduction, and cytokine production. However, more validatory experiments are needed to confirm their interaction with TRIF and the role that these proteins may play in regulating TLR signalling.

## **Chapter 4**

### **Investigating the novel role of human ADAM15 in TLR3 and TLR4 signalling**

## **4.1 Introduction**

### **4.1.1 Background**

Metalloproteases are a large family of important proteases that include matrix metalloproteases (MMPs) and proteins with a disintegrin and metalloproteinase domain (ADAM). They are also referred to as MDC (Metallo-protease, Disintegrin, Cysteine-rich) proteins (Rosenberg, 2009). ADAMs are members of the zinc protease superfamily and may be subdivided according to the primary structure of their catalytic sites. ADAMs belong to the metzincin subgroup which may be further divided into serralyins, astacins, matrixins, and adamalysins (Seals and Contrtneidge, 2003). Thus, ADAMs are MMPs which belong to the the matrixin subgroup of metzincin proteins. These enzymes are responsible for extracellular matrix degradation and remodelling and play important roles in development, wound healing, and in the pathology of diseases such as Rheumatoid arthritis (RA) and cancer (Visse and Nagase, 2003). ADAMs are found in vertebrates, as well as in *Caenorhabditis elegans*, *Drosophila*, and *Xenopus*. In contrast, ADAMs are not expressed in *Escherichia coli*, *Saccharomyces cerevisiae*, or plants (Seals and Contrtneidge, 2003). Several ADAMs are expressed as multiple splice variants *e.g.*, ADAM22, ADAM29 and ADAM30 exist as two to three splice variants that vary in terms of the length of their cytoplasmic tails, although no functional differences in these isoforms have been reported. In other cases, alternative splicing produces proteins with markedly different activity (Sagane et al., 1998; Cerretti et al., 1999).

### **4.1.2 ADAM Domain structure and function**

To date, about 40 members of the ADAMs family have been described in many different species (Paulissen et al., 2009). The domain structure of the ADAMs consists of a prodomain, a metalloprotease domain, a disintegrin domain, a cysteine-rich domain, an EGF-like domain, a transmembrane domain and a cytoplasmic tail (Figure 4.1).

#### **4.1.2.1 The Prodomain**

The signal sequence at the N-terminus directs ADAMs to the secretory pathway and the prodomain functions to facilitate the maturation of ADAMs. The prodomain keeps the metalloprotease site of ADAMs inactive through a cysteine switch. Several ADAMs are

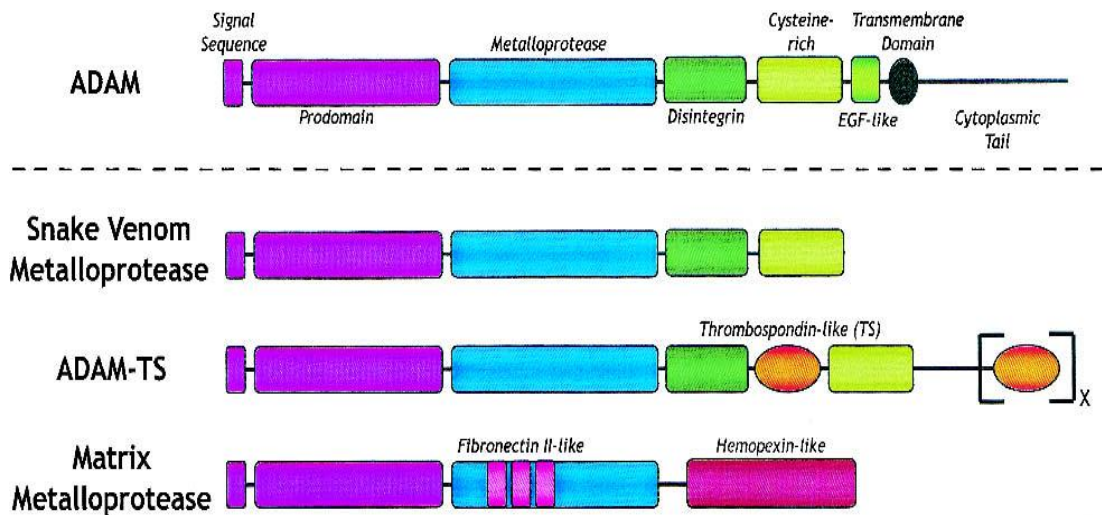


**Figure 4.1: Domain structure of ADAMs and MMPs.** The figure shows general domain structure of ADAMs compared to snake venom metalloproteases (SVMP), ADAMs with thrombospondin-like motif (ADMTS) and MMP. The MMP shown is of the gelatinase class. Other subclasses of MMPs lack hemopexin-like sequences and/or fibronectin type II-like sequences. It should be noted that alternative splicing results in some ADAMs lacking one or more domain. (Adapted from Seals and Contrneidge, 2003).

kept inactive state through the interaction of a cysteine residue at the prodomain with the zinc in the metalloprotease domain. During maturation which takes place in the endoplasmic reticulum, the prodomain is cleaved by furin or furin-like proprotein convertases, and the resulting protein constitutes the mature form with an active metalloprotease domain. However, maturation of some ADAMs such as ADAM8 and ADAM28 occurs as an autocatalytic process (Primakoff and Myles, 2000; Paulissen et al., 2009). The prodomain appears to be necessary for the correct folding of the ADAMs metalloprotease domain and to facilitate the transport of ADAMs through the secretory pathway (Blobel, 2005).

#### **4.1.2.2 The metalloprotease domain**

The metalloprotease domain contains zinc and water atoms that are necessary for the hydrolytic processing of protein substrates, and which are coordinated by three conserved histidine residues and a downstream methionine. Whilst all ADAMs possess a metalloprotease domain, only about 50 % exhibit protease activity. ADAMs which display protease activity include ADAM 8, 9, 10, 12, 15, 17, 19, 28, and 33 (Duffy et al., 2011). Once activated, ADAMs regulate many biological functions, including proteolysis, cell adhesion, cell fusion, inflammation, angiogenesis and intracellular signalling. Several ADAM family members have been found to mediate the release of cytokines, growth factors, receptors, adhesion molecules and other membrane bound proteins from the cell surface, a process termed ectodomain shedding (Nath et al., 1999; Zhong et al., 2008). Examples of cell surface proteins shed by ADAMs include the IL-6 receptor, FAS-ligand, transforming growth factor  $\alpha$  (TGF $\alpha$ ) and TNF $\alpha$ , (Zigrino et al., 2007). Inhibitors of ADAMs metalloprotease activity fall into four broad classes: those that inhibit by denaturation, those that inhibit by Zn-chelation, small molecule inhibitors and tissue inhibitors of metalloproteases (TIMPs). The first two categories represent non-selective inhibitors such as reducing agents or zinc chelating agents. The third class arose from efforts to develop inhibitors of both MMPs and ADAMs, and include hydroxamate-based inhibitors that bind competitively to the active site. Tissue inhibitors of metalloproteases, or TIMPs, are endogenous regulators of MMPs and ADAMs. Four TIMPs are now known and they cause inactivation by binding to the catalytic site of MMPs. However, the TIMPs are not totally selective for MMPs, TIMP3 also inhibits ADAM17 and ADAM12. ADAM10 is inhibited by both TIMP1 and TIMP3 but not all

ADAMs are sensitive to TIMP3. ADAM8 and ADAM9 processing of myelin basic protein is not inhibited by any TIMP (Amour et al., 2000; Loechel et al., 2000).

#### **4.1.2.3 The disintegrin domain**

The disintegrin domain within ADAMs is approximately 90 amino acids in length and displays sequence similarity to the disintegrin domain in snake venom metalloproteases (SVMPs). Disintegrins have an arginine-glycine-aspartic acid (RGD) integrin-binding site, bind to the platelet integrin GPIIb-IIIa ( $\alpha_{IIb}\beta_3$ ) and inhibit platelet aggregation (Primakoff and Myle, 2000; Seal and Contrtneidge, 2003). Human ADAM15 is the only known ADAM to contain a RGD binding site in the disintegrin domain. (Chen et al., 2008; Zhong et al., 2008).

#### **4.1.2.4 The cysteine-rich and EGF-like domains**

The function of the cysteine-rich and EGF-like domains is not fully understood. Structurally, the cysteine-rich and EGF-like domains are approximately 160 amino acids in length. The two domains may be important for interaction or cell fusion of ADAMs with other proteins such as chaperons. In some cases, the cysteine-rich region has been implicated in regulating protease activity and controlling substrate specificity (Reiss et al., 2006). It is also believed that the cysteine-rich domain complements the binding capacity of the disintegrin domain (Serrano et al., 2005). Surprisingly, ADAM10 and ADAM17, the only known ADAMs lacking the EGF-like domain, are the most effective at ectodomain shedding. This suggests that the EGF-like-domain may hinder the ectodomain shedding (Page-McCaw et al., 2007).

#### **4.1.2.5 The cytoplasmic tail**

The cytoplasmic tail of the ADAMs family is highly variable both in length and in sequence and serves to transduce signals between the interior and exterior of cells. Phosphorylation dependent and independent protein interactions with the cytosolic tail of ADAMs have been shown to regulate their maturation, subcellular localization and metalloprotease activation (Seal and Contrtneidge, 2003). The domain contains specialized motifs. The most common motifs are PxxP binding sites for SH3 domain-containing proteins. These SH3-binding sites are present in human ADAMs 7, 8, 9, 10, 12, 15, 17, 19, 22, 29, and 33. Several ADAMs also have potential phosphorylation sites for serine-threonine and/or tyrosine kinases. Consequently, ADAMs may serve as

adaptors to facilitate the assembly of protein complexes at critical functional locations (Yong et al., 2001; Seal and Contrtneidge, 2003).

#### **4.1.3 Subcellular localisation of ADAM**

Data indicate that ADAMs are probably synthesized in the rough endoplasmic reticulum and mature in the late Golgi compartment. Maturation involves the removal of the prodomain from the ADAM precursor protein, which facilitates the activation of the metalloprotease domain of ADAMs (Roghani et al., 1999; Hougaard et al., 1999). Some studies have showed that certain ADAMs reside in a region near the nucleus. However, ADAMs can also be detected on the cell surface. For example, ADAMs 9, 10, 15 and 17 are expressed on the cell surface in a processed catalytically active form (Black et al., 1997; Hougaard et al., 1999; Lammich et al., 1999). Thus, the subcellular localization and activity of ADAMs depends on the specific ADAM, the cell type and the substrate involved.

#### **4.1.4 ADAM-mediated shedding**

ADAMs facilitate the shedding of cytokines, cytokine receptors and growth factors (Herren et al., 2002). One of the most well-studied members of the ADAMs family, TNF converting enzyme (TACE) also called ADAM17 (Black et al., 2002). It has been implicated in the release of multiple transmembrane molecules including TNF $\alpha$ , TNFRII (p75) and L-selectin. It was shown that TNF $\alpha$  processing was significantly inhibited in ADAM17 knockout mice, though limited processing of TNF $\alpha$  can still occur in cells derived from ADAM17-deficient mice. This residual sheddase activity is inhibited by the metalloprotease inhibitor IC-3, suggesting that other ADAMs family members may also process TNF $\alpha$  (Reddy et al., 2000). A dominant negative form of ADAM17, which lacks a metalloprotease domain, blocked the proteolysis of the TNF receptor (Solomon et al., 1999). Also, IL-1 receptor-II shedding does not occur in ADAM17-deficient fibroblasts. In fact, reconstitution of these cells with ADAM17, but not ADAM10 was capable of restoring shedding (Reddy et al., 2000). Other molecules that have been reported to be cleaved by ADAMs are the extracellular matrix proteins, type IV collagen, gelatine and fibronectin (Millichip et al., 1998; Alfandari et al., 2001; Martin et al., 2002). It is speculated that such activity may assist in cell migration.

#### **4.1.5 ADAMs and human diseases**

ADAMs have been implicated in a variety of human disease processes, such as cancer, neuroinflammation, Alzheimers's disease and RA. Studies from cell lines grown in culture, animal models and human malignancies suggest that a number of ADAMs are involved in cancer formation and/or progression, for example, ADAM9, 10, 12, 15 and 17 (Duffey et al., 2009). ADAMs could potentially promote cancer formation/progression through several different mechanisms *e.g.*, release or activation of growth factors. Many growth factors are initially synthesised as inactive transmembrane precursor proteins that require conversion and the best-studied of these are the EGFR/HER family of ligands. All of these receptors, apart from HER2, can be directly activated following ligand binding leading to activation of several different signalling pathways including the MAPK, the PI3K and the janus kinase/signal transducer and activator of transcriptional (JAK/STAT) pathways. Activation of these signalling events results in activation of the classical hall markers of malignancy such as enhanced cell proliferation and increased cell survival (Bublil et al., 2007).

#### **4.1.6 The ADAM15 gene**

ADAM15 is a type I transmembrane glycoprotein belonging to the ADAMs proteins family and is widely expressed in different tissues and cell types with high level in vascular cells, the endocardium bone and some region in the brain (Zhong et al., 2008; Klino et al., 2009). Human ADAM 15 is located at 1q21.3 of chromosome 1, and was cloned in 1996 from MDA-MB-468 adenocarcinoma cells (Krätzschmar et al., 1996). The chromosomal region 1q21.3 has been reported to contain genes amplified in breast cancer and sarcomas, thus suggesting an association between ADAM15 and cancer (Kuefer et al., 2006). Human ADAM15 gene contains 23 exons varying in length from 63 to 316 bp, and 22 introns (from 79 to 1283 bp). Exons 19-21 are used alternatively in human tissues (Kleino et al., 2007; Lu et al., 2010). Alternative mRNA splicing generates several ADAM15 isoforms which contain different combinations of putative Src homology-3 (SH3) domain binding sites in their cytosolic tails. A total of 6 isoforms of ADAM15 have been described, and an alternative use of ADAM15 exons was found to profoundly influence selection of SH3-containing cellular partner proteins. Also, the amino acid sequence of the cytoplasmic tail of ADAM15 contains potential tyrosine phosphorylation sites, suggesting that ADAM15 could interact with SH2 domain-containing proteins via phosphotyrosines, as well as potential serine and

threonine phosphorylation sites. Indeed, interaction of ADAM15 with Src, growth factor receptor binding protein2 (Grb2), endophilin, p85 (the regulatory subunit of Phosphatidylinositol-3 kinases) and mitotic arrest deficient2 (MAD2) has been reported (Howard et al., 1999; Poghosyan et al., 2002; Zhong et al., 2008). Thus, ADAM15 is involved in regulating many cellular signalling pathways. Also, alternative mRNA splicing provides a useful mechanism through which ADAM15 may regulate intracellular protein interactions which may help explain the association of some, but not all, ADAM15 isoforms with cancer (Yasui et al., 2004; Kleino et al 2009).

The human ADAM15 has also been termed metargidin (for metalloprotease-RGD disintegrin) as it is the only ADAM which contains an RGD sequence in a similar position to that in snake venom disintegrins. Interestingly, the mouse and rat orthologues of ADAM15 lack an RGD sequence. The presence of the RGD sequence suggests a specific role for ADAM15 in integrin binding and therefore, in cell-cell interactions (Lum et al., 1998; Horiuchi et al, 2003). Although human ADAM15 can indeed interact with RGD-binding integrins  $\alpha v\beta 3$  and  $\alpha 5\beta 1$ , the mouse ADAM15 does not. Instead, the mouse ADAM15 has been implicated as a ligand for integrin  $\alpha 9\beta 1$ . Both the human and mouse ADAM15 contain a catalytic site consensus sequence for zinc-dependent metalloproteases and purified recombinant ADAM15 is catalytically active. Known ADAM15 substrates include FGFR2iiiib and N- and E-cadherin, the shedding of which has been implicated in prostate and breast cancer pathogenesis (Klino et al., 2009).

Atherosclerosis is a chronic inflammatory disorder that is the underlying cause of most cardiovascular diseases. Interestingly, ADAM15 expression was detected in the macrophage-rich regions of atherosclerotic lesions (Herren et al., 1997). This work demonstrated that ADAM15 was upregulated during atherosclerosis suggesting a potential involvement of ADAM15 in this pathology. Also, upregulation of  $\alpha 5\beta 1$  and  $\alpha v\beta 3$  integrins was detected in atherosclerosis (Al-Fakhri, et al., 2003). These integrins bind to ADAM15 and have been shown to be involved in the development and progression of atherosclerosis. These findings suggest that ADAM15 expressed on endothelial cells could act as a receptor for platelets or as a receptor involved in the recruitment of immune cells during inflammation (Al-Fakhri et al., 2003; Nath et al., 1999). Also, upregulation of ADAM15 mRNA and protein levels during inflammatory bowel disease (IBD) was detected, suggesting a role of ADAM15 in intestinal inflammation (Mosnier et al., 2006). ADAM15 has been also shown to be involved in

RA, an inflammatory degenerative joint disease, whereby ADAM15 may be involved in cleaving extracellular matrix (ECM) components such as gelatin and IV collagen (Martin et al., 2002).

Herein, following the immunoprecipitation of TRIF and analysis of interacting partners using LC-MS techniques, ADAM15 was identified as a novel TRIF interacting partner following stimulation of HEK293-TLR3 cells with poly(I:C) for 60 min. Interestingly, TRIF and ADAM15 coimmunoprecipitated in a ligand-independent manner in HEK293-TLR4 cells. The aim of this chapter was to investigate the role played by ADAM15 in TRIF mediated TLR3 and TLR4 signalling.

## 4.2 Results

### 4.2.1 ADAM15 interacts with TRIF

Analysis of TRIF interacting partners using a proteomics approach revealed that TRIF interacted with ADAM15. Thus, to confirm the interaction, co-immunoprecipitation of epitope-tagged TRIF (HA-TRIF) with epitope tagged ADAM15 (V5-ADAM15) was performed in HEKT293-TLR3. Cells were transfected with HA-TRIF and EV, or HA-TRIF and V5-ADAM15 and treated as indicated. Thereafter, immunoprecipitation of HA-TRIF was performed as described (Materials and methods, section 2.2.9). As shown in Figure 4.2 panel A, ADAM15 co-immunoprecipitated with TRIF following stimulation of cells with poly(I:C) for 60 min and there is no association in the absence of poly(I:C). It should be mentioned that downregulation of TRIF expression was observed when co-expressed with ADAM15 and that ADAM15 probably causing TRIF processing (discussed in more details in section 4.2.9). Interestingly, in HEK293-TLR4 cells, proteomics analysis showed that ADAM15 interacted with TRIF in a ligand independent manner and suggests that TLR4 or another auxiliary molecule may facilitate ligand-independent interaction of ADAM15 with TRIF when TLR4 is overexpressed in the cell. Many different anti-human TRIF antibodies were tested for their ability to detect TRIF, especially at the endogenous level. It was found that an anti-TRIF polyclonal antibody obtained from Exalpa detected endogenous TRIF and was chosen for IP and western blot (discussed further in chapter 6). Thereafter, IP of endogenous TRIF from human astrocytoma cell line U373-CD14 was performed as described (Materials and methods, section 2.2.10). These cells were used as a model since they express TLR3 and TLR4 mRNA and respond well to poly(I:C) and LPS. As illustrated in Figure 4.2, panel B, endogenous ADAM15 interacted with endogenous TRIF following stimulation of U373-CD14 cells with poly(I:C) and LPS for 60 and 20 min, respectively. The interaction of TRIF with ADAM15 upon LPS stimulation for 20 min was also confirmed by LC-MS analysis of the endogenous TRIF immunocomplex (discussed further in chapter 6).

### 4.2.2 ADAM15 inhibited TRIF-dependent reporter gene assays

Initially, the ability of ADAM15 to modulate TRIF-mediated luciferase reporter gene activity was investigated. Thus, HEKT293 cells were transiently transfected with the NF- $\kappa$ B, IFN- $\beta$  and CCL5 (Rantes) reporter gene constructs and increasing amounts of

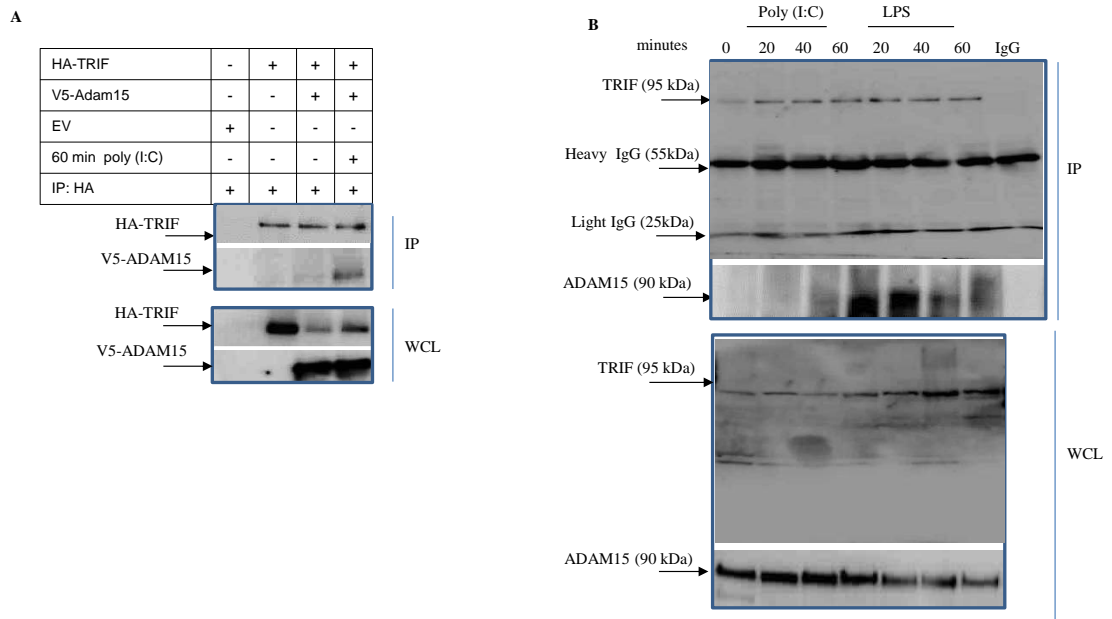


**Figure 4.2: Co-immunoprecipitation of human TRIF and human ADAM15.** (A). HEK293-TLR3 were seeded into 6 well plates. When the cells become confluent (80 %), cells were co-transfected with 2  $\mu$ g of HA-TRIF and 1  $\mu$ g of EV or co-transfected with 2  $\mu$ g of HA-TRIF and 1  $\mu$ g of V5-ADAM15. 20 h after transfection, cells were left unstimulated or stimulated with 20  $\mu$ g/ml poly(I:C) for 60 min. Thereafter cells were lysed in lysis buffer (50 mM HEPES, pH 7.5, 150 mM NaCl, 2 mM EDTA, pH 8.0, 1 % NP-40, 0.5 % sodium deoxycholate supplemented with 1 mM PMSF, 1 mM DDT, 1 mM NaVO<sub>3</sub>, 5 mM EGTA and protease inhibitor cocktail). Cleared cell lysates were incubated with 1  $\mu$ g of anti-HA monoclonal antibody precoupled to 50  $\mu$ l of Protein A/G Plus-Agarose beads for 2 h at 4 °C with gentle shaking. Immunoprecipitation complexes were washed 4 times with lysis buffer and then released from the beads by addition of 40  $\mu$ l of Laemmli loading buffer, followed by boiling for 5 min. Proteins were separated by SDS-PAGE gel electrophoresis and subjected to immuno-blotting using anti-HA and anti-V5 monoclonal antibodies. (B) U373-CD14 cells were cultured into T175 flasks. When the cells were 90-95 % confluent, they were stimulated with either 20  $\mu$ g/ml poly(I:C) or 1  $\mu$ g/ml LPS for time indicated. Thereafter cells were scrapped into 10 ml ice cold PBS and spun down for 10 min at 4 °C at 220 g. Cell pellets were lysed as per panel A and cleared cell lysates were incubated with 2  $\mu$ g of anti-hTRIF polyclonal antibody precoupled to 50  $\mu$ l of Protein A/G Plus-Agarose beads for 2 h at 4 °C with gentle shaking. Proteins were separated by SDS-PAGE gel electrophoresis and immunoblot analysis was performed using anti-hTRIF (Exalpa) and anti-hADAM15 (R&D) antibodies. Rabbit IgG (Sigma) was used as negative control. Images were captured using the G: box system (Syngene). Results represent at least three independent experiments.

ADAM15 in the presence of a constant concentration of TRIF or MyD88. Overexpression of ADAM15 significantly inhibited TRIF-dependent activation of the NF- $\kappa$ B, IFN- $\beta$  (p125-luc) and Rantes reporter genes (Figure 4.3 panels A, B and C). Moreover, overexpression of ADAM15 also significantly inhibited TRIF-dependent activation of the NF- $\kappa$ B-driven PRDII and IRF3/IRF7-dependent PRDIII-I reporter genes (Figure 4.3 panels D and E). As a control, the effect of ADAM15 on MyD88 driven NF- $\kappa$ B, IFN- $\beta$  and Rantes promoter activity was also tested. Overexpression of ADAM15 significantly inhibited MyD88-dependent activation of the NF- $\kappa$ B and Rantes promoter (Figure 4.3 panels F and H). However, overexpression of low levels of ADAM15 (5-20 ng) increased MyD88 dependent activation of the IFN- $\beta$  (p125-luc) reporter gene (Figure 4.3 panel G).

#### **4.2.3 ADAM15 inhibited TLR3 and TLR4-mediated reporter gene activity**

AS TRIF mediates TLR3 and TLR4 signalling, the effect of ADAM15 on TLR3 and TLR4-dependent NF- $\kappa$ B, IFN- $\beta$  and Rantes activation was investigated using HEK293 cells stably expressing either TLR3 or TLR4. In HEK293-TLR3 cells, overexpression of ADAM15 significantly inhibited TLR3-dependent activation of NF- $\kappa$ B, IFN- $\beta$  and Rantes reporter genes (Figure 4.4). Interestingly, the inhibition effect on the reporter gene activation of NF- $\kappa$ B and Rantes was stronger than the effect on IFN- $\beta$  reporter gene activity (Figure 4.4 panels A-C). Furthermore, in HEK293-TLR4 cells, overexpression of ADAM15 significantly reduced TLR4-dependent NF- $\kappa$ B, IFN- $\beta$  reporter gene activation (Figure 4.4 panels D and E). In our hands, HEK293-TLR4 cells did not induce LPS mediated activation of the Rantes reporter gene. Also, there was difficulty using HEK293-TLR4 for reporter gene assays as the fold induction of NF- $\kappa$ B, IFN- $\beta$  relative luciferase activity (RLA) was always low when compared to HEK293-TLR3.

#### **4.2.4 Poly(I:C) increased ADAM15 transcription**

Some MMPs including MMP9 and MMP3 contain an NF- $\kappa$ B binding site in their promoter region that regulates their expression (Mishra et al., 2011). Moreover, it has been demonstrated that poly(I:C) induces MMP9 expression in HaCat keratinocytes through NF- $\kappa$ B, p38 MAPK and PI-3K signal transduction pathways (Voss et al., 2011). Therefore, the effect of poly(I:C) and LPS on ADAM15 transcription was investigated.

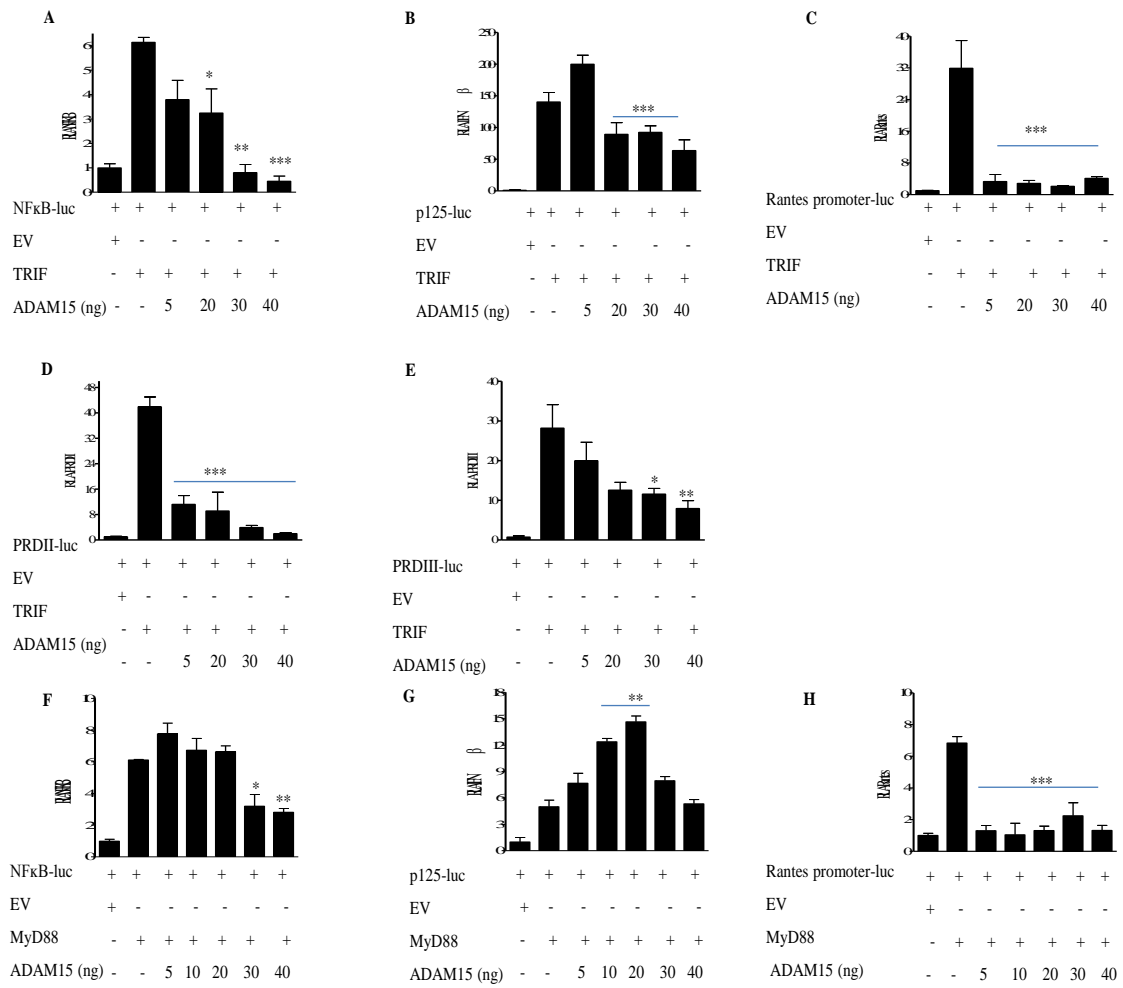


**Figure 4.3: ADAM15 inhibited TRIF-dependent reporter gene activity.** (A-E) HEKT293 cells were plated into 96 well plates at a density of  $5 \times 10^4$  cells/well. After 24 h, cells were transfected with expression vectors encoding either the reporter genes NF- $\kappa$ B (A), IFN- $\beta$  promoter p125 (B), Rantes (C), IFN- $\beta$  PRDII (D) or IFN- $\beta$  PRDIII-I (E) and co-transfected with either EV or expression vectors encoding the full length human HA-TRIF (20 ng) and increasing amounts of expression vectors encoding full length human V5-ADAM15 (5, 20, 30 and 40 ng) as indicated. After 24 h, cells were harvested and lysed. The cell lysates were stored at  $-80^\circ\text{C}$  for at least 24 h, followed by assessment of luciferase reporter gene activity. (F-H) HEKT293 cells were plated into 96 well plates at density of  $5 \times 10^4$  cells/well. After 24 h, cells were transfected with expression vectors encoding either reporter genes for the NF- $\kappa$ B (F), full-length IFN- $\beta$  promoter (p125) (G) and Rantes (H) as indicated, and co-transfected with either EV or an expression vector encoding full length human Myc-MyD88 (20 ng) and increasing amounts of an expression vector encoding full length human V5-ADAM15 as indicated. After 24 h, cells were lysed and the cell lysates were stored at  $-80^\circ\text{C}$  for at least 24 h. Thereafter, luciferase reporter gene activity was assessed using the dual luciferase system (Promega). The results presented are representative of at least three independent experiments, each experiment was done in triplicate. \*  $P < 0.05$ , \*\*  $P < 0.01$  and \*\*\*  $P < 0.001$ .

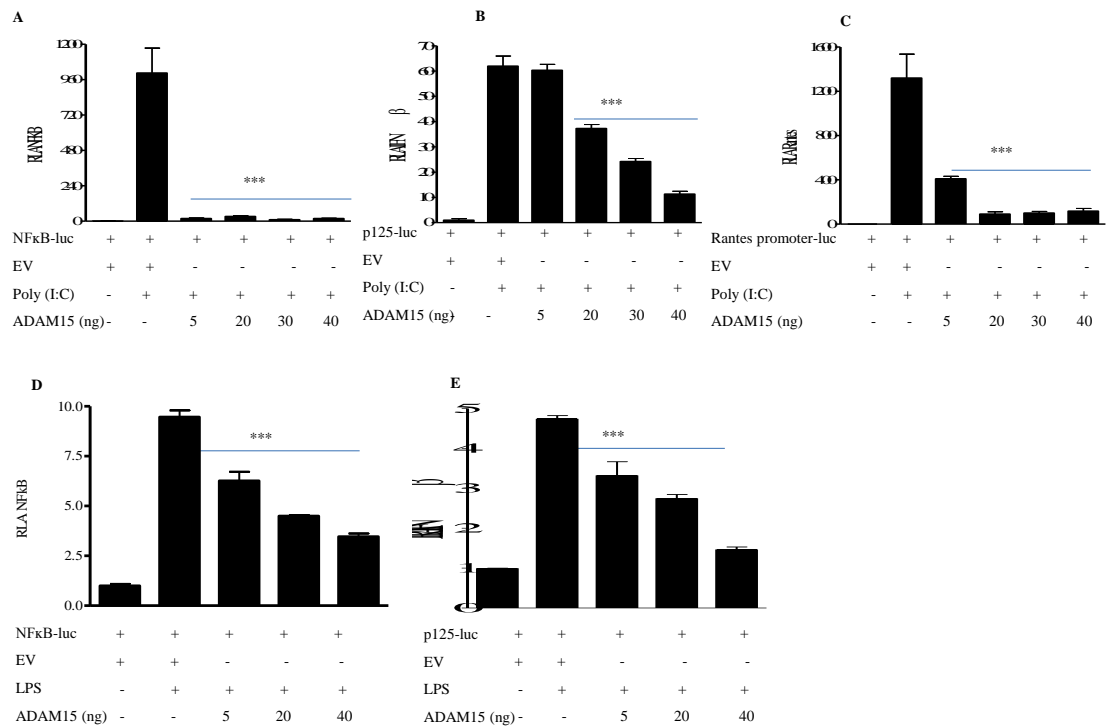


**Figure 4.4: Overexpression of ADAM15 inhibited TLR3 and TLR4 mediated reporter gene activity.** (A-C) HEK293-TLR3 cells were plated into 96 well plates at density of  $5 \times 10^4$  cells/well. After 24 h, cells were transfected with expression vectors encoding either the NF- $\kappa$ B (A), full-length IFN- $\beta$  promoter (p125) (B), or Rantes promoter (C) reporter gene plasmids, and co-transfected with either an EV or and increasing amounts of V5-ADAM15. After 24 h, cells were left untreated (control) or stimulated with 20  $\mu$ g/ml poly (I:C) for an additional 24 h, followed by harvesting of cell lysates. Cell lysates were left at  $-80^\circ\text{C}$  for at least 24 h and assessment of luciferase reporter gene activity was performed. (D and E) HEK293-TLR4 were transfected with reporter genes for the NF- $\kappa$ B (D) or full-length IFN- $\beta$  promoter (p125) (E), and co-transfected with either an EV or increasing amount of expression vector encoding full length human V5-ADAM15 as indicated. After 24 h, cells were left untreated (control) or stimulated with 1  $\mu$ g/ml LPS for 24 h, followed by harvesting and cell lysis. Cell lysates were left at  $-80^\circ\text{C}$  for at least 24 h, followed by assessment of luciferase reporter gene activity using dual luciferase system (Promega). The results presented are representative of at least three independent experiments each experiment was done in triplicate. \*\*\*  $P < 0.001$ .

using the human astrocytoma cell line U373-CD14 as a model. Cells were stimulated with either poly(I:C) or LPS for different time points followed by RNA isolation, cDNA synthesis and Q-RT-PCR. Poly(I:C) stimulation modestly increased ADAM15 mRNA compared to the control, while LPS did not have an effect on ADAM15 mRNA expression (Figure 4.5 panel A and B).

#### **4.2.5 Downregulation of ADAM15 by esiRNA.**

To investigate the role played by ADAM15 in TLR3 and TLR4 signalling, knockdown of ADAM15 was performed using MISSION esiRNA technology in U373-CD14 cells. MISSION esiRNA are end-ribonuclease prepared siRNA. They are a heterogeneous mixture of siRNAs that all target the same mRNA sequence. These multiple silencing triggers lead to highly specific and effective gene silencing. To monitor the knockdown, U373-CD14 cells were transfected with esiRNA-control or esiRNA against human ADAM15, then ADAM mRNA and protein levels were measured by using RT-PCR and immunoblotting, respectively. It was found that esiRNA significantly decreased ADAM15 mRNA compare to the control (Figure 4.6, panel A and B). In addition, the ADAM15 protein expression was also downregulated by the ADAM15 esiRNA compared to the control as measured by western blot (Figure 4.6, panel C).

#### **4.2.6 Suppression of ADAM15 expression enhanced IFN- $\beta$ , TNF- $\alpha$ and Rantes mRNA expression.**

To investigate the potential role of ADAM15 in TLR3 and TLR4 signalling, levels of IFN- $\beta$ , TNF- $\alpha$  and Rantes mRNAs were measured in U373-CD14 cells transfected with esiRNA control or esiRNA against ADAM15. After 48 h, cells were stimulated with either poly(I:C) or LPS for 3 h. Downregulation of ADAM15 significantly increased poly(I:C) and LPS induce IFN- $\beta$ , TNF- $\alpha$  and Rantes transcription compared to the control (Figure 4.7, panels A, B, C and F, G, H). Also knockdown of ADAM15 increased slightly the basal level of IFN  $\beta$  mRNA compared to the control (Figure 4.7 panel A and F). It has been reported that MMP9 secretion and activity was abolished in PC-3 cell line in response to ADAM15 reduction by short hairpin RNA technology (Najy et al., 2008). Furthermore ADAM15 has been shown to cleave the ectodomain of MMP10 (Tousseyn et al., 2009; Friedrichet et al., 2011). Therefore, the effect of ADAM15 knockdown on the transcription of these two MMPs was studied. Surprisingly, reduction of ADAM15 significantly increased poly(I:C) induced MMP9

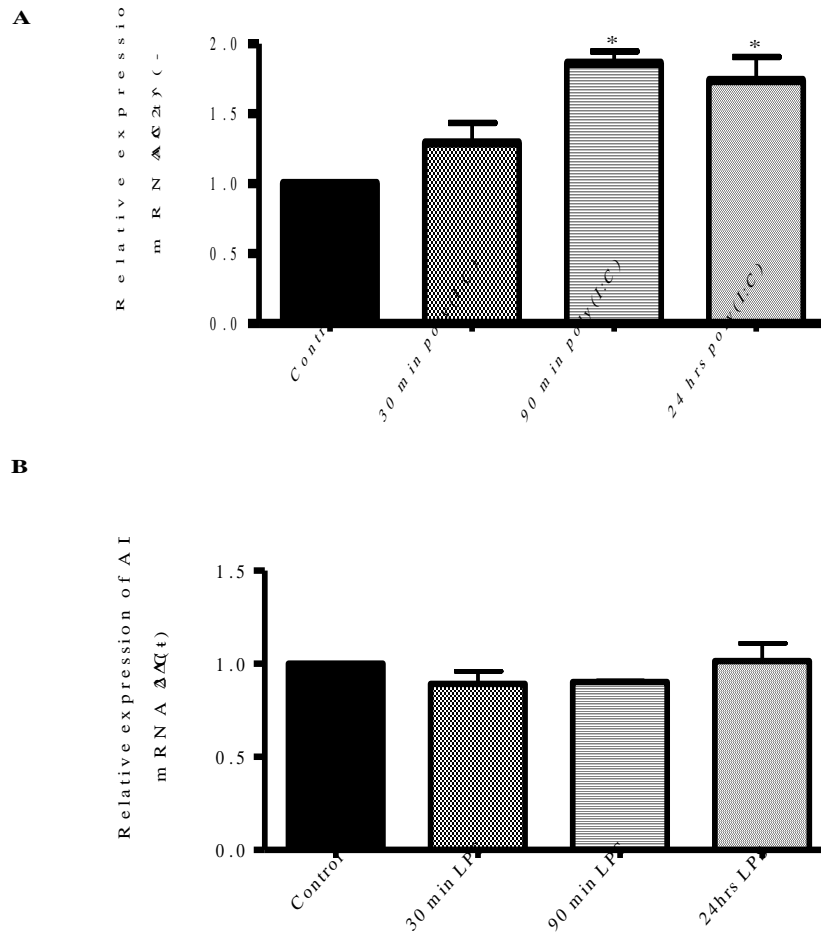


**Figure 4.5: poly (I:C) increased ADAM15 mRNA.** U373-CD14 cells were plated into 6-well plates. When cells were 80 % confluent, they were left un-stimulated (control) or stimulated with either 20  $\mu\text{g}/\text{ml}$  poly(I:C) (A) or 1  $\mu\text{g}/\text{ml}$  LPS (B) for the time indicated. Thereafter, total RNA was isolated, and reverse transcribed into cDNA. The cDNA were used as a template whereby it was diluted 25 times and ADAM15 mRNA was measured by Q-RT-PCR using primer specific to human ADAM15. GAPDH was used as housekeeping gene. The results presented are representative of at least three independent experiments each experiment was done in duplicate. \*  $P < 0.05$ .

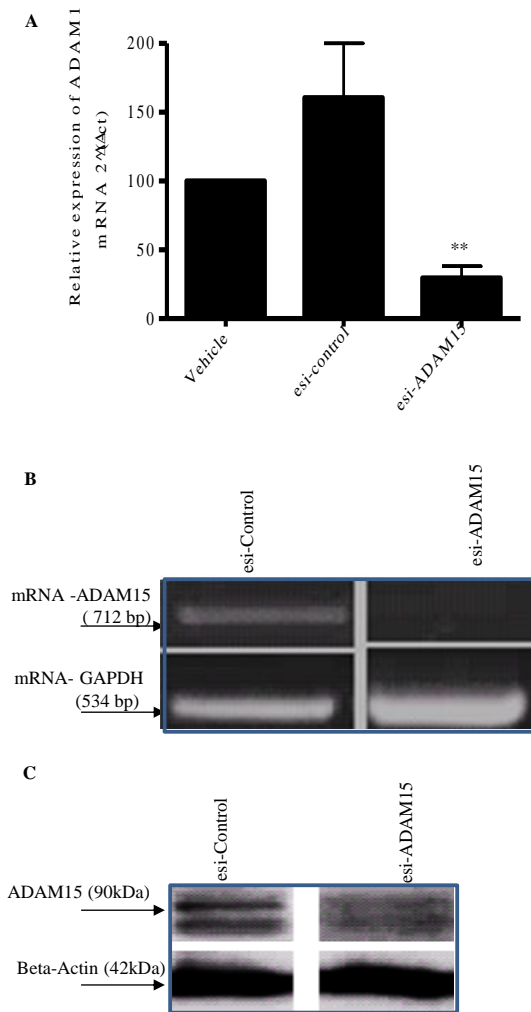


**Figure 4.6: Suppression of ADAM15 in human astrocytoma U373-CD14 cells.** (A) Cells were seeded into 6-well plate. When cells were 80 % confluent, they were transfected with 20 nM esiRNA control or 20 nM esiRNA against human ADAM15. Cells were harvested 24 h after transfection and total RNA was isolated and reverse transcribed into cDNA. The cDNA template was diluted 25 times and ADAM15 mRNA was measured by Q-RT-PCR using primer specific to human ADAM15. GAPDH was used as housekeeping gene. (B) The cDNAs were diluted 100 times and RT-PCR was performed using specific primer for human ADAM15. GAPDH was used as housekeeping gene. RT-PCR products were separated by agarose gel electrophoresis for 1 h at 100 V. Images were captured using the G:box documentation system (Syngene). (C) Cells were plated into 6-well plates. After 24 h, cells were transfected with 20 nM esiRNA control or esiRNA against human ADAM15. Cells were collected 48 h after transfection in 1 ml cold ice PBS and centrifuged for 10 min at 380 g at 4 °C. Cells were lysed in RIPA buffer (25 mM Tris-HCl pH 7.6, 150 mM NaCl, 1 % NP-40, 1 % sodium deoxycholate, 0.1 % SDS, supplemented with protease inhibitor cocktail, 1 mM PMSF 1 mM Na<sub>3</sub>VO<sub>4</sub> , and 1 mM DDT). Proteins were separated by SDS-PAGE gel electrophoresis and subject to immunoblotting. ADAM15 was detected using anti-human ADAM15 monoclonal antibody (R&D). β-Actin was used as loading control. Images were captured using the G:box documentation system (Syngene). \*\*P < 0.01.

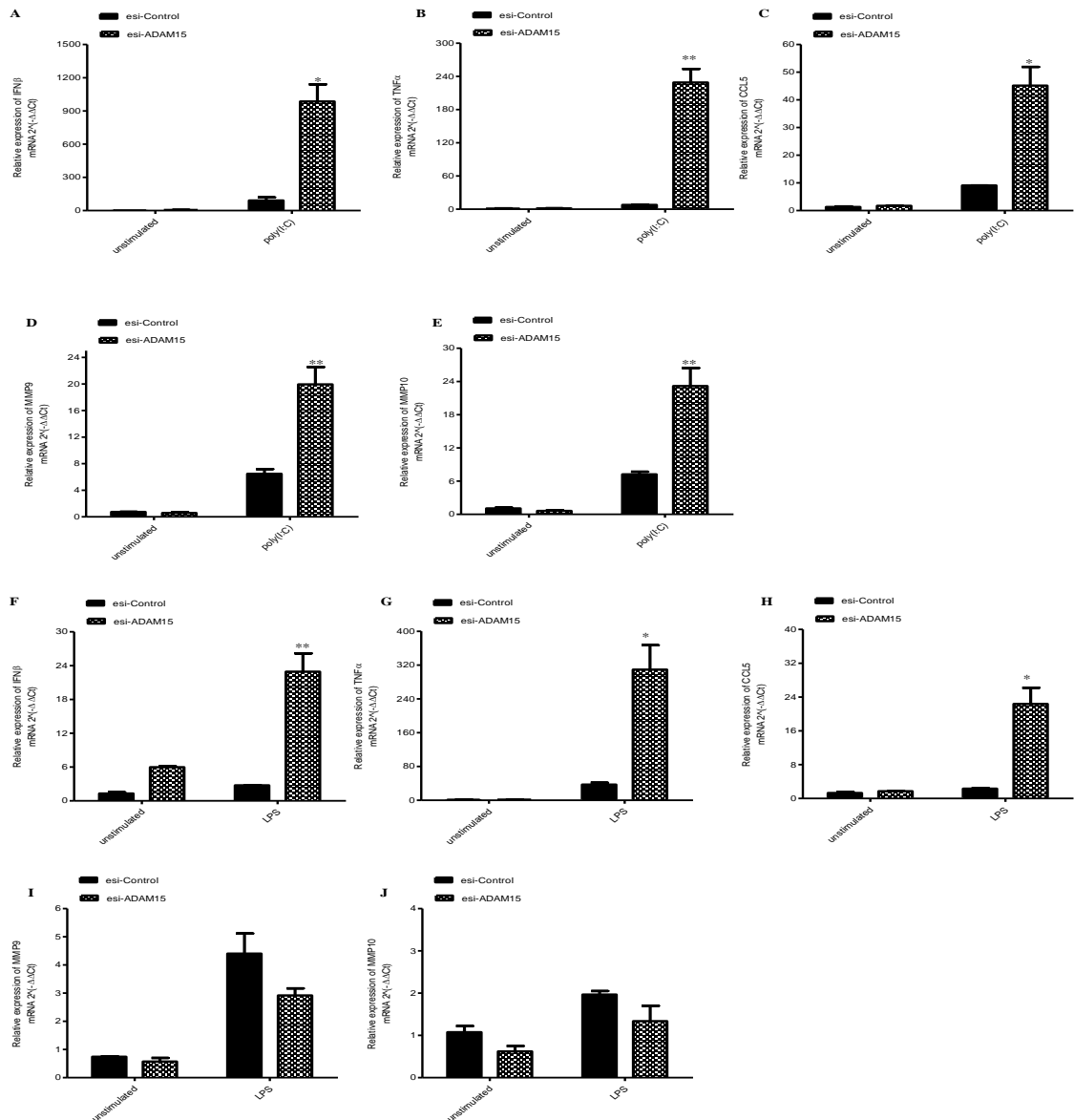


**Figure 4.7: Suppression of ADAM15 expression enhanced IFN- $\beta$ , TNF- $\alpha$  and Rantes mRNA transcripts (A and C)** U373-CD14 cells were seeded into 6 well plates. When the cells were 80 % confluent, they were transfected with 20 nM esiRNA control or esiRNA directed against ADAM15. After 48 h, cells were stimulated with either 20  $\mu$ g/ml poly(I:C) (panel A) or 1  $\mu$ g/ml LPS (panel C) for 3 h. Thereafter, cells were harvested and total RNA was isolated and reverse transcribed into cDNA. The cDNA was used as template and then diluted 25 times. Next, levels of IFN- $\beta$ , TNF- $\alpha$  and Rantes mRNAs were measured by Q-RT-PCR using specific human IFN- $\beta$ , TNF- $\alpha$  and Rantes primers. (Panels, B and D) Cells were seeded into a 6-well plate and when cells become 80 % confluent, cells were transfected with 20 nM esiRNA control or esiRNA against ADAM15. After 24 h, cells were stimulated with either 20  $\mu$ g/ml poly(I:C) (panel B) or 1  $\mu$ g/ml LPS (panel D) for an additional 24 h. Thereafter cells were collected, total RNA was isolated and reverse transcribed into cDNA. cDNA was used as template and then diluted 25 times. Levels of mRNA for MMP9 and MMP10 were measured by Q-RT-PCR using specific human MMP9 and MMP10 primers. GAPDH was used as housekeeping gene. Data are representative of two independent experiments each experiment was done in duplicates. \* P < 0.05 and \*\* P < 0.01.

and MMP10 mRNA compared to the control (Figure 4.7 panels D and E). However, reduction of ADAM15 slightly decreased LPS induced MMP9 and MMP10 mRNA Compared to the control (Figure 4.7, panels I and J). Suppression of ADAM15 had no effect on basal MMP9 transcription however it decreased slightly the MMP 10 mRNA compared to the control (Figure4.7, panels I and J).

#### **4.2.7 Downregulation of ADAM15 increased cytokine and chemokine secretion**

Next, the effect of ADAM15 on TLR3 and TLR4 mediated cytokine and chemokine induction was assessed. To this end, U373-CD14 cells were transfected with esiRNA control or esiRNA against ADAM15 for 24 h, followed by stimulation with either poly(I:C) or LPS for additional 24 h. Thereafter, cell free supernatants were collected and cyto/chemokine secretion was measured using the human Meso ELISA system as described (Materials and methods section 2.2.21). Suppression of ADAM15 expression significantly increased poly(I:C) induced IFN- $\beta$ , IFN- $\gamma$ , IL- 12p70, Rantes and TNF- $\alpha$  (Figure 4.8 panels A-E) secretion compared to the control. Furthermore, down-regulation of ADAM15 enhanced LPS induced IFN- $\beta$  and IFN- $\gamma$ , IL-12p70 and Rantes (Figure 4.8, panel E), secretion compared to the control (Figure 4.8, panels I-L). TNF- $\alpha$  is slightly increased but the difference is not significant (Figure 4.8, panel M).

The transcription of many MMPs is promoted by inflammatory cytokines and chemokines (Yong et al et al., 2001). Also Voss et al. (2011) reported that poly(I:C) stimulation in chondrocytes leads to TRIF-dependent induction of MMP1 and MMP13 , thus the levels of MMP 1, 3 and 9 in cell free supernatants was also measured using the human Meso ELISA system. Reduction of ADAM15 significantly enhanced poly(I:C) induced MMP1 MMP3 and MMP9 compared to the control (Figure 4.8, panels F-H). Alternatively, knockdown of ADAM15 significantly decreased/increased LPS induced MMP9/MMP3 secretion compared to the control, MMP1 was not affected (Figure 4.8, panels N-P). It should be mentioned that knockdown of ADAM15 had negligible effect on cytokines/chemokine and MMPs basal levels.

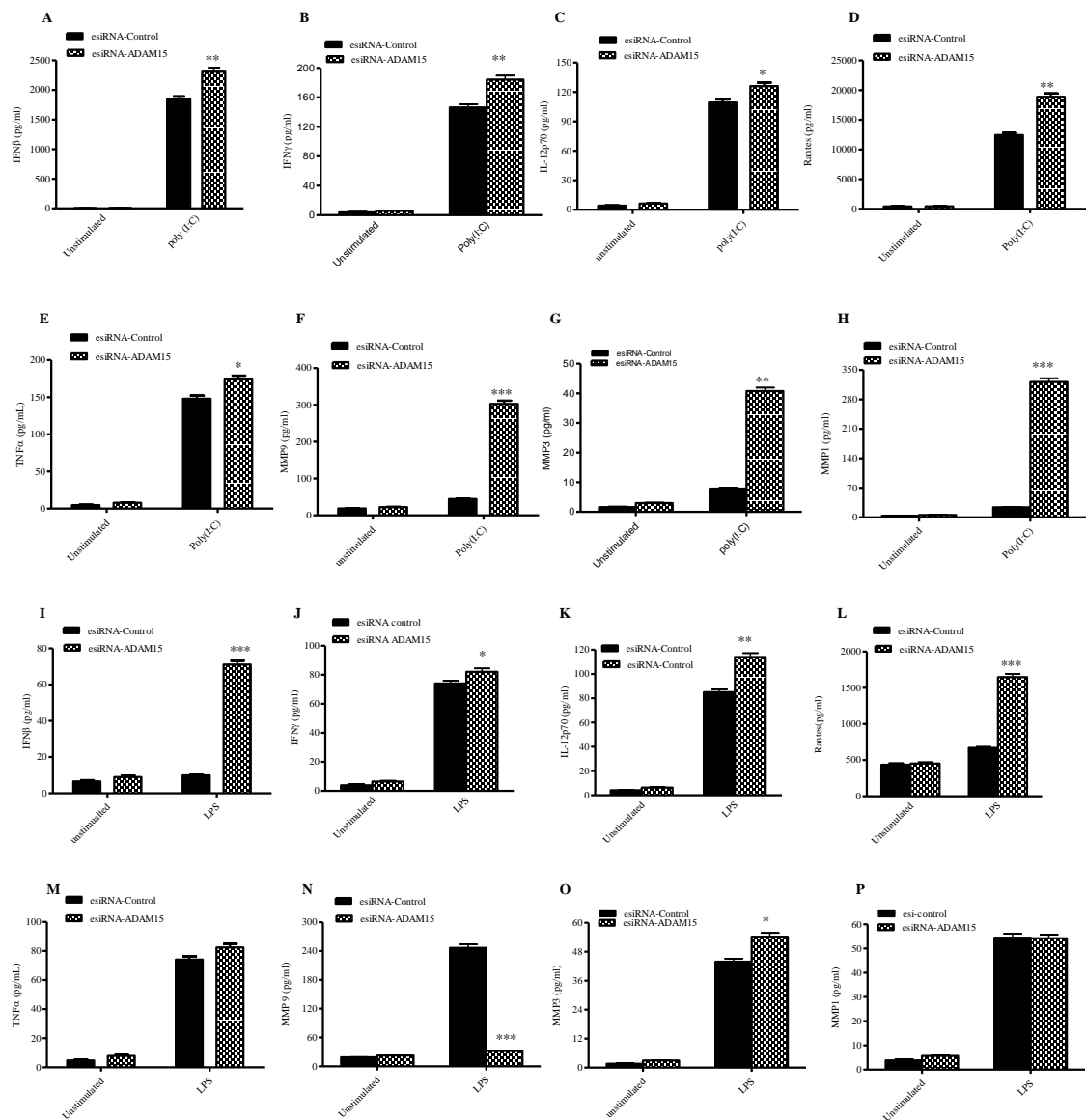


**Figure 4.8: Suppression of ADAM15 enhanced TLR3 and TLR4 mediated cytokine and chemokine induction.** U373-CD14 cells were plated into 6-well plates. When the cells were 80 % confluent, cells were transfected with 20 nM esiRNA control or esiRNA against ADAM15. After 24 h, cells were stimulated with either 20  $\mu$ g/ml poly(I:C) (panels A, B, C, D) or 1  $\mu$ g/ml LPS (panels E, F, G, H) for an additional 24 h. Thereafter, cell free supernatants were collected and ELISA was performed using the Meso system. IFN- $\gamma$ , IL-12p70, IL-6, TNF- $\alpha$  were measured in the cell free supernatants using human Pro-Inflammatory 7-plex Meso kit. Rantes and IFN- $\beta$  were measured using the human single plex Meso kit. MMP 1, 3 and 9 were measured using the human 3 plex Meso kit. \* P < 0.05, \*\* P < 0.01 and \*\*\* P < 0.001.

#### **4.2.8 Knockdown of ADAM15 increased the phosphorylation of p65**

As TRIF mediates NF- $\kappa$ B activation and phosphorylation of both p65 and IRF3, it was of interest to investigate whether ADAM15 reduction affected I $\kappa$ B $\alpha$  degradation, phosphorylation of p65 and IRF3. To this end, U373-CD14 cells were transfected with esiRNA control or esiRNA against ADAM15 for 48 h followed by stimulation with either poly(I:C) or LPS at the indicated time points. Then, I $\kappa$ B $\alpha$  degradation, phosphorylation of p65 and IRF3 was investigated in whole cell lysates. Suppression of ADAM15 expression increased delayed I $\kappa$ B $\alpha$  degradation and phosphorylation of p65 (120 min) upon LPS stimulation (Figure 4.9) compared to the control. However, suppression of ADAM15 expression had no effect on I $\kappa$ B $\alpha$  degradation and phosphorylation of p65 upon poly(I:C) (data not shown). Additionally, phosphorylation of IRF3 was not detected in this cell line.

#### **4.2.9 ADAM15 mediates TRIF degradation**

In an effort to define the mechanism that underlying ADAM15 negatively regulates TRIF mediated TLR3 and TLR4 signalling and as ADAM15 exhibits protease activity (Martin et al., 2002; Duffey et al., 2011), the ability of ADAM15 to mediate the degradation of TRIF was investigated. To this end, HEK293-TLR3 were transfected with HA-TRIF and EV or HA-TRIF and V5-ADAM15. Thereafter, cells were left untreated (control) or stimulated with poly(I:C) as indicated. It should be mentioned that during co-immunoprecipitation of TRIF and ADAM15 in HEK293-TLR3, degradation of TRIF was observed. To inhibit the catalytic activity of ADAM15, ethylene glycol tetraacetic acid (EGTA) and EDTA were used. Chen et al. (2007) reported that ADAM and MMP family members are Zn-dependent proteinases. Thus, their activities were reported to be inhibited by the metal ion chelators such as EDTA and EGTA. Results showed that ADAM10 and ADAM17 sheddase activity was inhibited by both EDTA and EGTA (Chen et al., 2007). For this reason EGTA and EDTA were not used in this experiment to keep ADAM15 in its catalytic active form. As shown in Figure 4.10 panel A, overexpression of 1  $\mu$ g ADAM15 caused TRIF degradation in HEK293-TLR3 even in the absent of poly(I:C) stimulation. As a control and to eliminate the possibility that the degradation effect could be caused by overexpression of two proteins within a cell at the same time, the modulatory effect of ADAM15 on MyD88 was tested.

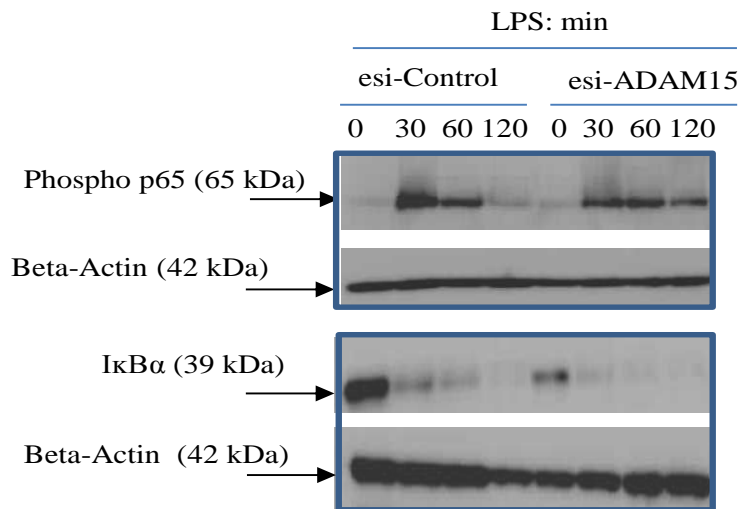


**Figure 4.9: Attenuation of ADAM15 increased phosphorylation of p65.** U373-CD14 cells were seeded into 6-well plates. When the cells were 80 % confluent, they were transfected with 20 nM esiRNA control or esiRNA against ADAM15. After 48 h, cells were stimulated with 1  $\mu$ g/ml LPS for the indicated time points. Thereafter, cells were collected in 1 ml PBS and centrifuged for 10 min at 4 °C at 380 g. Cell pellets were lysed in RIPA buffer (25 mM Tris-HCl pH 7.6, 150 mM NaCl, 1 % NP-40, 1 % sodium deoxycholate, 0.1 % SDS, supplemented with protease inhibitor cocktail, 1 mM PMFS 1 mM Na<sub>3</sub>VO<sub>4</sub> and 1 mM DDT). Next, cell lysates were mixed with Laemmli loading buffer and boiled for 5 min. Proteins were separated by SDS-PAGE and subjected to immunoblot analysis using mouse anti-I $\kappa$ B $\alpha$  and rabbit anti pp65 monoclonal antibodies.  $\beta$ -actin was used as loading control. Images were captured using the G:Box system (Syngene). Results represent three independent experiments.

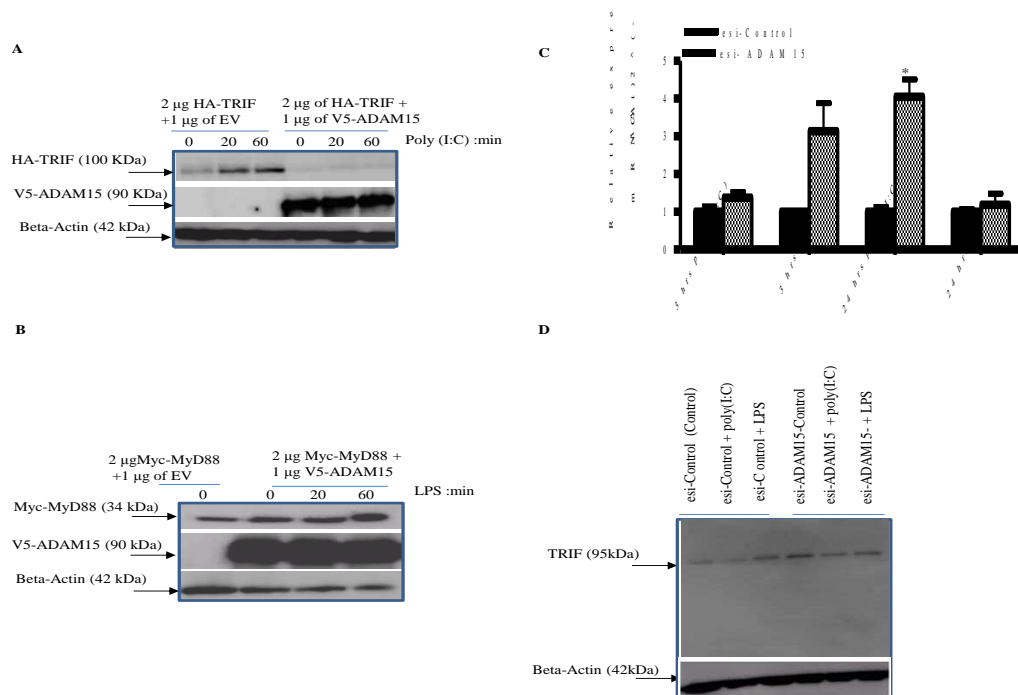


**Figure 4.10 : ADAM15 mediates TRIF degradation.** (Panel A), HEK293-TLR3, (Panel B), HEK293-TLR4 were seeded into 6-well plates. When the cells were 80 % confluent, HEK293-TLR3 were co-transfected with either 2  $\mu$ g of HA-TRIF and 1  $\mu$ g of EV or with 2  $\mu$ g of HA-TRIF and 1 $\mu$ g of V5-ADAM15. HEK293-TLR4 were co-transfected with 2  $\mu$ g of Myc-MyD88 and 1  $\mu$ g of EV or with 2  $\mu$ g of Myc-MyD88 and 1  $\mu$ g of V5-ADAM15. After 20 h, cells were left unstimulated or treated with 20  $\mu$ g/ml poly(I:C) (HEK293-TLR3) or 1  $\mu$ g/ml LPS (HEK293TLR4) for the indicated times. Thereafter, cells were harvested and lysed in RIPA buffer (25 mM Tris-HCl pH 7.6, 150 mM NaCl, 1 % NP-40, 1 % sodium deoxycholate, 0.1 % SDS, supplemented with protease inhibitor cocktail, 1 mM PMSF, 1 mM Na<sub>3</sub>VO<sub>4</sub> and 1 mM DDT). Proteins were separated by SDS-PAGE and immunoblotting was performed using anti-HA, anti-Myc and anti-V5 monoclonal antibodies whereby  $\beta$ -actin was used as loading control. (Panel C) U373-CD14 cells were seeded into 6 well plates. When the cells were 80 % confluent, they were transfected with 20 nM esiRNA control or 20 nM esiRNA against ADAM15. After 24 h, cells were stimulated with either 20  $\mu$ g/ml poly(I:C) or 1  $\mu$ g/ml LPS for 3 or 24 h as indicated. Thereafter, total RNA was isolated and reverse transcribed into cDNA which was diluted 25 times and then used as a template for Q-RT-PCR. TRIF mRNA was measured by Q-RT-PCR using specific primer to human TRIF. (Panel D) U373-CD14 cells were seeded into 6-well plates. When cells were 80 % confluent, they were transfected with 20 nM esiRNA control or 20 nM esiRNA against ADAM15. After 24 h, cells were stimulated with either 20  $\mu$ g/ml poly(I:C) or 1  $\mu$ g/ml LPS for additional 24 h. Thereafter, cells were collected in 1 ml PBS and centrifuged for 10 min at 4 °C at 380 g. Cell pellets were lysed in RIPA buffer (25 mM Tris-HCl pH 7.6, 150 mM NaCl, 1 % NP-40, 1 % sodium deoxycholate, 0.1 % SDS, supplemented with protease inhibitor cocktail, 1 mM PMSF, 1 mM Na<sub>3</sub>VO<sub>4</sub> and 1 mM DDT). Cell lysates were mixed with Laemmli loading buffer and boiled for 5 min. Proteins were separated by SDS-PAGE and subjected to immunoblotting using a rabbit anti-TRIF polyclonal antibody (Exalpha).  $\beta$ -actin was used as loading control. Images were captured using the G:Box system (Syngene). Results represent two independent experiments.

It was found that ADAM15 overexpression in HEK293-TLR4 had no effect on MyD88 expression (Figure 4.10 panel B). To support these findings, levels of endogenous TRIF mRNA and protein level were measured following suppression of endogenous ADAM15 by esiRNA. Suppression of ADAM15 resulted in a significant increase of TRIF mRNA 24 h upon poly(I:C) stimulation compared to the control. However, suppression of ADAM15 only slightly increased LPS induces TRIF transcription upon LPS stimulation at 3 h compared to the control (Figure 4.10 panel C). Next, TRIF protein expression was detected by western blot using a specific anti human-TRIF antibody. Suppression of ADAM15 resulted in the upregulation of TRIF protein expression upon poly(I:C) and LPS stimulation (Figure 4.10 panel and D).

#### **4.2.10 Cellular localization of ADAM15**

It has been reported that some ADAMs may be cleaved and subsequently translocate to the nucleus (Friedrich et al., 2011; Mishra et al., 2011). For that reason, the subcellular distribution of ADAM15 was investigated following stimulation of cells with poly(I:C). To this end, ADAM15 was overexpressed in HEK293-TLR3. Thereafter, cells were stimulated with poly(I:C) and subcellular localisation was investigated by confocal microscopy. To avoid potential artifacts due to high levels of overexpression, the amount of plasmid DNA transfected into the cells was maintained at low levels (200 ng). As illustrated in Figure 4.11, ADAM15 showed perinuclear distribution and poly (I:C) stimulation had no effect on its cellular location.

#### **4.2.11 Interaction network**

To investigate whether ADAM15 and TRIF are involved in the co-regulation of similar proteins or share some common targets, ADAM15 and TRIF were inputted into the Pathway Studio Software and a search was performed to identify common targets and common regulator networks. As illustrated in Figure 4.12, TRIF regulates IFN- $\gamma$  expression which is indirectly regulated by ADAM15. TNF $\alpha$  is directly regulated by TRIF and its expression is also regulated by ADAM15. Also, it was found that ADAM15 and TRIF indirectly regulate MAPK1 and MMP9 and MAPK3 is regulated by ADAM15. Interestingly, ADAM15 expression was previously reported to be upregulated in cells treated with pro-inflammatory cytokines and in tissues of inflammatory diseases (Charrier-Hisamuddin et al., 2008). Also, overexpression of ADAM15 causes increased ERK1/2 activation in endothelial (Sun et al., 2010). It is

known that TRIF induces proinflammatory cytokine which is dependent on NF- $\kappa$ B and MAPK activation (Qi et al., 2005). This indicates that both ADAM15 and TRIF are involved in MAPK activation and it is possible they may counterregulate each other. Ras GTPase-activating-like protein (IQGAP1) was another protein that was identified by LC-MS in HEK293-TLR3 together with ADAM15 upon poly(I:C) stimulation for 60 min. IQGAP1 is also involved in MAPK activation and has been reported to play a positive role in viral replication (Leung et al., 2006). Research has shown that IQGAP1 binds to and modulates the activity of multiple proteins that participate in bacterial invasion (Hugh et al., 2012). Interestingly, this protein has been reported to be involved in invadopodial matrix degradation (Sakurai-Yageta et al., 2008). Invadopodia are actin-based membrane protrusions with a matrix degradation activity and represent sites where cell signalling, proteolytic, adhesive, cytoskeletal, and membrane trafficking pathways physically converge (Weaver, 2006). Actin regulatory proteins participate in invadopodia formation whereas the matrix degradation activity requires MMPs. Stimulation of invadopodial activity by constitutively active IQGAP1 requires the CLIP170 and adenomatous polyposis coli (APC) (Sakurai-Yageta et al., 2008). These two proteins were also identified in the TRIF protein complex upon stimulation of HEK293-TLR3 with poly(I:C) for 60 min. Both CLIP170 and APC bind to IQGAP1 as shown in chapter 3 Figure 3.12. This may indicate that ADAM15 could cause TRIF degradation through IQGAP and their binding partners CLIP170 and APC. To investigate whether TRIF, ADAM15 and IQGAP share similar regulation of cellular processes, TRIF, ADAM15 and IQGAP were uploaded to the Pathway Studio Software and a cellular processes network was created. TRIF and IQGAP1 share the regulation of viral reproduction, phagocytosis and endothelial cell proliferation. Interestingly IQGAP1 regulates almost all cellular processes regulated by ADAM15. These include leukocyte migration, cell proliferation, cell migration, cell differentiation, vascularization, cell motility and cell invasion (Figure 4.13). Thus, there is a strong association between ADAM15 and IQGAP1. Therefore, IQGAP1 could be a target of choice in investigating the mechanism by which ADAM15 causes TRIF degradation and thereby negatively regulates TLR3 and TLR4 signalling.

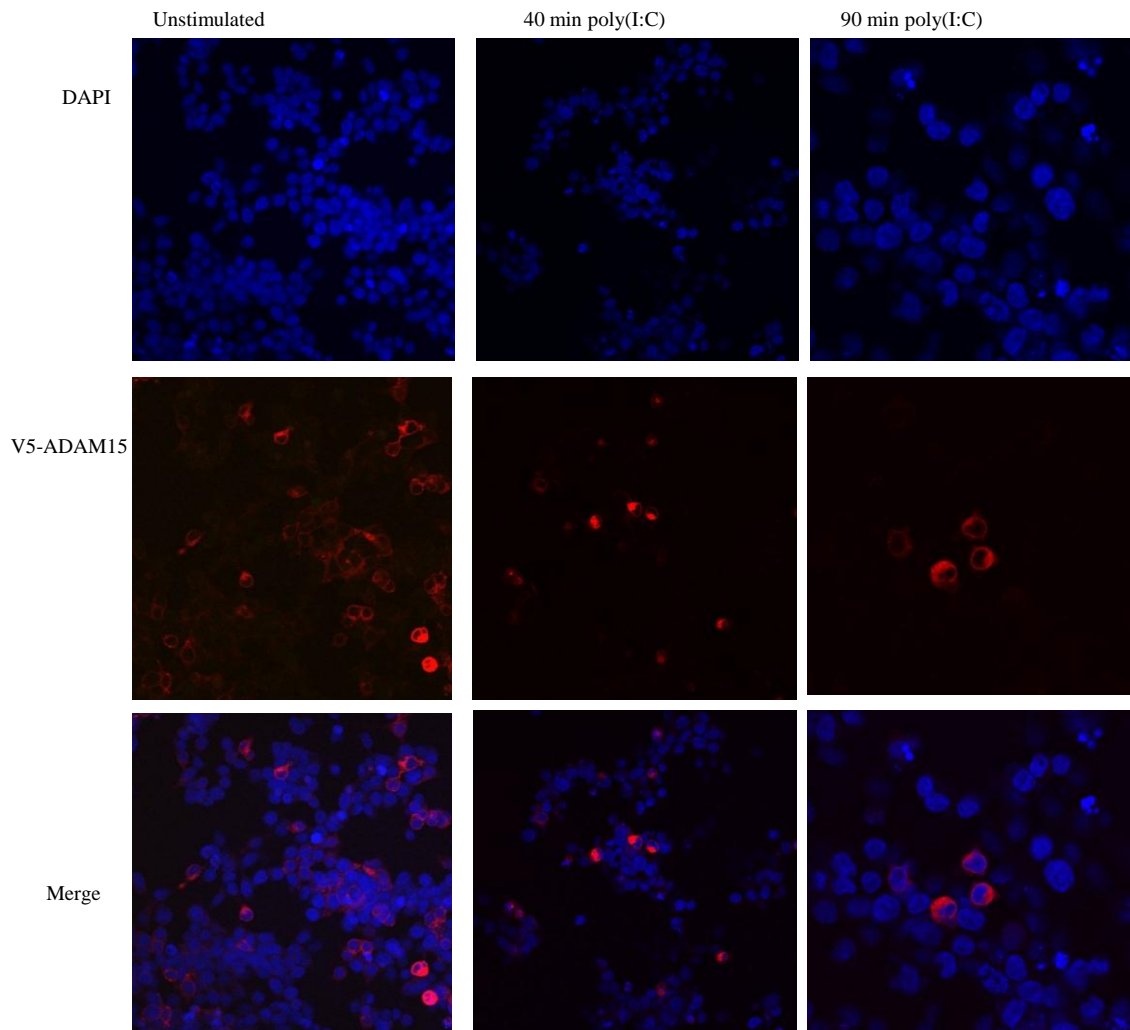


**Figure 4.11: Cellular distribution of ADAM15 upon TLR engagement.** HEK293-TLR3 were seeded on pre-collagen coated coverslip in 6-well plates. When the cells become 80 % confluent, they were transfected with 200 ng of V5-ADAM15. After 24 h, cells were left untreated or treated with 20  $\mu\text{g}/\text{ml}$  poly(I:C) for 40 or 90 min as indicated. Thereafter, cells were fixed in 4 % paraformaldehyde in PBS, permeabilized in 0.5 % triton X-100 in PBS and blocked for 1 h in 1 % BSA in PBS. Next, cells were incubated with 200  $\mu\text{l}$  of anti-V5 monoclonal primary antibody (diluted 1:50 in blocking buffer) for 2 h at RT with gentle shaking. Thereafter, cells were washed for 10 min with 0.05 % Tween 20 in PBS three times. Then, cells were incubated with Alexa fluoro 568 secondary antibody (diluted 1:200 in blocking buffer) for 1 h at RT in the dark, followed by three washes with 0.05 % Tween 20 in PBS. The nucleus was stained with DAPI (10  $\mu\text{g}/\text{ml}$  in PBS). Then, cells were washed twice in PBS and the coverslips were mounted on glass slide using mounting medium and kept in the fridge until analysed. Images were captured using Olympus 1000 confocal microscopy and Flouview Software.

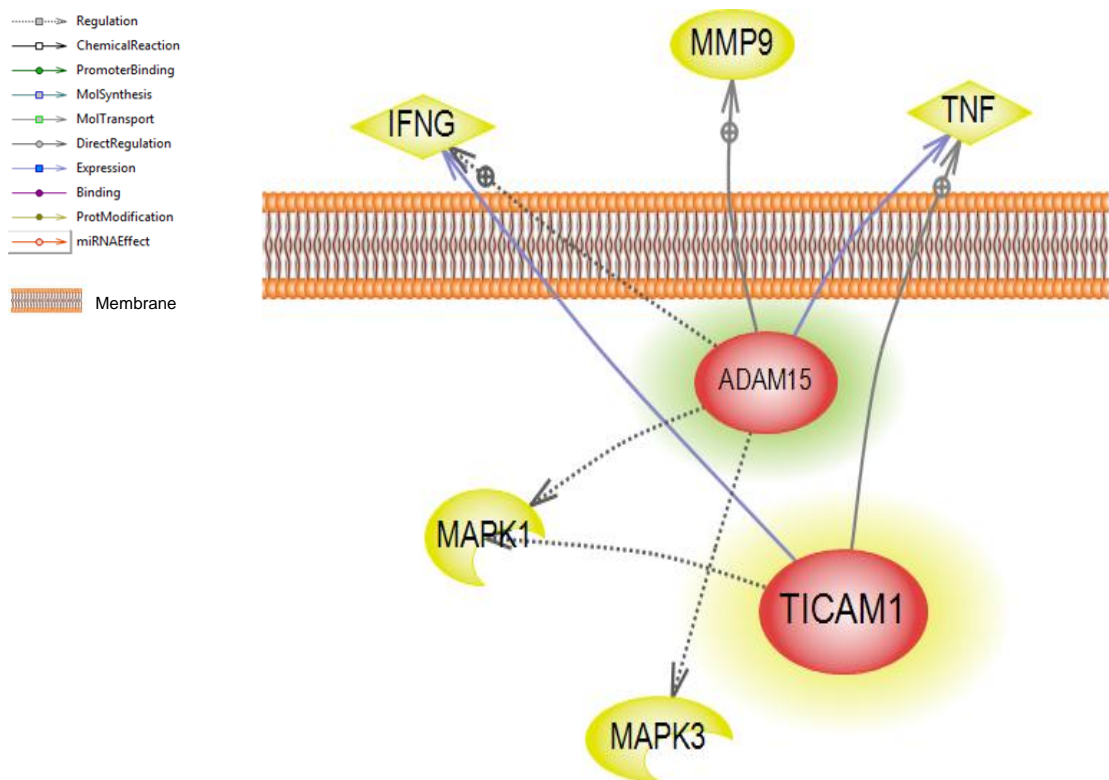


**Figure 4.12: Common targets/regulator network of ADAM15 and TRIF as constructed using Pathway Studio Software.** In HEK293-TLR3 cells, following immunoprecipitation of HA-TRIF and LC-MS analysis of TRIF interactors, ADAM15 was identified upon stimulation of cells with poly(I:C) for 60 min. TRIF (Ticam-1) is indicated in red with yellow surround. ADAM15 is indicated in red with green surround. Yellow entities indicate the proteins that are co-regulated by TRIF and ADAM15, as derived from the software programme. Grey dotted line indicates regulation, grey solid line indicates direct regulation and purple solid line indicates expression.

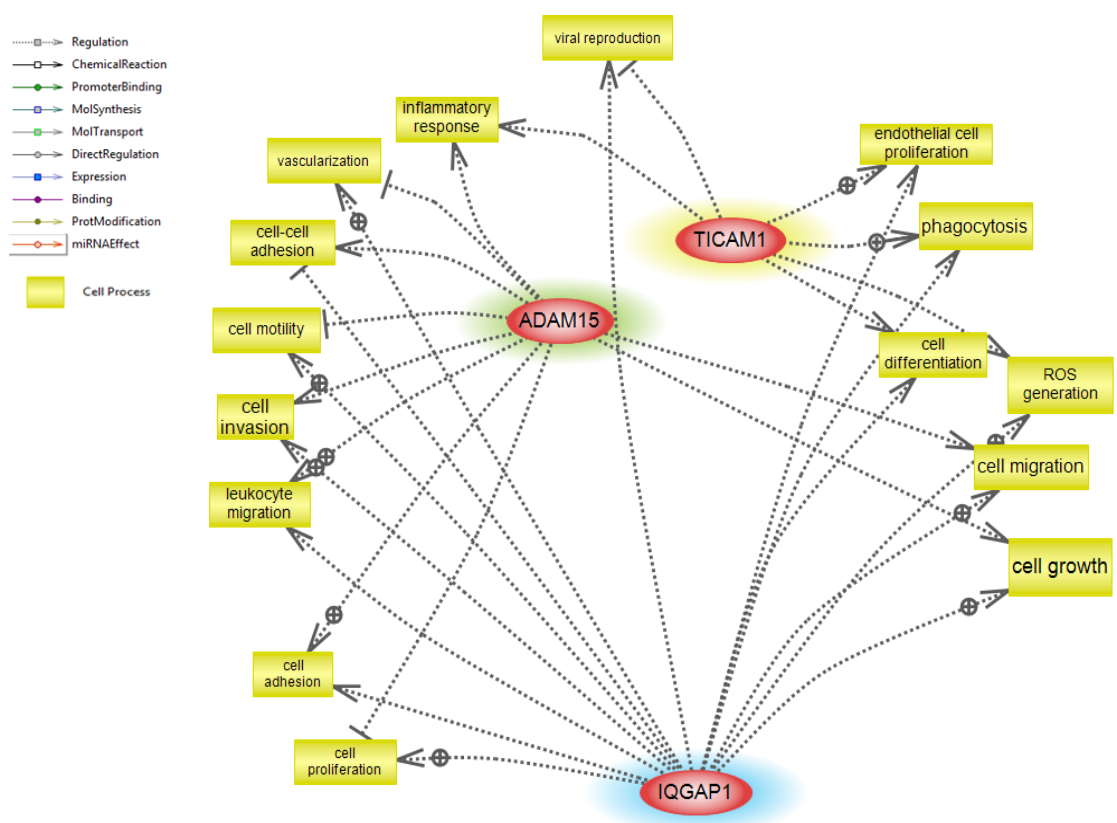


**Figure 4.13: Cell processes regulated by TRIF, ADAM15 and IQGAP1.** In HEK293-TLR3 cells, following IP and LC-MS of HA-TRIF immunocomplexes, ADAM15 and IQGAP1 were identified upon stimulation of cells with poly(I:C) for 60 min. Newly identified protein interactors were uploaded to Pathway Studio software analysis program. Next, cell processes that were commonly modulated by TRIF and the newly identified proteins were identified by Software analysis. Yellow entities indicate the cellular processes that are co-regulated by the identified proteins and TRIF. The red entity with yellow surround indicates TRIF (Ticam-1), red entity with green surround indicates ADAM15 and red entity with blue surround indicates IQGAP1. Grey dotted lines indicate regulation.

### 4.3 Discussion

This study has shown for the first time that TRIF interacts with the disintegrin metalloprotease ADAM15 upon stimulation of the cells with poly(I:C) and LPS. ADAM15 was found to function as a negative regulator of TRIF mediated activation of NF $\kappa$ B, IFN- $\beta$  and Rantes promoter activity. Also, efficient suppression of ADAM15 expression was achieved by using esiRNA technology. Knockdown of ADAM15 resulted in enhanced TLR3 and TLR4 signalling leading to the enhanced production of pro-inflammatory cytokines and chemokines and increased TRIF mRNA and protein levels compared to the control. Several MMPs including MMP3 and 9 contain NF- $\kappa$ B binding site within their promoter region that regulate their expression (Overall et al., 2002). In this study, it was found that reduction of ADAM15 significantly enhanced poly(I:C) induced MMP1, 3 and 9 secretion. In agreement with this finding Zhang et al. (2008) reported TRIF-dependent induction of MMP1 and MMP13 in chondrocytes upon poly(I:C) stimulation. This induction was dependent on the NF- $\kappa$ B pathway, but was differentially inhibited by various mitogen-activated protein kinase inhibitors. Moreover, MMP9 has been shown to be upregulated upon poly(I:C) stimulation in HaCaT keratinocytes (Voss et al., 2011). It has previously been reported that LPS induces MMP9 expression in macrophages through a ROS-p38 kinase dependent pathway (Woo et al., 2004). Interestingly, we show that whilst LPS induced MMP9 induction, suppression of ADAM15 expression significantly decreased LPS induced MMP9 secretion. MMP9 expression appears to be regulated by a number of different signalling pathways in different cell types. For example, protein kinases, MAPKs, transcription factors such as NF- $\kappa$ B, and AP-1 have all been reported to involve in the induction of MMP9 (Gum et al., 1996). Thus, the differences in terms of the role played by ADAM15 may be due to differences in signalling pathway that are instigated.

Despite the potentially important role that ADAM15 may play in cancer, little is known about the regulation of ADAM15 activity, though many studies suggest that ADAM15 could play a role in cell signalling events. The intracellular domain of ADAM15 contains proline-rich sequences, suggesting possible interaction with Src homology (SH) 3 domain-containing proteins. Poghosyan and colleagues showed that the cytoplasmic domain of ADAM15 can form specific, phosphorylation-dependent interactions with Src family protein-tyrosine kinases and with the Grb2 adaptor protein in hematopoietic cell lines (Poghosyan et al., 2002).

ADAM15 expression has also been detected in atherosclerotic lesions, indicating its involvement in this pathology (Herren et al., 1997). In RA, an inflammatory degenerative joint disease involving tissue remodeling, increased ADAM15 expression was found in rheumatoid synovial tissue compared with normal synovial tissue or even osteoarthritic synovial tissue. The expression of ADAM15 in endothelial cells and immune cell infiltrates in RA synovium implies a role for ADAM15 in RA via immune cell recruitment (Komiya et al., 2005 and Böhm et al., 2001). It was also speculated that in RA ADAM15 could degrade the extracellular matrix (ECM) directly through its metalloprotease activity or indirectly through proteolytic activation of MMPs (Charrier-Hisamuddin et al., 2008). Upregulation of ADAM15 was also reported during intestine bowel disease, suggested its involvement in intestinal inflammation.

Whilst most of the published data suggest that ADAM15 is a mediator of inflammation, the possibility that ADAM15 could present both pro- and anti-inflammatory activities cannot be precluded (Charrier-Hisamuddin et al., 2008; Kleino et al., 2008). Wound healing experiments showed that overexpression of ADAM15 inhibits the mechanisms of wound repair in Caco2-BBE cells (Charrier et al., 2005; Charrier et al., 2007). This is supported by Herren and colleagues showing that ADAM15 inhibits wound healing mechanisms in the fibroblastic cell line NIH3T3 (Herren et al., 2001). Recently Friedrich et al. (2011) reported that knockdown of ADAM15 significantly reduced HIV-1 replication in U373-MAGI-CCR5 cells, through a mechanism involving cleavage of ADAM10 by ADAM15. This indicates that ADAM15 is involved in viral replication.

Notably, a total of 6 isoforms of ADAM15 have been described, thus different expression of ADAM15 could result in different cellular events (Yasui et al., 2004). Herein, we have shown that full length ADAM15 binds to TRIF, however, the ability of the other ADAM15 splice variants to bind TRIF and to modulate TLR signalling remain to be investigated. Also, the availability of a specific ADAM15 inhibitor will greatly enhance the capability to study the effect of ADAM15 on other TLRs in various cell types.

In conclusion, this study shows for the first time that ADAM15 interacts with TRIF upon poly (I:C) and LPS stimulation, and that ADAM15 functions as a negative regulator of TLR3 and TLR4 signalling by a mechanism involving TRIF degradation.

## **Chapter 5**

### **Role of Dishevelled in TLR signalling**

## 5.1 Introduction

### 5.1.1 Wnt signalling pathway

The Wnt signalling pathway is a well conserved signalling pathway necessary for embryonic development, tissue self-renewal, cellular proliferation and homeostasis. Dysregulation of Wnt signalling has been linked to cancer (Wang et al., 2010; Bernatik et al., 2011). Wnts are secreted glycoproteins that can activate several downstream signalling pathways including the canonical Wnt/ $\beta$ -catenin pathway and other non-canonical pathways. These non-canonical pathways include the planar cell polarity (Rho/c-Jun N-terminal kinase), the Wnt/ $\text{Ca}^{2+}$  pathway, and other less-known signalling cascades (Uemastu et al., 2007; Gao et al., 2010). The canonical Wnt signalling pathway is the most well studied of the pathways and is involved in regulating diverse cellular processes, such as cell embryonic development, tissue homeostasis, stem cell maintenance, tumor suppression and oncogenesis (Logan et al., 2004). Many genes such as cyclin D1, c-myc, fibronectin, matrix metalloproteases (MMPs) and vascular endothelial growth factor (VEGF) have been identified as Wnt target genes (Staal et al., 2004; Ziegler et al., 2005).

### 5.1.2 Canonical Wnt Signalling

In the absence of a Wnt signal, cytoplasmic  $\beta$ -catenin is recruited into a destruction complex that contains adenomatous polyposis coli (APC) and Axin which facilitates the phosphorylation of  $\beta$ -catenin by Casein kinase I (CKI) and Glycogen synthase kinase (GSK3 $\beta$ ). Phosphorylated  $\beta$ -catenin is then ubiquitinated and destroyed by the proteasome (Figure 5.1, panel A). When a Wnt ligand binds to a Frizzled (Fzd) family of receptors and a low density lipoprotein (LRP) co-receptor of the LRP-5/6, the destruction complex is inhibited and the signalling cascade is initiated. LRP is phosphorylated by CKI and GSK3 $\beta$ , and Axin is then recruited to the plasma membrane. The kinases in the  $\beta$ -catenin destruction complex are then inactivated and  $\beta$ -catenin translocates to the nucleus. In the nucleus,  $\beta$ -catenin interacts with the T cell factor (TCF)/lymphoid enhancer factor (LEF) family transcription factors and activates the transcription of various target genes (Eisenmann et al., 2005; Choi et al., 2007; Zhou et al., 2009) (Figure 5.1, panel B).

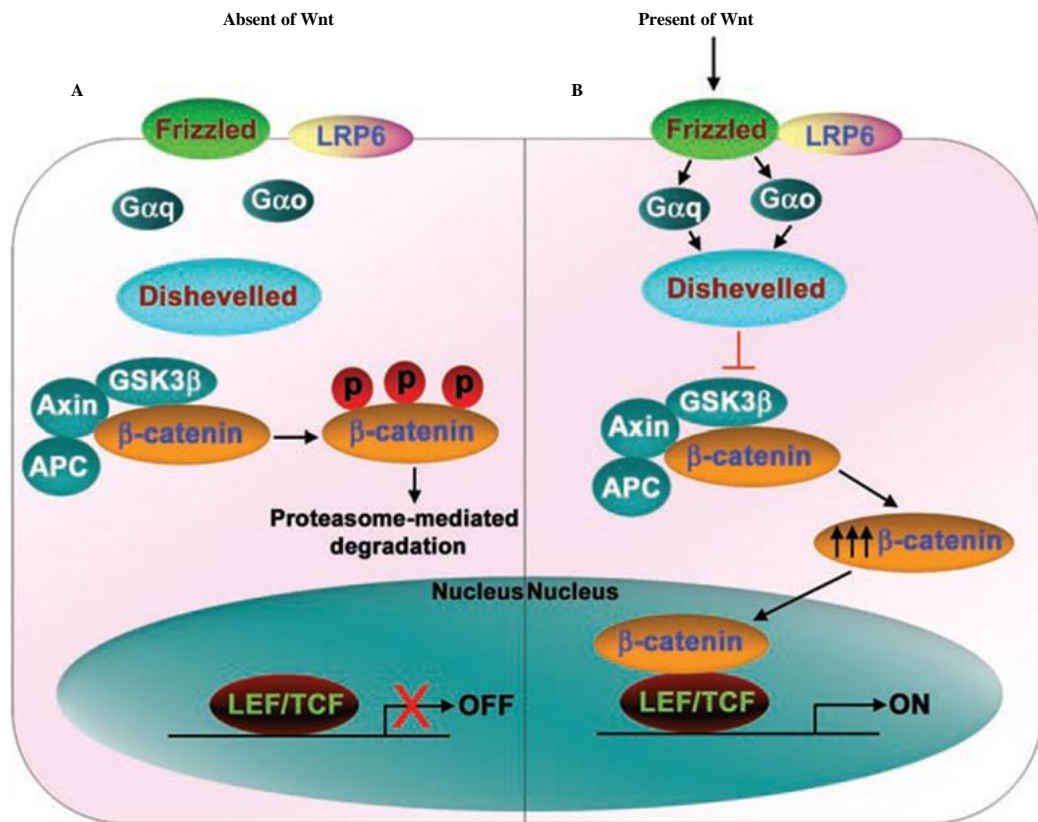


**Figure 5.1: Schematic representation of the canonical Wnt/ $\beta$ -catenin pathway.** (A) In the absence of the Wnt protein ligands, the destruction complex (Axin, APC and GSK3 $\beta$ ) facilitates  $\beta$ -catenin phosphorylation and its ubiquitination and degradation by the proteasome. (B) Binding of the Wnt ligand to a Frizzled/LRP-5/6 receptor complex activates the downstream signalling components including the G-proteins, G $\alpha$ o and G $\alpha$ q, and the phosphoprotein, DVL. DVL reduces GSK3 $\beta$  kinase activity, which lead to  $\beta$ -catenin stabilisation and its translocation to the nucleus, where it interacts with TCF/LEF proteins in the nucleus to activate transcription. (Adapted from Bikkavilli and Malbon, 2009).

To date, 19 different Wnt ligands have been identified in humans and all are lipid-modified glycoproteins (Liang et al., 2007; Muralidharan et al., 2011). The  $\beta$ -catenin pathway is mainly activated by the ligands Wnt1, Wnt3A and Wnt8.

### **5.1.3 Non-canonical WNT signalling.**

There are many non-canonical Wnt signalling pathways, but the two best-studied pathways are the Planar Cell Polarity (PCP) and Wnt/Calcium pathways (Staal et al., 2008) (Figure 5.2, panel A and B). Activation of the non-canonical Wnt signalling pathway is initiated by the ligands Wnt4, Wnt5A and Wnt11 which interact with Frizzled and DVL (Grumolato et al., 2010). In the PCP pathway, which does not involve  $\beta$ -catenin, LRP or TCF molecules, ligand binding to the receptor recruits Dishevelled (DVL), which forms a complex with Daam1. Daam1 then activates the small G-protein Ras homologue gene-family member A (Rho A) through a guanine exchange factor. Rho A then activates Rho-associated kinase (ROCK), a cytoskeletal regulator. DVL also forms a complex with Ras-related C3 botulinum toxin substrate 1 (Rac 1) and mediates profilin binding to actin. Rac1 activates JNK and can also lead to actin polymerization. Profilin binding to actin results in restructuring of the cytoskeleton and changes in cell adhesion and motility. Through largely unknown mechanisms, canonical  $\beta$ -catenin signalling can be inhibited by the PCP signalling pathway (Staal et al., 2008; Liang et al., 2007).

In the Wnt/Calcium pathway, Wnt5A and Fzd regulate intracellular calcium levels. Ligand binding initiates activation of the coupled G-protein to activate phospholipase C (PLC), leading to the generation of Diacyl glycerol (DAG) and Inositol 1,4,5-trisphosphate ( $IP_3$ ). When  $IP_3$  binds to its receptor on the ER, levels of intracellular calcium increase. Ligand binding also activates cGMP-specific phosphodiesterase (PDE), which depletes cGMP and leads to further increases in intracellular calcium. The increased concentrations of calcium and DAG then activate cell division control protein 42 (cdc42) through PKC (Habas and Dawid, 2005; Staal et al., 2008). Cdc42 itself serves to regulate cell adhesion, migration, and tissue separation. Increased calcium also activates calcineurin (Calc) and CamKII (calcium/calmodulin-dependent kinase). Whereas Calc induces activation of transcription factor NFAT, which regulates ventral patterning, CamKII activates TAK1 and Nemo-like kinase (NLK) which interferes with TCF/ $\beta$ -catenin signalling in the canonical pathway. Thus,

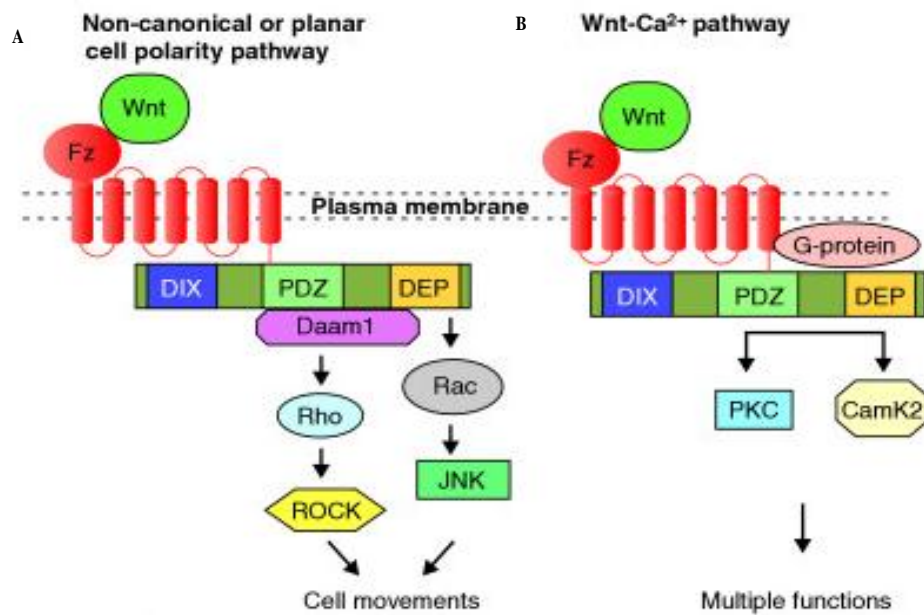


**Figure 5.2: A schematic representation of the non-canonical Wnt signalling pathways.** (A) For planar cell polarity (PCP) signalling, Wnt signalling is transduced through Frizzled independent of LPR5/6. Utilizing the PDZ and DEP domains of DVL, this pathway mediates cytoskeletal changes through activation of the small GTPases Rho and Rac. (B) The Wnt-Ca<sup>2+</sup> pathway, Wnt signalling via Frizzled mediates activation of heterotrimeric G-proteins, which engage DVL, calcium-calmodulin kinase 2 (CamK2) and protein kinase C (PKC). This pathway also uses the PDZ and DEP domains of DVL to modulate cell adhesion and motility (Adapted from Habas and Dawid, 2005).

The Wnt/Calcium pathway can influence the activity of both the non-canonical and canonical Wnt signalling pathways (Habas and Dawid, 2005; Liang et al., 2007; Staal et al., 2008).

#### **5.1.4 Wnt signalling in immune system**

In blood and immune cells, Wnt signalling controls the proliferation of progenitor cells. Wnt proteins also regulate effector T-cell development, regulatory T-cell activation and dendritic cell maturation (Staal et al., 2008). The Wnt/ $\beta$ -catenin signalling pathway plays an important role in thymocyte development and induces T cell production of MMPs which are required for T cell migration (Wu et al., 2007). However, Muralidharan and colleagues have since reported that activation of the Wnt/ $\beta$ -catenin signalling pathway inhibits human peripheral T cell differentiation (Muralidharan et al., 2011). Interestingly, Wnt protein production by macrophages has been shown to depend on microbial stimulation. For example, stimulation of macrophages and monocytes with LPS or Pam<sub>3</sub>CSK<sub>4</sub> (TLR2 ligand) induced the production of Wnt5A (George, 2011). It was noted that TLR ligand induced Wnt5A induction was restricted to macrophages, DCs and monocytes, as T cells, B cells and natural killer (NK) cells did not express Wnt5A after TLR stimulation. TLR-induced Wnt5A production was dependent on the NF- $\kappa$ B pathway and it was also reported that microbe-induced Fzd1 mRNA was TLR2, TLR4, MyD88 and NF- $\kappa$ B pathway dependent (Neumann et al., 2009).

#### **5.1.5 Dishevelled**

The segment polarity genes dishevelled (DVLs) are key components in the Wnt signalling pathways. Mammalian cells express 3 isoforms of the phosphoprotein DVL, namely DVL1, DVL2 and DVL3. All three human DVL genes are expressed in foetal and adult tissues, including lung, kidney, heart, brain and skeletal muscle (Shan et al., 2005). The DVLs are composed of three well known conserved domains (Figure 5.3), a N-terminal DIX (Dishevelled-Axin) domain, a central PDZ (post synaptic density-95, disc large and zonular occludens-1) domain and a C-terminal DEP (Dishevelled-EGL10-Pleckstrin) domain (Lee et al., 2008). The DIX domain is necessary for DVL-DVL or DVL-Axin dimerization. The PDZ domain is essential for Wnt canonical and non-canonical signalling pathways. The DEP domain is essential for the PCP pathway.

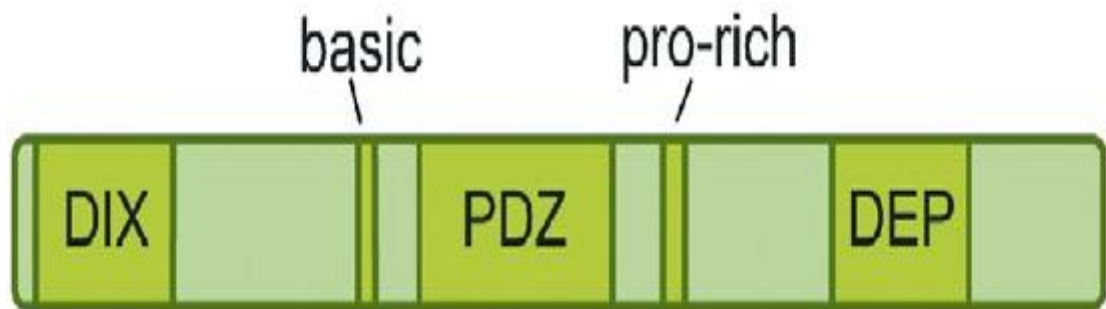


**Figure 5.3: Dishevelled domain structure.** DVL proteins possess three conserved domains an amino terminal DIX domain of 80 amino acids, a central PDZ domain of about 90 amino acids, and a carboxyl-terminal DEP domain of 80 amino acids. In addition, another two conserved regions, the basic region and the proline-rich region, are also implicated to mediate protein-protein interaction and/or phosphorylation (Adapted from Gao and Chen, 2010).

Deletion of either the DIX or PDZ domain of DVL blocks the Wnt canonical pathway (Gao and Chen, 2010). Mammalian DVLs are approximately 70 % homologous and appear to function cooperatively as well as uniquely (lee et al., 2008; Śmietana et al., 2011) DVLs act as scaffolding proteins which interact with many proteins and serve as key signalling intermediate between the Wnt receptor Fzd and downstream components in the Wnt/ $\beta$ -catenin and non-canonical Wnt signalling pathways (Bernatik et al., 2011). The current model of Wnt/ $\beta$ -catenin signal transduction proposes that DVLs are a core protein of dynamic protein assemblies called signalosomes. The signalosome hypothesis proposes that upon stimulation of the Wnt pathway, the DVL proteins multimerise via the DIX domains and form a platform which then recruits other proteins including Axin, which is required for the phosphorylation of LRP6 (Bilic et al., 2007; Romond et al., 2007). When DVL is overexpressed in mammalian cells, it is present in dynamic protein aggregates and is visible as DVL punctuate structures, which most likely represent DVL multimers. Wnt induced activation of DVL is visible as a Wnt-induced shift in the electrophoretic mobility of all three DVL isoforms, forming the so called phosphorylated and shifted-(PS) DVL. It has been clearly demonstrated that both the activation of DVL in the Wnt/ $\beta$ -catenin pathway and Wnt-induced PS-DVL formation is dependent on CK1 (Jose´ et al 2004; Bryja et al., 2007). The fact that there are three DVLs in mammals and that they interact with a great variety of proteins suggest that DVLs may have other functions in addition to Wnt signalling. Recently, it was found that all three DVLs isoforms directly interact with NF- $\kappa$ B (p65) and overexpression of DVLs inhibit TNF- $\alpha$ -induce activation of the NF- $\kappa$ B transcriptional activity (Deng et al., 2010).

As mentioned in Chapter 3, using proteomics, DVL3 was identified as a TRIF interacting partner upon stimulation of HEK-TLR4 with LPS for 20 min. Another Wnt pathway protein, APC, was also identified as a TRIF interacting partner following stimulation of HEK293-TLR3 with poly(I:C) for 60 min. As mention earlier (section, 5.1.4) WNT signalling reported to play different roles in immune system. Interestingly recently TLR4 has been reported to negatively regulate WNT signalling in enterocytes in the ileum of new born mice and suppressed Wnt signalling in Muller glia by reducing phosphorylation and therefore activation of LRP6 (Yi et al., 2012, sodhi et al., 2010). As DVLs are essential proteins in the WNT signalling pathway and shown to bind NF $\kappa$ B it was of interest to study the role of DVLs in TLR3 and TLR4 signalling and the counterregulation of DVLs/Wnt- $\beta$ -catenin signalling by TLR ligands in this Chapter.

## 5.2 Results

### 5.2.1 DVLs interact with TRIF

Using a proteomics approach, DVL3 was identified as a TRIF interacting partner upon stimulation of HEK-TLR4 with LPS for 20 min. To confirm the interaction between DVL3 and TRIF, HEK293-TLR4 were co-transfected with HA-TRIF and Myc-DVL3 and IP of HA-TRIF was implemented as described (Materials and methods, section 2.2.9). As shown in Figure 5.4 panel A, Myc-DVL3 co-immunoprecipitated with HA-TRIF even in a ligand independent manner. Next, an IP of endogenous TRIF from U373-CD14 cells following stimulation with either poly(I:C) or LPS was performed as described (Materials and methods, section 2.2.10). Herein, we show that endogenous DVL3 interacts with endogenous TRIF following stimulation with LPS for 20-40 min. However, DVL3 did not interact with TRIF upon poly(I:C) stimulation (Figure 5.4 panel B). Next, it was decided to examine whether DVL1 and DVL2 also interacted with TRIF. HEK293-TLR4 cells were co-transfected with either HA-TRIF and Myc-DVL1 or HA-TRIF and Myc-DVL2 and IP of HA-TRIF was implemented as described (Materials and methods, section 2.2.9). As shown in Figure 5.5, panel A and B, Myc-DVL1 and Myc-DVL2, respectively, both co-immunoprecipitated with HA-TRIF even in the absence of the ligand. These data indicate that co-overexpression of DVLs and TRIF facilitated their interaction in a ligand independent manner. It was previously reported that overexpression of TRIF resulted in its activation and concomitant induction of the IFN- $\beta$  promoter in a receptor-independent manner (Funami et al., 2007; Funami et al., 2008). Thus, it may be implicated that activation of TRIF is required to facilitate its interaction with the DVLs.

### 5.2.2 DVLs inhibited TRIF-dependent reporter gene activity

The ability of the DVLs to modulate TRIF signalling cascades was investigated. Initially, luciferase reporter gene assays were performed using HEK293 cells. Overexpression of all the DVLs isoforms significantly inhibited TRIF-dependent activation of NF- $\kappa$ B, IFN- $\beta$  (p125-luc), Rantes, PRDII and PDRIII reporter gene activity (Figure 5.6). The results showed that DVL3 exhibited a strong inhibitory effect on TRIF mediated reporter activity when cells were transfected with as little as 1ng of DVL3 (Figure 5.6, panel A-E). Overexpression of DVL1 and DVL2 also strongly reduced

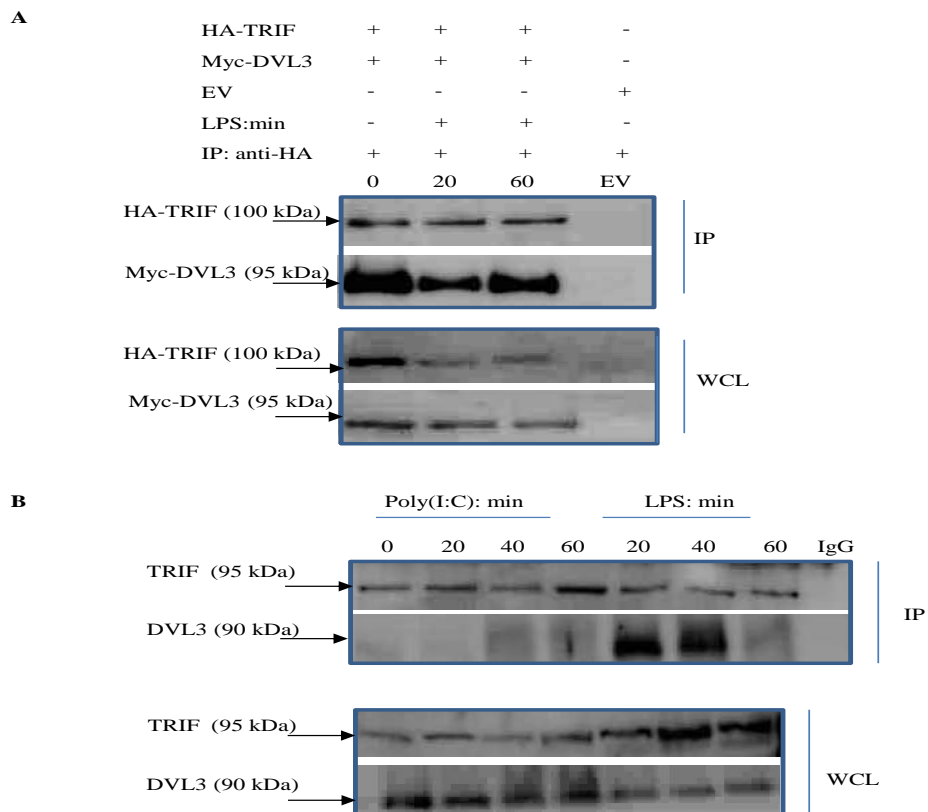


**Figure 5.4: Co-immunoprecipitation of human TRIF and human DVL3.** (A), HEK293-TLR4 were seeded into 6 well plates. When the cells become confluent (80 %) they were transfected with 3  $\mu$ g of EV (control) or co-transfected with 2  $\mu$ g of HA-TRIF and 1  $\mu$ g of Myc-DVL3. Next, 20 h after transfection cells were left un-stimulated or stimulated with 1  $\mu$ g/ml LPS for 20 and 60 min as indicated. Thereafter, cells were lysed in lysis buffer (50 mM HEPES, pH 7.5, 150 mM NaCl, 2 mM EDTA, pH 8.0, 1 % NP-40, 0.5 % sodium deoxycholate supplemented with 1 mM PMSF, 1 mM DDT, 1 mM  $\text{NaVO}_3$  and protease inhibitor cocktail). Cleared cell lysates were incubated with 1  $\mu$ g of anti-HA monoclonal antibody precoupled to 50  $\mu$ l of Protein A/G Plus-Agarose beads for 2 h at 4  $^\circ$ C with gentle shaking. Immuno-precipitation complexes were washed 4 times with lysis buffer and then released from the beads by addition of Laemmli loading buffer, followed by boiling for 5 min. Proteins were separated by SDS-PAGE gel electrophoresis and subjected to immunoblotting using anti-HA and anti-Myc monoclonal antibodies. (B) U373-CD14 cells were cultured into T175 flasks. When the cells were 90-95 % confluent, they were stimulated with either 20  $\mu$ g/ml poly(I:C) or 1  $\mu$ g/ml LPS for times indicated. Thereafter, cells were scrapped into 10 ml ice cold PBS and spun down for 10 min at 4  $^\circ$ C at 220 g. Cell pellets were lysed as described in panel A. Cleared cell lysates were incubated with 2  $\mu$ g of anti-hTRIF polyclonal antibody precoupled to 50  $\mu$ l of Protein A/G Plus-Agarose beads for 2 h at 4  $^\circ$ C with gentle shaking. Proteins were separated by SDS-PAGE and immunoblot analysis was performed using rabbit polyclonal anti-hTRIF and anti-hDVL3 antibodies. Rabbit IgG was used as negative control. Images were captured using the G: box system (Syngene). Results represent at least two independent experiments.

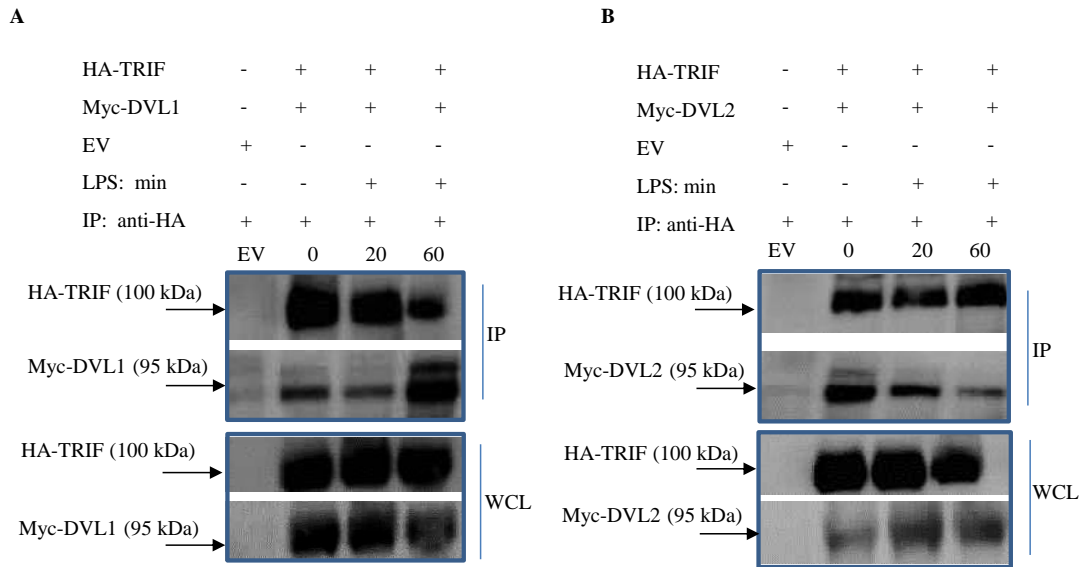


**Figure 5.5: DVL1 and DVL2 interact with TRIF.** HEK293-TLR4 cells were seeded into a 6 well plate. When the cells become confluent (80 %), they were transfected with either 3  $\mu$ g of EV (control) or co-transfected with 2  $\mu$ g of HA-TRIF and 1  $\mu$ g of Myc-DVL1 (A) or 2  $\mu$ g of HA-TRIF and 1  $\mu$ g of Myc-DVL2 (B). After 20 h, cells were left unstimulated or stimulated with 1  $\mu$ g/ml LPS for 20 and 60 min as indicated. Thereafter, cells were lysed in lysis buffer (50 mM HEPES, pH 7.5, 150 mM NaCl, 2 mM EDTA, pH8.0, 1 % NP-40, 0.5 % sodium deoxycholate supplemented with 1 mM PMSF, 1 mM DDT, 1 mM NaVO<sub>3</sub> and protease inhibitor cocktail). Cleared cell lysates were incubated with 1  $\mu$ g of anti-HA monoclonal antibody precoupled to 50  $\mu$ l of Protein A/G Plus-Agarose beads for 2 h at 4 °C with gentle shaking. Immuno-precipitation complexes were washed 4 times with lysis buffer and then released from the beads by addition of Laemmli loading buffer, followed by boiling for 5 min. Proteins were separated by SDS-PAGE and subjected to immunoblot analysis using anti-HA and anti-Myc monoclonal antibodies. Images were captured using the G: box system (Syngene).

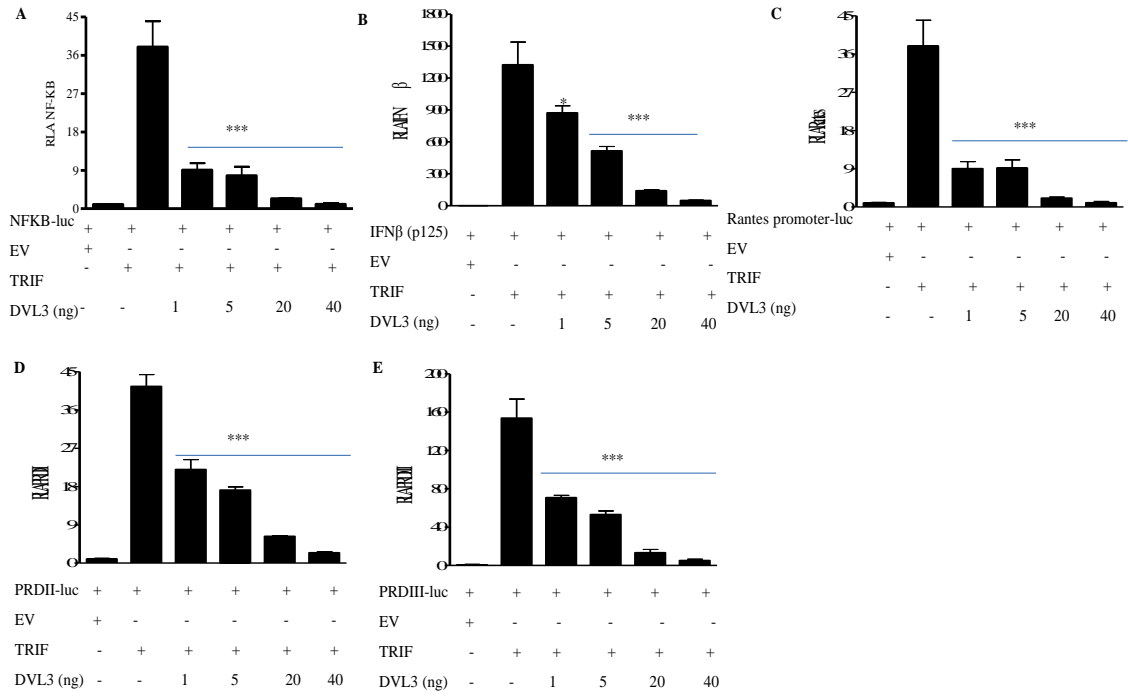


**Figure 5.6: DVL3 inhibited TRIF-dependent reporter gene activity.** HEKT293 cells were plated into 96 well plates at a density of  $5 \times 10^4$  cells/well. After 24 h, cells were transfected with expression vectors encoding either NF- $\kappa$ B (A), full-length IFN- $\beta$  promoter p125 (B), Rantes promoter (C), IFN- $\beta$  PRDII (D) or IFN- $\beta$  PRDIII-I (E) luciferase reporter gene plasmids and co-transfected with either EV or expression vector encoding full length human HA-TRIF (20 ng) and increasing amounts of expression vector encoding full length human Myc-DVL3 (1, 5, 20 and 40 ng) as indicated. After 24 h, cells were harvested and lysed and the cell lysates were kept at  $-80^\circ\text{C}$  for at least 24 h, followed by assessment of luciferase reporter gene activity using dual luciferase system (Promega). The results presented are representative of at least three independent experiments, each experiment was done in triplicate. \*  $P < 0.05$ , and \*\*\*  $P < 0.001$ .

TRIF-mediated NF- $\kappa$ B and Rantes reporter gene activity (Figure 5.7, panel A, C, D and F). However, both DVL1 and DVL2 reduced TRIF mediated IFN- $\beta$  (p125-luc) reporter gene activation at a higher concentration (20 ng) (Figure 5.7, panel B and E). In an agreement with these results, Deng et al. (2010) showed that overexpression of DVLS dramatically reduced TNF- $\alpha$ -induced NF- $\kappa$ B transcriptional activity.

### **5.2.3 DVLS inhibited TLR3-dependent reporter gene activity**

To investigate the role of DVL3 in TLR3 signalling, HEK293-TLR3 were transfected with NF- $\kappa$ B, IFN- $\beta$  and Rantes reporter gene constructs and increasing amount of full length human Myc-DVL3. Despite the fact that DVL3 did not co-immunoprecipitate with TRIF in U373-CD14 cells upon poly(I:C) stimulation, surprisingly, its overexpression in HEK293-TLR3 resulted in a markedly decrease in TLR3-dependent transcription of NF- $\kappa$ B, IFN- $\beta$  and Rantes (Figure 5.8, panel A-C). This could be due to cell lines used or the possibility that DVL3 may exert its effects on TLR3 signalling through another intermediate protein molecule involved in the pathway and not directly through TRIF. Thereafter, the effect of DVL1 and DVL2 on TLR3 signalling was studied. Results showed that DVL1 and DVL2 function as potent inhibitors of TLR3 signalling pathway as they significantly reduced TLR3-dependent activation of NF- $\kappa$ B, IFN- $\beta$  and Rantes promoter (Figure 5.8, panels D-I). Reporter gene assays in HEK293-TLR4 were not possible as the cells that were available had lost their responsiveness to LPS.

### **5.2.4 Effect of DVLS on MyD88-dependent reporter activity**

As both TRIF and MyD88 mediate TLR4 signalling the ability of DVLS to modulate MyD88 mediated reporter gene activity was investigated. Cells were co-transfected with either NF- $\kappa$ B, and IFN- $\beta$  (p125) constructs and MyD88 and increasing amounts of DVL1, DVL2 and DVL3. Overexpression of DVL1 had a negligible effect on MyD88-induced NF- $\kappa$ B reporter gene activity. However, DVL1 significantly decreased MyD88-induced IFN- $\beta$  reporter gene activity at concentrations of 20-40 ng (Figure 5.9, panel A and B). Interestingly, DVL2 overexpression significantly enhanced MyD88-dependent activation of NF- $\kappa$ B, and IFN- $\beta$  reporter genes at a concentration of 1-20 ng (Figure 5.9, panel C and D). On the other hand, overexpression of DVL3 significantly inhibited MyD88-induced NF- $\kappa$ B transcriptional activity even at very low concentration (1 ng) (Figure 5.9, panel E).

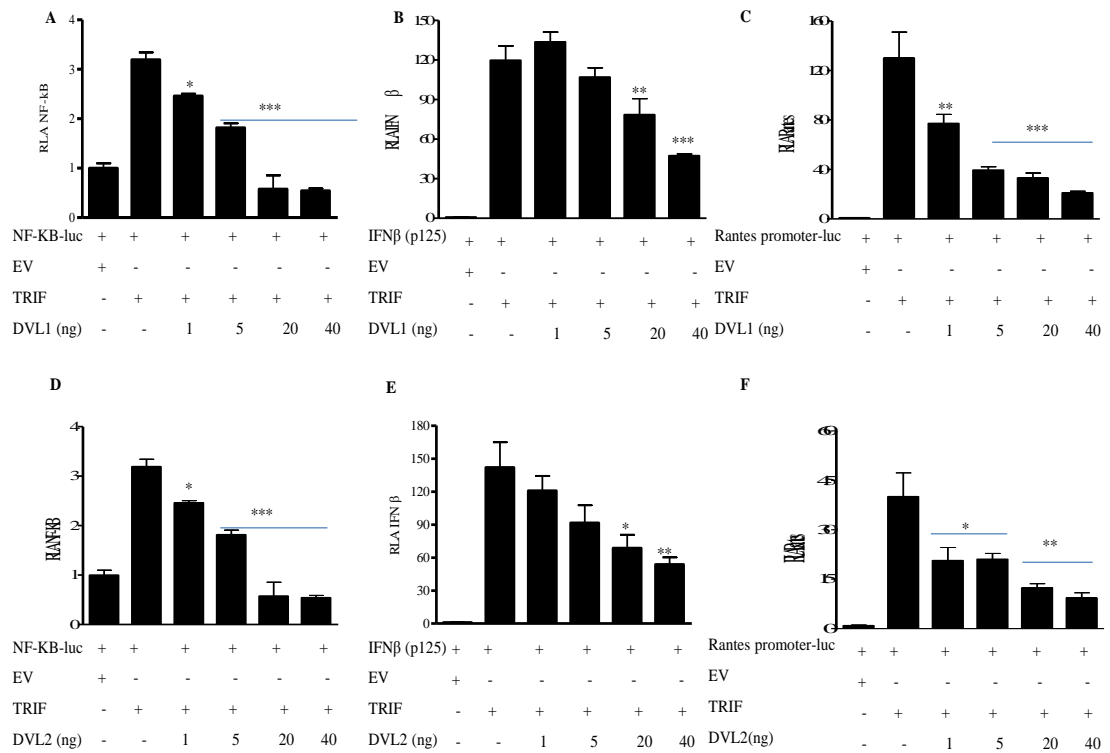


**Figure 5.7: DVL1 and DVL2 reduced TRIF-dependent reporter gene activity.** HEK293 cells were plated into a 96 well plate at a density of  $5 \times 10^4$  cells/well. After 24 h, cells were transfected with expression vectors encoding either NF- $\kappa$ B (A and D), IFN- $\beta$  promoter (p125) (B and E), Rantes promoter (C and F) luciferase reporter gene plasmids and co-transfected with either EV or expression vector encoding full length human HA-TRIF (20 ng) and increasing amounts of expression vector encoding full length human Myc-DVL1 (A-C) or DVL2 (D-F) as indicated. After 24 h, cells were harvested and lysed and the cell lysate were kept at  $-80^\circ\text{C}$  for at least 24 h, followed by assessment of luciferase reporter gene activity using dual luciferase system (Promega). The results presented are representative of at least two independent experiments, each experiment was done in triplicate. \*  $P < 0.05$ , \*\*  $P < 0.01$  and \*\*\*  $P < 0.001$ .

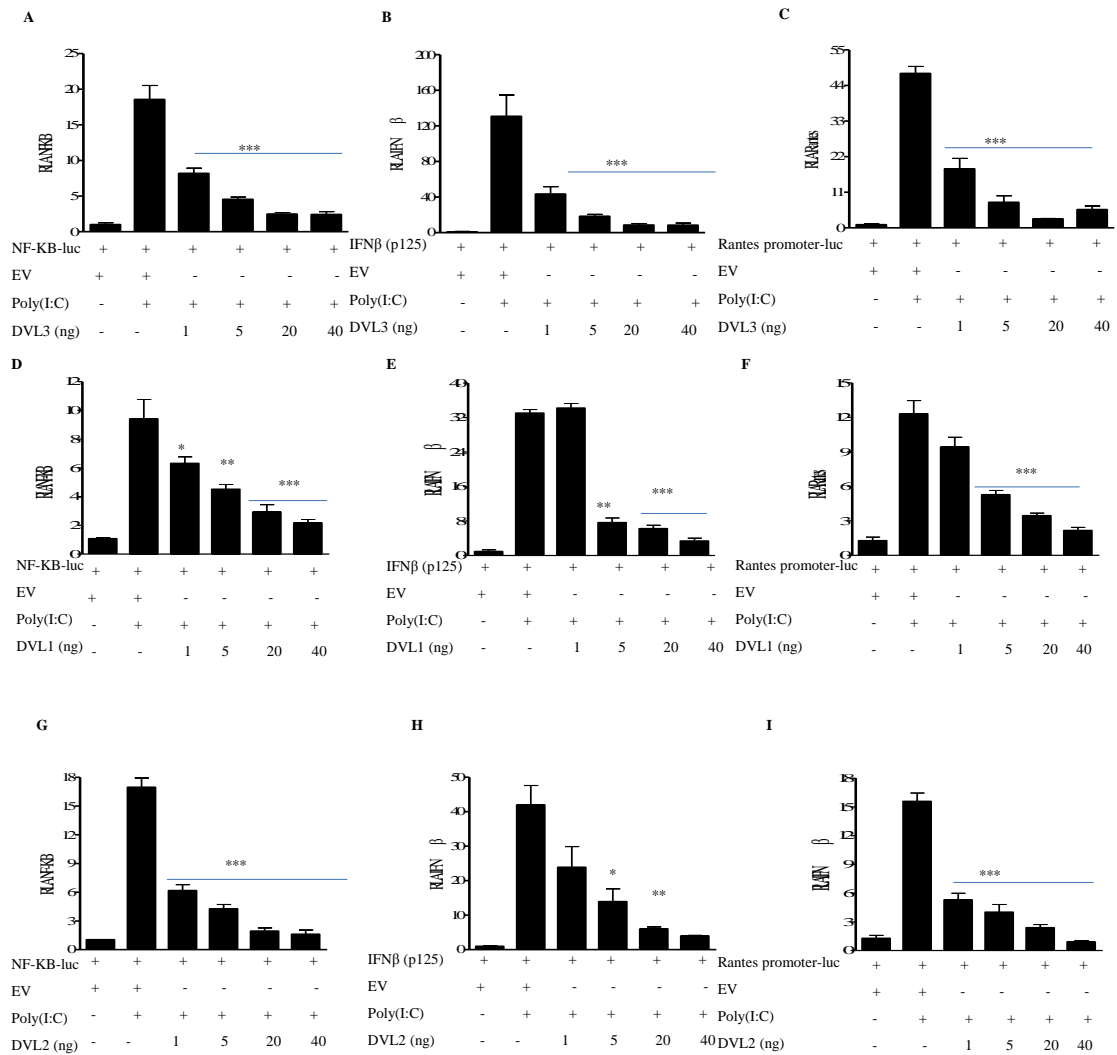


**Figure 5.8: DVLs represses TLR3-dependent reporter gene activity.** HEK293-TLR3 cells were plated into a 96 well plate at a density of  $5 \times 10^4$  cells/well. After 24 h, cells were transfected with expression vectors encoding NF- $\kappa$ B (A, D, G), IFN- $\beta$  (p125) (B, E, H) and Rantes promoter (C, F, I) reporter gene constructs and co-transfected with either EV or increasing amounts of expression vector encoding full length human Myc-DVL3 (A-C) or expression vector encoding full length human Myc-DVL1 (D-F) expression vector encoding full length human or Myc-DVL2 (G-I) as indicated. After 24 h, cells were stimulated with 20  $\mu$ g/ml poly(I:C) for an additional 24 h. Thereafter, cells were harvested and lysed and cell lysate were kept at  $-80^\circ\text{C}$  for at least 24 h, followed by assessment of luciferase reporter gene activity using dual luciferase system (Promega). The results presented are representative of at least two independent experiments, each experiment was done in triplicate. \*  $P < 0.05$ , \*\*  $P < 0.01$  and \*\*\*  $P < 0.001$ .

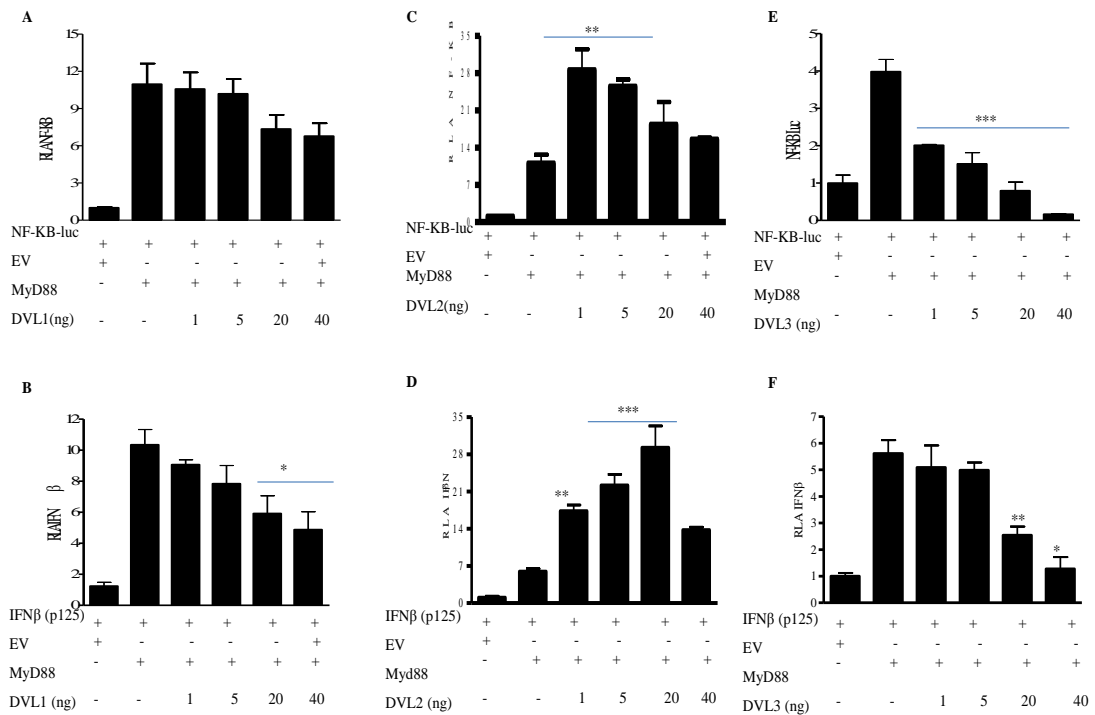


**Figure 5.9: Effect of DVLs on MyD88-dependent reporter gene activity.** HEKT293 cells were plated into 96 well plates at a density of  $5 \times 10^4$  cells/well. After 24 h, cells were transfected with expression vectors encoding either a reporter gene NF- $\kappa$ B (A, C and E), IFN- $\beta$  promoter (p125) (B, D and F), and co-transfected with either EV or expression vector encoding full length human Myc-MyD88 (20 ng) and increasing amounts of expression vector encoding full length human Myc-DVL1 (A, and B) or expression vector encoding full length human Myc-DVL2 (C and D) or expression vector encoding full length human Myc-DVL3 (E and F) as indicated. After 24 h, cells were harvested and lysed and cell lysates were kept at  $-80^\circ\text{C}$  for at least 24 h, followed by assessment of luciferase reporter gene activity using dual luciferase system (Promega). The results presented are representative of at least two independent experiments, each experiment was done in triplicate. \*  $P < 0.05$ , \*\*  $P < 0.01$  and \*\*\*  $P < 0.001$ .

Nevertheless, its overexpression significantly decreased MyD88-induced IFN- $\beta$  reporter gene activity at concentration of 20-40 ng (Figure 5.9, panel F). Collectively, these results indicate that DVLs are capable of regulating NF- $\kappa$ B and IFN- $\beta$  transcription, and among all DVLs isoforms DVL3 strongly represses TRIF and MyD88-dependent activation of NF- $\kappa$ B and IFN- $\beta$ .

### **5.2.5 Inhibition of DVLs attenuates TLR3 and TLR4 signalling**

As mentioned in sections 5.2.2 and 5.2.4, DVLs were capable of regulating TRIF and MyD88-dependent reporter gene activity. Therefore, it was of interest to study the effect of DVLs inhibition on TLR3 and TLR4-dependent signalling in wild-type murine bone-derived macrophages (wt-BMDMs). The DVLs were inhibited by the cell permeable amidobenzanilide. This compound targets the DVLs PDZ domain which is essential for DVLs mediated canonical and non-canonical WNT pathways. In addition, this compound has been reported to block WNT signalling in different biological systems. It suppresses WNT pathway-dependent growth of prostate cancer PC-3 cells by 16 % in 72 h at  $\geq 50$   $\mu$ M, it also inhibit WNT-pathway-mediated apoptosis of the hyaloid endothelial cells in the mouse eyes (Grandy et al., 2009). Next, wt-BMDMs were treated with DMSO or 100  $\mu$ M DVL inhibitor (in DMSO solvent) for 48 h and subsequently stimulated with either 20  $\mu$ g/ml poly(I:C) or 100 ng/ml LPS for 3 h. Thereafter, total RNA was isolated as described (Materials and methods, section 2.2.14) and cytokine mRNA was measured using Q-RT-PCR. Surprisingly, results showed that inhibition of DVLs significantly reduced poly(I:C) and LPS-induce TNF- $\alpha$  and Rantes transcription compared to the control. However, basal transcriptions of TNF- $\alpha$  and Rantes were slightly increased due to the DVL inhibition (Figure 5.10, panels, B, D, G, and I). IFN- $\beta$  mRNA was also reduced but not statistical significant (Figure 5.10, panels A and F). Interestingly, DVL inhibition significantly increased LPS-induce IFN- $\alpha$  transcription but slightly decreased poly(I:C)-induce IFN- $\alpha$  transcription compared to the control (Figure 5.10, panels C and D). Nevertheless, overexpression of all DVLs in HEK293-TLR3 reduced TLR3-dependent gene transcription. Here, DVLs inhibition did not increase poly(I:C) induces signalling. This could be due to the fact that poly(I:C) can be sensed by RLRs such as MDA-5 (Siednienko et al., 2011) which may suggest the involvement of DVLs in other signalling pathways induced by poly(I:C). These results showed that DVLs are needed for poly(I:C) and LPS induce signalling in murine BMDMs.

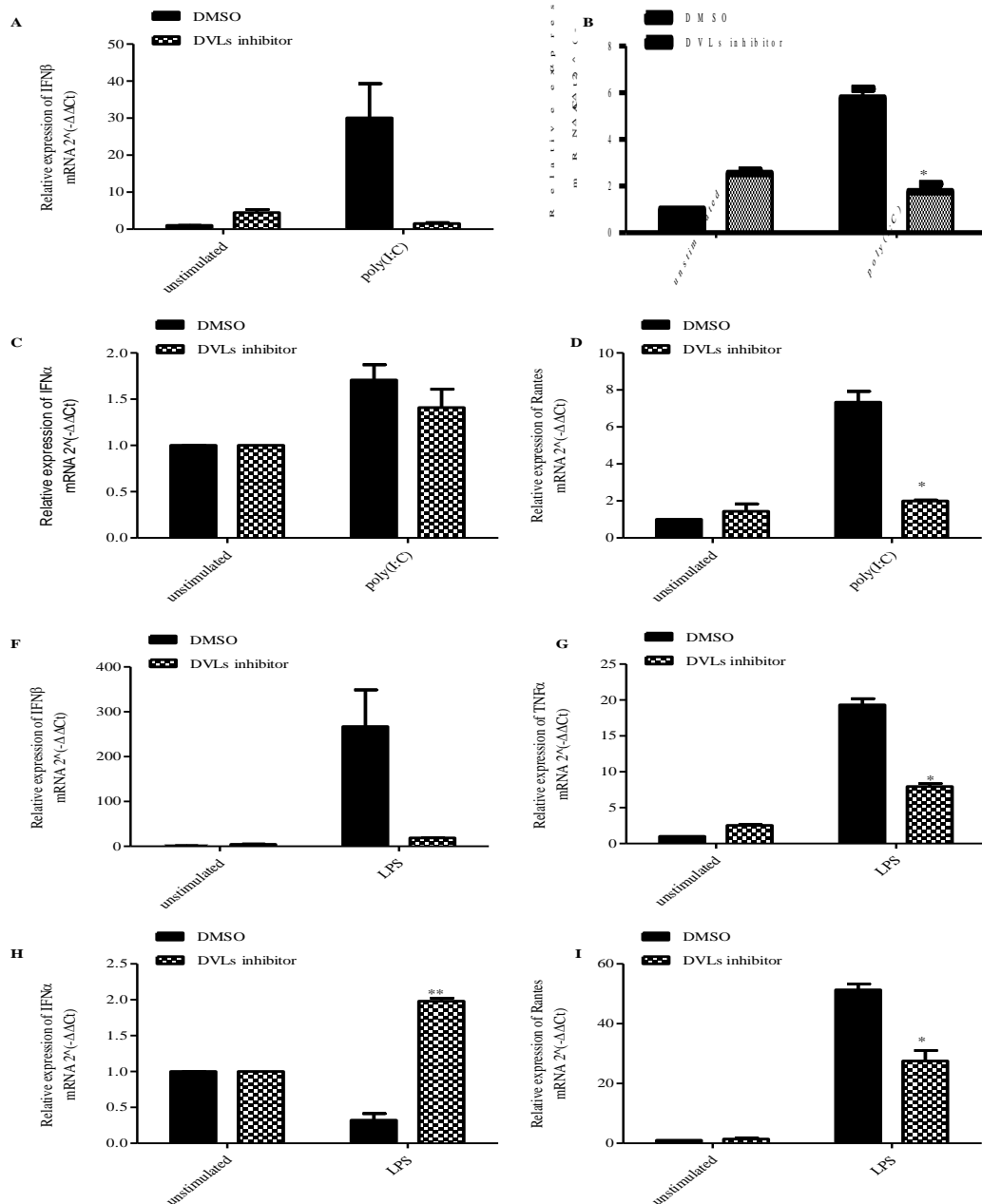


**Figure 5.10: Inhibition of DVLs attenuated TLR3 and TLR4 signalling.** Wt-BMDMs were plated into 6 well plates. When cells became confluent (60 %), they were treated with either DMSO or 100  $\mu$ M DVLs inhibitor for 48 h. Thereafter, cells were stimulated with either 20  $\mu$ g/ml poly(I:C) (A - D) or 100 ng/ml LPS (F - I) for 3 h. Next, total RNA was isolated and reverse transcribed into cDNA. The cDNA was used as a template and samples were diluted 25 times and cytokines were measured by Q-RT-PCR using specific primer to murine IFN- $\beta$ , IFN- $\alpha$ , TNF $\alpha$ , and Rantes. Mouse GAPDH was used as a housekeeping gene. Results are representing two independent experiments each done in duplicates. \* P < 0.05, \*\* P < 0.01.

### **5.2.6 Inhibition of DVLs decreased I $\kappa$ B $\alpha$ degradation and phosphorylation of IRF3.**

To understand the molecular mechanism by which DVLs inhibition reduced the cytokines mRNA, their ability to modulate I $\kappa$ B $\alpha$  degradation and phosphorylation of p65 and IRF3 was investigated. To this end, Wt-BMDMs were pretreated with either the DVL inhibitor or DMSO and subsequently stimulated with either poly(I:C) or LPS for different time points. Then, I $\kappa$ B $\alpha$  degradation and phosphorylation of p65 and IRF3 in whole cell lysates were studied by western blot. As shown in Figure 5.11 panel A, inhibition of DVL decreased I $\kappa$ B $\alpha$  degradation 60-120 min upon poly(I:C) stimulation compared to the control. Phosphorylation of p65 and IRF3 was not detected. On the other hand, inhibition of DVLs decreased I $\kappa$ B degradation and phosphorylation of IRF3 upon LPS stimulation for 60 min compared to the control (Figure 5.11, panel B). Here, phosphorylation of p65 was not detected. It has been reported that, in human macrophages, LPS induced a strong IFN- $\beta$  mRNA response within a short time frame. These responses were associated with NF- $\kappa$ B and IRF3 activation. However, poly(I:C) induced a strong and long-lasting IFN- $\beta$  mRNA and protein response in the absence of detectable IRF3 and NF- $\kappa$ B signalling (Reimer et al., 2008). These results confirmed that DVLs are needed for NF- $\kappa$ B and IRF3 activation upon poly(I:C) and LPS stimulation in murine BMDMs. Whether DVLs inhibition promote stabilization and resynthesis of I $\kappa$ B protein following poly(I:C) and LPS stimulation respectively is need to be investigated.

### **5.2.7 Effect of $\beta$ -catenin activation on TLR3 and TLR4 signalling**

Physically interaction between  $\beta$ -catenin and NF- $\kappa$ B has been reported in human colon and breast cancer cells. This interaction resulted in a reduction of NF- $\kappa$ B DNA binding (Deng et al., 2002). Sun and colleagues also reported that Salmonella-induced IL-8 secretion is completely abolished by the activity of  $\beta$ -catenin in human intestinal epithelia (Sun et al., 2005). Thus, it was of interest to study whether activation of  $\beta$ -catenin affects TLR3 and TLR4 signalling. It has been previously demonstrated that epidermal growth factor (EGF) treatment inactivates GSK-3 $\beta$  and thereby, activates  $\beta$ -catenin and caused its nuclear translocation (Lee et al., 2010; Hu et al., 2010). Therefore, herein, EGF was used as a  $\beta$ -catenin activator. Initially, wt-BMDMs were pretreated with 10  $\mu$ g/ml EGF for 24 h, followed by stimulation with either poly(I:C)

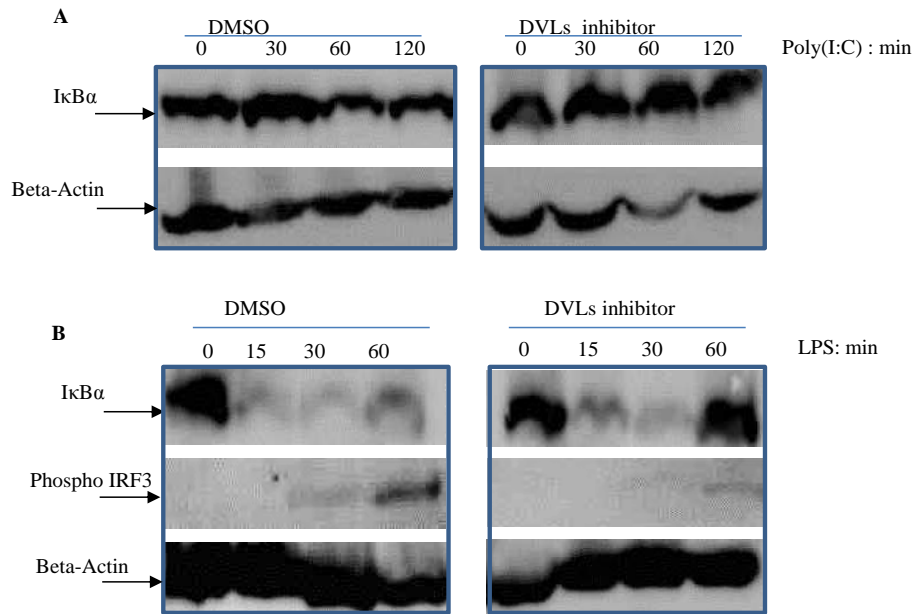


**Figure 5.11: DVLs inhibition reduced IκBα degradation and phosphorylation of IRF3.** Wt-BMDMS were seeded into 6 well plates when cell become confluent (60 %) cells were treated with either DMSO or 100 μM DVLs inhibitor for 48 h. Thereafter cells were treated with either 20 μg/ml poly(I:C) or 100 ng/ml LPS for times indicated. Then cells were collected in 1 ml PBS and spun down for 10 min at 4 °C at 380 g. Cell pellets were lysed in RIPA buffer (25 mM Tris-HCl pH 7.6, 150 mM NaCl, 1 % NP-40, 1 % sodium deoxycholate, 0.1 % SDS, supplemented with protease inhibitor cocktail, 1 mM PMFS 1 mM Na<sub>3</sub>VO<sub>4</sub> and 1 mM DDT). Cell lysates were mixed with Laemmli loading buffer and boiled for 5 minutes. Proteins were separated by SDS-PAGE gel electrophoresis and subjected to immunoblotting using anti-IκBα, and anti-phospho-IRF3 monoclonal antibodies. β-Actin was used as loading control. Images were captured using the G: Box system (Syngene). Results are representing of three independent experiments.

and LPS for 3 h. Thereafter, RNA was isolated and cytokines mRNA was measured using Q-RT-PCR. EGF treatment was found to increase IFN- $\beta$  and Rantes, but decrease IFN $\alpha$  transcriptions upon poly(I:C) stimulation compared to the control (Figure 5.12). In contrast, expression of TNF- $\alpha$  mRNA was not affected. Furthermore, EGF treatment significantly increased IFN- $\beta$  and Rantes and decreased IFN- $\alpha$  and TNF- $\alpha$  upon LPS stimulation compared to the control (Figure 5.12). To confirm these results HEK293-TLR3 were transfected with NF- $\kappa$ B, IFN- $\beta$  (p125), IFN- $\alpha$  and Rantes promoter reporter gene constructs in the presence of EGF. Then, cells were left untreated or stimulated with 20  $\mu$ g/ml poly (I:C) followed by assessment of reporter gene activity. In accordance with the Q-RT-PCR data, results showed that EGF treatment significantly decreased TLR3-dependent NF- $\kappa$ B and IFN- $\alpha$  reporter gene activation (Figure 5.13, panels A and B). However, EGF increased slightly TLR3-dependent IFN- $\beta$  and Rantes reporter gene activity (Figure 5.13, panels C and D).

### **5.2.8 EGF stimulation decreased I $\kappa$ B $\alpha$ degradation and increased phosphorylation of IRF3 and p38**

Wnts are capable of activating p38 MAPKs and this activation dependent on the DVLs (Bikkavilli and Malbon, 2009). Activation of p38 MAPK by Wnt inhibits GSK3 $\beta$  and leads to an increase in cytosolic  $\beta$ -catenin levels and Wnt-sensitive gene transcription. Therefore, the effects of EGF-induced  $\beta$ -catenin activation on TLR-mediated I $\kappa$ B $\alpha$  degradation and phosphorylation of IRF3 and p38 was investigated. Wt-BMDMs were pretreated with 10  $\mu$ g/ml EGF for 24 h followed by stimulation with either poly(I:C) or LPS for different time points as indicated. Thereafter, cells were collected and I $\kappa$ B $\alpha$ , phospho IRF3 and phospho p38 were detected in whole cell lysates. Results showed that pretreatment of cells with EGF inhibited poly(I:C) mediated I $\kappa$ B $\alpha$  degradation (60-120 min) compared to the control. Moreover, EGF increased basal levels of phospho p38 but has a negligible effect on p38 phosphorylation upon poly(I:C) stimulation compared to the control (Figure 5.14, panel A). Phosphorylation of IRF3 was not detected. However, EGF stimulation reduced early and late I $\kappa$ B $\alpha$  degradation (15-60 min), and increased phosphorylation of IRF3 and p38 (30-60 min) upon LPS stimulation compared to the control (Figure 5.14, panel B). This suggests that the increase in IFN- $\beta$  and Rantes transcription was due to increase IRF3 phosphorylation. However, as EGF reported to activates an extensive network of signal transduction pathways that include activation of

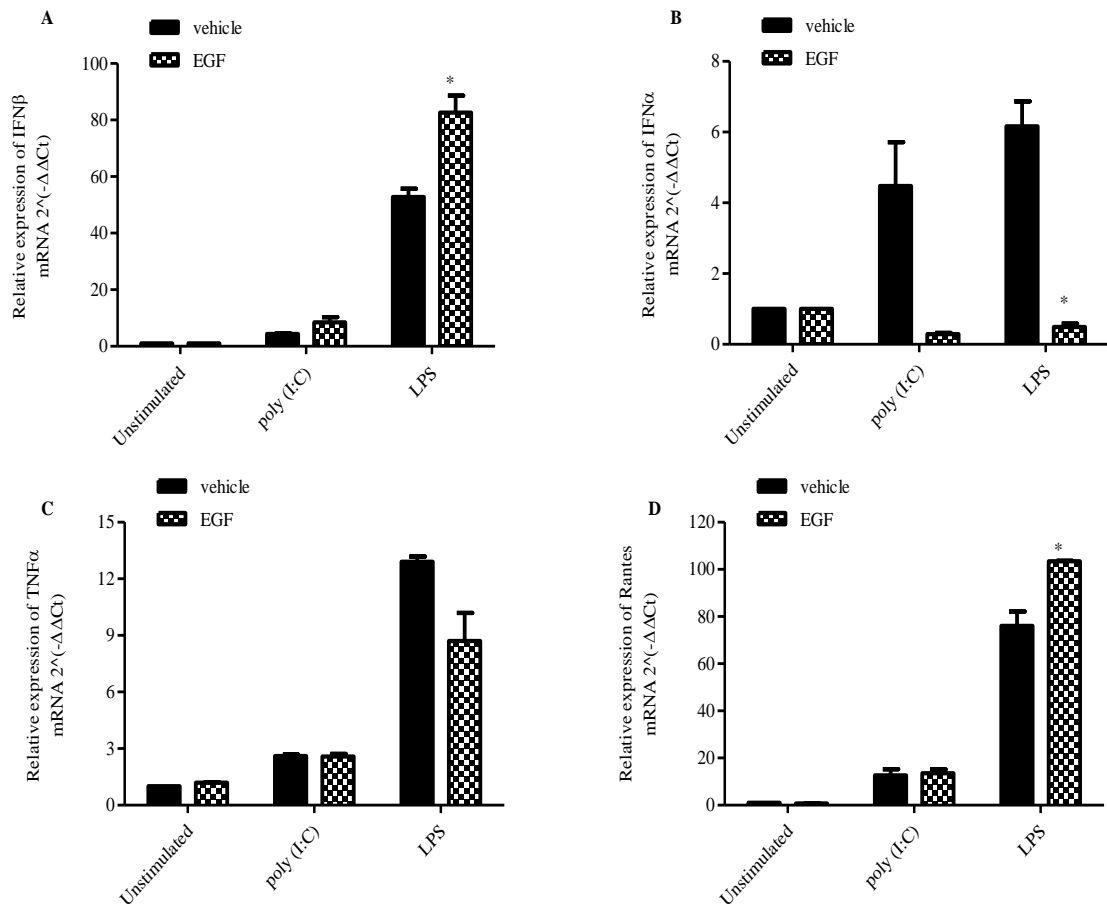


**Figure 5.12: Effect EGF on TLR3 and TLR4 signalling.** Wt-BMDMs were plated into a 6 well plate. When cells become confluent (80 %), they were left untreated or treated with 10  $\mu$ g/ml EGF for 24 h. Thereafter, cells were stimulated with either 20  $\mu$ g/ml poly(I:C) or 100 ng/ml LPS for 3 h. Next, total RNA was isolated and reverse transcribed in to cDNA. cDNA was used as templates and samples were diluted 25 times and cytokines were measured by Q-RT-PCR using specific primer to murine IFN- $\beta$ , IFN- $\alpha$ , TNF- $\alpha$ , Rantes and IL-6. Mouse GAPDH was used as housekeeping gene. Results are representing two independent experiments each done in duplicates. \*  $P < 0.05$ .

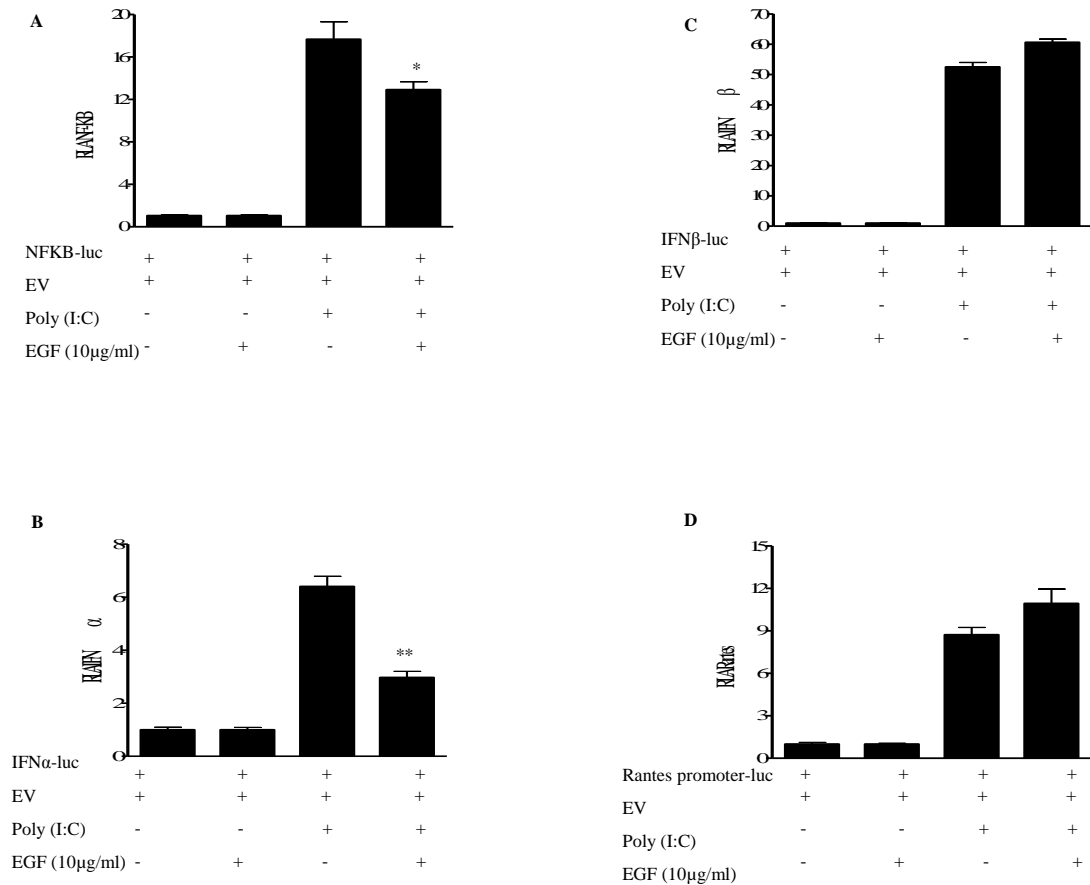


**Figure 5.13: Effect of EGF activation on TLR3-dependent signalling.** HEK293-TLR3 were plated in to 96 well plate at density of  $5 \times 10^4$  cells/well. After 24 h, the medium on the cells was removed and replaced by fresh medium containing 10 µg/ml EGF. After 3 h, cells were transfected with (80 ng) of reporter gene constructs encoding either NF- $\kappa$ B (A), IFN- $\alpha$  (B), IFN- $\beta$  (p125) (C) and Rantes promoter (D). 24 h after transfection cells were left untreated or treated with 20 µg/ml poly(I:C) for additional 24 h. Thereafter, cells were harvested and lysed, cell lysates were kept at - 80 °C for at least 24 h. Then, luciferase assay was performed using dual luciferase system (Promega). The results presented are representative of at least two independent experiments, each experiment was done in triplicate. \* P < 0.05, \*\* P < 0.01.

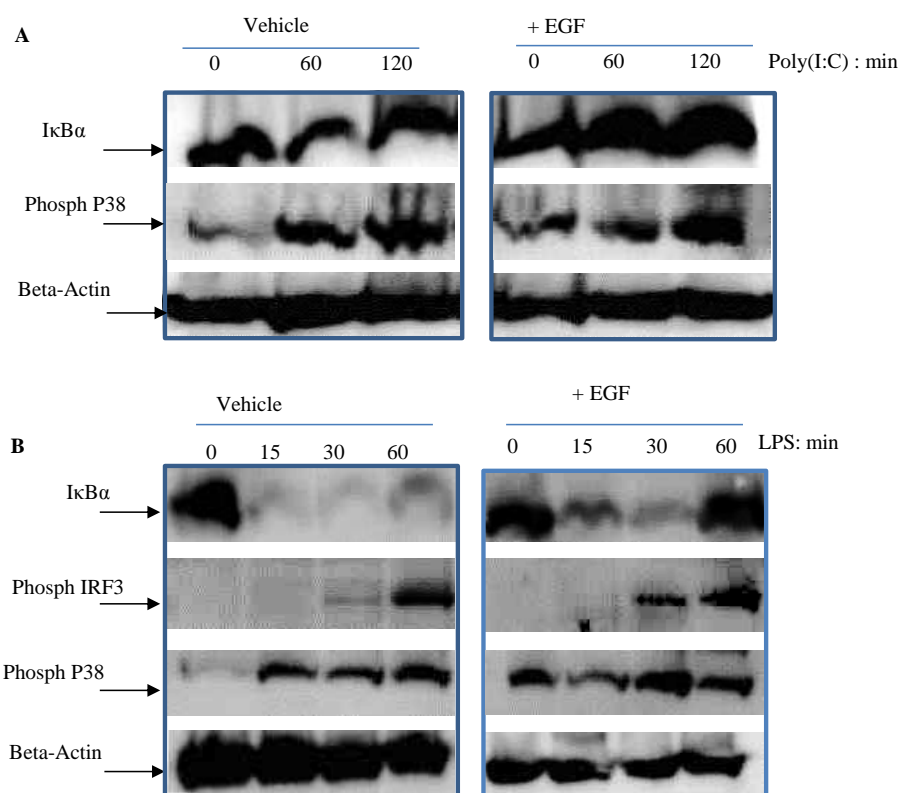


**Figure 5.14: EGF stimulation inhibited IκBα degradation and increased phosphorylation of IRF3 and p38.** Wt-BMDMs were seeded into 6 well plates. When cells became confluent (80 %), they were either left untreated or treated with 10 μg/ml EGF for 24 h. Thereafter, cells were treated with either 20 μg/ml poly(I:C) or 100 ng/ml LPS for times indicated. Then, cells were collected in 1 ml PBS and spun down for 10 min at 4 °C at 380 g. Cell pellets were lysed in RIPA buffer (25 mM Tris-HCl pH 7.6, 150 mM NaCl, 1 % NP-40, 1 % sodium deoxycholate, 0.1 % SDS, supplemented with protease inhibitor cocktail, 1 mM PMSF 1 mM Na<sub>3</sub>VO<sub>4</sub> and 1 mM DDT). Cell lysates were mixed with Laemmli loading buffer and boiled for 5 min. Proteins were separated by SDS-PAGE and subjected to immunoblot analysis using anti-IκBα, anti phosph p38 and IRF3 monoclonal antibodies. β-Actin was used as loading control. Images were captured using the G:Box system (Syngene). Results represent two independent experiments.

the MAPK, PI3K/AKT, RAS/ERK and JAK/STAT pathways (Henson and Gibson, 2006; Ji et al., 2009) more direct experiments are needed to confirm the role of  $\beta$ -catenin in TLR signalling.

### **5.2.9 Regulation of DVLs by the TLRs**

Autophagy is a newly recognised innate defence mechanism, acting as a cell-autonomous system for the elimination of intracellular pathogens. TLRs have been shown to induce TRIF and MyD88-dependent autophagy in macrophages (Delgado et al., 2008; Shi et al., 2008). Interestingly, autophagy negatively regulates Wnt signalling by promoting the degradation of DVLs (Gao et al., 2010). Thus, we propose that TLR activation may lead to the degradation of DVL protein and concomitant inhibition of Wnt signalling. To test this hypothesis, the effect of poly(I:C), LPS and R848 (TLR7 and 8 ligand) on DVLs mRNA expression levels was investigated. Wt-BMDMs were treated with either poly(I:C) or LPS or R848 for different time points, followed by RNA isolation and measurement of DVL1, DVL2, and DVL3 mRNA by Q-RT-PCR. Results showed that poly(I:C) significantly increased all three DVLs mRNA at 3 and 24 h compared to the control (Figure 5.15, panels A-C). LPS treatment significantly increased DVL1 and DVL3 mRNA at 90 min but significantly decreased DVL3 at 30 min and at 24 h compared to the control (Figure 5.14, panels D and F). DVL2 mRNA significantly decreased at 90 min, at 3 and 24 h (Figure 5.15, panel E). On the other hand, R848 significantly induced DVL1 transcription at 30 and 90 min but decreased it at 3 h compared to the control (Figure 5.15, panel G). DVL2 mRNA was also significantly increased at 90 min and decreased at 24 h (Figure 5.15, panel H). DVL3 transcription was significantly reduced at 24 h. This showed that TLRs differently regulated DVLs expression.

### **5.2.10 TRIF and MyD88 inhibit $\beta$ -catenin-induced Lef promoter activation**

It has been previously reported that downregulation of Wnt/ $\beta$ -catenin signalling occurred during *Mycobacterium tuberculosis* infection, characterised by TLR activation, in mice (Schaale et al., 2011). Therefore, the ability of TRIF and MyD88 to regulate  $\beta$ -catenin induced Lef transcription was studied in HEK293. Cells were co-transfected with Lef reporter construct,  $\beta$ -catenin and increasing amount of either TRIF or MyD88. It was found that TRIF significantly reduced  $\beta$ -catenin-induced Lef transcriptional activity even at a concentration of 1 ng (Figure 5.15, panel B).

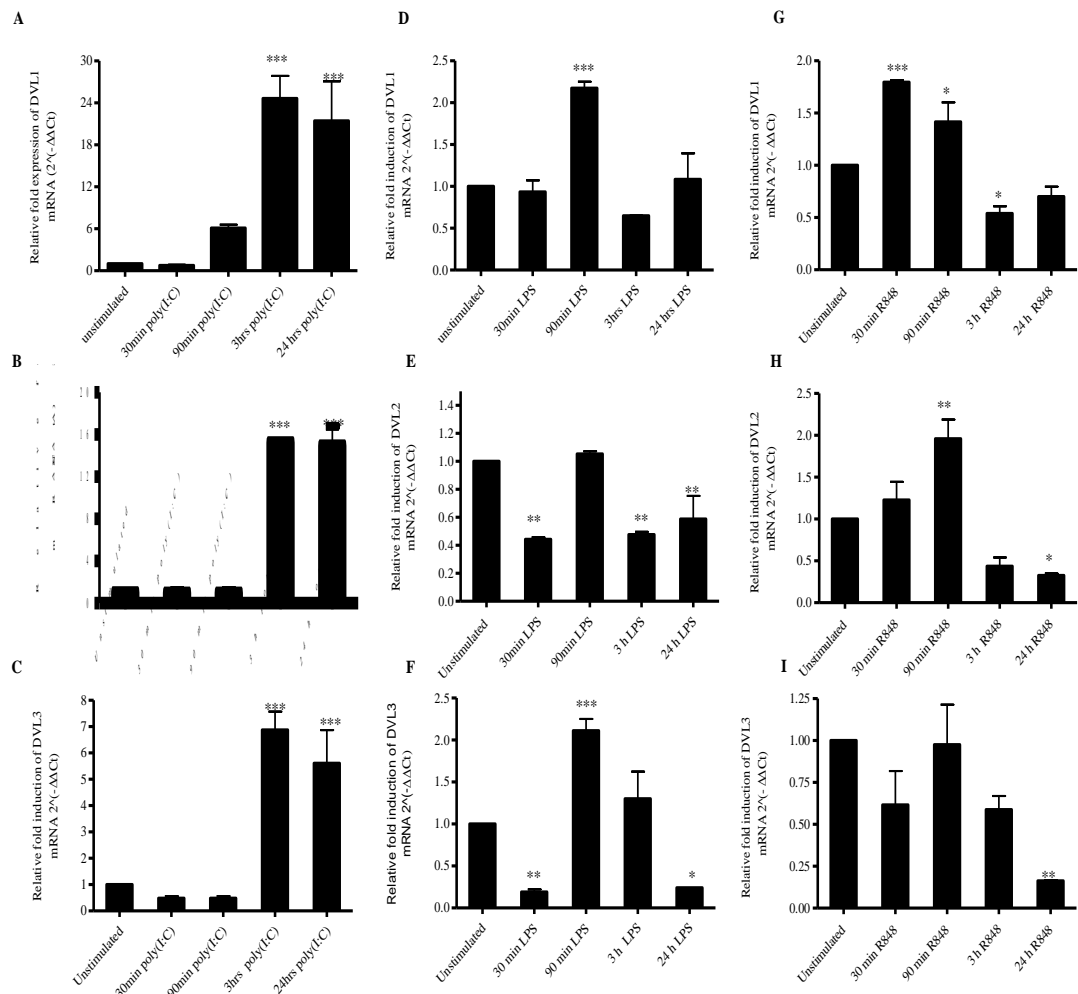


**Figure 5.15: Regulation of DVLs transcription by TLRs.** Wt-BMDMs were plated into 6 well plates. When the cells were confluent, they were treated with either 20  $\mu\text{g}/\text{ml}$  poly(I:C) (A, B and C) or 100  $\text{ng}/\text{ml}$  LPS (D, E and F) or 1  $\mu\text{g}/\text{ml}$  R848 (G, H and I) for times indicated. Thereafter, cells were collected and total RNA was isolated and reverse transcribed into cDNA. cDNA was used as templates and samples were diluted 25 times and DVLs mRNA were measured by Q-RT-PCR using specific primer to murine DVL1 (A, D, G), DVL2 (B, E, H), and DVL3 (C, F, I). Mouse GAPDH was used as housekeeping gene. Results are representing two independent experiments each done in duplicates. \*  $P < 0.05$ , \*\*  $P < 0.01$ , \*\*\*  $P < 0.001$ .

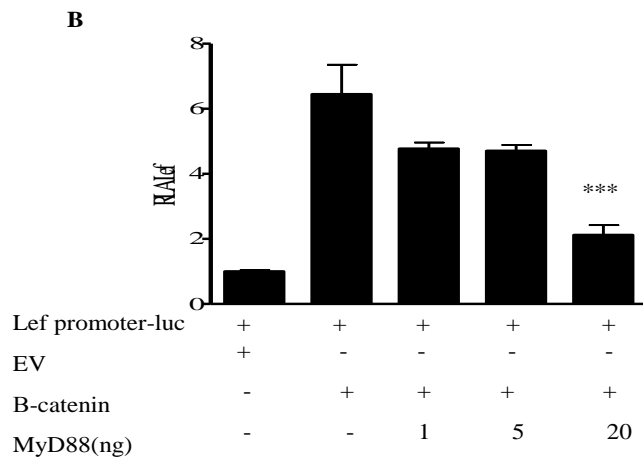
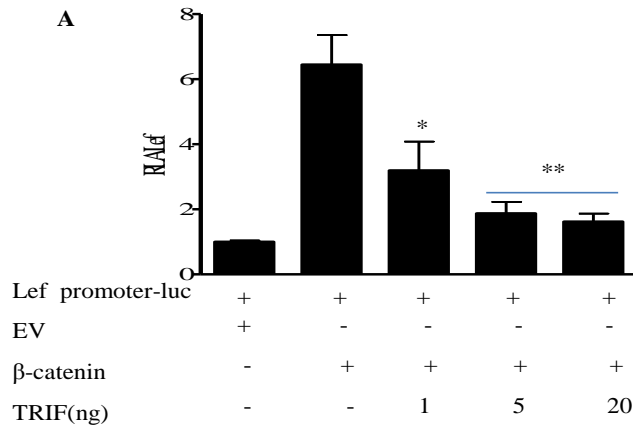


**Figure 5.16: TRIF and MyD88 inhibited  $\beta$ -catenin-induced Lef transcription**

HEKT293 were plated into a 96 well plate at a density of  $5 \times 10^4$  cells/well. After 24 h, cells were transfected with expression vectors encoding a reporter gene construct for Lef and co-transfected with either EV or expression vector encoding full length human HA- $\beta$ -catenin (20 ng) and increasing amounts of expression vector encoding full length human HA-TRIF (A), or an expression vector encoding full length human Myc-MyD88 (B). After 24 h, cells were harvested and lysed and cell lysates were kept at  $-80^\circ\text{C}$  for at least 24 h, followed by assessment of luciferase reporter gene activity using dual luciferase system (Promega). The results presented are representative of at least two independent experiments, each experiment was done in triplicate. \*  $P < 0.05$ , \*\*  $P < 0.01$  and \*\*\*  $P < 0.001$ .

MyD88 inhibited  $\beta$ -catenin-induced Lef promoter activation at a concentration of 20 ng (Figure 5.15, panel B). This may suggest reciprocal regulation of the TLRs and the Wnt/ $\beta$ -catenin pathway.

#### **5.2.11 poly(I:C) and LPS inhibited $\beta$ -catenin expression**

Following the finding that TRIF and MyD88 negatively regulate  $\beta$ -catenin-induced lef promoter transcription, the effect of poly(I:C) and LPS on  $\beta$ -catenin expression and its nuclear translocation was investigated. HeLa cells were transfected with either  $\beta$ -catenin or  $\beta$ -catenin and DVL3. Thereafter, cells were treated with poly(I:C) or LPS for 60 min followed by immunostaining of  $\beta$ -catenin and analyses by confocal microscopy. The expressed  $\beta$ -catenin was found to mostly co-localize in the cytoplasm but partially in the nucleus (Figure 5.17 panel A). DVL3 expression caused  $\beta$ -catenin nuclear translocation (Figure 5.17, panel B). However, poly(I:C) and LPS stimulation decreased  $\beta$ -catenin expression and partially inhibited DVL3-dependent  $\beta$ -catenin translocation (Figure 5.17, panels C and D).

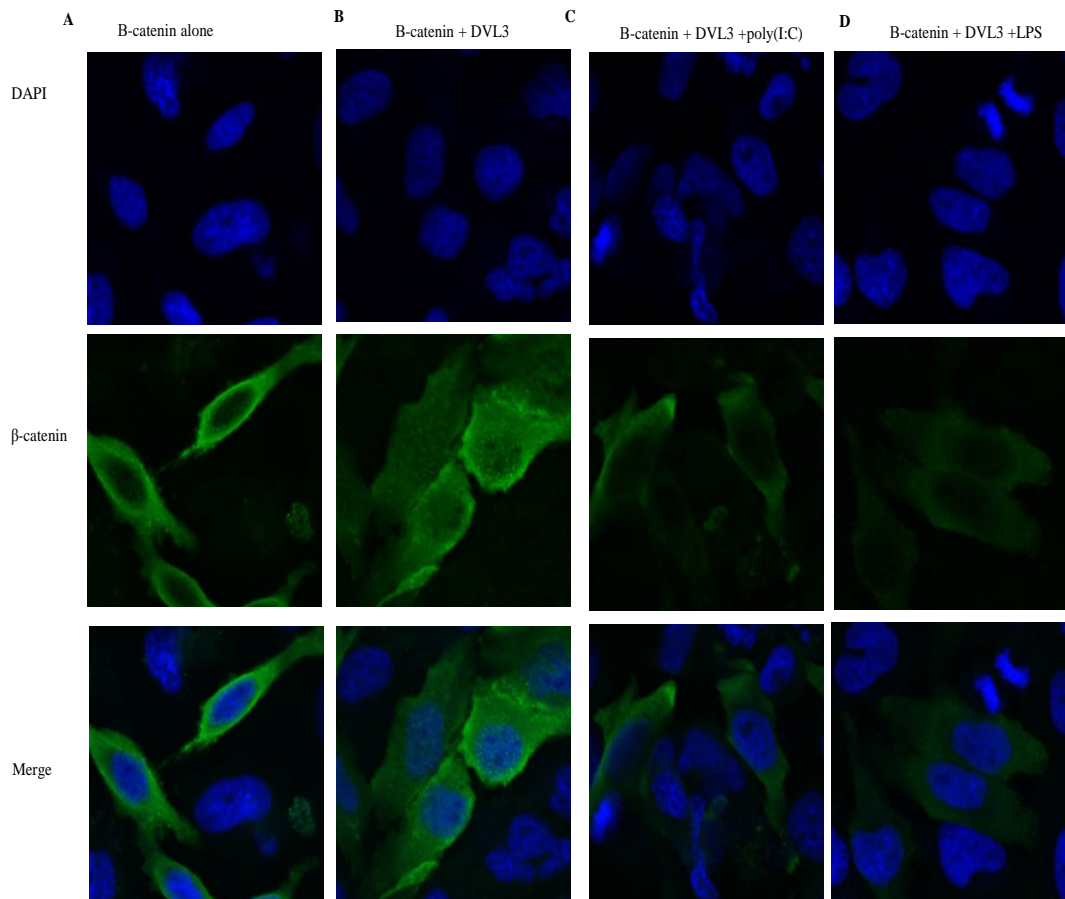


**Figure 5.17: Poly(I:C) and LPS inhibited  $\beta$ -catenin expression.** HeLa cells were seeded on precollagen coated glass coverslip into 6 wells plate. After 24 h, cells were transfected with either 200 ng of expression vector encoding full length human HA- $\beta$ -catenin (A) or co-transfected with either 200 ng of expression vector encoding full length human HA- $\beta$ -catenin and 200 ng of EV or 200 ng of expression vector encoding full length human HA- $\beta$ -catenin and full length human Myc-DVL3 (B-D). After 24 h cells were left untreated (A, B) or treated with either 20  $\mu$ g/ml poly (I:C) (C) or 1  $\mu$ g/ml LPS (D) for 60 min as indicated. Thereafter, cells were fixed in 4 % paraformaldehyde in PBS, permeabilised in 0.5 % triton X-100 in PBS and blocked for 1 h in 1 % BSA in PBS. Then, cells were incubated with 200  $\mu$ l of anti-HA monoclonal primary antibody (diluted 1:50 in blocking buffer) for 2 h at RT with gentle shaking. Thereafter, cells were washed with 0.05 % Tween 20 in PBS three times each 10 min. Then, cells were incubated with Alexa fluoro 488 secondary antibody (diluted 1:200 in blocking buffer) for 1 h at RT in the dark, followed by three washes with 0.05 % Tween 20 in PBS. Nucleus was stained with DAPI (10  $\mu$ g/ml in PBS). Then cell were washed twice in PBS and coverslip were mounted on glass slide using mounting medium and kept in the fridge until analysed. Images were captured using Olympus 1000 confocal microscopy and Flouview Software.

### 5.3 Discussion

The fact that there are three DVLs in mammals and that they are found to interact with a great variety of proteins including NF- $\kappa$ B suggests that DVLs may have other functions in addition to their vital role in Wnt signalling. In this study, role of DVLs in the regulation of TLR3 and TLR4 was investigated. It was found for the first time that all DVLs isoforms interacted with TRIF. Overexpression of all DVLs isoforms negatively regulated TRIF and TLR3-induce NF- $\kappa$ B, IFN- $\beta$  and Rantes promoter activation. However, only DVL2 had a positive effect on MyD88-dependent activation of NF- $\kappa$ B and IFN- $\beta$  promoter at low concentration. Recently, it has been reported that DVLs interact with NF- $\kappa$ B in the nucleus and their overexpression dramatically reduced TNF- $\alpha$ -induced NF- $\kappa$ B transcriptional activity (Deng et al., 2010). However, the inhibition of NF- $\kappa$ B by the DVLs was not dependent on Wnt signalling or  $\beta$ -catenin (Deng et al., 2010).

Inhibition of DVLs reduced TLR3 and TLR4-induce IFN- $\beta$ , TNF- $\alpha$  and Rantes transcription. This reduction could be explained by the decreased in I $\kappa$ B $\alpha$  degradation and the phosphorylation of IRF3 observed after DVLs inhibition. In contrast, the DVLs negatively regulated TRIF and TLR3 signalling in reporter gene assays. These differential effects could be due to the cell lines used in the study. Several studies suggested that different cell types may use different receptors to sense poly(I:C) or viral dsRNA. Although TLR3 was reported to play a key role in sensing poly(I:C) by epithelial cells (Guillot et al., 2005; Rudd et al., 2006; Matsukura et al., 2007), it only played a moderate or minor role in sensing poly(I:C) in macrophages (Alexopoulou et al., 2001; Yamamoto et al., 2003; López et al., 2004). Upregulation of Wnt5A in human macrophages stimulated with different mycobacterial species and conserved bacterial structures has been reported and the expression was dependent upon TLRs and NF- $\kappa$ B activation. Functional studies showed that Wnt5A is necessary for the regulation IL-12 and interferon  $\gamma$  in response to infectious agents (Blumenthal et al., 2006). A potential regulatory function of Wnt5A on cytokine expression is further supported by the observation that in patients with rheumatoid arthritis, Wnt5A modulates IL-6 and IL-15 expression in synoviocytes (Sen et al., 2001). Collectively, these data indicate the involvement of Wnt signalling in regulation of TLR signalling cascades. Our data showed that DVLs were needed for poly(I:C) and LPS induce cytokines transcription and may suggest that DVLs and Wnt5A activate the noncanonical pathway via calcium/

calmodulin dependent kinase II (CAMKII) which results in sustained upregulation of inflammatory cytokines (Figure 5.18).

Stimulation with EGF which was used here as of  $\beta$ -catenin activator increased IFN- $\beta$  and Rantes and decreased IFN $\alpha$  and TNF $\alpha$  transcription upon poly(I:C) and LPS stimulation. Also, it increased phosphorylation of IRF3 and p38 after LPS stimulation. However, I $\kappa$ B $\alpha$  degradation was reduced upon poly(I:C) and LPS stimulation. This may suggest that that  $\beta$ -catenin may play a positive and a negative role in regulating TLR signalling. In agreement with this result,  $\beta$ -catenin has been shown to interact with NF- $\kappa$ B and this interaction inhibited NF- $\kappa$ B activation in human colon and breast cancer cells (Deng et al., 2002). In another study, overexpression of  $\beta$ -catenin inhibited NF- $\kappa$ B reporter gene activity in a dose-dependent manner (Du et al., 2009). Also, Sun and colleagues reported that in cell lines expressing constitutively active  $\beta$ -catenin, I $\kappa$ B $\alpha$  protein was indirectly stabilised and NF- $\kappa$ B activity was repressed after wild-type *Salmonella* colonisation (Sun et al., 2005).

This study showed that DVLs transcriptions are differentially regulated by the TLRs, and that TRIF and MyD88 inhibited  $\beta$ -catenin-induces Lef transcription. Also, poly(I:C) and LPS stimulation decreased  $\beta$ -catenin expression in HeLa cells and partially inhibited DVL3-dependent  $\beta$ -catenin translocation. TLR4 activation has been shown to inhibits enterocyte proliferation in vitro and in vivo via impaired  $\beta$ -catenin signalling through activation of the GSK3 $\beta$  (Sodhi et al., 2010). In mice infected with *M. tuberculosis*, while inducible nitric oxide synthase (iNOS) and IFN- $\gamma$  formation were increased, the transcription of  $\beta$ -catenin dependent target genes were significantly reduced (Neumann et al., 2009; Schaale et al., 2011).

In conclusion this study demonstrates for the first time, that an interaction occurs between TRIF and the DVLs isoforms and shows that DVLs were needed for poly(I:C) and LPS induced cytokines transcription in wt-BMDMs. Specific DVL inhibitors or esiRNA against individual DVL may be useful to define the role that each DVL play in regulating TLR signalling. This study also demonstrated a cross regulation between  $\beta$ -catenin and TLR/NF- $\kappa$ B-mediated signalling.

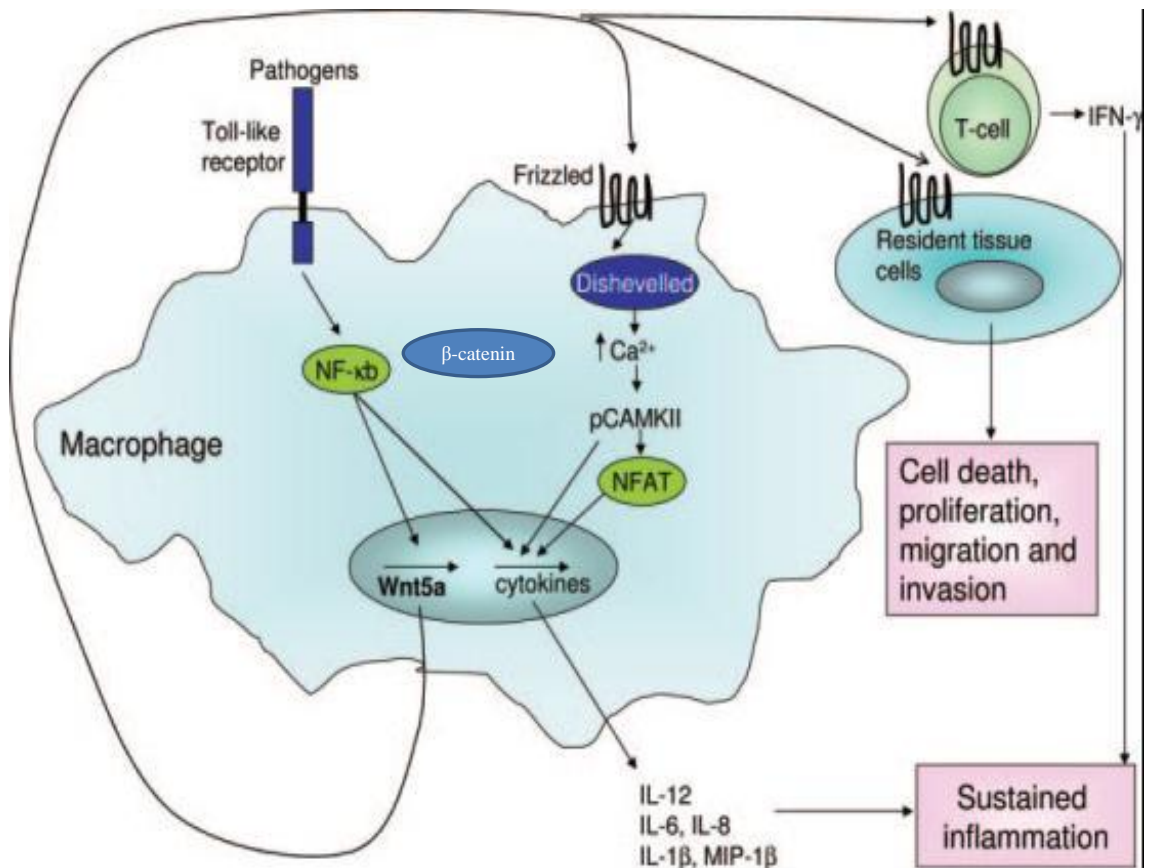


**Figure 5.18: Working hypothesis of the role of Wnt5A in the inflammatory response.** Activation of TLRs in macrophages by pathogens leads to activation of NF-κB and upregulation of Wnt5A and cytokines. Wnt5A independently of β-catenin activates the noncanonical pathway via calcium/calmodulin dependent kinase II (CAMKII) which results in sustained upregulation of inflammatory cytokines including IL-12, IL-6, IL-8, IL-1β, and macrophage inflammatory protein-1β (MIP-1β) either in a nuclear factor of activated T-cells (NFAT)-dependent or independent manner. Additionally, increased levels of Wnt5A and cytokines may affect other mononuclear cells including T-cells and surrounding resident tissue cells. (Adapted from George, 2008).

## **Chapter 6**

### **Proteomic analysis of endogenous TRIF interactome and the negative regulation of TRIF signalling by Optineurin**

## 6.1 Introduction

Mammalian cell lines provide several advantages over other cellular systems for the production of recombinant proteins, most notably the correct processing and modification of mammalian proteins (Mallory et al., 2007). However, still several problems such as protein yield, protein solubility and toxicity are associated with protein expression in mammalian cells. To date, most, if not all, studies concerning the subcellular localization of TRIF use over-expression models (Funami et al., 2008). These systems, though inherently useful, may not accurately reflect the true *in vivo* status of TRIF. For example, the correct subcellular localization of TRIF may not be apparent due to the large fluorescent tag which may impede cellular trafficking. An important problem associated with TRIF overexpression is the fact that induction of RIP/FADD/caspase8-dependent apoptosis is apparent (Han et al., 2004). Also, the expression of TRIF protein was always very low when compared to cells that were similarly transfected with MyD88 or other proteins that were utilised used during this project. This finding is supported by work undertaken by Funami and colleagues who reported lower expression level of wild-type TRIF when compared to mutated forms of TRIF (Funami et al., 2008). They suggested that wild-type TRIF may be rapidly degraded via some protein modifications.

Given the issues surrounding the overexpression of TRIF, the aim of the current chapter was to identify an anti-TRIF antibody that is capable of detecting endogenous human TRIF. Subsequently, the antibody will be used for pull-down assays and western blot analysis towards defining the time-dependent association of TRIF interacting proteins. Likewise, we aim to find a mammalian cell line that responds to both TLR3 and TLR4 ligands. The cell line would then be used to investigate the role played by TRIF and novel TRIF interacting proteins in TLR3 and TLR4 signalling.

## 6.2 Results

### 6.2.1 Characterisation of commercially available TRIF antibodies

To find an antibody that specifically recognises endogenous TRIF, a number of different commercial anti-TRIF antibodies were characterised. The antibodies were tested for their specificity towards the detection of TRIF by using different approaches namely western blotting, immunoprecipitation and immunohistochemistry. The antibodies that were tested are as follows:

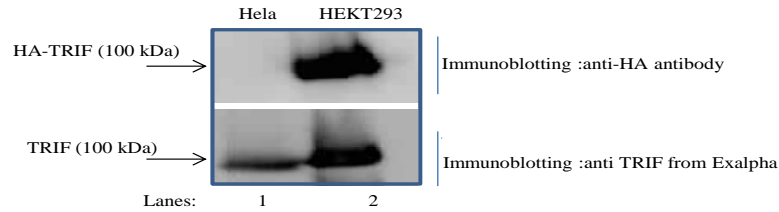
Rabbit polyclonal anti-human TRIF (Alexis, Cat. no. AL227 ).

Rabbit polyclonal anti-human and anti-mouse TRIF (Abnova, Cat. no. PAB0317).

Rabbit polyclonal anti-human TRIF antibody (Exalpa, Cat. no. X1827P).

Following transfection of HEKT293 cells with a plasmid encoding HA-TRIF, it was found that the anti-TRIF antibody that was purchased from Exalpa was capable of detecting HA-TRIF. In contrast, the anti-TRIF antibodies that were purchased from Alexis and Abnova did not detect HA-TRIF, despite confirmation of HA-TRIF expression following western blotting using an anti-HA antibody (data not shown). Regarding the anti-TRIF antibody from Exalpa, the antibody was examined for its ability to detect epitope-tagged full length human HA-TRIF using whole cell lysate (WCL) from HEKT293 cells transfected with 3 µg of HA-TRIF. To detect endogenous TRIF, whole cell lysate from un-transfected HeLa cells was used as these cells have been reported to express TRIF mRNA (Nishimura et al., 2005). Proteins were separated by SDS-PAGE electrophoresis. Immunoblotting was performed using either the anti-HA antibody or the anti-TRIF antibody (Exalpa). A band close to the 100 kDa molecular weight marker was detected in HeLa WCL (Figure 6.1 panel A, lane 1) and this band was also detected in HEKT293 WCL following HA-TRIF overexpression (Figure 6.1, panel A, lane 2). To confirm that the antibody was capable of immunoprecipitating TRIF, HEKT293 cells were transfected with 3 µg EV or 3 µg HA-TRIF and IP of HA-TRIF was performed as described (Materials and methods, section 2.2.9) using either an anti-HA or an anti-TRIF antibody (Exalpa). Immunoprecipitation of HA-TRIF using both the anti-TRIF antibody (Exalpa) and the anti-HA antibody was confirmed (Figure 6.1, panel B). These data confirm that the anti-TRIF antibody (Exalpa) can detect TRIF and be used in western blot and IP studies. As mentioned in Chapter 4 and

A



B

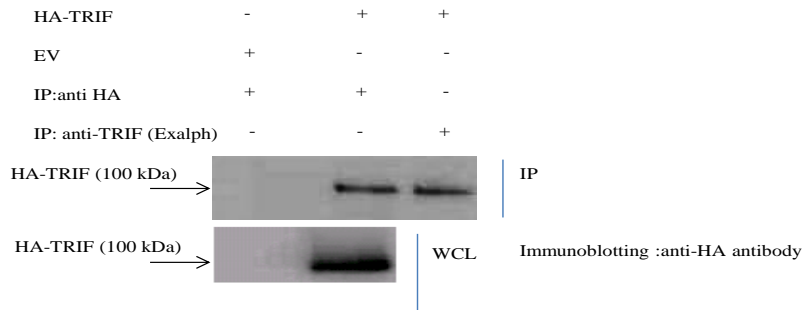


**Figure 6.1: Characterisation of Exalpa anti-hTRIF polyclonal antibody.** (A, lane 1) HeLa were seeded into T175 flasks and when the cells were 90-95 % confluent, they were collected in 10 ml ice cold PBS and spun down 10 min at 4 °C at 2000 rpm. Thereafter, the cell pellet was lysed in RIPA buffer (25 mM Tris-HCl pH 7.6, 150 mM NaCl, 1 % NP-40, 1 % sodium deoxycholate, 0.1 % SDS, supplemented with protease inhibitor cocktail, 1 mM PMSF 1 mM Na<sub>3</sub>VO<sub>4</sub> and 1 mM DDT). Cell lysates were mixed with Laemmli loading buffer and boiled for 5 min. Proteins were separated by SDS-PAGE and subjected to immunoblotting using anti-TRIF polyclonal antibody (Exalpa) and anti-HA antibodies. (A, lane 2) HEKT293 cell were seeded into 6 well plates. When cells were 80 % confluent, they were transfected with 3 µg of HA-TRIF. After 20 h, cells were lysed in RIPA buffer as mentioned in lane 1. Cell lysates were mixed with Laemmli loading buffer and boiled for 5 min. Proteins were separated by SDS-PAGE and subjected to immunoblotting using anti-HA and anti-TRIF(Exalpa) antibodies. (B) HEKT293 cells were seeded into 6 well plates. When the cells 80 % confluent, they were transfected with either 3 µg EV or 3 µg of HA-TRIF. After 20 h, transfected cells were lysed in lysis buffer (50mM HEPES, pH 7.5, 150 mM NaCl, 2 mM EDTA, pH8.0, 1 % NP-40, 0.5 % sodium deoxycholate supplemented with 1 mM PMFS, 1 mM DDT, 1 mM NaVO<sub>3</sub>, 5 and protease inhibitor cocktail). Cleared cell lysates were incubated with either 1 µg of anti-HA monoclonal or 2 µg of anti-TRIF (Exalpa) antibodies precoupled to 50 µl of Protein A/G Plus-Agarose beads for 2 h at 4 °C with gentle shaking. IP complexes were washed 4 times with lysis buffer and then released from the beads by addition of 40 µl of Laemmli loading buffer, followed by boiling for 5 min. Proteins were separated by SDS-PAGE and subjected to immunoblotting using anti-HA monoclonal antibody. Images were captured G: box system (Snygene). Results represent at least two independent experiments.

5, the anti-TRIF antibody was used to confirm an interaction between ADAM15 and TRIF and DVL3 and TRIF, respectively.

### **6.2.2 Examination of TLR3 and TLR4 responsiveness in U373-CD14 cells**

Having established that the TRIF antibody obtained from Exalpha can be used to detect endogenous TRIF, different cell lines were tested for their responsiveness to TLR3 and TLR4 ligands with the ultimate aim of the comparative characterisation of the endogenous TRIF immunocomplex following TLR3 and TLR4 engagement. Cells of relevance to innate immunity namely, human alveolar epithelial (A549) cells, bronchial epithelial (BEAS-2B) cells and human astrocytoma (U373-CD14) cells were tested. To test the cellular responsiveness, cells were stimulated with either poly(I:C) or LPS for different time points. Thereafter, cytokines were measured at both mRNA and protein level using by Q-RT PCR and ELISA, respectively. It was found that the U373-CD14 cell line was the only cell line that responded well to poly(I:C) and LPS as demonstrated by the upregulation of mRNA and secretion of cytokines and chemokines as measured by Q-RT-PCR and ELISA, respectively (Figure 6.2). Stimulation of U373 CD14 cells with poly(I:C) and LPS resulted in a significant upregulation of TNF- $\alpha$ , IFN- $\beta$ , and Rantes mRNAs compared to the control (Figure 6.2, panels A-C). In agreement with the mRNA data, poly(I:C) and LPS stimulation significantly increased the TNF- $\alpha$ , IL-6, and Rantes secretion in the cell free supernatant when compared to the control (Figure 6.2, panels, D-F). These results indicate that U373-CD14 respond to both TLR3 and TLR4 ligands, which make them suitable cell line for the proposed study.

### **6.2.3 Immunoprecipitation of endogenous TRIF**

IP of endogenous TRIF using an anti-hTRIF antibody obtained from Exalpha was performed using U373-CD14 cells as a model. To ensure adequate protein recovery and to achieve optimal TRIF detection, the IP was performed using the protein obtained from T175 flasks which were 90-95 % confluent. To this end, U373-CD14 cells were treated with either poly(I:C) or LPS for different time points followed by IP of endogenous TRIF as described (Materials and methods, section 2.2.10). Proteins were separated by SDS-PAGE and subjected to immunoblotting. As shown in Figure 6.3, panel A, whilst immuno-

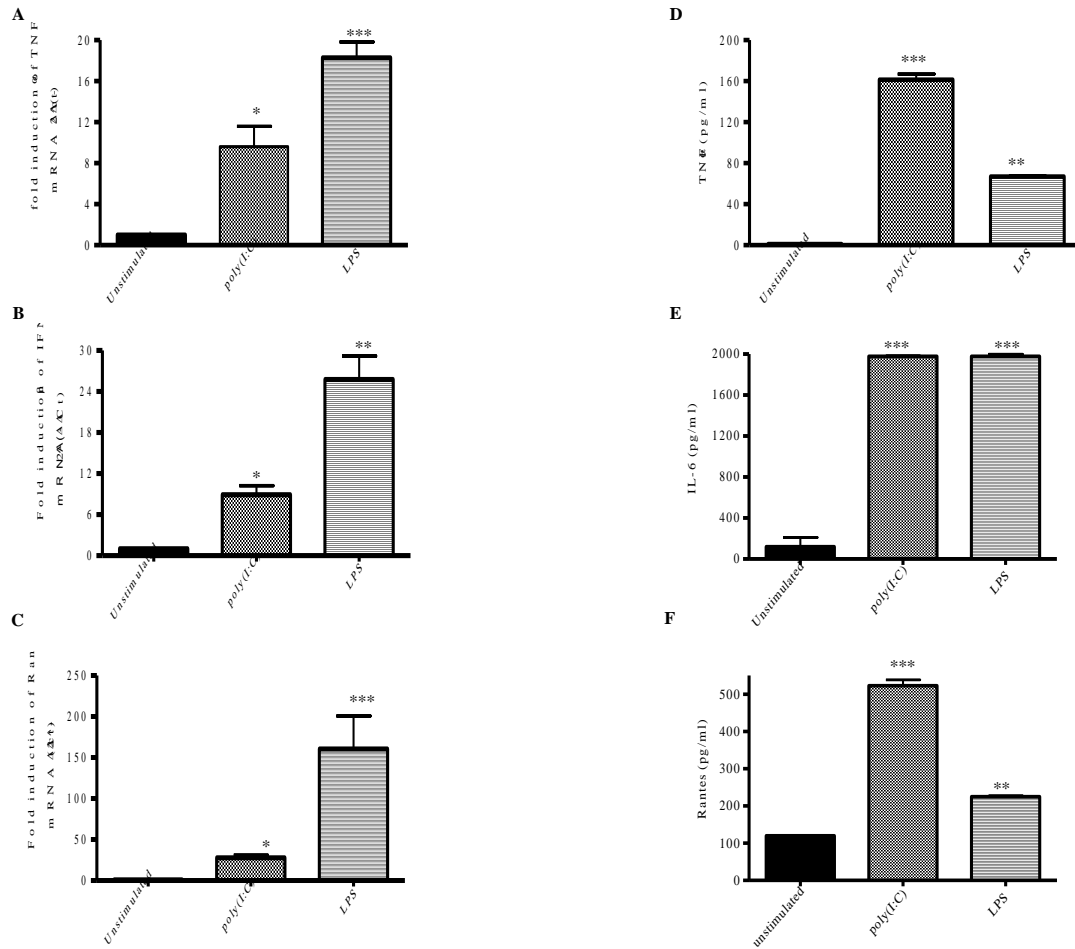


**Figure 6.2: Examination of TLR3 and TLR4 responsiveness in U373-CD14 cells (A-C)** U373-CD14 cells were seeded into 6 well plates. When the cells were 80 % confluent, they were stimulated with either 20  $\mu\text{g/ml}$  poly(I:C) or 1 $\mu\text{g/ml}$  LPS for 3 h. Thereafter, cells were collected and total RNA was isolated and reverse transcribed into cDNA. The cDNA was then diluted 25 times and Q-RT-PCR was performed using primers specific for human TNF- $\alpha$  (A), IFN- $\beta$  (B) and Rantes (C). Human GAPDH was used as housekeeping gene. (D-F) Cells were plated into 6 well plate. When the cells were 80 % confluent, they were stimulated with either 20  $\mu\text{g/ml}$  poly(I:C) or 1 $\mu\text{g/ml}$  LPS for additional 24 h. Thereafter, cell free supernatants were collected and sandwich ELISA was performed to measure the protein level of TNF- $\alpha$  (D), IL-6 (E) and Rantes (F). Data are representative of three independent experiments. \*  $P < 0.05$ , \*\*  $P < 0.01$ , and \*\*\*  $P < 0.001$ .

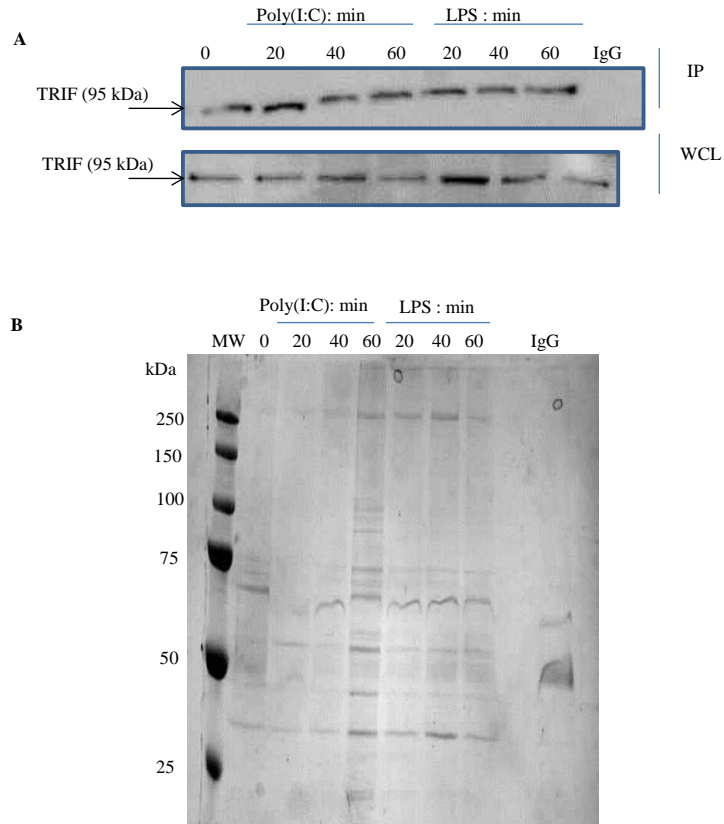


**Figure 6.3: Immunoprecipitation of endogenous TRIF.** (A) U373-CD14 cells were cultured into T175 flasks. When the cells were 90-95 % confluent, they were stimulated with either 20  $\mu\text{g/ml}$  poly(I:C) or 1  $\mu\text{g/ml}$  LPS for the times indicated. Thereafter, cells were scraped into 10 ml ice cold PBS and spun down for 10 min at 4  $^{\circ}\text{C}$  at 1200 rpm. Cell pellets were lysed in of lysis buffer (50 mM HEPES, pH 7.5, 150 mM NaCl, 2 mM EDTA, pH 8.0, 1 % NP-40, 0.5 % sodium deoxycholate supplemented with 1 mM PMSF, 1 mM DDT, 1 mM  $\text{NaVO}_3$  and protease inhibitor cocktail). Cleared cell lysates were incubated with 2  $\mu\text{g}$  of anti-hTRIF polyclonal antibody precoupled to 50  $\mu\text{l}$  of Protein A/G Plus-Agarose beads for 2 h at 4  $^{\circ}\text{C}$  with gentle shaking. Proteins were separated by SDS-PAGE and immunoblot analysis was performed using anti-hTRIF (Exalpha). Rabbit IgG (Sigma) was used as negative control. To visualize protein bands for tryptic digestion and LC-MS analysis, gels were stained in instant blue overnight (B) Images were captured using the G:box system (Syngene).

precipitated endogenous TRIF was detected at all-time points, a band was not detected in the control IP using a rabbit IgG. It must be noted that whilst the predicted molecular weight of TRIF is 76-78 kDa, routinely, in the current study, endogenous TRIF was detected at approximately 95 kDa. This finding is supported by Qu and colleagues whom showed that endogenous TRIF was detected at ~ 90 kDa (Qu et al., 2011). Further, an aliquot of the protein sample was subjected to SDS-PAGE followed by instant blue staining to visualise the protein bands (Figure 6.3, panel B). Here, to avoid the loss of protein, the gel was not destained, although, it is a less sensitive detection method when compared to the silver staining method.

#### **6.2.4 Identification of endogenous TRIF interactors**

The aim of this aspect of the study was to identify the binding partners for endogenous TRIF, without putting the cells under stress associated with transfection or TRIF overexpression. As the study investigated TRIF interactors at the endogenous level, receptor-independent TRIF activation associated with TRIF overexpression was avoided (Funami et al., 2007; Funami et al., 2008). We aimed here to identify ligand and receptor-dependent TRIF interacting proteins. Each gel lane was cut into 24 gel pieces, followed by in-gel tryptic digestion and LC-MS analysis as described (Materials and methods, section 2.2.12). Samples were analysed using Agilent 6340 Ion trap LC-MS machine. The MS spectra of the peptide ions were identified using the Mascot software programme ([www.matrixscience.com](http://www.matrixscience.com)) to search against the publicly available NCBI nonredundant protein database ([www.ncbi.nlm.nih.gov](http://www.ncbi.nlm.nih.gov)). The results generated at each time point was compared to the controls (un-stimulated and the IgG). Proteins which were similar to that identified in the controls were excluded from further analysis and considered as unspecific binding. Poly(I:C)-dependent TRIF interacting proteins are listed in Table 6.1 and LPS-dependent TRIF interacting proteins were listed in Table 6.2. Following analysis of the TRIF interactors, it was found that Menin, adenomatous polyposis coli (APC), CAP-Gly domain-containing linker protein 1 (CLIP), Prohibitin, ADAM15, IQ motif containing GTPase activating protein1 (IQGAP1), and 14-3-3 protein Zeta/delta proteins interacted with endogenous TRIF upon poly(I:C) and LPS stimulation. All of these proteins were also identified following LC-MS analysis of the overexpressed TRIF immunocomplex (Chapter 3). Together, these data confirm the association of these proteins with TRIF, both at

endogenous and at overexpressed level. Unfortunately, following analysis of the TRIF immunocomplex, TRIF itself was not identified, and as described in Chapter 3 (section 3.3), this may be due to mobility issues relating to TRIF. It must be emphasised that whilst TRIF was not detected by LC-MS it was detected in the concomitant sample following immunoblot analysis.

A significant number of proteins were identified as TRIF interactors. Due to the time course of this project validation of these protein interactors by immunoprecipitation or other direct experiments was not possible. However, it was decided to establish the role of a novel TRIF interactor, Optineurin (OPTN), in TLR signalling. Optineurin was identified as being a TRIF interactor following stimulation of cells with poly(I:C) for 20 min and will be further discussed herein. In addition, another interesting TRIF interactor identified upon stimulation of cells with poly(I:C) and LPS for 60 min and 40-60 min, respectively, was Prolow-density lipoprotein receptor-related protein 1 (LRP1). The LRP1 is multifunctional cell surface receptor and member of the low density lipoprotein (LDL)-receptor family. LRP1 play an important role in endocytosis and phagocytosis of apoptotic cells and involves in the regulation of many signalling pathway including lipid metabolism, proliferation of vascular smooth muscle, neurodevelopment and cancer (Campana et al., 2006; Francini et al., 2011). LRP1 induces the expression of matrix metalloproteinase 2 (MMP2) and MMP9 and thereby promotes the migration and invasion of human glioblastoma U87 cells (Song, et al., 2009). Zurhove et al. (2008) showed that LRP1 interacted with IRF3 in the nucleus and promotes its nuclear export and proteasomal degradation. Moreover, basal transcription of LPS target genes and LPS-induced secretion of proinflammatory cytokines are increased in the absence of LRP1. It has been reported that LRP1 sequestered frizzled receptor and thereby disrupts the frizzled receptor-LRP5/LRP6 complex and ultimately represses the canonical Wnt pathway (Lindner et al., 2010). This may suggest that the LRP1 is involved in TLRs mediated negative regulation to the Wnt/ $\beta$ -catenin pathway.

**Table 6.1 poly(I:C)-dependent TRIF interacting proteins.**

U373-CD14 cell line was stimulated with poly(I:C) for 20, 40 and 60 min, then TRIF immunoprecipitation was performed and proteins were separated by 1D SDS-PAGE gel electrophoresis followed by tryptic digestion and LC-MS analysis.

Protein name	NCBI accession no	Mascot score	PI	MW	Peptide Match	Sequence Coverage %	Time point
Adenomatous polyposis coli protein	53759122	57	7.92	313659	3	1	20 min
CAP-Gly domain-containing linker protein 1	109658674	51	5.29	162901	3	2	20 min
A disintegrin and metalloproteinase with thrombospondin motifs 13	21265034	51	6.96	158261	3	3	20 min
Optineurin/FIP2	20149572	53	5.14	66286	2	3	20 min
14-3-3 protein zeta/delta	4507953	134	4.73	26943	3	23	20 min
Very low-density lipoprotein receptor	65301167	249	4.62	99856	5	7	40, 60 min
NF-kappa-B-repressing factor	63003897	64	8.94	78308	2	3	40 min
Pyruvate kinase isozymes M1/M2	33286418	127			3	5	40 min and 60 min
Pro-low-density lipoprotein receptor-related protein 1	126012562	585	5.16	523476	16	4	60 min
Ras GTPase-activating-like protein IQGAP1	4506787	78	6.08	189772	2	1	60 min
prohibitin	4505773	74	5.75	29843	2	16	60 min

**Table 6.2 LPS-dependent TRIF interacting proteins.** U373-CD14 cells were stimulated with LPS for 20, 40 and 60 min, then TRIF immunoprecipitation was performed and proteins was separated by 1D SDS-PAGE followed by tryptic digestion and LC-MS analysis.

Protein name	NCBI accession no	Mascot score	PI	MW	Peptides Match	Sequence Coverage %	Time point
Desmoplakin	58530840	88	6.44	334021	2	1	20 min
Vascular endothelial growth factor receptor 1	156104876	53	8.66	152554	2	1	20 min
Junction plakoglobin	4504811	134	5.75	82434	4	6	20 min
Disintegrin and metalloproteinase domain-containing protein 15	15778976	52	6.3	95636	2	2	20 min
Growth factor receptor-bound protein 10	48762679	51	8.07	68158	2	5	20 min
Lysozyme C	4557894	132	9.38	16982	2	16	20 min
Prolow-density lipoprotein receptor-related protein 1	12667788	378	5.16	523150	12	3	40 min and 60 min
Very low-density lipoprotein receptor	65301167	147	4.62	99856	3	6	40 min and 60 min
Menin	1945390	53	6.14	68380	5	2	40 min
Monocyte differentiation antigen CD14	4557417	72	5.84	40689	2	5	40 min and 60min
Granulins	4504151	49	6.43	6815	2	3	60 min

Another interesting TRIF interactor that was identified upon LPS stimulation for 20 min was growth factor receptor-bound protein 10 (GRB10). GRB10 encodes an intracellular adaptor protein that can interact with several receptor tyrosine kinases and downstream signalling molecules (Garfield et al., 2011). GRB10 has been shown to interact with insulin receptor (IR), insulin-like growth factor 1 receptor (IGF1R), Raf1 kinase, and MEK1 kinase and to be involved in cell growth regulation. It is also negatively regulate insulin and IGF1 signalling by mediating insulin receptor and IGF1R degradation through ubiquitination (Huang et al., 2010; Doiron et al., 2012). In this regard, it has been reported that activation of the innate immune system via TLRs is implicated in the pathogenesis of insulin resistance and diabetes (Shi et al., 2006; Grishman et al., 2012). In accordance with this, Dasu and colleagues reported a significant increase in TLR2 and TLR4 expression in monocytes isolated from type 2 diabetes patients. They also showed increased phosphorylation of MyD88, TRIF, IRF3, IRAK1 and p65 in type 2 diabetes monocytes (Dasu et al., 2010).

## **6.3 Optineurin negatively regulates TRIF signalling**

### **6.3.1 Introduction**

Following the immunoprecipitation of endogenous TRIF using anti-TRIF antibody (from Exalpha) and analysis of interacting partners using LC-MS techniques, Optineurin (OPTN) was identified as a novel TRIF interacting partner following stimulation U373-CD14 cells with poly(I:C) for 20 min. Therefore the aim of this part was to investigate the role played by OPTN in TRIF mediated TLR3 and TLR4 signalling. OPTN is a Golgi complex-associated ubiquitous protein with high expression in skeletal muscle, heart, brain and pancreas (Sippl et al., 2011). It was first discovered as a binding partner of the adenoviral protein E3-14.7K and was shown to protect infected cells from TNF-induced cytolysis (Li et al., 1998). OPTN is a conserved 67-kD protein with multiple leucine zipper domains and a putative zinc finger domain at the C-terminus. OPTN shows strong homology (53 % identity) with NF- $\kappa$ B essential modulator and was therefore also called NEMO-related protein (Schwamborn et al., 2000).

Mutations in OPTN have been observed in rare hereditary cases of glaucoma (neurodegenerative eye diseases that cause blindness) and therefore named Optic neuropathy-inducing protein (Chalasanani et al., 2007). Recently, mutations in OPTN were identified in patients with familial amyotrophic lateral sclerosis (ALS) (Maruyama et al., 2010). ALS is an adult onset progressive neurodegenerative disorder whose hallmark is the selective death of motor neurons of primary motor cortex, brainstem, and spinal cord. The mechanisms by which mutant OPTN causes glaucoma or ALS have not been clarified yet. However, overexpression of glaucoma-causing mutant of OPTN in culture cells causes apoptotic and Golgi fragmentation leads to cell death and receptor mediated endocytosis (Sippl et al., 2011). OPTN also bind to Rab8, a member of small GTPase family known to be involve in vesicular transport (Hattula and Peränen, 2000) and link myosin VI to the Golgi complex and is involved in Golgi organization and exocytosis (Sahlender et al., 2005).

OPTN plays an important role in NF- $\kappa$ B regulation. Suppression of OPTN expression increases basal as well as TNF- $\alpha$ -induced NF- $\kappa$ B activity whereas overexpressed OPTN inhibits it. This negative regulation of NF- $\kappa$ B activity is believed to

be the result of competition of OPTN with NEMO for binding to polyubiquitinated RIP (Zhu et al., 2007). However, in human T-lymphotropic virus type1 (HTLV-1) infected cells, OPTN interacts with TAX1BP1 and a viral protein TAX1 resulting in sustained activation of NF- $\kappa$ B and ubiquitination of TAX1 (Jouno et al., 2009). Importantly, OPTN was identified as TBK1 binding partner (Morton et al., 2008). Overexpression of OPTN inhibited Sendai virus (SeV) and dsRNA triggered induction of IFN- $\beta$ , whereas depletion of OPTN with siRNA promoted virus-induced IFN- $\beta$  production and decreased RNA virus replication. This signalling involves interaction of OPTN with the antiviral protein kinase TBK1 and ubiquitin ligase TRAF3 (Mankouri et al., 2010). However, Gleason and colleagues reported a significant reduction in TBK1 activity and decreased phosphorylation of IRF3 in response to activation of TLR3 and TLR4 in BMDMs expressing a polyubiquitin-binding defective OPTN mutant. The production of IFN- $\beta$  mRNA and IFN- $\beta$  secretion was also impaired (Gleason et al., 2011).

## 6.3.2 Results

### 6.3.2.1 OPTN interacts with TRIF

Analysis of endogenous TRIF interacting partners using a proteomics approach revealed that TRIF interacts with OPTN. Thus, to confirm the interaction, co-immunoprecipitation of epitope-tagged TRIF (HA-TRIF) with epitope tagged OPTN (Myc-OPTN) was performed in HEK293-TLR3. Cells were transfected with either HA-TRIF and EV, or HA-TRIF and Myc-OPTN and treated as indicated. Thereafter, immunoprecipitation of HA-TRIF was performed as described (Materials and methods, section 2.2.9). As shown in Figure 6.4, panel A, OPTN constitutively co-immunoprecipitated with TRIF. Interestingly, Mankouri and colleagues reported a constitutive interaction between OPTN and TBK1 in HEK293 infected with Sendai virus or HEK293-TLR3 treated with poly(I:C) (Mankouri et al., 2010). This finding was recently supported by Gleason and colleagues who showed constitutive interaction between endogenous OPTN and endogenous TBK1 in BMDMs (Gleason et al., 2011). To investigate whether endogenous TRIF and OPTN interact constitutively with each other, IP of TRIF was performed in U373-CD14. Cells were treated with either poly(I:C) or LPS for 20 and 60 min followed by IP of endogenous TRIF as described (Materials and methods, section 2.2.10). Results showed that TRIF and OPTN interact in ligand-dependent manner. However, OPTN proved difficult to detect in whole cell lysates (Figure 6.4, panel, B).

### 6.3.2.2 Poly(I:C) and LPS induce OPTN expression

It has been reported that expression of OPTN is induced in response to viral infection (Mankouri et al., 2010). TNF- $\alpha$  stimulation in HeLa and A549 cells also activates OPTN promoter activity in a NF- $\kappa$ B dependent manner (Sudhakar et al., 2009). Therefore, the effect of poly(I:C) and LPS on OPTN expression was investigated in U373-CD14. Cells were stimulated with either poly(I:C) or LPS for different time points followed by RNA isolation, cDNA synthesis and Q-RT-PCR. Poly(I:C) significantly increased OPTN mRNA after 24 h compared to the control, LPS also increased OPTN expression at 24 h but the difference was not statistically significant (Figure 6.5, panels, A and B).

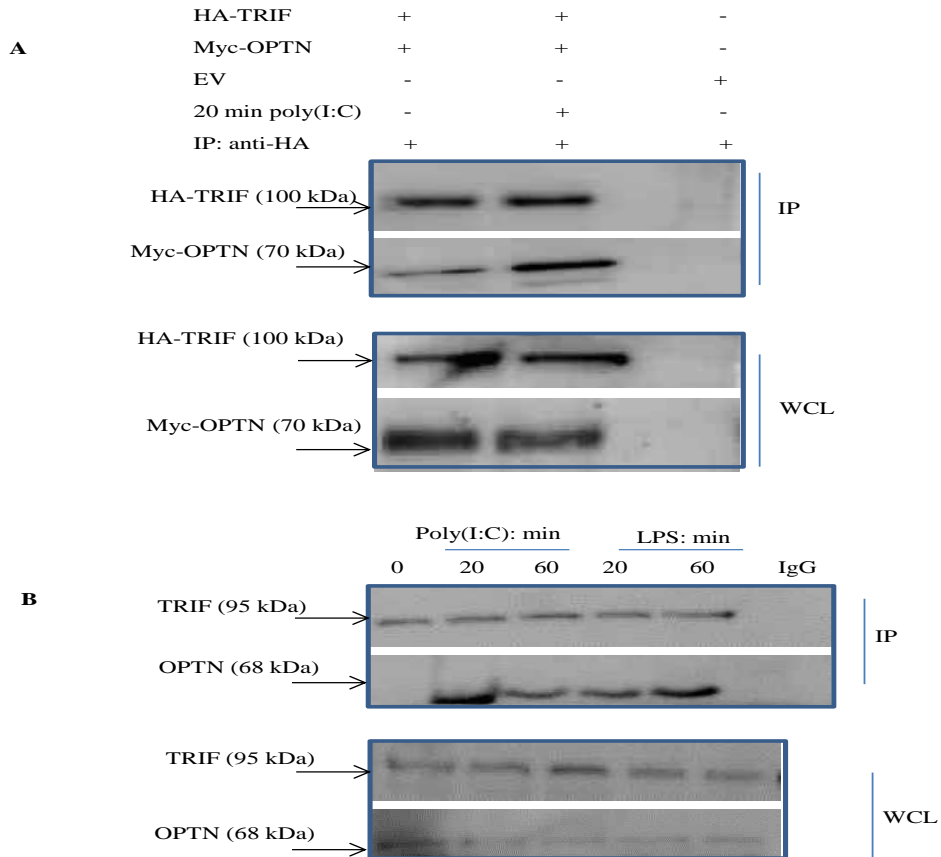


**Figure 6.4: Co-immunoprecipitation of TRIF and OPTN.** (A) HEK293-TLR3 were seeded into 6 well plates. When confluent (80 %), cells were co-transfected with 2  $\mu$ g of HA-TRIF and 1  $\mu$ g of EV or co-transfected with 2  $\mu$ g of HA-TRIF and 1  $\mu$ g of Myc-OPTN. After 20 h, cells were left unstimulated or stimulated with 20  $\mu$ g/ml poly(I:C) for 20 min. Thereafter, cells were lysed in lysis buffer (50 mM HEPES, pH 7.5, 150 mM NaCl, 2 mM EDTA, pH 8.0, 1 % NP-40, 0.5 % sodium deoxycholate supplemented with 1 mM PMSF, 1 mM DDT, 1 mM NaVO<sub>3</sub>, and protease inhibitor cocktail). Cleared cell lysates were incubated with 1  $\mu$ g of anti-HA monoclonal antibody precoupled to 50  $\mu$ l of Protein A/G Plus-Agarose beads for 2 h at 4 °C with gentle shaking. Immunoprecipitation complexes were washed 4 times with lysis buffer and then released from the beads by addition of 40  $\mu$ l of Laemmli loading buffer, followed by boiling for 5 min. Proteins were separated by SDS-PAGE and subjected to immunoblotting using anti-HA and anti-Myc monoclonal antibodies. (B) U373-CD14 cells were cultured into T175 flasks. When the cells were 90-95 % confluent, they were stimulated with either 20  $\mu$ g/ml poly(I:C) or 1  $\mu$ g/ml LPS for time indicated. Thereafter cells were scrapped into 10 ml ice cold PBS and spun down for 10 min at 4 °C at 1200 rpm. Cell pellets were lysed as per panel A and cleared cell lysates were incubated with 2  $\mu$ g of anti-hTRIF polyclonal antibody precoupled to 50  $\mu$ l of Protein A/G Plus-Agarose beads for 2 h at 4 °C with gentle shaking. Proteins were separated by SDS-PAGE and immunoblot analysis was performed using anti-hTRIF (Exalpha) and anti-hOPTN (Santa cruz) antibodies. Rabbit IgG (Sigma) was used as negative control. Images were captured using the G:box system (Syngene).

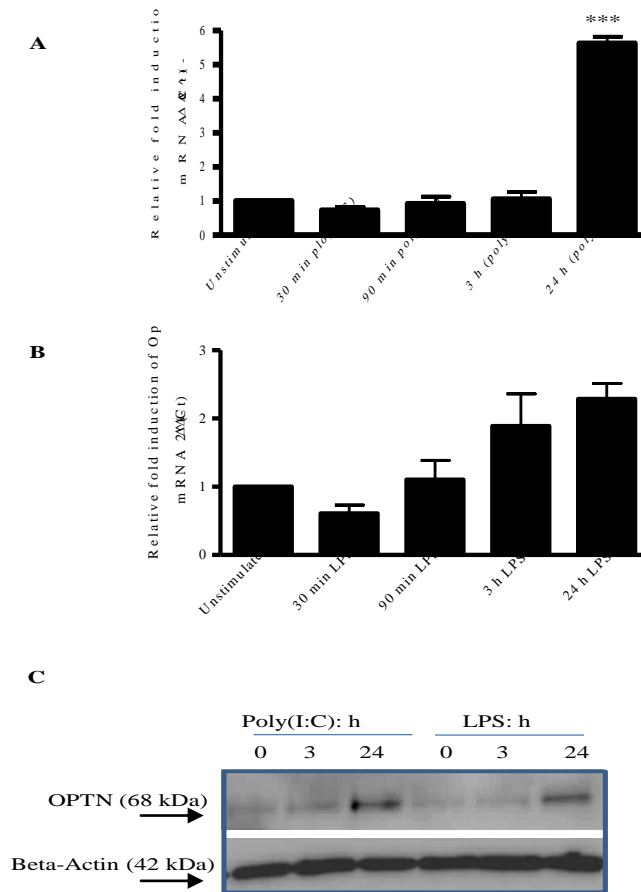


**Figure 6.5: poly(I:C) and LPS induce OPTN expression.** (A, B). U373-CD14 cells were plated into 6-well plates. When cells were 80 % confluent, they were left unstimulated (control) or stimulated with either 20  $\mu\text{g/ml}$  poly(I:C) (A) or 1  $\mu\text{g/ml}$  LPS (B) for the time indicated. Thereafter, total RNA was isolated, and reverse transcribed into cDNA. The cDNA were used as a template whereby it was diluted 25 times and OPTN mRNA was measured by Q-RT-PCR using primer specific to human OPTN. GAPDH was used as housekeeping gene. (C) U373-CD14 cells were plated in T175 flasks. When cells were 80 % confluent, they were stimulated with either 20  $\mu\text{g/ml}$  poly(I:C) or 1  $\mu\text{g/ml}$  LPS for the time indicated. Thereafter, cells were collected in 10 ml ice cold PBS and spun down for 10 min at 4  $^{\circ}\text{C}$  at 1200 rpm. Cell pellets were lysed in RIPA buffer (25 mM Tris-HCl pH 7.6, 150 mM NaCl, 1 % NP-40, 1 % sodium deoxycholate, 0.1 % SDS, supplemented with protease inhibitor cocktail, 1 mM PMSF, 1 mM  $\text{Na}_3\text{VO}_4$  and 1 mM DDT). Next, cell lysates were mixed with Laemmli loading buffer and boiled for 5 min. Proteins were separated by SDS-PAGE and subjected to immunoblot analysis using mouse anti-OPTN monoclonal antibody and  $\beta$ -actin was used as loading control. Images were captured using the G:Box system (Syngene). The results presented are representative of at least two independent experiments. \*\*\*  $P < 0.001$ .

However, poly(I:C) and LPS both increased OPTN protein expression levels after 24 h (Figure 6.5, panel C).

### **6.3.2.3 OPTN inhibits TRIF and TLR3-dependent reporter gene activity.**

The ability of OPTN to modulate TRIF-mediated luciferase reporter gene activity was investigated. Thus, HEK293 cells were transiently transfected with the NF- $\kappa$ B, IFN- $\beta$  and CCL5 (Rantes) reporter gene constructs and increasing amounts of OPTN in the presence of a constant concentration of TRIF. OPTN significantly inhibited TRIF-dependent activation of the NF- $\kappa$ B, IFN- $\beta$  (p125-luc) and Rantes reporter genes (Figure 6.6, panels, A-C). Furthermore, overexpression of OPTN also significantly inhibited TRIF-dependent activation of the NF- $\kappa$ B-driven PRDII and IRF3/IRF7-dependent PRDIII-I reporter genes (Figure 6.6, panels D and E). As TRIF mediates TLR3 signalling, the effect of OPTN on TLR3-dependent NF- $\kappa$ B, IFN- $\beta$  and Rantes activation was investigated using HEK293 cells stably expressing TLR3. In HEK293-TLR3 cells, overexpression of OPTN significantly inhibited TLR3-dependent activation of NF- $\kappa$ B, IFN- $\beta$  and Rantes reporter genes (Figure 6.6 panels F-H).

### **6.3.2.4 Suppression of OPTN by esiRNA.**

To investigate the role played by OPTN in TLR3 and TLR4 signalling, knockdown of OPTN was performed using esiRNA technology in U373-CD14 cells. To monitor the knockdown, U373-CD14 cells were transfected with esiRNA control or esiRNA against human OPTN, then OPTN mRNA and protein levels were measured by using Q-RT-PCR and immunoblotting, respectively. It was found that esiRNA successfully reduced OPTN mRNA by at least 70 % compared to the control (Figure 6.7 panel, A). In addition, the OPTN protein expression was also downregulated following suppression of OPTN expression by esiRNA compared to the control as measured by western blot (Figure 6.6 panel C).

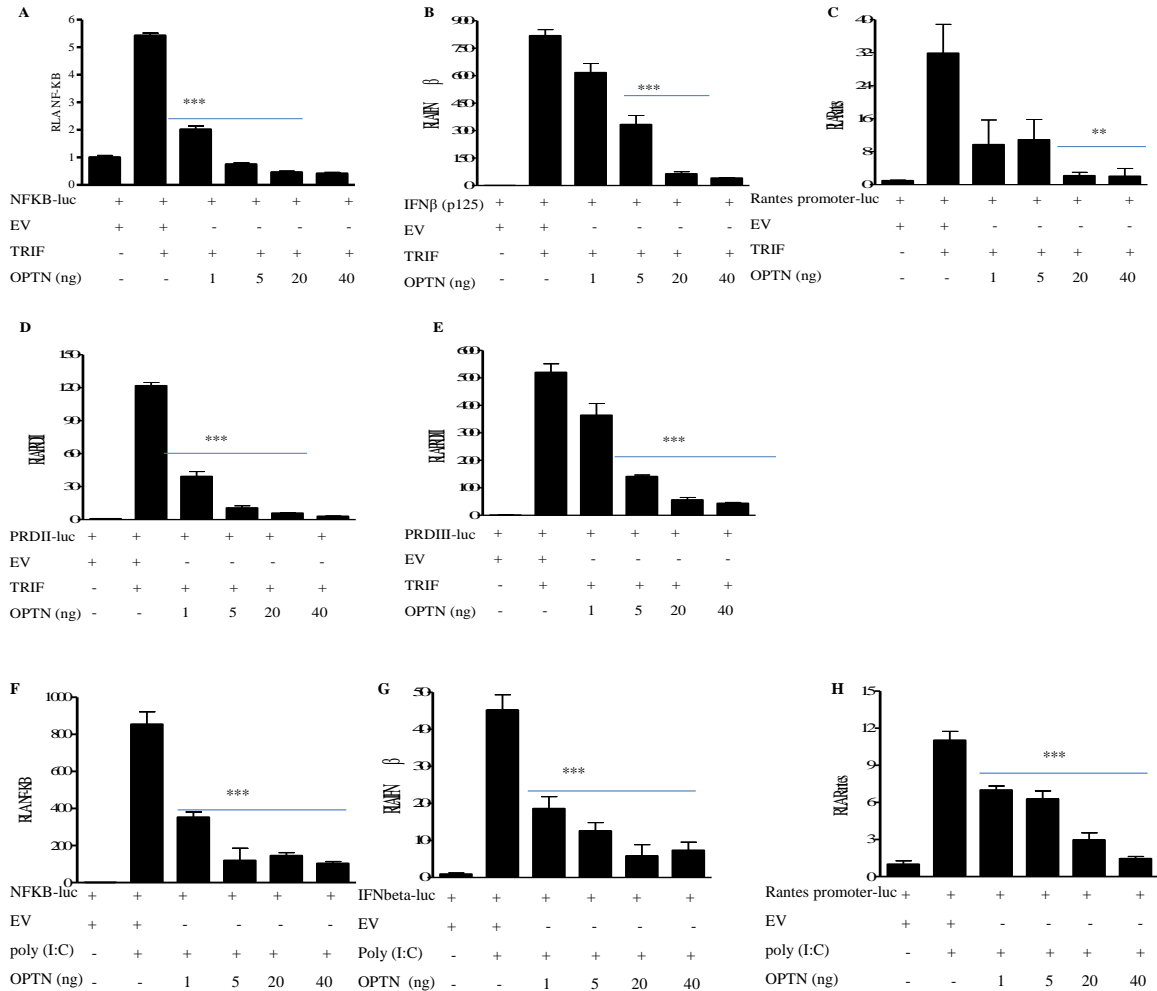


**Figure 6.6: OPTN inhibited TRIF and TLR3-dependent reporter gene activity.** (A-E) HEK293 cells were plated into 96 well plates at a density of  $5 \times 10^4$  cells/well. After 24 h, cells were transfected with expression vectors encoding either the reporter genes NF- $\kappa$ B (A), IFN- $\beta$  promoter p125 (B), Rantes promoter (C), IFN- $\beta$  PRDII (D) or IFN- $\beta$  PRDIII-I (E) and co-transfected with either EV or expression vectors encoding the full length human HA-TRIF (20 ng) and increasing amounts of expression vectors encoding full length human Myc-OPTN (5, 20, 30 and 40 ng) as indicated. After 24 h, cells were harvested and lysed. The cell lysates were stored at  $-80^\circ\text{C}$  for at least 24 h, followed by assessment of luciferase reporter gene activity. (F-H) HEK293-TLR3 cells were plated into 96 well plates at a density of  $5 \times 10^4$  cells/well. After 24 h, cells were transfected with expression vectors encoding either the NF- $\kappa$ B (F), IFN- $\beta$  promoter p125 (G), or Rantes promoter (H) reporter gene plasmids, and co-transfected with either an EV or and increasing amounts of OPTN. After 24 h, cells were left untreated (control) or stimulated with  $20 \mu\text{g/ml}$  poly(I:C) for an additional 24 h, followed by harvesting of cell lysates. Cell lysates were left at  $-80^\circ\text{C}$  for at least 24 h and assessment of luciferase reporter gene activity was performed using the dual luciferase system (Promega). The results presented are representative of at least three independent experiments, each experiment was done in triplicate. \*\*  $P < 0.01$  and \*\*\*  $P < 0.001$ .

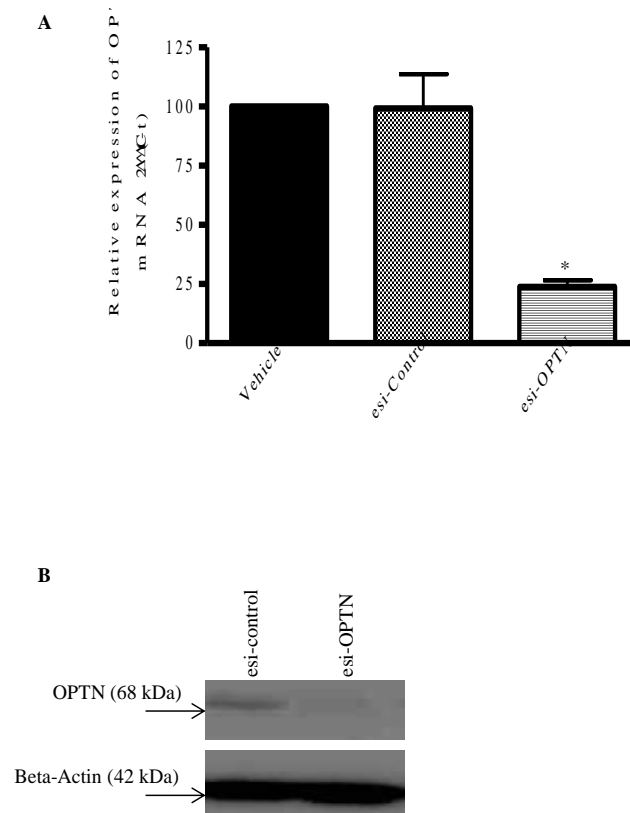


**Figure 6.7: Suppression of OPTN in human astrocytoma U373-CD14 cells.** (A) Cells were seeded into 6-well plate. When cells were 80 % confluent, they were transfected with 20 nM esiRNA control or 20 nM esiRNA against human OPTN. Cells were harvested 24 h after transfection and total RNA was isolated and reverse transcribed into cDNA. The cDNA template was diluted 25 times and OPTN mRNA was measured by Q-RT-PCR using primer specific to human OPTN. GAPDH was used as housekeeping gene. (B). Cells were plated into 6-well plates. After 24 h, cells were transfected with 20 nM esiRNA control or esiRNA against human OPTN. Cells were collected 48 h after transfection in 1 ml cold ice PBS and centrifuged for 10 min at 2000 rpm at 4 °C. Cells were lysed in RIPA buffer (25 mM Tris-HCl pH 7.6, 150 mM NaCl, 1 % NP-40, 1 % sodium deoxycholate, 0.1 % SDS, supplemented with protease inhibitor cocktail, 1 mM PMSF, 1 mM Na<sub>3</sub>VO<sub>4</sub>, and 1 mM DDT). Proteins were separated by SDS-PAGE and subjected to immunoblot analysis using an anti-human OPTN mouse monoclonal antibody (Santa Cruz) and β-Actin was used as loading control. Images were captured using the G:box documentation system (Syngene). \*P < 0.05.

### **6.3.2.5 Downregulation of OPTN expression enhanced IFN- $\beta$ , and Rantes mRNA expression.**

To investigate the potential role of OPTN in TLR3 and TLR4 signalling, levels of IFN- $\beta$ , TNF- $\alpha$  and Rantes mRNAs were measured in U373-CD14 cells following transfection with esiRNA control or esiRNA against OPTN. After 48 h post transfection, cells were stimulated with either poly(I:C) or LPS for 3 h, followed by RNA isolation, cDNA synthesis and Q-RT-PCR. It was found that suppression of OPTN expression significantly increased poly(I:C)-induces IFN- $\beta$  transcription compared to the control (Figure 6.8, panel A) Rantes mRNA was also increased but the difference is not statistically significant. However, suppression of OPTN expression had a negligible effect on TNF- $\alpha$ . (Figure 6.8 panels B and C). Suppression of OPTN had a negligible effect on LPS-induces IFN- $\beta$ , TNF- $\alpha$  and Rantes transcription (Figure 6.8 panels D-F). In general knockdown of OPTN increased slightly the basal levels IFN- $\beta$ , TNF- $\alpha$  and Rantes transcriptions

### **6.3.2.6 Effect of OPTN suppression on cytokine and chemokine secretion**

Next, the effect of OPTN on TLR3 and TLR4-mediated cytokine and chemokine secretion were assessed. To this end, U373-CD14 cells were transfected with esiRNA control or esiRNA against OPTN for 24 h, followed by stimulation with either poly(I:C) or LPS for additional 24 h. Thereafter, cell free supernatants were collected and cyto/chemokine secretion was measured in cell free supernatants using the Sandwich ELISA as described (Materials and method, section 2.2.20). Suppression of OPTN expression significantly increased poly(I:C) induced TNF- $\alpha$ , and Rantes compared to the control, IL-6 was slightly increased but the difference was not statistically significant, Surprisingly reduction of OPTN significantly decreased/increased LPS-induces TNF- $\alpha$ /Rantes, respectively (Figure 6.9, panels, A-C). Basal induction of TNF- $\alpha$  and Rantes was slightly increased when OPTN was suppressed.

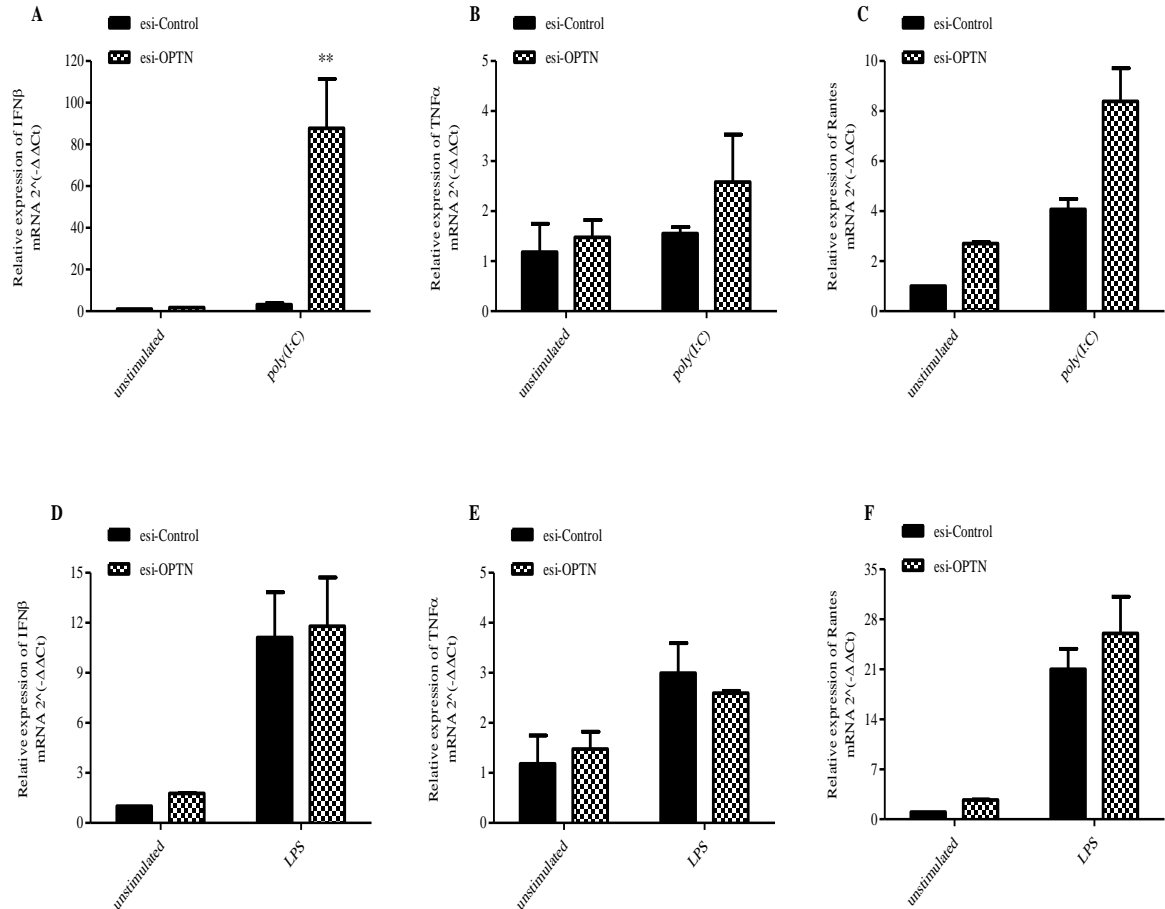


**Figure 6.8: Suppression of OPTN expression enhanced IFN- $\beta$  mRNA transcription.** U373-CD14 cells were seeded into 6 well plates. When the cells were 80 % confluent, they were transfected with 20 nM esiRNA control or esiRNA directed against OPTN. After 48 h, cells were stimulated with either 20  $\mu$ g/ml poly(I:C) (panels, A-C) or 1  $\mu$ g/ml LPS (panels D-F) for 3 h. Thereafter, cells were harvested and total RNA was isolated and reverse transcribed into cDNA. The cDNA was used as template and then diluted 25 times. Next, levels of IFN- $\beta$  (A, D), TNF- $\alpha$  (B, E) and Rantes (C, F) mRNAs were measured by Q-RT-PCR using specific human IFN- $\beta$ , TNF- $\alpha$  and Rantes primers. GAPDH was used as housekeeping gene. Data are representative of two independent experiments each experiment was done in duplicates. \* P < 0.05.

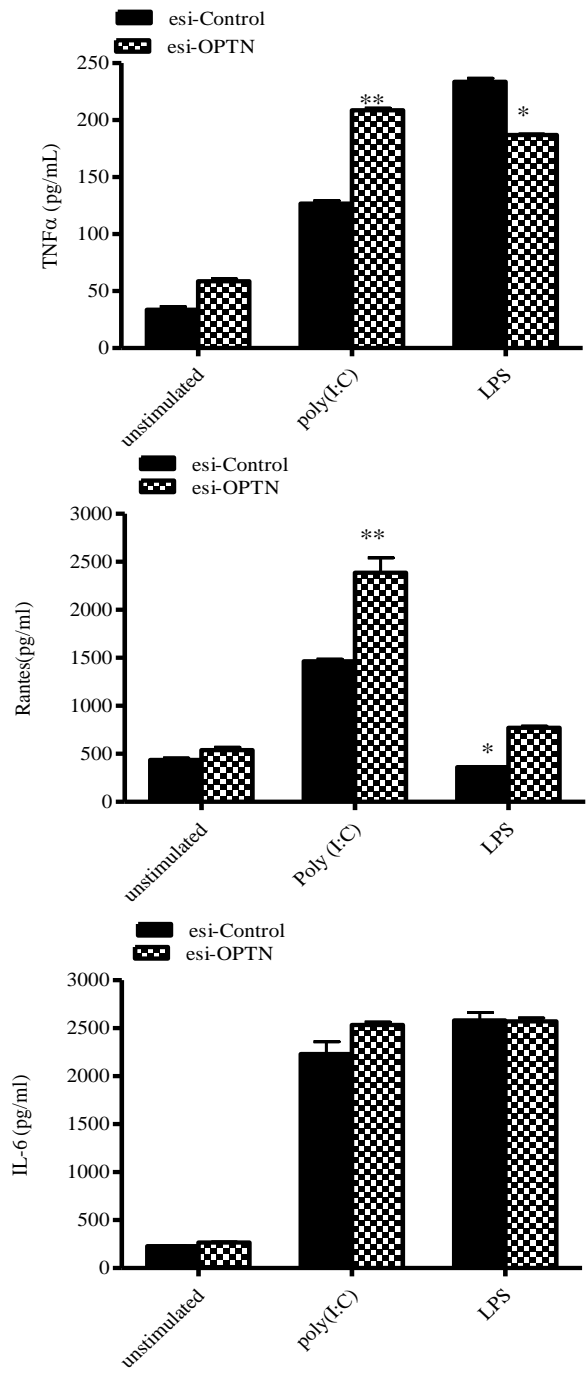


**Figure 6.9: Effect of OPTN suppression on cytokine and chemokine secretion** U373-CD14 cells were plated into 6-well plates. When the cells were 80 % confluent, cells were transfected with 20 nM esiRNA control or esiRNA against OPTN. After 24 h, cells were stimulated with either 20 µg/ml poly(I:C) or 1 µg/ml LPS for an additional 24 h. Thereafter, cell free supernatants were collected and ELISA was performed to detect human TNF-α (A), Rantes (B) and IL-6 (C). Data are representative of two independent experiments each experiment was done in triplicates. \* P < 0.05, \*\* P < 0.01.

## 6.4 Discussion

The aim of this chapter was to characterise the endogenous TRIF immunocomplex following TLR3 and TLR4 ligand stimulation. To this end, we characterised a suitable antibody and cell line that facilitated the activation of TLR3 and TLR4 signalling and subsequent immunoprecipitation of endogenous TRIF. This study has showed that an anti-TRIF antibody obtained from Exalpa can be used to detect and immunoprecipitate endogenous TRIF. The anti-TRIF antibody was used to confirm an interaction between endogenous TRIF and some novel TRIF interacting proteins such as ADAM15, DVL3 and OPTN. The human astrocytoma cell line U373-CD14 was found to be a good cell model to study TRIF mediated TLR3 and TLR4 signalling as they showed good response to poly(I:C) and LPS. This is in contrast to A549 cells which showed upregulation of TNF- $\alpha$  and IFN- $\beta$  mRNA upon poly(I:C) and LPS stimulation. However, secretion of TNF- $\alpha$ , Rantes and IL-6 was not detected in cell free supernatant following stimulation with these ligands, as measured by ELISA (data not shown). In BEAS-2B cells, poly(I:C) stimulation resulted in increased TNF- $\alpha$  and IFN- $\beta$  mRNA and, in agreement with the mRNA data, the BEAS-2B cells showed significant increase in IL-6 and Rantes secretion in cell free supernatant. However, LPS stimulation increased TNF- $\alpha$  mRNA, but not cytokine/chemokine secretion in cell free supernatant (data not shown). MacRedmond et al. (2005) reported that expression of TLR4 in A549 cells showed that the cells respond to LPS. Hou et al. (2006) also reported that Poly(I:C) upregulated TLR3 mRNA, stimulated IL-8 secretion and enhanced phosphorylation of NF- $\kappa$ B in A549 cells. Regarding the BEAS-2B, it has been reported that these cells express functionally active TLR3 and TLR4 (Sha et al., 2004). The difference here, may be due the cells passage that used in this study or the cells may secrete other cytokine/chemokine than what we measured in response to poly(I:C) and LPS.

Following immunoprecipitation of endogenous TRIF and subsequent LC-MS analysis a potential number of poly(I:C) and LPS-dependent TRIF protein interactors were identified in this study. Proteins such ADAM15, CLIP, APC, Menin, IQGAP1 and prohibitin were identified in this screening and also identified in the proteomic analysis of overexpressed TRIF protein complex (Chapter 3). These data confirm an association between these proteins and TRIF at the endogenous level. However, further validation by

direct experiments is required to study their potential role in TRIF signalling. New interesting TRIF interactors such as LRP1 and GRB10 were also identified, thus linking TRIF to other signalling pathways such as endocytosis and phagocytosis and diseases such as diabetes. As mentioned earlier LRP1 play an important role in endocytosis and phagocytosis (Campana et al., 2005; Francini et al., 2011) and GRB10 negatively regulates insulin and IGF1 signalling by mediating insulin receptor and IGF1R degradation through ubiquitination (Huang et al., 2010; Doiron et al., 2012).

Results showed that OPTN, a TBK1 binding protein also interacted with TRIF constitutively when overexpressed in HEK293-TLR3. It also binds to endogenous TRIF upon poly(I:C) and LPS stimulation for 20-60 min in U373-CD14. It was found that OPTN expression was increased following stimulation with poly(I:C) and LPS for 24 h. In agreement with this result, Mankouri and colleagues reported that increased OPTN expression was evident in HEK293 infected with Sendai virus, an activator of the RIG-I pathway and following stimulation of HEK293-TLR3 with poly(I:C) (Mankouri et al., 2010). Activation of OPTN promoter upon TNF- $\alpha$  stimulation in Hela and A549 cells has also been reported (Sudhakar et al., 2009).

Overexpression of OPTN in HEK293 or HEK-TLR3 strongly inhibited TRIF and TLR3-dependent activation of NF- $\kappa$ B, IFN- $\beta$  and Rantes promoter activity respectively. Moreover, overexpression of OPTN in HEK293 also significantly inhibited TRIF-dependent activation of the NF- $\kappa$ B-driven PRDII and IRF3/IRF7-dependent PRDIII-I reporter genes. Furthermore knockdown of endogenous OPTN using esiRNA technology in U373-CD14 significantly increased IFN- $\beta$  mRNA and secretion of TNF- $\alpha$  and Rantes upon poly(I:C) stimulation. However, suppression of OPTN significantly increased LPS-induced Rantes and decreased LPS-induced TNF- $\alpha$  secretion. In this regard, Gleason and colleagues reported that OPTN is required for optimal activation of TBK1 and production of IFN- $\beta$  in BMDMs upon TLR3 and TLR4 activation (Gleason et al., 2011). This is in contrast with another study which reported that poly(I:C) and virus-induced activation of IFN- $\beta$  reporter gene and IFN- $\beta$  secretion was inhibited upon OPTN overexpression and enhanced by siRNA knockdown of OPTN in HEK293-TLR3 (Mankouri et al., 2010). However, another study showed that overexpression of OPTN inhibited TNF- $\alpha$ -induced NF- $\kappa$ B activation in

Hela cells (Nagabhushana et al. 2011). Collectively, these data suggest that the role of OPTN in regulating NF- $\kappa$ B and IFN- $\beta$  depends on the cell type and the stimulus.

In conclusion, this study demonstrates that an anti-TRIF antibody obtained from Exalpha can be used to detect and immunoprecipitate endogenous TRIF, and characterisation of the TRIF immunocomplex has identified a number of TRIF interacting partners. OPTN has been identified as a negative regulator of TRIF and TLR3-mediated reporter gene activation. However, further future work is need to determine the mechanisms by which OPTN inhibits TRIF and TLR3 signalling.

## **Chapter 7**

### **General Discussion**

## 7.1 General discussion

While it is well appreciated that the TLRs are responsible for the recognition of pathogens and emanation of the appropriate responses, increasing evidence suggests that the family of five cytosolic TIR-adaptor proteins also play a crucial role in the specificity of the response (Jenkenis and Mansell, 2010). The TRIF adaptor protein is a key adaptor for TLR3 and TLR4-mediated signalling. It was first shown to serve as an adaptor for the TLR3-mediated signalling pathway with studies showing an association between TRIF and TLR3 and the ability of a mutant form of TRIF to inhibit the TLR3-dependent activation of NF- $\kappa$ B (Hardy et al., 2004). Further, studies using TRIF-deficient mice have demonstrated that TRIF plays a key role in both TLR3- and TLR4-mediated signal transduction via both NF- $\kappa$ B and IRF3, with the induction of IFN- $\beta$  and inflammatory cytokines being severely impaired (Yammato et al., 2003). Recently, it was shown that TRIF also mediates TLR5 signalling in intestinal epithelial cells and that DDX1, DDX21 and DHX36 use TRIF to activate the NF- $\kappa$ B pathway and type I IFN responses (Choi et al., 2010; Zhang et al., 2011).

Herein, proteomic analysis of overexpressed and endogenous TRIF interactomes was performed with a view to identifying novel TRIF interacting proteins towards a better understanding of how TRIF-mediates TLRs signalling. Proteomic analysis of overexpressed TRIF in HEK293-TLR3 and HEK293-TLR4 cells led to the identification of many novel TRIF interacting proteins. Interestingly, many of the newly identified TRIF interacting proteins have been previously reported to be involved in modulation of proteins such as MAPKs (MAPK1, 2, 3, 8, and 9), Caspases (Caspase 1, 3, and 8), BCL2, JUN, IKBKB and NFKBIA. Moreover, they were reported to modulate cellular processes such as apoptosis, immune response, inflammatory response, autophagy, phagocytosis, endocytosis, cytokine production, cell differentiation, cell proliferation and a lot of more. However, there was no previous report showing interaction between TRIF and these new identified proteins. Unfortunately, TRIF itself was not identified in the overexpression and endogenous IP complex in the LC-MS analysis. However, the expression of TRIF was always confirmed by immunoblot analysis. Recently, Li et al. (2011) performed proteomic analysis of the human innate immunity interactome for type I interferon. Proteins such as Optineurin (OPTN), NF $\kappa$ B repressing factor (NFRF), and Growth factor receptor-bound

protein 2 (GRB2) were among the identified hits. OPTN and NFRF, GRB2-associated-binding protein 3 and GRB10 were identified herein in TRIF IP complex this may confirm association of these proteins with TRIF. This approach, although useful, it may result in identification of false positive interacting protein hits. As the cells already expressed endogenous TRIF, overexpression of TRIF could increase the TRIF expression level in the cells, which may lead to induction of some proteins that are not present in its physiological condition. The overexpression of TRIF was also associated with apoptosis and cell death. Thus, the output from this approach requires intensive validations by direct experiments to filter out nonspecific binding proteins. Another method used to identify protein-protein interaction is the tandem affinity purification (TAP)-tags technique (Li et al., 2011; Pichlmair et al., 2012). The TAP tag is a composite tag consisting of two different epitope domains and a protease cleavage site, and it facilitates the purification of the tagged protein in two consecutive, high-affinity chromatography steps (Gunzl and Schimanski, 2009). An important advantage of the TAP-technique is that the amount of nonspecific binding is reduced compared to approach used in this study. Although the TAP-tag method is highly sensitive and selective, a potential problem with the method is that the increased purity leads to the loss of transient nature protein-protein interaction during the series of purification steps. Another problem is that a relatively large amount of starting material is required, which makes purification and identification of low abundance binding partners a difficult task (Berggård et al., 2007; Gunzl and Schimanski, 2009).

Proteins such ADAM15, Menin, Prohibitin, 14-3-3 protein Zeta/delta, IQ motif containing GTPase activating protein1, NF $\kappa$ B repressing factor (NFKRF) and adenomatous polyposis coli were identified following the proteomic analysis of the overexpressed and endogenous TRIF protein complex (Chapter 3 and 6). These data confirm an association between these proteins and TRIF at the endogenous level. However, further validation by direct experiments is required to study their potential role in TRIF signalling. Due to the time course of this project, three identified proteins namely ADAM15 and DVL3 and OPTN were selected for further study. These were selected because they have been shown to have potential role in inflammation, Wnt signalling pathway and antiviral signalling, respectively (Charrier-Hisamuddin, 2008; Mankouri et al., 2010; Bernatik et al., 2011).

In this study, it was found that ADAM15 interacted with TRIF upon poly(I:C) and LPS stimulation for 60 and 20 min, respectively. Moreover, ADAM15 acted as a negative regulator of TRIF, TLR3 and TLR4-mediated activation of the NF- $\kappa$ B, IFN $\beta$  (p125-luc) and Rantes reporter genes. In addition, overexpression of ADAM15 also significantly inhibited TRIF-dependent activation of the NF- $\kappa$ B-driven PRDII and IRF3/IRF7-dependent PRDIII-I reporter genes. Importantly, downregulation of ADAM-15 by esiRNA significantly enhanced poly(I:C) and LPS-induced cytokine/chemokine secretion in cell free supernatant in U373-CD14. Furthermore, overexpression of ADAM15 in HEK293-TLR3 caused TRIF degradation and the use of EGTA in combination with EDTA partially inhibited this effect. ADAM and MMP family members are Zn-dependent proteinases. Thus, their activities were reported to be inhibited by the metal ion chelators such as EDTA and EGTA (Chen et al., 2007). In agreement with these results, knockdown of ADAM15 increased TRIF mRNA and protein levels upon poly(I:C) stimulation. This lead to the speculation that ADAM15 inhibited TLR3 and TLR4 signalling by a mechanism involved TRIF degradation. In contrast to our finding, many of the published data consider ADAM15 as an inflammatory mediator (Herren et al., 1997; Al-Fakhri et al., 2003; Mosnier et al., 2006). However, the possibility that ADAM15 could present both pro-and anti-inflammatory activities cannot be precluded (Charrier et al., 2005; Charrier et al., 2007).

Furthermore, this study also investigated the role of DVL1, DVL2 and DVL3 in TRIF mediating TLRs signalling. It was found that all DVLS isoforms constitutively interacted with TRIF when overexpressed in HEK293-TLR4. However, immunoprecipitation of endogenous TRIF showed that DVL3 interacted with TRIF only following stimulation with LPS for 20-40 min. Moreover, overexpression of all DVLS isoform inhibited TRIF and TLR3-mediated activation of the NF- $\kappa$ B, IFN $\beta$  (p125-luc) and Rantes reporter genes in HEK293 and HEK293-TLR3, respectively. In agreement with our results, Deng et al. (2010) showed that all three DVLS isoforms directly interact with NF- $\kappa$ B (p65), and overexpression of DVLS inhibited TNF- $\alpha$  induced activation of NF- $\kappa$ B transcriptional activity. Surprisingly, in wild-type murine BMDMs, the inhibition of DVLS reduced poly(I:C)-induced upregulation of TNF- $\alpha$ , IFN- $\beta$  and Rantes mRNA as well as decreased I $\kappa$ B degradation. This could be due to the cells line used in this study. TLR3 was reported to play a key role in sensing poly(I:C) by epithelial cells (Guillot et al., 2005; Matsukura et al., 2007), but it played a moderate or minor role in sensing poly(I:C) in macrophages (Alexopoulou et al., 2001; Yamamoto

et al., 2003). Importantly, it was found that DVLs were also needed for LPS-induced upregulation of cytokine/chemokine transcription as well as phosphorylation of IRF3. In agreement with our results, Blumenthal et al. (2006) showed that TLRs activation resulted in upregulation of Wnt5A in human macrophages and that Wnt5A is necessary for the regulation of IL-12 and IFN- $\gamma$  in response to infectious agents. In addition, our study showed that DVLs transcriptions are differentially regulated by TLRs activation, and that both TRIF and MyD88 inhibit  $\beta$ -catenin-induced Lef transcription. Also, poly(I:C) and LPS stimulation decreased  $\beta$ -catenin expression in HeLa cells and partially inhibited DVL3-dependent  $\beta$ -catenin nuclear translocation. Correlating with this data, it has been shown that TLR4 activation inhibits enterocyte proliferation in vitro and in vivo via the impairment of  $\beta$ -catenin signalling through activation of GSK3 $\beta$  (Sodhi et al., 2010).

Importantly, it has been demonstrated that  $\beta$ -catenin-dependent Wnt signalling is also active in mature, peripheral blood T cells and that Wnts induce MMP expression and augment T cell transmigration (Wu et al., 2007). Masckauchán et al. (2006) showed that Wnt5A signalling induced proliferation and survival of endothelial cells in vitro and expression of MMP1. In addition, Blavier et al. (2006) reported that MMPs (MMP2, MMP3, MMP9, MMP13 and MMP14) play an active role in Wnt1-induced tumorigenesis in mice. Interestingly, high expression of ADAM 15 has been reported in lung, gastric, ovarian breast and prostate carcinoma cell lines and tissues (Zhong et al., 2008). Moreover, ADAM15 expression was shown to be associated with aggressive prostate and breast cancer (Kuefer et al., 2006). Furthermore, both ADAM15 and DVLs are involved in MAPK activation and in particular the extracellular signal regulated kinase 1/2 (ERK1/2) (Bikkavilli and Malbon, 2009; Sun et al., 2010). Schlange et al. (2007) showed that Wnt signalling activates the ERK1/2 pathway and suppression of the DVLs serves to decrease active  $\beta$ -catenin levels, lowering ERK1/2 activity, blocking proliferation and inducing apoptosis in the human breast cancer cell line MCF-7. The effects of Wnt signalling are mediated partly by EGFR transactivation in human breast cancer cells in a metalloprotease- and Src-dependent manner (Schlange et al., 2007). Interestingly ADAMs, including ADAM15, have been reported to be involved in EGFR transactivation (Seals and Courtneidge, 2003). Moreover in breast cancer cells, ADAM15 deletion decreases ERK1/2 phosphorylation impairing migration

and proliferation (Najy et al., 2008). Consistently, Sun et al. (2010) demonstrated that ADAM15 overexpression stimulates ERK1/2 phosphorylation in endothelial cells.

As mentioned earlier, TRIF activation induces Caspase-8-dependent cell death and studies have shown that TLR3 activation can trigger apoptosis of human prostate cells and breast cancer cells (Salaun et al., 2006; Paone et al., 2008). It is plausible to speculate that ADAM15 and DVLs may inhibit TRIF-induced cell death and thereby promote cell growth and tumor formation. As Wnts have been shown to induce MMPs expression (Blavier et al., 2006), it may be suggested that activation of Wnt signalling by DVLs may lead to ADAM15 expression which then can inhibit TLRs signalling in a negative feedback mechanism to prevent overproduction of pro-inflammatory cytokine and thereby, suppress the inflammation associated with bacterial and viral infections.

Herein, Optineurin (OPTN) was also identified as a TRIF interacting partner. OPTN constitutively interacted with TRIF when overexpressed in HEK293-TLR3. However, endogenously expressed OPTN and TRIF interacted in a ligand dependent manner only (20 and 60 min upon poly(I:C) and LPS stimulation). OPTN is a multifunctional protein involved in several functions such as vesicular trafficking from the Golgi to the plasma membrane, NF- $\kappa$ B regulation, signal transduction, endocytosis and gene expression (Nagabhushana et al., 2010). In this study, OPTN was found to act as a negative regulator of TRIF and TLR3-mediated activation of the NF- $\kappa$ B, IFN- $\beta$  (p125-luc) and Rantes reporter genes in HEK293 and HEK293-TLR3, respectively. Moreover, knockdown of endogenous OPTN using esiRNA technology in U373-CD14 significantly increased IFN- $\beta$  mRNA and secretion of TNF- $\alpha$  and Rantes upon poly(I:C) stimulation. However, suppression of OPTN significantly increased LPS-induced Rantes and decreased LPS-induced TNF- $\alpha$  secretion. The data regarding the role of OPTN in regulating NF- $\kappa$ B and IFN- $\beta$  are controversial and seem to be dependent on the cell type and the stimulus. In agreement with our results, Mankouri et al. (2010) reported that poly(I:C) and virus-induced activation of IFN- $\beta$  reporter gene and IFN- $\beta$  secretion was inhibited upon OPTN overexpression and enhanced by siRNA knockdown of OPTN in HEK293-TLR3. However, Gleason et al. (2011) reported that OPTN is required for optimal activation of TBK1 and production of IFN- $\beta$  in BMDMs upon TLR3 and TLR4 activation. Furthermore, Nagabhushana et al. (2010) demonstrated that OPTN is involved in endocytosis. It should be mentioned that 24 h poly(I:C) and LPS stimulation in U373-CD14 cell line resulted in increased OPTN

protein level, which may suggest that TLRs induced OPTN in a negative feedback mechanism to reduce the signal. Interestingly, Bryja et al. (2007) showed that endocytosis is important for DVL2 stability and blocking of endocytosis leads to rapid DVL2 degradation and prevents Wnt/ $\beta$ -catenin signalling. Importantly, the endocytosis receptor, low-density lipoprotein receptor-related protein 1 (LRP1) was also identified in the endogenous TRIF-IP complex following stimulation with poly(I:C) for 60 min and LPS for 40-60 min. Song et al. (2009) demonstrated that LRP1 induces the expression of MMP2 and MMP9 and thereby, promotes the migration and invasion of human glioblastoma U87 cells. Interestingly, it has been reported that LRP1 sequestered frizzled receptor and thereby, disrupts the frizzled receptor-LRP5/LRP6 complex and ultimately represses the canonical Wnt pathway (Lindner et al., 2010). Thus, it may be speculated that TLRs act through OPTN or LRP1 to regulate endocytosis and thereby, negatively or positively regulate Wnt signalling.

In conclusion, proteomic analysis of the overexpressed and endogenous TRIF immunocomplex led to the identification of many novel TRIF interacting proteins. These proteins indicate that TRIF may be linked to inflammasome activation, NOTCH signalling, Wnt signalling, cancer and diabetes. Overall, to our knowledge this is the first study performed to analyse whole TRIF-IP complex. Future studies are needed to validate the potential role of many of the TRIF-interactor proteins in TRIF signalling and to investigate whether TRIF can be associated with signalling pathways that are distinct from its role as an activator of TLR signalling.

# **Bibliography**

## Bibliography

- ABDOLLAHI-ROODSAZ, S., JOOSTEN, L. A., KOENDERS, M. I., DEVESA, I., ROELOFS, M. F., RADSTAKE, T. R., HEUVELMANS-JACOBS, M., AKIRA, S., NICKLIN, M. J., RIBEIRO-DIAS, F. & VAN DEN BERG, W. B. 2008. Stimulation of TLR2 and TLR4 differentially skews the balance of T cells in a mouse model of arthritis. *J Clin Invest*, 118, 205-16.
- ABDOLLAHI-ROODSAZ, S., JOOSTEN, L. A., ROELOFS, M. F., RADSTAKE, T. R., MATERA, G., POPA, C., VAN DER MEER, J. W., NETEA, M. G. & VAN DEN BERG, W. B. 2007. Inhibition of Toll-like receptor 4 breaks the inflammatory loop in autoimmune destructive arthritis. *Arthritis Rheum*, 56, 2957-67.
- AHMAD-NEJAD, P., HACKER, H., RUTZ, M., BAUER, S., VABULAS, R. M. & WAGNER, H. 2002. Bacterial CpG-DNA and lipopolysaccharides activate Toll-like receptors at distinct cellular compartments. *Eur J Immunol*, 32, 1958-68.
- AKIRA, S. & HEMMI, H. 2003. Recognition of pathogen-associated molecular patterns by TLR family. *Immunol Lett*, 85, 85-95.
- AKIRA, S. & SATO, S. 2003. Toll-like receptors and their signaling mechanisms. *Scand J Infect Dis*, 35, 555-62.
- AKSOY, E., VANDEN BERGHE, W., DETIENNE, S., AMRAOUI, Z., FITZGERALD, K. A., HAEGEMAN, G., GOLDMAN, M. & WILLEMS, F. 2005. Inhibition of phosphoinositide 3-kinase enhances TRIF-dependent NF-kappa B activation and IFN-beta synthesis downstream of Toll-like receptor 3 and 4. *Eur J Immunol*, 35, 2200-9.
- ALEXOPOULOU, L., HOLT, A. C., MEDZHITOV, R. & FLAVELL, R. A. 2001. Recognition of double-stranded RNA and activation of NF-kappaB by Toll-like receptor 3. *Nature*, 413, 732-8.
- AL-FAKHRI, N., WILHELM, J., HAHN, M., HEIDT, M., HEHRLEIN, F. W., ENDISCH, A. M., HUPP, T., CHERIAN, S. M., BOBRYSEV, Y. V., LORD, R. S. & KATZ, N. 2003. Increased expression of disintegrin-metalloproteinases ADAM-15 and ADAM-9 following upregulation of integrins alpha5beta1 and alphavbeta3 in atherosclerosis. *J Cell Biochem*, 89, 808-23.
- ALFANDARI, D., COUSIN, H., GAULTIER, A., SMITH, K., WHITE, J. M., DARRIBERE, T. & DESIMONE, D. W. 2001. Xenopus ADAM 13 is a metalloprotease required for cranial neural crest-cell migration. *Curr Biol*, 11, 918-30.

AMOUR, A., KNIGHT, C. G., WEBSTER, A., SLOCOMBE, P. M., STEPHENS, P. E., KNAUPER, V., DOCHERTY, A. J. & MURPHY, G. 2000. The in vitro activity of ADAM-10 is inhibited by TIMP-1 and TIMP-3. *FEBS Lett*, 473, 275-9.

AMSEN, D., BLANDER, J. M., LEE, G. R., TANIGAKI, K., HONJO, T. & FLAVELL, R. A. 2004. Instruction of distinct CD4 T helper cell fates by different notch ligands on antigen-presenting cells. *Cell*, 117, 515-26.

AN, H., ZHAO, W., HOU, J., ZHANG, Y., XIE, Y., ZHENG, Y., XU, H., QIAN, C., ZHOU, J., YU, Y., LIU, S., FENG, G. & CAO, X. 2006. SHP-2 phosphatase negatively regulates the TRIF adaptor protein-dependent type I interferon and proinflammatory cytokine production. *Immunity*, 25, 919-28.

AN, H. J., CHO, N. H., YANG, H. S., KWAK, K. B., KIM, N. K., OH, D. Y., LEE, S. W., KIM, H. O. & KOH, J. J. 2007. Targeted RNA interference of phosphatidylinositol 3-kinase p110-beta induces apoptosis and proliferation arrest in endometrial carcinoma cells. *J Pathol*, 212, 161-9.

ANDERSEN-NISSEN, E., SMITH, K. D., STROBE, K. L., BARRETT, S. L., COOKSON, B. T., LOGAN, S. M. & ADEREM, A. 2005. Evasion of Toll-like receptor 5 by flagellated bacteria. *Proc Natl Acad Sci U S A*, 102, 9247-52.

ANDREJEVA, J., CHILDS, K. S., YOUNG, D. F., CARLOS, T. S., STOCK, N., GOODBOURN, S. & RANDALL, R. E. 2004. The V proteins of paramyxoviruses bind the IFN-inducible RNA helicase, mda-5, and inhibit its activation of the IFN-beta promoter. *Proc Natl Acad Sci U S A*, 101, 17264-9.

ARTAVANIS-TSAKONAS, S., RAND, M. D. & LAKE, R. J. 1999. Notch signaling: cell fate control and signal integration in development. *Science*, 284, 770-6.

AUBRY, C., CORR, S. C., WIENERROITHER, S., GOULARD, C., JONES, R., JAMIESON, A. M., DECKER, T., O'NEILL, L. A., DUSSURGET, O. & COSSART, P. 2012. Both TLR2 and TRIF contribute to interferon-beta production during *Listeria* infection. *PLoS One*, 7, e33299.

AWOMOYI, A. A., RALLABHANDI, P., POLLIN, T. I., LORENZ, E., SZTEIN, M. B., BOUKHVALOVA, M. S., HEMMING, V. G., BLANCO, J. C. & VOGEL, S. N. 2007. Association of TLR4 polymorphisms with symptomatic respiratory syncytial virus infection in high-risk infants and young children. *J Immunol*, 179, 3171-7.

BAILEY, D., URENA, L., THORNE, L. & GOODFELLOW, I. 2012. Identification of protein interacting partners using tandem affinity purification. *J Vis Exp*.

BALASHOV, K. E., AUNG, L. L., VAKNIN-DEMBINSKY, A., DHIB-JALBUT, S. &

- WEINER, H. L. 2010. Interferon-beta inhibits toll-like receptor 9 processing in multiple sclerosis. *Ann Neurol*, 68, 899-906.
- BARNES, B. J., FIELD, A. E. & PITHA-ROWE, P. M. 2003. Virus-induced heterodimer formation between IRF-5 and IRF-7 modulates assembly of the IFN $\alpha$  enhanceosome in vivo and transcriptional activity of IFN $\alpha$  genes. *J Biol Chem*, 278, 16630-41.
- BARNES, B. J., KELLUM, M. J., FIELD, A. E. & PITHA, P. M. 2002. Multiple regulatory domains of IRF-5 control activation, cellular localization, and induction of chemokines that mediate recruitment of T lymphocytes. *Mol Cell Biol*, 22, 5721-40.
- BARTON, G. M. & MEDZHITOV, R. 2002. Control of adaptive immune responses by Toll-like receptors. *Curr Opin Immunol*, 14, 380-3.
- BARTON, G. M. & MEDZHITOV, R. 2002. Toll-like receptors and their ligands. *Curr Top Microbiol Immunol*, 270, 81-92.
- BELINDA, L. W., WEI, W. X., HANH, B. T., LEI, L. X., BOW, H. & LING, D. J. 2008. SARM: a novel Toll-like receptor adaptor, is functionally conserved from arthropod to human. *Mol Immunol*, 45, 1732-42.
- BELL, J. K., ASKINS, J., HALL, P. R., DAVIES, D. R. & SEGAL, D. M. 2006. The dsRNA binding site of human Toll-like receptor 3. *Proc Natl Acad Sci U S A*, 103, 8792-7.
- BERNATIK, O., GANJI, R. S., DIJKSTERHUIS, J. P., KONIK, P., CERVENKA, I., POLONIO, T., KREJCI, P., SCHULTE, G. & BRYJA, V. 2011. Sequential activation and inactivation of Dishevelled in the Wnt/beta-catenin pathway by casein kinases. *J Biol Chem*, 286, 10396-410.
- BERNHAGEN, J., CALANDRA, T., CERAMI, A. & BUCALA, R. 1994. Macrophage migration inhibitory factor is a neuroendocrine mediator of endotoxaemia. *Trends Microbiol*, 2, 198-201.
- BIKKAVILLI, R. K., FEIGIN, M. E. & MALBON, C. C. 2008. G alpha o mediates WNT-JNK signaling through dishevelled 1 and 3, RhoA family members, and MEKK 1 and 4 in mammalian cells. *J Cell Sci*, 121, 234-45.
- BIKKAVILLI, R. K., FEIGIN, M. E. & MALBON, C. C. 2008. p38 mitogen-activated protein kinase regulates canonical Wnt-beta-catenin signaling by inactivation of GSK3beta. *J Cell Sci*, 121, 3598-607.
- BIKKAVILLI, R. K. & MALBON, C. C. 2009. Mitogen-activated protein kinases and Wnt/beta-catenin signaling: Molecular conversations among signaling pathways.

*Commun Integr Biol*, 2, 46-9.

BILIC, J., HUANG, Y. L., DAVIDSON, G., ZIMMERMANN, T., CRUCIAT, C. M., BIENZ, M. & NIEHRS, C. 2007. Wnt induces LRP6 signalosomes and promotes dishevelled-dependent LRP6 phosphorylation. *Science*, 316, 1619-22.

BLACK, R. A., RAUCH, C. T., KOZLOSKY, C. J., PESCHON, J. J., SLACK, J. L., WOLFSON, M. F., CASTNER, B. J., STOCKING, K. L., REDDY, P., SRINIVASAN, S., NELSON, N., BOIANI, N., SCHOOLEY, K. A., GERHART, M., DAVIS, R., FITZNER, J. N., JOHNSON, R. S., PAXTON, R. J., MARCH, C. J. & CERRETTI, D. P. 1997. A metalloproteinase disintegrin that releases tumour-necrosis factor-alpha from cells. *Nature*, 385, 729-33.

BLAVIER, L., LAZARYEV, A., DOREY, F., SHACKLEFORD, G. M. & DECLERCK, Y. A. 2006. Matrix metalloproteinases play an active role in Wnt1-induced mammary tumorigenesis. *Cancer Res*, 66, 2691-9.

BLOBEL, C. P. 2005. ADAMs: key components in EGFR signalling and development. *Nat Rev Mol Cell Biol*, 6, 32-43.

BLUMENTHAL, A., EHLERS, S., LAUBER, J., BUER, J., LANGE, C., GOLDMANN, T., HEINE, H., BRANDT, E. & REILING, N. 2006. The Wingless homolog WNT5A and its receptor Frizzled-5 regulate inflammatory responses of human mononuclear cells induced by microbial stimulation. *Blood*, 108, 965-73.

BOHM, B., HESS, S., KRAUSE, K., SCHIRNER, A., EWALD, W., AIGNER, T. & BURKHARDT, H. 2010. ADAM15 exerts an antiapoptotic effect on osteoarthritic chondrocytes via up-regulation of the X-linked inhibitor of apoptosis. *Arthritis Rheum*, 62, 1372-82.

BOLOS, M., FERNANDEZ, S. & TORRES-ALEMAN, I. 2010. Oral administration of a GSK3 inhibitor increases brain insulin-like growth factor I levels. *J Biol Chem*, 285, 17693-700.

BOO, K. H. & YANG, J. S. 2010. Intrinsic cellular defenses against virus infection by antiviral type I interferon. *Yonsei Med J*, 51, 9-17.

BOUWMEESTER, T., BAUCH, A., RUFFNER, H., ANGRAND, P. O., BERGAMINI, G., CROUGHTON, K., CRUCIAT, C., EBERHARD, D., GAGNEUR, J., GHIDELLI, S., HOPF, C., HUHSE, B., MANGANO, R., MICHON, A. M., SCHIRLE, M., SCHLEGL, J., SCHWAB, M., STEIN, M. A., BAUER, A., CASARI, G., DREWES, G., GAVIN, A. C., JACKSON, D. B., JOBERTY, G., NEUBAUER, G., RICK, J., KUSTER, B. & SUPERTI-FURGA, G. 2004. A physical and functional map of the

human TNF-alpha/NF-kappa B signal transduction pathway. *Nat Cell Biol*, 6, 97-105.

BRENTANO, F., SCHORR, O., GAY, R. E., GAY, S. & KYBURZ, D. 2005. RNA released from necrotic synovial fluid cells activates rheumatoid arthritis synovial fibroblasts via Toll-like receptor 3. *Arthritis Rheum*, 52, 2656-65.

BRİKOS, C. & O'NEILL, L. A. 2008. Signalling of toll-like receptors. *Handb Exp Pharmacol*, 21-50.

BRYJA, V., CAJANEK, L., GRAHN, A. & SCHULTE, G. 2007. Inhibition of endocytosis blocks Wnt signalling to beta-catenin by promoting dishevelled degradation. *Acta Physiol (Oxf)*, 190, 55-61.

BRYJA, V., SCHAMBONY, A., CAJANEK, L., DOMINGUEZ, I., ARENAS, E. & SCHULTE, G. 2008. Beta-arrestin and casein kinase 1/2 define distinct branches of non-canonical WNT signalling pathways. *EMBO Rep*, 9, 1244-50.

BUBLIL, E. M. & YARDEN, Y. 2007. The EGF receptor family: spearheading a merger of signaling and therapeutics. *Curr Opin Cell Biol*, 19, 124-34.

BUCHANAN, S. G. & GAY, N. J. 1996. Structural and functional diversity in the leucine-rich repeat family of proteins. *Prog Biophys Mol Biol*, 65, 1-44.

BYRUM, S. D., TAVERNA, S. D. & TACKETT, A. J. 2011. Quantitative analysis of histone exchange for transcriptionally active chromatin. *J Clin Bioinforma*, 1, 17.

CADIGAN, K. M. & PEIFER, M. 2009. Wnt signaling from development to disease: insights from model systems. *Cold Spring Harb Perspect Biol*, 1, a002881.

CALANDRA, T., BERNHAGEN, J., MITCHELL, R. A. & BUCALA, R. 1994. The macrophage is an important and previously unrecognized source of macrophage migration inhibitory factor. *J Exp Med*, 179, 1895-902.

CAMPANA, W. M., LI, X., DRAGOJLOVIC, N., JANES, J., GAULTIER, A. & GONIAS, S. L. 2006. The low-density lipoprotein receptor-related protein is a pro-survival receptor in Schwann cells: possible implications in peripheral nerve injury. *J Neurosci*, 26, 11197-207.

CARIO, E. 2010. Toll-like receptors in inflammatory bowel diseases: a decade later. *Inflamm Bowel Dis*, 16, 1583-97.

CARIO, E. & PODOLSKY, D. K. 2000. Differential alteration in intestinal epithelial cell expression of toll-like receptor 3 (TLR3) and TLR4 in inflammatory bowel disease. *Infect Immun*, 68, 7010-7.

CARPENTIER, P. A., DUNCAN, D. S. & MILLER, S. D. 2008. Glial toll-like receptor signaling in central nervous system infection and autoimmunity. *Brain Behav Immun*,

22, 140-7.

CARTY, M., GOODBODY, R., SCHRODER, M., STACK, J., MOYNAGH, P. N. & BOWIE, A. G. 2006. The human adaptor SARM negatively regulates adaptor protein TRIF-dependent Toll-like receptor signaling. *Nat Immunol*, 7, 1074-81.

CERRETTI, D. P., DUBOSE, R. F., BLACK, R. A. & NELSON, N. 1999. Isolation of two novel metalloproteinase-disintegrin (ADAM) cDNAs that show testis-specific gene expression. *Biochem Biophys Res Commun*, 263, 810-5.

CHAKRAVARTI, D. N., CHAKRAVARTI, B. & MOUTSATSOS, I. 2002. Informatic tools for proteome profiling. *Biotechniques*, Suppl, 4-10, 12-5.

CHALASANI, M. L., RADHA, V., GUPTA, V., AGARWAL, N., BALASUBRAMANIAN, D. & SWARUP, G. 2007. A glaucoma-associated mutant of optineurin selectively induces death of retinal ganglion cells which is inhibited by antioxidants. *Invest Ophthalmol Vis Sci*, 48, 1607-14.

CHANG, L. & KARIN, M. 2001. Mammalian MAP kinase signalling cascades. *Nature*, 410, 37-40.

CHAO, M. P., JAISWAL, S., WEISSMAN-TSUKAMOTO, R., ALIZADEH, A. A., GENTLES, A. J., VOLKMER, J., WEISKOPF, K., WILLINGHAM, S. B., RAVEH, T., PARK, C. Y., MAJETI, R. & WEISSMAN, I. L. 2010. Calreticulin is the dominant pro-phagocytic signal on multiple human cancers and is counterbalanced by CD47. *Sci Transl Med*, 2, 63ra94.

CHARRIER, L., YAN, Y., DRISS, A., LABOISSE, C. L., SITARAMAN, S. V. & MERLIN, D. 2005. ADAM-15 inhibits wound healing in human intestinal epithelial cell monolayers. *Am J Physiol Gastrointest Liver Physiol*, 288, G346-53.

CHARRIER, L., YAN, Y., NGUYEN, H. T., DALMASSO, G., LABOISSE, C. L., GEWIRTZ, A. T., SITARAMAN, S. V. & MERLIN, D. 2007. ADAM-15/metargidin mediates homotypic aggregation of human T lymphocytes and heterotypic interactions of T lymphocytes with intestinal epithelial cells. *J Biol Chem*, 282, 16948-58.

CHARRIER-HISAMUDDIN, L., LABOISSE, C. L. & MERLIN, D. 2008. ADAM-15: a metalloprotease that mediates inflammation. *FASEB J*, 22, 641-53.

CHATURVEDI, A., DORWARD, D. & PIERCE, S. K. 2008. The B cell receptor governs the subcellular location of Toll-like receptor 9 leading to hyperresponses to DNA-containing antigens. *Immunity*, 28, 799-809.

CHEN, C. D., PODVIN, S., GILLESPIE, E., LEEMAN, S. E. & ABRAHAM, C. R. 2007. Insulin stimulates the cleavage and release of the extracellular domain of Klotho

by ADAM10 and ADAM17. *Proc Natl Acad Sci U S A*, 104, 19796-801.

CHEN, Q., MENG, L. H., ZHU, C. H., LIN, L. P., LU, H. & DING, J. 2008. ADAM15 suppresses cell motility by driving integrin alpha5beta1 cell surface expression via Erk inactivation. *Int J Biochem Cell Biol*, 40, 2164-73.

CHEN, Z. J. 2005. Ubiquitin signalling in the NF-kappaB pathway. *Nat Cell Biol*, 7, 758-65.

CHEUNG, H. C., CORLEY, L. J., FULLER, G. N., MCCUTCHEON, I. E. & COTE, G. J. 2006. Polypyrimidine tract binding protein and Notch1 are independently re-expressed in glioma. *Mod Pathol*, 19, 1034-41.

CHOI, Y. J., IM, E., CHUNG, H. K., POTHOUKAKIS, C. & RHEE, S. H. 2010. TRIF mediates Toll-like receptor 5-induced signaling in intestinal epithelial cells. *J Biol Chem*, 285, 37570-8.

CHOI, Y. J., IM, E., POTHOUKAKIS, C. & RHEE, S. H. 2010. TRIF modulates TLR5-dependent responses by inducing proteolytic degradation of TLR5. *J Biol Chem*, 285, 21382-90.

CHOI, Y. S., HUR, J. & JEONG, S. 2007. Beta-catenin binds to the downstream region and regulates the expression C-reactive protein gene. *Nucleic Acids Res*, 35, 5511-9.

CRELLIN, N. K., GARCIA, R. V., HADISFAR, O., ALLAN, S. E., STEINER, T. S. & LEVINGS, M. K. 2005. Human CD4+ T cells express TLR5 and its ligand flagellin enhances the suppressive capacity and expression of FOXP3 in CD4+CD25+ T regulatory cells. *J Immunol*, 175, 8051-9.

CURTISS, L. K. & TOBIAS, P. S. 2009. Emerging role of Toll-like receptors in atherosclerosis. *J Lipid Res*, 50 Suppl, S340-5.

CUSSON-HERMANCE, N., KHURANA, S., LEE, T. H., FITZGERALD, K. A. & KELLIHER, M. A. 2005. Rip1 mediates the Trif-dependent toll-like receptor 3- and 4-induced NF- $\kappa$ B activation but does not contribute to interferon regulatory factor 3 activation. *J Biol Chem*, 280, 36560-6.

DAMICO, R. L., CHESLEY, A., JOHNSTON, L., BIND, E. P., AMARO, E., NIJMEH, J., KARAKAS, B., WELSH, L., PEARSE, D. B., GARCIA, J. G. & CROW, M. T. 2008. Macrophage migration inhibitory factor governs endothelial cell sensitivity to LPS-induced apoptosis. *Am J Respir Cell Mol Biol*, 39, 77-85.

DANSAKO, H., IKEDA, M., ARIUMI, Y., WAKITA, T. & KATO, N. 2009. Double-stranded RNA-induced interferon-beta and inflammatory cytokine production modulated by hepatitis C virus serine proteases derived from patients with hepatic

diseases. *Arch Virol*, 154, 801-10.

DANSEREAU, D. A., LUNKE, M. D., FINKIELSZTEIN, A., RUSSELL, M. A. & BROOK, W. J. 2002. Hephaestus encodes a polypyrimidine tract binding protein that regulates Notch signalling during wing development in *Drosophila melanogaster*. *Development*, 129, 5553-66.

DASU, M. R., DEVARAJ, S., PARK, S. & JIALAL, I. 2010. Increased toll-like receptor (TLR) activation and TLR ligands in recently diagnosed type 2 diabetic subjects. *Diabetes Care*, 33, 861-8.

DE KONING, H. D., SIMON, A., ZEEUWEN, P. L. & SCHALKWIJK, J. 2012. Pattern recognition receptors in infectious skin diseases. *Microbes Infect*, 14, 881-93.

DE WEVER, O., DERYCKE, L., HENDRIX, A., DE MEERLEER, G., GODEAU, F., DEPYPERE, H. & BRACKE, M. 2007. Soluble cadherins as cancer biomarkers. *Clin Exp Metastasis*, 24, 685-97.

DELGADO, M. A., ELMAOUED, R. A., DAVIS, A. S., KYEI, G. & DERETIC, V. 2008. Toll-like receptors control autophagy. *EMBO J*, 27, 1110-21.

DENG, J., MILLER, S. A., WANG, H. Y., XIA, W., WEN, Y., ZHOU, B. P., LI, Y., LIN, S. Y. & HUNG, M. C. 2002. beta-catenin interacts with and inhibits NF-kappa B in human colon and breast cancer. *Cancer Cell*, 2, 323-34.

DENG, N., YE, Y., WANG, W. & LI, L. 2010. Dishevelled interacts with p65 and acts as a repressor of NF-kappaB-mediated transcription. *Cell Res*, 20, 1117-27.

DOIRON, B., HU, W., NORTON, L. & DEFRONZO, R. A. 2012. Lentivirus shRNA Grb10 targeting the pancreas induces apoptosis and improved glucose tolerance due to decreased plasma glucagon levels. *Diabetologia*, 55, 719-28.

DOW, L. E., ELSUM, I. A., KING, C. L., KINROSS, K. M., RICHARDSON, H. E. & HUMBERT, P. O. 2008. Loss of human Scribble cooperates with H-Ras to promote cell invasion through deregulation of MAPK signalling. *Oncogene*, 27, 5988-6001.

DUFFY, M. J., MCKIERNAN, E., O'DONOVAN, N. & MCGOWAN, P. M. 2009. The role of ADAMs in disease pathophysiology. *Clin Chim Acta*, 403, 31-6.

DUFFY, M. J., MULLOOLY, M., O'DONOVAN, N., SUKOR, S., CROWN, J., PIERCE, A. & MCGOWAN, P. M. 2011. The ADAMs family of proteases: new biomarkers and therapeutic targets for cancer? *Clin Proteomics*, 8, 9.

EGAWA, T., ALBRECHT, B., FAVIER, B., SUNSHINE, M. J., MIRCHANDANI, K., O'BRIEN, W., THOME, M. & LITTMAN, D. R. 2003. Requirement for CARMA1 in antigen receptor-induced NF-kappa B activation and lymphocyte proliferation. *Curr*

*Biol*, 13, 1252-8.

EISENMANN, D. M. 2005. Wnt signaling. *WormBook*, 1-17.

EWALD, S. E., LEE, B. L., LAU, L., WICKLIFFE, K. E., SHI, G. P., CHAPMAN, H. A. & BARTON, G. M. 2008. The ectodomain of Toll-like receptor 9 is cleaved to generate a functional receptor. *Nature*, 456, 658-62.

FAN, J., KAPUS, A., MARSDEN, P. A., LI, Y. H., OREOPOULOS, G., MARSHALL, J. C., FRANTZ, S., KELLY, R. A., MEDZHITOV, R. & ROTSTEIN, O. D. 2002. Regulation of Toll-like receptor 4 expression in the lung following hemorrhagic shock and lipopolysaccharide. *J Immunol*, 168, 5252-9.

FAUSTIN, B., CHEN, Y., ZHAI, D., LE NEGRATE, G., LARTIGUE, L., SATTERTHWAIT, A. & REED, J. C. 2009. Mechanism of Bcl-2 and Bcl-X(L) inhibition of NLRP1 inflammasome: loop domain-dependent suppression of ATP binding and oligomerization. *Proc Natl Acad Sci U S A*, 106, 3935-40.

FITZGERALD, K. A., PALSSON-MCDERMOTT, E. M., BOWIE, A. G., JEFFERIES, C. A., MANSELL, A. S., BRADY, G., BRINT, E., DUNNE, A., GRAY, P., HARTE, M. T., MCMURRAY, D., SMITH, D. E., SIMS, J. E., BIRD, T. A. & O'NEILL, L. A. 2001. Mal (MyD88-adaptor-like) is required for Toll-like receptor-4 signal transduction. *Nature*, 413, 78-83.

FITZGERALD, K. A., ROWE, D. C., BARNES, B. J., CAFFREY, D. R., VISINTIN, A., LATZ, E., MONKS, B., PITHA, P. M. & GOLENBOCK, D. T. 2003. LPS-TLR4 signaling to IRF-3/7 and NF-kappaB involves the toll adapters TRAM and TRIF. *J Exp Med*, 198, 1043-55.

FLANNERY, S. & BOWIE, A. G. 2010. The interleukin-1 receptor-associated kinases: critical regulators of innate immune signalling. *Biochem Pharmacol*, 80, 1981-91.

FRANCHINI, M. & MONTAGNANA, M. 2011. Low-density lipoprotein receptor-related protein 1: new functions for an old molecule. *Clin Chem Lab Med*, 49, 967-70.

FRIEDRICH, B. M., MURRAY, J. L., LI, G., SHENG, J., HODGE, T. W., RUBIN, D. H., O'BRIEN, W. A. & FERGUSON, M. R. 2011. A functional role for ADAM10 in human immunodeficiency virus type-1 replication. *Retrovirology*, 8, 32.

FUNAMI, K., SASAI, M., OHBA, Y., OSHIUMI, H., SEYA, T. & MATSUMOTO, M. 2007. Spatiotemporal mobilization of Toll/IL-1 receptor domain-containing adaptor molecule-1 in response to dsRNA. *J Immunol*, 179, 6867-72.

FUNAMI, K., SASAI, M., OSHIUMI, H., SEYA, T. & MATSUMOTO, M. 2008. Homo-oligomerization is essential for Toll/interleukin-1 receptor domain-containing

adaptor molecule-1-mediated NF-kappaB and interferon regulatory factor-3 activation. *J Biol Chem*, 283, 18283-91.

GAIDE, O., FAVIER, B., LEGLER, D. F., BONNET, D., BRISSONI, B., VALITUTTI, S., BRON, C., TSCHOPP, J. & THOME, M. 2002. CARMA1 is a critical lipid raft-associated regulator of TCR-induced NF-kappa B activation. *Nat Immunol*, 3, 836-43.

GALLI, R., STARACE, D., BUSA, R., ANGELINI, D. F., PAONE, A., DE CESARIS, P., FILIPPINI, A., SETTE, C., BATTISTINI, L., ZIPARO, E. & RICCIOLI, A. 2010. TLR stimulation of prostate tumor cells induces chemokine-mediated recruitment of specific immune cell types. *J Immunol*, 184, 6658-69.

GALLO, A., CUOZZO, C., ESPOSITO, I., MAGGIOLINI, M., BONOFILGIO, D., VIVACQUA, A., GARRAMONE, M., WEISS, C., BOHMANN, D. & MUSTI, A. M. 2002. Menin uncouples Elk-1, JunD and c-Jun phosphorylation from MAP kinase activation. *Oncogene*, 21, 6434-45.

GANTNER, B. N., SIMMONS, R. M., CANAVERA, S. J., AKIRA, S. & UNDERHILL, D. M. 2003. Collaborative induction of inflammatory responses by dectin-1 and Toll-like receptor 2. *J Exp Med*, 197, 1107-17.

GAO, C., CAO, W., BAO, L., ZUO, W., XIE, G., CAI, T., FU, W., ZHANG, J., WU, W., ZHANG, X. & CHEN, Y. G. 2010. Autophagy negatively regulates Wnt signalling by promoting Dishevelled degradation. *Nat Cell Biol*, 12, 781-90.

GARAY-MALPARTIDA, H. M., MOURAO, R. F., MANTOVANI, M., SANTOS, I. A., SOGAYAR, M. C. & GOLDBERG, A. C. 2011. Toll-like receptor 4 (TLR4) expression in human and murine pancreatic beta-cells affects cell viability and insulin homeostasis. *BMC Immunol*, 12, 18.

GARFIELD, A. S., COWLEY, M., SMITH, F. M., MOORWOOD, K., STEWART-COX, J. E., GILROY, K., BAKER, S., XIA, J., DALLEY, J. W., HURST, L. D., WILKINSON, L. S., ISLES, A. R. & WARD, A. 2011. Distinct physiological and behavioural functions for parental alleles of imprinted Grb10. *Nature*, 469, 534-8.

GAY, N. J. & KEITH, F. J. 1991. Drosophila Toll and IL-1 receptor. *Nature*, 351, 355-6.

GEORGE, S. J. 2008. Wnt pathway: a new role in regulation of inflammation. *Arterioscler Thromb Vasc Biol*, 28, 400-2.

GEORGEL, P., JIANG, Z., KUNZ, S., JANSSEN, E., MOLS, J., HOEBE, K., BAHRAM, S., OLDSTONE, M. B. & BEUTLER, B. 2007. Vesicular stomatitis virus

glycoprotein G activates a specific antiviral Toll-like receptor 4-dependent pathway. *Virology*, 362, 304-13.

GEORGES, E., BONNEAU, A. M. & PRINOS, P. 2011. RNAi-mediated knockdown of alpha-enolase increases the sensitivity of tumor cells to antitubulin chemotherapeutics. *Int J Biochem Mol Biol*, 2, 303-8.

GLEASON, C. E., ORDUREAU, A., GOURLAY, R., ARTHUR, J. S. & COHEN, P. 2011. Polyubiquitin binding to optineurin is required for optimal activation of TANK-binding kinase 1 and production of interferon beta. *J Biol Chem*, 286, 35663-74.

GODOWSKI, P. J. 2005. A smooth operator for LPS responses. *Nat Immunol*, 6, 544-6.

GONZALEZ-SANCHO, J. M., BRENNAN, K. R., CASTELO-SOCCIO, L. A. & BROWN, A. M. 2004. Wnt proteins induce dishevelled phosphorylation via an LRP5/6-independent mechanism, irrespective of their ability to stabilize beta-catenin. *Mol Cell Biol*, 24, 4757-68.

GORDEN, K. K., QIU, X., BATTISTE, J. J., WIGHTMAN, P. P., VASILAKOS, J. P. & ALKAN, S. S. 2006. Oligodeoxynucleotides differentially modulate activation of TLR7 and TLR8 by imidazoquinolines. *J Immunol*, 177, 8164-70.

GOULD, T. D. & MANJI, H. K. 2005. Glycogen synthase kinase-3: a putative molecular target for lithium mimetic drugs. *Neuropsychopharmacology*, 30, 1223-37.

GOVINDARAJ, R. G., MANAVALAN, B., BASITH, S. & CHOI, S. 2011. Comparative analysis of species-specific ligand recognition in Toll-like receptor 8 signaling: a hypothesis. *PLoS One*, 6, e25118.

GREGO-BESSA, J., DIEZ, J., TIMMERMAN, L. & DE LA POMPA, J. L. 2004. Notch and epithelial-mesenchyme transition in development and tumor progression: another turn of the screw. *Cell Cycle*, 3, 718-21.

GRISHMAN, E. K., WHITE, P. C. & SAVANI, R. C. 2012. Toll-like receptors, the NLRP3 inflammasome, and interleukin-1beta in the development and progression of type 1 diabetes. *Pediatr Res*.

GROSKREUTZ, D. J., MONICK, M. M., POWERS, L. S., YAROVINSKY, T. O., LOOK, D. C. & HUNNINGHAKE, G. W. 2006. Respiratory syncytial virus induces TLR3 protein and protein kinase R, leading to increased double-stranded RNA responsiveness in airway epithelial cells. *J Immunol*, 176, 1733-40.

GRUMOLATO, L., LIU, G., MONG, P., MUDBHARY, R., BISWAS, R., ARROYAVE, R., VIJAYAKUMAR, S., ECONOMIDES, A. N. & AARONSON, S. A. 2010. Canonical and noncanonical Wnts use a common mechanism to activate

completely unrelated coreceptors. *Genes Dev*, 24, 2517-30.

GUILLOT, L., LE GOFFIC, R., BLOCH, S., ESCRIOU, N., AKIRA, S., CHIGNARD, M. & SI-TAHAR, M. 2005. Involvement of toll-like receptor 3 in the immune response of lung epithelial cells to double-stranded RNA and influenza A virus. *J Biol Chem*, 280, 5571-80.

GUM, R., LENGYEL, E., JUAREZ, J., CHEN, J. H., SATO, H., SEIKI, M. & BOYD, D. 1996. Stimulation of 92-kDa gelatinase B promoter activity by ras is mitogen-activated protein kinase kinase 1-independent and requires multiple transcription factor binding sites including closely spaced PEA3/ets and AP-1 sequences. *J Biol Chem*, 271, 10672-80.

GUO, B. & CHENG, G. 2007. Modulation of the interferon antiviral response by the TBK1/IKKi adaptor protein TANK. *J Biol Chem*, 282, 11817-26.

HABAS, R. & DAWID, I. B. 2005. Dishevelled and Wnt signaling: is the nucleus the final frontier? *J Biol*, 4, 2.

HACKER, H., REDECKE, V., BLAGOEV, B., KRATCHMAROVA, I., HSU, L. C., WANG, G. G., KAMPS, M. P., RAZ, E., WAGNER, H., HACKER, G., MANN, M. & KARIN, M. 2006. Specificity in Toll-like receptor signalling through distinct effector functions of TRAF3 and TRAF6. *Nature*, 439, 204-7.

HAN, K. J., SU, X., XU, L. G., BIN, L. H., ZHANG, J. & SHU, H. B. 2004. Mechanisms of the TRIF-induced interferon-stimulated response element and NF-kappaB activation and apoptosis pathways. *J Biol Chem*, 279, 15652-61.

HAN, K. J., YANG, Y., XU, L. G. & SHU, H. B. 2010. Analysis of a TIR-less splice variant of TRIF reveals an unexpected mechanism of TLR3-mediated signaling. *J Biol Chem*, 285, 12543-50.

HARDY, M. P., MC, G. A. F. & O'NEILL, L. A. 2004. Transcriptional regulation of the human TRIF (TIR domain-containing adaptor protein inducing interferon beta) gene. *Biochem J*, 380, 83-93.

HASAN, U. A., BATES, E., TAKESHITA, F., BILIATO, A., ACCARDI, R., BOUVARD, V., MANSOUR, M., VINCENT, I., GISSMANN, L., IFTNER, T., SIDERI, M., STUBENRAUCH, F. & TOMMASINO, M. 2007. TLR9 expression and function is abolished by the cervical cancer-associated human papillomavirus type 16. *J Immunol*, 178, 3186-97.

HATTULA, K. & PERANEN, J. 2000. FIP-2, a coiled-coil protein, links Huntingtin to Rab8 and modulates cellular morphogenesis. *Curr Biol*, 10, 1603-6.

- HEMMI, H., TAKEUCHI, O., KAWAI, T., KAISHO, T., SATO, S., SANJO, H., MATSUMOTO, M., HOSHINO, K., WAGNER, H., TAKEDA, K. & AKIRA, S. 2000. A Toll-like receptor recognizes bacterial DNA. *Nature*, 408, 740-5.
- HENSON, E. S. & GIBSON, S. B. 2006. Surviving cell death through epidermal growth factor (EGF) signal transduction pathways: implications for cancer therapy. *Cell Signal*, 18, 2089-97.
- HEPPNER, C., BILIMORIA, K. Y., AGARWAL, S. K., KESTER, M., WHITTY, L. J., GURU, S. C., CHANDRASEKHARAPPA, S. C., COLLINS, F. S., SPIEGEL, A. M., MARX, S. J. & BURNS, A. L. 2001. The tumor suppressor protein menin interacts with NF-kappaB proteins and inhibits NF-kappaB-mediated transactivation. *Oncogene*, 20, 4917-25.
- HERREN, B. 2002. ADAM-mediated shedding and adhesion: a vascular perspective. *News Physiol Sci*, 17, 73-6.
- HERREN, B., RAINES, E. W. & ROSS, R. 1997. Expression of a disintegrin-like protein in cultured human vascular cells and in vivo. *FASEB J*, 11, 173-80.
- HONDA, K., OHBA, Y., YANAI, H., NEGISHI, H., MIZUTANI, T., TAKAOKA, A., TAYA, C. & TANIGUCHI, T. 2005. Spatiotemporal regulation of MyD88-IRF-7 signalling for robust type-I interferon induction. *Nature*, 434, 1035-40.
- HONDA, K., YANAI, H., MIZUTANI, T., NEGISHI, H., SHIMADA, N., SUZUKI, N., OHBA, Y., TAKAOKA, A., YEH, W. C. & TANIGUCHI, T. 2004. Role of a transductional-transcriptional processor complex involving MyD88 and IRF-7 in Toll-like receptor signaling. *Proc Natl Acad Sci U S A*, 101, 15416-21.
- HONDA, K., YANAI, H., NEGISHI, H., ASAGIRI, M., SATO, M., MIZUTANI, T., SHIMADA, N., OHBA, Y., TAKAOKA, A., YOSHIDA, N. & TANIGUCHI, T. 2005. IRF-7 is the master regulator of type-I interferon-dependent immune responses. *Nature*, 434, 772-7.
- HORIUCHI, K., WESKAMP, G., LUM, L., HAMMES, H. P., CAI, H., BRODIE, T. A., LUDWIG, T., CHIUSAROLI, R., BARON, R., PREISSNER, K. T., MANOVA, K. & BLOBEL, C. P. 2003. Potential role for ADAM15 in pathological neovascularization in mice. *Mol Cell Biol*, 23, 5614-24.
- HORNG, T., BARTON, G. M., FLAVELL, R. A. & MEDZHITOV, R. 2002. The adaptor molecule TIRAP provides signalling specificity for Toll-like receptors. *Nature*, 420, 329-33.
- HORNUNG, V., ABLASSER, A., CHARREL-DENNIS, M., BAUERNFEIND, F.,

- HORVATH, G., CAFFREY, D. R., LATZ, E. & FITZGERALD, K. A. 2009. AIM2 recognizes cytosolic dsDNA and forms a caspase-1-activating inflammasome with ASC. *Nature*, 458, 514-8.
- HORTON, C. G., PAN, Z. J. & FARRIS, A. D. 2010. Targeting Toll-like receptors for treatment of SLE. *Mediators Inflamm*, 2010.
- HOSHINO, K., TAKEUCHI, O., KAWAI, T., SANJO, H., OGAWA, T., TAKEDA, Y., TAKEDA, K. & AKIRA, S. 1999. Cutting edge: Toll-like receptor 4 (TLR4)-deficient mice are hyporesponsive to lipopolysaccharide: evidence for TLR4 as the Lps gene product. *J Immunol*, 162, 3749-52.
- HOU, Y. F., ZHOU, Y. C., ZHENG, X. X., WANG, H. Y., FU, Y. L., FANG, Z. M. & HE, S. H. 2006. Modulation of expression and function of Toll-like receptor 3 in A549 and H292 cells by histamine. *Mol Immunol*, 43, 1982-92.
- HOUGAARD, S., LOECHEL, F., XU, X., TAJIMA, R., ALBRECHTSEN, R. & WEWER, U. M. 2000. Trafficking of human ADAM 12-L: retention in the trans-Golgi network. *Biochem Biophys Res Commun*, 275, 261-7.
- HOWARD, L., NELSON, K. K., MACIEWICZ, R. A. & BLOBEL, C. P. 1999. Interaction of the metalloprotease disintegrins MDC9 and MDC15 with two SH3 domain-containing proteins, endophilin I and SH3PX1. *J Biol Chem*, 274, 31693-9.
- HU, L. W., KAWAMOTO, E. M., BRIETZKE, E., SCAVONE, C. & LAFER, B. 2011. The role of Wnt signaling and its interaction with diverse mechanisms of cellular apoptosis in the pathophysiology of bipolar disorder. *Prog Neuropsychopharmacol Biol Psychiatry*, 35, 11-7.
- HU, T. & LI, C. 2010. Convergence between Wnt-beta-catenin and EGFR signaling in cancer. *Mol Cancer*, 9, 236.
- HUANG, B., ZHAO, J., LI, H., HE, K. L., CHEN, Y., CHEN, S. H., MAYER, L., UNKELESS, J. C. & XIONG, H. 2005. Toll-like receptors on tumor cells facilitate evasion of immune surveillance. *Cancer Res*, 65, 5009-14.
- HUANG, B., ZHAO, J., UNKELESS, J. C., FENG, Z. H. & XIONG, H. 2008. TLR signaling by tumor and immune cells: a double-edged sword. *Oncogene*, 27, 218-24.
- HUANG, Q. & SZEBENYI, D. M. 2010. Structural basis for the interaction between the growth factor-binding protein GRB10 and the E3 ubiquitin ligase NEDD4. *J Biol Chem*, 285, 42130-9.
- HUPPERT, S. S., LE, A., SCHROETER, E. H., MUMM, J. S., SAXENA, M. T., MILNER, L. A. & KOPAN, R. 2000. Embryonic lethality in mice homozygous for a

processing-deficient allele of Notch1. *Nature*, 405, 966-70.

INOHARA, N., OGURA, Y., CHEN, F. F., MUTO, A. & NUNEZ, G. 2001. Human Nod1 confers responsiveness to bacterial lipopolysaccharides. *J Biol Chem*, 276, 2551-4.

IWASAKI, A. & MEDZHITOV, R. 2004. Toll-like receptor control of the adaptive immune responses. *Nat Immunol*, 5, 987-95.

JANEWAY, C. A., JR. 1989. Approaching the asymptote? Evolution and revolution in immunology. *Cold Spring Harb Symp Quant Biol*, 54 Pt 1, 1-13.

JANEWAY, C. A., JR. & MEDZHITOV, R. 2002. Innate immune recognition. *Annu Rev Immunol*, 20, 197-216.

JANSSENS, S., BURNS, K., TSCHOPP, J. & BEYAERT, R. 2002. Regulation of interleukin-1- and lipopolysaccharide-induced NF-kappaB activation by alternative splicing of MyD88. *Curr Biol*, 12, 467-71.

JENKINS, K. A. & MANSELL, A. 2010. TIR-containing adaptors in Toll-like receptor signalling. *Cytokine*, 49, 237-44.

JI, H., WANG, J., NIKA, H., HAWKE, D., KEEZER, S., GE, Q., FANG, B., FANG, X., FANG, D., LITCHFIELD, D. W., ALDAPE, K. & LU, Z. 2009. EGF-induced ERK activation promotes CK2-mediated disassociation of alpha-Catenin from beta-Catenin and transactivation of beta-Catenin. *Mol Cell*, 36, 547-59.

JIANG, W., MCDONALD, D., HOPE, T. J. & HUNTER, T. 1999. Mammalian Cdc7-Dbf4 protein kinase complex is essential for initiation of DNA replication. *EMBO J*, 18, 5703-13.

JIANG, Z., JOHNSON, H. J., NIE, H., QIN, J., BIRD, T. A. & LI, X. 2003. Pellino 1 is required for interleukin-1 (IL-1)-mediated signaling through its interaction with the IL-1 receptor-associated kinase 4 (IRAK4)-IRAK-tumor necrosis factor receptor-associated factor 6 (TRAF6) complex. *J Biol Chem*, 278, 10952-6.

JIANG, Z., MAK, T. W., SEN, G. & LI, X. 2004. Toll-like receptor 3-mediated activation of NF-kappaB and IRF3 diverges at Toll-IL-1 receptor domain-containing adapter inducing IFN-beta. *Proc Natl Acad Sci U S A*, 101, 3533-8.

JIANG, Z., ZAMANIAN-DARYOUSH, M., NIE, H., SILVA, A. M., WILLIAMS, B. R. & LI, X. 2003. Poly(I-C)-induced Toll-like receptor 3 (TLR3)-mediated activation of NFkappa B and MAP kinase is through an interleukin-1 receptor-associated kinase (IRAK)-independent pathway employing the signaling components TLR3-TRAF6-TAK1-TAB2-PKR. *J Biol Chem*, 278, 16713-9.

- JOHNSON, A. C., LI, X. & PEARLMAN, E. 2008. MyD88 functions as a negative regulator of TLR3/TRIF-induced corneal inflammation by inhibiting activation of c-Jun N-terminal kinase. *J Biol Chem*, 283, 3988-96.
- JONES, J. W., KAYAGAKI, N., BROZ, P., HENRY, T., NEWTON, K., O'ROURKE, K., CHAN, S., DONG, J., QU, Y., ROOSE-GIRMA, M., DIXIT, V. M. & MONACK, D. M. 2010. Absent in melanoma 2 is required for innate immune recognition of *Francisella tularensis*. *Proc Natl Acad Sci U S A*, 107, 9771-6.
- JOURNO, C., FILIPE, J., ABOUT, F., CHEVALIER, S. A., AFONSO, P. V., BRADY, J. N., FLYNN, D., TANGY, F., ISRAEL, A., VIDALAIN, P. O., MAHIEUX, R. & WEIL, R. 2009. NRP/Optineurin Cooperates with TAX1BP1 to potentiate the activation of NF-kappaB by human T-lymphotropic virus type 1 tax protein. *PLoS Pathog*, 5, e1000521.
- KAGAN, J. C., SU, T., HORNG, T., CHOW, A., AKIRA, S. & MEDZHITOV, R. 2008. TRAM couples endocytosis of Toll-like receptor 4 to the induction of interferon-beta. *Nat Immunol*, 9, 361-8.
- KANEDA, K., TAKASAKI, Y., TAKEUCHI, K., YAMADA, H., NAWATA, M., MATSUSHITA, M., MATSUDAIRA, R., IKEDA, K., YAMANAKA, K. & HASHIMOTO, H. 2004. Autoimmune response to proteins of proliferating cell nuclear antigen multiprotein complexes in patients with connective tissue diseases. *J Rheumatol*, 31, 2142-50.
- KANZLER, H., BARRAT, F. J., HESSEL, E. M. & COFFMAN, R. L. 2007. Therapeutic targeting of innate immunity with Toll-like receptor agonists and antagonists. *Nat Med*, 13, 552-9.
- KATO, H., SATO, S., YONEYAMA, M., YAMAMOTO, M., UEMATSU, S., MATSUI, K., TSUJIMURA, T., TAKEDA, K., FUJITA, T., TAKEUCHI, O. & AKIRA, S. 2005. Cell type-specific involvement of RIG-I in antiviral response. *Immunity*, 23, 19-28.
- KATO, H., TAKEUCHI, O., MIKAMO-SATOH, E., HIRAI, R., KAWAI, T., MATSUSHITA, K., HIIRAGI, A., DERMODY, T. S., FUJITA, T. & AKIRA, S. 2008. Length-dependent recognition of double-stranded ribonucleic acids by retinoic acid-inducible gene-I and melanoma differentiation-associated gene 5. *J Exp Med*, 205, 1601-10.
- KATO, H., TAKEUCHI, O., SATO, S., YONEYAMA, M., YAMAMOTO, M., MATSUI, K., UEMATSU, S., JUNG, A., KAWAI, T., ISHII, K. J., YAMAGUCHI, O.,

- OTSU, K., TSUJIMURA, T., KOH, C. S., REIS E SOUSA, C., MATSUURA, Y., FUJITA, T. & AKIRA, S. 2006. Differential roles of MDA5 and RIG-I helicases in the recognition of RNA viruses. *Nature*, 441, 101-5.
- KAWAI, T., ADACHI, O., OGAWA, T., TAKEDA, K. & AKIRA, S. 1999. Unresponsiveness of MyD88-deficient mice to endotoxin. *Immunity*, 11, 115-22.
- KAWAI, T. & AKIRA, S. 2006. TLR signaling. *Cell Death Differ*, 13, 816-25.
- KAWAI, T., SATO, S., ISHII, K. J., COBAN, C., HEMMI, H., YAMAMOTO, M., TERAII, K., MATSUDA, M., INOUE, J., UEMATSU, S., TAKEUCHI, O. & AKIRA, S. 2004. Interferon-alpha induction through Toll-like receptors involves a direct interaction of IRF7 with MyD88 and TRAF6. *Nat Immunol*, 5, 1061-8.
- KEATING, S. E., BARAN, M. & BOWIE, A. G. 2011. Cytosolic DNA sensors regulating type I interferon induction. *Trends Immunol*, 32, 574-81.
- KENNY, E. F. & O'NEILL, L. A. 2008. Signalling adaptors used by Toll-like receptors: an update. *Cytokine*, 43, 342-9.
- KIECHL, S., LORENZ, E., REINDL, M., WIEDERMANN, C. J., OBERHOLLENZER, F., BONORA, E., WILLEIT, J. & SCHWARTZ, D. A. 2002. Toll-like receptor 4 polymorphisms and atherogenesis. *N Engl J Med*, 347, 185-92.
- KIM, D., KIM, Y. J., KOH, H. S., JANG, T. Y., PARK, H. E. & KIM, J. Y. 2010. Reactive Oxygen Species Enhance TLR10 Expression in the Human Monocytic Cell Line THP-1. *Int J Mol Sci*, 11, 3769-82.
- KIM, T., PAZHOOR, S., BAO, M., ZHANG, Z., HANABUCHI, S., FACCHINETTI, V., BOVER, L., PLUMAS, J., CHAPEROT, L., QIN, J. & LIU, Y. J. 2010. Aspartate-glutamate-alanine-histidine box motif (DEAH)/RNA helicase A helicases sense microbial DNA in human plasmacytoid dendritic cells. *Proc Natl Acad Sci U S A*, 107, 15181-6.
- KINLOCH, A., TATZER, V., WAIT, R., PESTON, D., LUNDBERG, K., DONATIEN, P., MOYES, D., TAYLOR, P. C. & VENABLES, P. J. 2005. Identification of citrullinated alpha-enolase as a candidate autoantigen in rheumatoid arthritis. *Arthritis Res Ther*, 7, R1421-9.
- KLEINO, I., ORTIZ, R. M. & HUOVILA, A. P. 2007. ADAM15 gene structure and differential alternative exon use in human tissues. *BMC Mol Biol*, 8, 90.
- KLEINO, I., ORTIZ, R. M., YRITYS, M., HUOVILA, A. P. & SAKSELA, K. 2009. Alternative splicing of ADAM15 regulates its interactions with cellular SH3 proteins. *J Cell Biochem*, 108, 877-85.

- KOBAYASHI, K., HERNANDEZ, L. D., GALAN, J. E., JANEWAY, C. A., JR., MEDZHITOV, R. & FLAVELL, R. A. 2002. IRAK-M is a negative regulator of Toll-like receptor signaling. *Cell*, 110, 191-202.
- KOLLN, J., ZHANG, Y., THAI, G., DEMETRIOU, M., HERMANOWICZ, N., DUQUETTE, P., VAN DEN NOORT, S. & QIN, Y. 2010. Inhibition of glyceraldehyde-3-phosphate dehydrogenase activity by antibodies present in the cerebrospinal fluid of patients with multiple sclerosis. *J Immunol*, 185, 1968-75.
- KONDRATENKO, I., PASCHENKO, O., POLYAKOV, A. & BOLOGOV, A. 2007. Nijmegen breakage syndrome. *Adv Exp Med Biol*, 601, 61-7.
- KONG, K. F., DELROUX, K., WANG, X., QIAN, F., ARJONA, A., MALAWISTA, S. E., FIKRIG, E. & MONTGOMERY, R. R. 2008. Dysregulation of TLR3 impairs the innate immune response to West Nile virus in the elderly. *J Virol*, 82, 7613-23.
- KRATZSCHMAR, J., LUM, L. & BLOBEL, C. P. 1996. Metargidin, a membrane-anchored metalloprotease-disintegrin protein with an RGD integrin binding sequence. *J Biol Chem*, 271, 4593-6.
- KUEFER, R., DAY, K. C., KLEER, C. G., SABEL, M. S., HOFER, M. D., VARAMBALLY, S., ZORN, C. S., CHINNAIYAN, A. M., RUBIN, M. A. & DAY, M. L. 2006. ADAM15 disintegrin is associated with aggressive prostate and breast cancer disease. *Neoplasia*, 8, 319-29.
- LAMKANFI, M. & DIXIT, V. M. 2009. The inflammasomes. *PLoS Pathog*, 5, e1000510.
- LAMKANFI, M. & DIXIT, V. M. 2009. Inflammasomes: guardians of cytosolic sanctity. *Immunol Rev*, 227, 95-105.
- LAMMICH, S., KOJRO, E., POSTINA, R., GILBERT, S., PFEIFFER, R., JASIONOWSKI, M., HAASS, C. & FAHRENHOLZ, F. 1999. Constitutive and regulated alpha-secretase cleavage of Alzheimer's amyloid precursor protein by a disintegrin metalloprotease. *Proc Natl Acad Sci U S A*, 96, 3922-7.
- LARANGE, A., ANTONIOS, D., PALLARDY, M. & Kerdine-Romer, S. 2009. TLR7 and TLR8 agonists trigger different signaling pathways for human dendritic cell maturation. *J Leukoc Biol*, 85, 673-83.
- LAUW, F. N., CAFFREY, D. R. & GOLENBOCK, D. T. 2005. Of mice and man: TLR11 (finally) finds profilin. *Trends Immunol*, 26, 509-11.
- LAZARUS, R., RABY, B. A., LANGE, C., SILVERMAN, E. K., KWIATKOWSKI, D. J., VERCELLI, D., KLIMECKI, W. J., MARTINEZ, F. D. & WEISS, S. T. 2004.

TOLL-like receptor 10 genetic variation is associated with asthma in two independent samples. *Am J Respir Crit Care Med*, 170, 594-600.

LE GOFFIC, R., BALLOY, V., LAGRANDERIE, M., ALEXOPOULOU, L., ESCRIOU, N., FLAVELL, R., CHIGNARD, M. & SI-TAHAR, M. 2006. Detrimental contribution of the Toll-like receptor (TLR)3 to influenza A virus-induced acute pneumonia. *PLoS Pathog*, 2, e53.

LEE, C. H., HUNG, H. W., HUNG, P. H. & SHIEH, Y. S. 2010. Epidermal growth factor receptor regulates beta-catenin location, stability, and transcriptional activity in oral cancer. *Mol Cancer*, 9, 64.

LEE, I. O., KIM, J. H., CHOI, Y. J., PILLINGER, M. H., KIM, S. Y., BLASER, M. J. & LEE, Y. C. 2010. Helicobacter pylori CagA phosphorylation status determines the gp130-activated SHP2/ERK and JAK/STAT signal transduction pathways in gastric epithelial cells. *J Biol Chem*, 285, 16042-50.

LEE, M. S. & KIM, Y. J. 2007. Signaling pathways downstream of pattern-recognition receptors and their cross talk. *Annu Rev Biochem*, 76, 447-80.

LEE, Y. N., GAO, Y. & WANG, H. Y. 2008. Differential mediation of the Wnt canonical pathway by mammalian Dishevelleds-1, -2, and -3. *Cell Signal*, 20, 443-52.

LEMAITRE, B., NICOLAS, E., MICHAUT, L., REICHHART, J. M. & HOFFMANN, J. A. 1996. The dorsoventral regulatory gene cassette spatzle/Toll/cactus controls the potent antifungal response in Drosophila adults. *Cell*, 86, 973-83.

LEUNG, J., YUEH, A., APPAH, F. S., JR., YUAN, B., DE LOS SANTOS, K. & GOFF, S. P. 2006. Interaction of Moloney murine leukemia virus matrix protein with IQGAP. *EMBO J*, 25, 2155-66.

LI, H. P., HUANG, P., PARK, S. & LAI, M. M. 1999. Polypyrimidine tract-binding protein binds to the leader RNA of mouse hepatitis virus and serves as a regulator of viral transcription. *J Virol*, 73, 772-7.

LI, K., FOY, E., FERREON, J. C., NAKAMURA, M., FERREON, A. C., IKEDA, M., RAY, S. C., GALE, M., JR. & LEMON, S. M. 2005. Immune evasion by hepatitis C virus NS3/4A protease-mediated cleavage of the Toll-like receptor 3 adaptor protein TRIF. *Proc Natl Acad Sci U S A*, 102, 2992-7.

LI, S., WANG, L., BERMAN, M., KONG, Y. Y. & DORF, M. E. 2011. Mapping a dynamic innate immunity protein interaction network regulating type I interferon production. *Immunity*, 35, 426-40.

LI, Y., KANG, J. & HORWITZ, M. S. 1998. Interaction of an adenovirus E3 14.7-

kilodalton protein with a novel tumor necrosis factor alpha-inducible cellular protein containing leucine zipper domains. *Mol Cell Biol*, 18, 1601-10.

LIANG, H., COLES, A. H., ZHU, Z., ZAYAS, J., JURECIC, R., KANG, J. & JONES, S. N. 2007. Noncanonical Wnt signaling promotes apoptosis in thymocyte development. *J Exp Med*, 204, 3077-84.

LIBERATI, N. T., FITZGERALD, K. A., KIM, D. H., FEINBAUM, R., GOLENBOCK, D. T. & AUSUBEL, F. M. 2004. Requirement for a conserved Toll/interleukin-1 resistance domain protein in the *Caenorhabditis elegans* immune response. *Proc Natl Acad Sci U S A*, 101, 6593-8.

LIN, Z., CROCKETT, D. K., LIM, M. S. & ELENITOBA-JOHNSON, K. S. 2003. High-throughput analysis of protein/peptide complexes by immunoprecipitation and automated LC-MS/MS. *J Biomol Tech*, 14, 149-55.

LINDNER, I., HEMDAN, N. Y., BUCHOLD, M., HUSE, K., BIGL, M., OERLECKE, I., RICKEN, A., GAUNITZ, F., SACK, U., NAUMANN, A., HOLLBORN, M., THAL, D., GEBHARDT, R. & BIRKENMEIER, G. 2010. Alpha2-macroglobulin inhibits the malignant properties of astrocytoma cells by impeding beta-catenin signaling. *Cancer Res*, 70, 277-87.

LOECHEL, F., FOX, J. W., MURPHY, G., ALBRECHTSEN, R. & WEWER, U. M. 2000. ADAM 12-S cleaves IGFBP-3 and IGFBP-5 and is inhibited by TIMP-3. *Biochem Biophys Res Commun*, 278, 511-5.

LOGAN, C. Y. & NUSSE, R. 2004. The Wnt signaling pathway in development and disease. *Annu Rev Cell Dev Biol*, 20, 781-810.

LORD, K. A., HOFFMAN-LIEBERMANN, B. & LIEBERMANN, D. A. 1990. Nucleotide sequence and expression of a cDNA encoding MyD88, a novel myeloid differentiation primary response gene induced by IL6. *Oncogene*, 5, 1095-7.

LUM, L., REID, M. S. & BLOBEL, C. P. 1998. Intracellular maturation of the mouse metalloprotease disintegrin MDC15. *J Biol Chem*, 273, 26236-47.

MACHIDA, K., CHENG, K. T., SUNG, V. M., LEVINE, A. M., FOUNG, S. & LAI, M. M. 2006. Hepatitis C virus induces toll-like receptor 4 expression, leading to enhanced production of beta interferon and interleukin-6. *J Virol*, 80, 866-74.

MACREDMOND, R., GREENE, C., TAGGART, C. C., MCELVANEY, N. & O'NEILL, S. 2005. Respiratory epithelial cells require Toll-like receptor 4 for induction of human beta-defensin 2 by lipopolysaccharide. *Respir Res*, 6, 116.

MALLORY, M., CHARTRAND, K. & GAUTHIER, E. R. 2007. GADD153 expression

does not necessarily correlate with changes in culture behavior of hybridoma cells. *BMC Biotechnol*, 7, 89.

MANKOURI, J., FRAGKLOUDIS, R., RICHARDS, K. H., WETHERILL, L. F., HARRIS, M., KOHL, A., ELLIOTT, R. M. & MACDONALD, A. 2010. Optineurin negatively regulates the induction of IFN $\beta$  in response to RNA virus infection. *PLoS Pathog*, 6, e1000778.

MANKOURI, J., TEDBURY, P. R., GRETTON, S., HUGHES, M. E., GRIFFIN, S. D., DALLAS, M. L., GREEN, K. A., HARDIE, D. G., PEERS, C. & HARRIS, M. 2010. Enhanced hepatitis C virus genome replication and lipid accumulation mediated by inhibition of AMP-activated protein kinase. *Proc Natl Acad Sci U S A*, 107, 11549-54.

MANSELL, A., BRINT, E., GOULD, J. A., O'NEILL, L. A. & HERTZOG, P. J. 2004. Mal interacts with tumor necrosis factor receptor-associated factor (TRAF)-6 to mediate NF-kappaB activation by toll-like receptor (TLR)-2 and TLR4. *J Biol Chem*, 279, 37227-30.

MANSELL, A., SMITH, R., DOYLE, S. L., GRAY, P., FENNER, J. E., CRACK, P. J., NICHOLSON, S. E., HILTON, D. J., O'NEILL, L. A. & HERTZOG, P. J. 2006. Suppressor of cytokine signaling 1 negatively regulates Toll-like receptor signaling by mediating Mal degradation. *Nat Immunol*, 7, 148-55.

MARSHAK-ROTHSTEIN, A. 2006. Toll-like receptors in systemic autoimmune disease. *Nat Rev Immunol*, 6, 823-35.

MARSILI, G., REMOLI, A. L., SGARBANTI, M., PERROTTI, E., FRAGALE, A. & BATTISTINI, A. 2012. HIV-1, interferon and the interferon regulatory factor system: An interplay between induction, antiviral responses and viral evasion. *Cytokine Growth Factor Rev*, 23, 255-70.

MARTIN, J., EYNSTONE, L. V., DAVIES, M., WILLIAMS, J. D. & STEADMAN, R. 2002. The role of ADAM 15 in glomerular mesangial cell migration. *J Biol Chem*, 277, 33683-9.

MARZOLO, M. P. & FARFAN, P. 2011. New insights into the roles of megalin/LRP2 and the regulation of its functional expression. *Biol Res*, 44, 89-105.

MASCKAUCHAN, T. N., AGALLIU, D., VORONTCHIKHINA, M., AHN, A., PARMALEE, N. L., LI, C. M., KHOO, A., TYCKO, B., BROWN, A. M. & KITAJEWSKI, J. 2006. Wnt5a signaling induces proliferation and survival of endothelial cells in vitro and expression of MMP-1 and Tie-2. *Mol Biol Cell*, 17, 5163-72.

MATSUKURA, S., KOKUBU, F., KUROKAWA, M., KAWAGUCHI, M., IEKI, K., KUGA, H., ODAKA, M., SUZUKI, S., WATANABE, S., HOMMA, T., TAKEUCHI, H., NOHTOMI, K. & ADACHI, M. 2007. Role of RIG-I, MDA-5, and PKR on the expression of inflammatory chemokines induced by synthetic dsRNA in airway epithelial cells. *Int Arch Allergy Immunol*, 143 Suppl 1, 80-3.

MATSUMOTO, M., FUNAMI, K., TANABE, M., OSHIUMI, H., SHINGAI, M., SETO, Y., YAMAMOTO, A. & SEYA, T. 2003. Subcellular localization of Toll-like receptor 3 in human dendritic cells. *J Immunol*, 171, 3154-62.

MCCORMACK, W. J., PARKER, A. E. & O'NEILL, L. A. 2009. Toll-like receptors and NOD-like receptors in rheumatic diseases. *Arthritis Res Ther*, 11, 243.

MCCULLY, R. R. & POMERANTZ, J. L. 2008. The protein kinase C-responsive inhibitory domain of CARD11 functions in NF-kappaB activation to regulate the association of multiple signaling cofactors that differentially depend on Bcl10 and MALT1 for association. *Mol Cell Biol*, 28, 5668-86.

MCDONNELL, J. M., JONES, G. E., WHITE, T. K. & TANZER, M. L. 1996. Calreticulin binding affinity for glycosylated laminin. *J Biol Chem*, 271, 7891-4.

MCGETTRICK, A. F., BRINT, E. K., PALSSON-MCDERMOTT, E. M., ROWE, D. C., GOLENBOCK, D. T., GAY, N. J., FITZGERALD, K. A. & O'NEILL, L. A. 2006. Trif-related adapter molecule is phosphorylated by PKC{epsilon} during Toll-like receptor 4 signaling. *Proc Natl Acad Sci U S A*, 103, 9196-201.

MEDZHITOV, R. & JANEWAY, C. A., JR. 1998. Innate immune recognition and control of adaptive immune responses. *Semin Immunol*, 10, 351-3.

MEDZHITOV, R. & JANEWAY, C. A., JR. 2002. Decoding the patterns of self and nonself by the innate immune system. *Science*, 296, 298-300.

MEDZHITOV, R., PRESTON-HURLBURT, P. & JANEWAY, C. A., JR. 1997. A human homologue of the Drosophila Toll protein signals activation of adaptive immunity. *Nature*, 388, 394-7.

MEDZHITOV, R., PRESTON-HURLBURT, P., KOPP, E., STADLEN, A., CHEN, C., GHOSH, S. & JANEWAY, C. A., JR. 1998. MyD88 is an adaptor protein in the hToll/IL-1 receptor family signaling pathways. *Mol Cell*, 2, 253-8.

MEYLAN, E., BURNS, K., HOFMANN, K., BLANCHETEAU, V., MARTINON, F., KELLIHER, M. & TSCHOPP, J. 2004. RIP1 is an essential mediator of Toll-like receptor 3-induced NF-kappa B activation. *Nat Immunol*, 5, 503-7.

MILLICHIP, M. I., DALLAS, D. J., WU, E., DALE, S. & MCKIE, N. 1998. The

metallo-disintegrin ADAM10 (MADM) from bovine kidney has type IV collagenase activity in vitro. *Biochem Biophys Res Commun*, 245, 594-8.

MINK, M., FOGELGREN, B., OLSZEWSKI, K., MAROY, P. & CSISZAR, K. 2001. A novel human gene (SARM) at chromosome 17q11 encodes a protein with a SAM motif and structural similarity to Armadillo/beta-catenin that is conserved in mouse, *Drosophila*, and *Caenorhabditis elegans*. *Genomics*, 74, 234-44.

MISHRA, A., PAUL, S. & SWARNAKAR, S. 2011. Downregulation of matrix metalloproteinase-9 by melatonin during prevention of alcohol-induced liver injury in mice. *Biochimie*, 93, 854-66.

MISHRA, B. B., GUNDRA, U. M. & TEALE, J. M. 2008. Expression and distribution of Toll-like receptors 11-13 in the brain during murine neurocysticercosis. *J Neuroinflammation*, 5, 53.

MISHRA, S., MURPHY, L. C., NYOMBA, B. L. & MURPHY, L. J. 2005. Prohibitin: a potential target for new therapeutics. *Trends Mol Med*, 11, 192-7.

MIYACHI, K., FRITZLER, M. J. & TAN, E. M. 1978. Autoantibody to a nuclear antigen in proliferating cells. *J Immunol*, 121, 2228-34.

MOGENSEN, T. H. 2009. Pathogen recognition and inflammatory signaling in innate immune defenses. *Clin Microbiol Rev*, 22, 240-73, Table of Contents.

MOLINARI, M., ERIKSSON, K. K., CALANCA, V., GALLI, C., CRESSWELL, P., MICHALAK, M. & HELENIUS, A. 2004. Contrasting functions of calreticulin and calnexin in glycoprotein folding and ER quality control. *Mol Cell*, 13, 125-35.

MONICK, M. M., YAROVINSKY, T. O., POWERS, L. S., BUTLER, N. S., CARTER, A. B., GUDMUNDSSON, G. & HUNNINGHAKE, G. W. 2003. Respiratory syncytial virus up-regulates TLR4 and sensitizes airway epithelial cells to endotoxin. *J Biol Chem*, 278, 53035-44.

MONTERO VEGA, M. T. & DE ANDRES MARTIN, A. 2009. The significance of toll-like receptors in human diseases. *Allergol Immunopathol (Madr)*, 37, 252-63.

MORTON, S., HESSON, L., PEGGIE, M. & COHEN, P. 2008. Enhanced binding of TBK1 by an optineurin mutant that causes a familial form of primary open angle glaucoma. *FEBS Lett*, 582, 997-1002.

MOSNIER, J. F., JARRY, A., BOU-HANNA, C., DENIS, M. G., MERLIN, D. & LABOISSE, C. L. 2006. ADAM15 upregulation and interaction with multiple binding partners in inflammatory bowel disease. *Lab Invest*, 86, 1064-73.

MUCCIOLI, M., SPRAGUE, L., NANDIGAM, H., PATE, M. & BENENCIA, F. 2012.

Toll-like receptors as novel therapeutic targets for ovarian cancer. *ISRN Oncol*, 2012, 642141.

MUKHERJEE, A., MOROSKY, S. A., DELORME-AXFORD, E., DYBDAHL-SISSOKO, N., OBERSTE, M. S., WANG, T. & COYNE, C. B. 2011. The coxsackievirus B 3C protease cleaves MAVS and TRIF to attenuate host type I interferon and apoptotic signaling. *PLoS Pathog*, 7, e1001311.

MULLER-TAUBENBERGER, A., BRETSCHEIDER, T., FAIX, J., KONZOK, A., SIMMETH, E. & WEBER, I. 2002. Differential localization of the Dictyostelium kinase DPAKa during cytokinesis and cell migration. *J Muscle Res Cell Motil*, 23, 751-63.

MURALIDHARAN, S., HANLEY, P. J., LIU, E., CHAKRABORTY, R., BOLLARD, C., SHPALL, E., ROONEY, C., SAVOLDO, B., RODGERS, J. & DOTTI, G. 2011. Activation of Wnt signaling arrests effector differentiation in human peripheral and cord blood-derived T lymphocytes. *J Immunol*, 187, 5221-32.

NAGABHUSHANA, A., BANSAL, M. & SWARUP, G. 2011. Optineurin is required for CYLD-dependent inhibition of TNF $\alpha$ -induced NF- $\kappa$ B activation. *PLoS One*, 6, e17477.

NAGABHUSHANA, A., CHALASANI, M. L., JAIN, N., RADHA, V., RANGARAJ, N., BALASUBRAMANIAN, D. & SWARUP, G. 2010. Regulation of endocytic trafficking of transferrin receptor by optineurin and its impairment by a glaucoma-associated mutant. *BMC Cell Biol*, 11, 4.

NAGASAKA, K., PIM, D., MASSIMI, P., THOMAS, M., TOMAIC, V., SUBBIAH, V. K., KRANJEC, C., NAKAGAWA, S., YANO, T., TAKETANI, Y., MYERS, M. & BANKS, L. 2010. The cell polarity regulator hScrib controls ERK activation through a KIM site-dependent interaction. *Oncogene*, 29, 5311-21.

NAIKI, Y., MICHELSEN, K. S., ZHANG, W., CHEN, S., DOHERTY, T. M. & ARDITI, M. 2005. Transforming growth factor- $\beta$  differentially inhibits MyD88-dependent, but not TRAM- and TRIF-dependent, lipopolysaccharide-induced TLR4 signaling. *J Biol Chem*, 280, 5491-5.

NAJY, A. J., DAY, K. C. & DAY, M. L. 2008. ADAM15 supports prostate cancer metastasis by modulating tumor cell-endothelial cell interaction. *Cancer Res*, 68, 1092-9.

NAJY, A. J., DAY, K. C. & DAY, M. L. 2008. The ectodomain shedding of E-cadherin by ADAM15 supports ErbB receptor activation. *J Biol Chem*, 283, 18393-401.

NAKAGAWA, T., ZHU, H., MORISHIMA, N., LI, E., XU, J., YANKNER, B. A. & YUAN, J. 2000. Caspase-12 mediates endoplasmic-reticulum-specific apoptosis and cytotoxicity by amyloid-beta. *Nature*, 403, 98-103.

NAKAMURA, K., MIYAZATO, A., KOGUCHI, Y., ADACHI, Y., OHNO, N., SAIJO, S., IWAKURA, Y., TAKEDA, K., AKIRA, S., FUJITA, J., ISHII, K., KAKU, M. & KAWAKAMI, K. 2008. Toll-like receptor 2 (TLR2) and dectin-1 contribute to the production of IL-12p40 by bone marrow-derived dendritic cells infected with *Penicillium marneffeii*. *Microbes Infect*, 10, 1223-7.

NANJI, A. A., LAU, G. K., TIPOE, G. L., YUEN, S. T., CHEN, Y. X., THOMAS, P. & LAN, H. Y. 2001. Macrophage migration inhibitory factor expression in male and female ethanol-fed rats. *J Interferon Cytokine Res*, 21, 1055-62.

NATH, D., SLOCOMBE, P. M., STEPHENS, P. E., WARN, A., HUTCHINSON, G. R., YAMADA, K. M., DOCHERTY, A. J. & MURPHY, G. 1999. Interaction of metargidin (ADAM-15) with alphavbeta3 and alpha5beta1 integrins on different haemopoietic cells. *J Cell Sci*, 112 ( Pt 4), 579-87.

NEGISHI, H., OHBA, Y., YANAI, H., TAKAOKA, A., HONMA, K., YUI, K., MATSUYAMA, T., TANIGUCHI, T. & HONDA, K. 2005. Negative regulation of Toll-like-receptor signaling by IRF-4. *Proc Natl Acad Sci U S A*, 102, 15989-94.

NEUMANN, S., COUDREUSE, D. Y., VAN DER WESTHUYZEN, D. R., ECKHARDT, E. R., KORSWAGEN, H. C., SCHMITZ, G. & SPRONG, H. 2009. Mammalian Wnt3a is released on lipoprotein particles. *Traffic*, 10, 334-43.

NISHIMURA, M. & NAITO, S. 2005. Tissue-specific mRNA expression profiles of human toll-like receptors and related genes. *Biol Pharm Bull*, 28, 886-92.

NOURBAKHS, M. & HAUSER, H. 1999. Constitutive silencing of IFN-beta promoter is mediated by NRF (NF-kappaB-repressing factor), a nuclear inhibitor of NF-kappaB. *EMBO J*, 18, 6415-25.

NUNEZ MIGUEL, R., WONG, J., WESTOLL, J. F., BROOKS, H. J., O'NEILL, L. A., GAY, N. J., BRYANT, C. E. & MONIE, T. P. 2007. A dimer of the Toll-like receptor 4 cytoplasmic domain provides a specific scaffold for the recruitment of signalling adaptor proteins. *PLoS One*, 2, e788.

NYMAN, T., STENMARK, P., FLODIN, S., JOHANSSON, I., HAMMARSTROM, M. & NORDLUND, P. 2008. The crystal structure of the human toll-like receptor 10 cytoplasmic domain reveals a putative signaling dimer. *J Biol Chem*, 283, 11861-5.

OBEID, M., TESNIERE, A., GHIRINGHELLI, F., FIMIA, G. M., APETOH, L.,

PERFETTINI, J. L., CASTEDO, M., MIGNOT, G., PANARETAKIS, T., CASARES, N., METIVIER, D., LAROCLETTE, N., VAN ENDERT, P., CICCOSANTI, F., PIACENTINI, M., ZITVOGEL, L. & KROEMER, G. 2007. Calreticulin exposure dictates the immunogenicity of cancer cell death. *Nat Med*, 13, 54-61.

OGURA, Y., BONEN, D. K., INOHARA, N., NICOLAE, D. L., CHEN, F. F., RAMOS, R., BRITTON, H., MORAN, T., KARALIUSKAS, R., DUERR, R. H., ACHKAR, J. P., BRANT, S. R., BAYLESS, T. M., KIRSCHNER, B. S., HANAUER, S. B., NUNEZ, G. & CHO, J. H. 2001. A frameshift mutation in NOD2 associated with susceptibility to Crohn's disease. *Nature*, 411, 603-6.

O'NEILL, L. 2000. The Toll/interleukin-1 receptor domain: a molecular switch for inflammation and host defence. *Biochem Soc Trans*, 28, 557-63.

O'NEILL, L. A. & BOWIE, A. G. 2007. The family of five: TIR-domain-containing adaptors in Toll-like receptor signalling. *Nat Rev Immunol*, 7, 353-64.

O'NEILL, L. A., BRYANT, C. E. & DOYLE, S. L. 2009. Therapeutic targeting of Toll-like receptors for infectious and inflammatory diseases and cancer. *Pharmacol Rev*, 61, 177-97.

O'NEILL, L. A., FITZGERALD, K. A. & BOWIE, A. G. 2003. The Toll-IL-1 receptor adaptor family grows to five members. *Trends Immunol*, 24, 286-90.

ONODERA, S., NISHIHARA, J., KOYAMA, Y., MAJIMA, T., AOKI, Y., ICHIYAMA, H., ISHIBASHI, T. & MINAMI, A. 2004. Macrophage migration inhibitory factor up-regulates the expression of interleukin-8 messenger RNA in synovial fibroblasts of rheumatoid arthritis patients: common transcriptional regulatory mechanism between interleukin-8 and interleukin-1beta. *Arthritis Rheum*, 50, 1437-47.

OSHIUMI, H., MATSUMOTO, M., FUNAMI, K., AKAZAWA, T. & SEYA, T. 2003. TICAM-1, an adaptor molecule that participates in Toll-like receptor 3-mediated interferon-beta induction. *Nat Immunol*, 4, 161-7.

OSHIUMI, H., SASAI, M., SHIDA, K., FUJITA, T., MATSUMOTO, M. & SEYA, T. 2003. TIR-containing adapter molecule (TICAM)-2, a bridging adapter recruiting to toll-like receptor 4 TICAM-1 that induces interferon-beta. *J Biol Chem*, 278, 49751-62.

OSORIO, F. & REIS E SOUSA, C. 2011. Myeloid C-type lectin receptors in pathogen recognition and host defense. *Immunity*, 34, 651-64.

OVERALL, C. M. & LOPEZ-OTIN, C. 2002. Strategies for MMP inhibition in cancer: innovations for the post-trial era. *Nat Rev Cancer*, 2, 657-72.

PAGE-MCCAW, A., EWALD, A. J. & WERB, Z. 2007. Matrix metalloproteinases and

the regulation of tissue remodelling. *Nat Rev Mol Cell Biol*, 8, 221-33.

PALAGA, T., BURANARUK, C., RENGPIPAT, S., FAUQ, A. H., GOLDE, T. E., KAUFMANN, S. H. & OSBORNE, B. A. 2008. Notch signaling is activated by TLR stimulation and regulates macrophage functions. *Eur J Immunol*, 38, 174-83.

PALAYOOR, S. T., YOUMELL, M. Y., CALDERWOOD, S. K., COLEMAN, C. N. & PRICE, B. D. 1999. Constitutive activation of IkappaB kinase alpha and NF-kappaB in prostate cancer cells is inhibited by ibuprofen. *Oncogene*, 18, 7389-94.

PALSSON-MCDERMOTT, E. M., DOYLE, S. L., MCGETTRICK, A. F., HARDY, M., HUSEBYE, H., BANAHAN, K., GONG, M., GOLENBOCK, D., ESPEVIK, T. & O'NEILL, L. A. 2009. TAG, a splice variant of the adaptor TRAM, negatively regulates the adaptor MyD88-independent TLR4 pathway. *Nat Immunol*, 10, 579-86.

PANCHANATHAN, R., DUAN, X., SHEN, H., RATHINAM, V. A., ERICKSON, L. D., FITZGERALD, K. A. & CHOUBEY, D. 2010. Aim2 deficiency stimulates the expression of IFN-inducible Ifi202, a lupus susceptibility murine gene within the Nba2 autoimmune susceptibility locus. *J Immunol*, 185, 7385-93.

PAONE, A., STARACE, D., GALLI, R., PADULA, F., DE CESARIS, P., FILIPPINI, A., ZIPARO, E. & RICCIOLI, A. 2008. Toll-like receptor 3 triggers apoptosis of human prostate cancer cells through a PKC-alpha-dependent mechanism. *Carcinogenesis*, 29, 1334-42.

PARK, S. J., SONG, H. Y. & YOUN, H. S. 2009. Suppression of the TRIF-dependent signaling pathway of toll-like receptors by isoliquiritigenin in RAW264.7 macrophages. *Mol Cells*, 28, 365-8.

PATTINGRE, S., TASSA, A., QU, X., GARUTI, R., LIANG, X. H., MIZUSHIMA, N., PACKER, M., SCHNEIDER, M. D. & LEVINE, B. 2005. Bcl-2 antiapoptotic proteins inhibit Beclin 1-dependent autophagy. *Cell*, 122, 927-39.

PAULISSEN, G., ROCKS, N., GUEDERS, M. M., CRAHAY, C., QUESADA-CALVO, F., BEKAERT, S., HACHA, J., EL HOUR, M., FOIDART, J. M., NOEL, A. & CATALDO, D. D. 2009. Role of ADAM and ADAMTS metalloproteinases in airway diseases. *Respir Res*, 10, 127.

PENG, J., YUAN, Q., LIN, B., PANNEERSELVAM, P., WANG, X., LUAN, X. L., LIM, S. K., LEUNG, B. P., HO, B. & DING, J. L. 2010. SARM inhibits both TRIF- and MyD88-mediated AP-1 activation. *Eur J Immunol*, 40, 1738-47.

PICHLMAIR, A., KANDASAMY, K., ALVISI, G., MULHERN, O., SACCO, R., HABJAN, M., BINDER, M., STEFANOVIC, A., EBERLE, C. A., GONCALVES, A.,

BURCKSTUMMER, T., MULLER, A. C., FAUSTER, A., HOLZE, C., LINDSTEN, K., GOODBOURN, S., KOCHS, G., WEBER, F., BARTENSCHLAGER, R., BOWIE, A. G., BENNETT, K. L., COLINGE, J. & SUPERTI-FURGA, G. 2012. Viral immune modulators perturb the human molecular network by common and unique strategies. *Nature*, 487, 486-90.

PIEREN, M., GALLI, C., DENZEL, A. & MOLINARI, M. 2005. The use of calnexin and calreticulin by cellular and viral glycoproteins. *J Biol Chem*, 280, 28265-71.

PIERIK, M., JOOSSENS, S., VAN STEEN, K., VAN SCHUERBEEK, N., VLIETINCK, R., RUTGEERTS, P. & VERMEIRE, S. 2006. Toll-like receptor-1, -2, and -6 polymorphisms influence disease extension in inflammatory bowel diseases. *Inflamm Bowel Dis*, 12, 1-8.

PIKARSKY, E., PORAT, R. M., STEIN, I., ABRAMOVITCH, R., AMIT, S., KASEM, S., GUTKOVICH-PYEST, E., URIELI-SHOVAL, S., GALUN, E. & BEN-NERIAH, Y. 2004. NF-kappaB functions as a tumour promoter in inflammation-associated cancer. *Nature*, 431, 461-6.

POECK, H., BSCHIEDER, M., GROSS, O., FINGER, K., ROTH, S., REBSAMEN, M., HANNESSCHLAGER, N., SCHLEE, M., ROTHENFUSSER, S., BARCHET, W., KATO, H., AKIRA, S., INOUE, S., ENDRES, S., PESCHEL, C., HARTMANN, G., HORNUNG, V. & RULAND, J. 2010. Recognition of RNA virus by RIG-I results in activation of CARD9 and inflammasome signaling for interleukin 1 beta production. *Nat Immunol*, 11, 63-9.

POGHOSYAN, Z., ROBBINS, S. M., HOUSLAY, M. D., WEBSTER, A., MURPHY, G. & EDWARDS, D. R. 2002. Phosphorylation-dependent interactions between ADAM15 cytoplasmic domain and Src family protein-tyrosine kinases. *J Biol Chem*, 277, 4999-5007.

POISSON, A., ZABLEWSKA, B. & GAUDRAY, P. 2003. Menin interacting proteins as clues toward the understanding of multiple endocrine neoplasia type 1. *Cancer Lett*, 189, 1-10.

PORTELIUS, E., ZHANG, B., GUSTAVSSON, M. K., BRINKMALM, G., WESTMAN-BRINKMALM, A., ZETTERBERG, H., LEE, V. M., TROJANOWSKI, J. Q. & BLENNOW, K. 2009. Effects of gamma-secretase inhibition on the amyloid beta isoform pattern in a mouse model of Alzheimer's disease. *Neurodegener Dis*, 6, 258-62.

PRATESI, F., MOSCATO, S., SABBATINI, A., CHIMENTI, D., BOMBARDIERI, S. & MIGLIORINI, P. 2000. Autoantibodies specific for alpha-enolase in systemic

autoimmune disorders. *J Rheumatol*, 27, 109-15.

PRIMAKOFF, P. & MYLES, D. G. 2000. The ADAM gene family: surface proteins with adhesion and protease activity. *Trends Genet*, 16, 83-7.

QI, H. Y. & SHELHAMER, J. H. 2005. Toll-like receptor 4 signaling regulates cytosolic phospholipase A2 activation and lipid generation in lipopolysaccharide-stimulated macrophages. *J Biol Chem*, 280, 38969-75.

QU, L., FENG, Z., YAMANE, D., LIANG, Y., LANFORD, R. E., LI, K. & LEMON, S. M. 2011. Disruption of TLR3 signaling due to cleavage of TRIF by the hepatitis A virus protease-polymerase processing intermediate, 3CD. *PLoS Pathog*, 7, e1002169.

REGIS, E. G., BARRETO-DE-SOUZA, V., MORGADO, M. G., BOZZA, M. T., LENG, L., BUCALA, R. & BOU-HABIB, D. C. 2010. Elevated levels of macrophage migration inhibitory factor (MIF) in the plasma of HIV-1-infected patients and in HIV-1-infected cell cultures: a relevant role on viral replication. *Virology*, 399, 31-8.

REIMER, T., BRCIC, M., SCHWEIZER, M. & JUNGI, T. W. 2008. poly(I:C) and LPS induce distinct IRF3 and NF-kappaB signaling during type-I IFN and TNF responses in human macrophages. *J Leukoc Biol*, 83, 1249-57.

REISS, K., LUDWIG, A. & SAFTIG, P. 2006. Breaking up the tie: disintegrin-like metalloproteinases as regulators of cell migration in inflammation and invasion. *Pharmacol Ther*, 111, 985-1006.

RIAD, A., WESTERMANN, D., ZIETSCH, C., SAVVATIS, K., BECHER, P. M., BERESWILL, S., HEIMESAAT, M. M., LETTAU, O., LASSNER, D., DORNER, A., POLLER, W., BUSCH, M., FELIX, S. B., SCHULTHEISS, H. P. & TSCHOPE, C. 2011. TRIF is a critical survival factor in viral cardiomyopathy. *J Immunol*, 186, 2561-70.

RITTER, K., UY, A., RITTER, S. & THOMSEN, R. 1994. Hemolysis and autoantibodies to triosephosphate isomerase in a patient with acute hepatitis A virus infection. *Scand J Infect Dis*, 26, 379-82.

RIZWANI, W., ALEXANDROW, M. & CHELLAPPAN, S. 2009. Prohibitin physically interacts with MCM proteins and inhibits mammalian DNA replication. *Cell Cycle*, 8, 1621-9.

ROELOFS, M. F., JOOSTEN, L. A., ABDOLLAHI-ROODSAZ, S., VAN LIESHOUT, A. W., SPRONG, T., VAN DEN HOOGEN, F. H., VAN DEN BERG, W. B. & RADSTAKE, T. R. 2005. The expression of toll-like receptors 3 and 7 in rheumatoid arthritis synovium is increased and costimulation of toll-like receptors 3, 4, and 7/8

results in synergistic cytokine production by dendritic cells. *Arthritis Rheum*, 52, 2313-22.

ROGHANI, M., BECHERER, J. D., MOSS, M. L., ATHERTON, R. E., ERDJUMENT-BROMAGE, H., ARRIBAS, J., BLACKBURN, R. K., WESKAMP, G., TEMPST, P. & BLOBEL, C. P. 1999. Metalloprotease-disintegrin MDC9: intracellular maturation and catalytic activity. *J Biol Chem*, 274, 3531-40.

ROMIEU-MOUREZ, R., SOLIS, M., NARDIN, A., GOUBAU, D., BARON-BODO, V., LIN, R., MASSIE, B., SALCEDO, M. & HISCOTT, J. 2006. Distinct roles for IFN regulatory factor (IRF)-3 and IRF-7 in the activation of antitumor properties of human macrophages. *Cancer Res*, 66, 10576-85.

ROSENBERG, G. A. 2009. Matrix metalloproteinases and their multiple roles in neurodegenerative diseases. *Lancet Neurol*, 8, 205-16.

ROWE, D. C., MCGETTRICK, A. F., LATZ, E., MONKS, B. G., GAY, N. J., YAMAMOTO, M., AKIRA, S., O'NEILL, L. A., FITZGERALD, K. A. & GOLENBOCK, D. T. 2006. The myristoylation of TRIF-related adaptor molecule is essential for Toll-like receptor 4 signal transduction. *Proc Natl Acad Sci U S A*, 103, 6299-304.

SAGANE, K., OHYA, Y., HASEGAWA, Y. & TANAKA, I. 1998. Metalloproteinase-like, disintegrin-like, cysteine-rich proteins MDC2 and MDC3: novel human cellular disintegrins highly expressed in the brain. *Biochem J*, 334 ( Pt 1), 93-8.

SAHLENDER, D. A., ROBERTS, R. C., ARDEN, S. D., SPUDICH, G., TAYLOR, M. J., LUZIO, J. P., KENDRICK-JONES, J. & BUSS, F. 2005. Optineurin links myosin VI to the Golgi complex and is involved in Golgi organization and exocytosis. *J Cell Biol*, 169, 285-95.

SAKURAI-YAGETA, M., RECCHI, C., LE DEZ, G., SIBARITA, J. B., DAVIET, L., CAMONIS, J., D'SOUZA-SCHOREY, C. & CHAVRIER, P. 2008. The interaction of IQGAP1 with the exocyst complex is required for tumor cell invasion downstream of Cdc42 and RhoA. *J Cell Biol*, 181, 985-98.

SALAUN, B., COSTE, I., RISSOAN, M. C., LEBECQUE, S. J. & RENNO, T. 2006. TLR3 can directly trigger apoptosis in human cancer cells. *J Immunol*, 176, 4894-901.

SASAI, M., LINEHAN, M. M. & IWASAKI, A. 2010. Bifurcation of Toll-like receptor 9 signaling by adaptor protein 3. *Science*, 329, 1530-4.

SATO, A., LINEHAN, M. M. & IWASAKI, A. 2006. Dual recognition of herpes simplex viruses by TLR2 and TLR9 in dendritic cells. *Proc Natl Acad Sci U S A*, 103,

17343-8.

SATO, S., SUGIYAMA, M., YAMAMOTO, M., WATANABE, Y., KAWAI, T., TAKEDA, K. & AKIRA, S. 2003. Toll/IL-1 receptor domain-containing adaptor inducing IFN-beta (TRIF) associates with TNF receptor-associated factor 6 and TANK-binding kinase 1, and activates two distinct transcription factors, NF-kappa B and IFN-regulatory factor-3, in the Toll-like receptor signaling. *J Immunol*, 171, 4304-10.

SCANGA, C. A., ALIBERTI, J., JANKOVIC, D., TILLOY, F., BENNOUNA, S., DENKERS, E. Y., MEDZHITOV, R. & SHER, A. 2002. Cutting edge: MyD88 is required for resistance to *Toxoplasma gondii* infection and regulates parasite-induced IL-12 production by dendritic cells. *J Immunol*, 168, 5997-6001.

SCHAALE, K., NEUMANN, J., SCHNEIDER, D., EHLERS, S. & REILING, N. 2011. Wnt signaling in macrophages: augmenting and inhibiting mycobacteria-induced inflammatory responses. *Eur J Cell Biol*, 90, 553-9.

SCHALLER, M. A., NEUPANE, R., RUDD, B. D., KUNKEL, S. L., KALLAL, L. E., LINCOLN, P., LOWE, J. B., MAN, Y. & LUKACS, N. W. 2007. Notch ligand Delta-like 4 regulates disease pathogenesis during respiratory viral infections by modulating Th2 cytokines. *J Exp Med*, 204, 2925-34.

SCHLANGE, T., MATSUDA, Y., LIENHARD, S., HUBER, A. & HYNES, N. E. 2007. Autocrine WNT signaling contributes to breast cancer cell proliferation via the canonical WNT pathway and EGFR transactivation. *Breast Cancer Res*, 9, R63.

SCHOENEMEYER, A., BARNES, B. J., MANCL, M. E., LATZ, E., GOUTAGNY, N., PITHA, P. M., FITZGERALD, K. A. & GOLENBOCK, D. T. 2005. The interferon regulatory factor, IRF5, is a central mediator of toll-like receptor 7 signaling. *J Biol Chem*, 280, 17005-12.

SCHONEVELD, A. H., HOEFER, I., SLUIJTER, J. P., LAMAN, J. D., DE KLEIJN, D. P. & PASTERKAMP, G. 2008. Atherosclerotic lesion development and Toll like receptor 2 and 4 responsiveness. *Atherosclerosis*, 197, 95-104.

SCHRODER, K. & TSCHOPP, J. 2010. The inflammasomes. *Cell*, 140, 821-32.

SCHRODER, M., BARAN, M. & BOWIE, A. G. 2008. Viral targeting of DEAD box protein 3 reveals its role in TBK1/IKKepsilon-mediated IRF activation. *EMBO J*, 27, 2147-57.

SCHWAMBORN, K., WEIL, R., COURTOIS, G., WHITESIDE, S. T. & ISRAEL, A. 2000. Phorbol esters and cytokines regulate the expression of the NEMO-related protein, a molecule involved in a NF-kappa B-independent pathway. *J Biol Chem*, 275,

22780-9.

SCHWARZ-ROMOND, T., FIEDLER, M., SHIBATA, N., BUTLER, P. J., KIKUCHI, A., HIGUCHI, Y. & BIENZ, M. 2007. The DIX domain of Dishevelled confers Wnt signaling by dynamic polymerization. *Nat Struct Mol Biol*, 14, 484-92.

SCOTT, A. M. & SALEH, M. 2007. The inflammatory caspases: guardians against infections and sepsis. *Cell Death Differ*, 14, 23-31.

SEALS, D. F. & COURTNEIDGE, S. A. 2003. The ADAMs family of metalloproteases: multidomain proteins with multiple functions. *Genes Dev*, 17, 7-30.

SEGUIN, B., ARROUAYS, D., BALESSENT, J., SOUSSANA, J.-F., BONDEAU, A., SMITH, P., ZAEHLE, S., DE NOBLET, N. & VIOVY, N. 2007. Moderating the impact of agriculture on climate. *Agricultural and Forest Meteorology*, 142, 278-287.

SELEDTSOV, V. I. & SELEDTSOVA, G. V. 2012. A balance between tissue-destructive and tissue-protective immunities: a role of toll-like receptors in regulation of adaptive immunity. *Immunobiology*, 217, 430-5.

SEN, M., CHAMORRO, M., REIFERT, J., CORR, M. & CARSON, D. A. 2001. Blockade of Wnt-5A/frizzled 5 signaling inhibits rheumatoid synoviocyte activation. *Arthritis Rheum*, 44, 772-81.

SERRANO, S. M., JIA, L. G., WANG, D., SHANNON, J. D. & FOX, J. W. 2005. Function of the cysteine-rich domain of the haemorrhagic metalloproteinase atrolysin A: targeting adhesion proteins collagen I and von Willebrand factor. *Biochem J*, 391, 69-76.

SHA, Q., TRUONG-TRAN, A. Q., PLITT, J. R., BECK, L. A. & SCHLEIMER, R. P. 2004. Activation of airway epithelial cells by toll-like receptor agonists. *Am J Respir Cell Mol Biol*, 31, 358-64.

SHAN, J., SHI, D. L., WANG, J. & ZHENG, J. 2005. Identification of a specific inhibitor of the dishevelled PDZ domain. *Biochemistry*, 44, 15495-503.

SHARMA, S., TENOEVER, B. R., GRANDVAUX, N., ZHOU, G. P., LIN, R. & HISCOTT, J. 2003. Triggering the interferon antiviral response through an IKK-related pathway. *Science*, 300, 1148-51.

SHI, C. S. & KEHRL, J. H. 2008. MyD88 and Trif target Beclin 1 to trigger autophagy in macrophages. *J Biol Chem*, 283, 33175-82.

SHI, H., KOKOEVA, M. V., INOUE, K., TZAMELI, I., YIN, H. & FLIER, J. S. 2006. TLR4 links innate immunity and fatty acid-induced insulin resistance. *J Clin Invest*, 116, 3015-25.

SHIN, O. S., MILLER, L. S., MODLIN, R. L., AKIRA, S., UEMATSU, S. & HU, L. T. 2009. Downstream signals for MyD88-mediated phagocytosis of *Borrelia burgdorferi* can be initiated by TRIF and are dependent on PI3K. *J Immunol*, 183, 491-8.

SHINOHARA, H., INOUE, A., TOYAMA-SORIMACHI, N., NAGAI, Y., YASUDA, T., SUZUKI, H., HORAI, R., IWAKURA, Y., YAMAMOTO, T., KARASUYAMA, H., MIYAKE, K. & YAMANASHI, Y. 2005. Dok-1 and Dok-2 are negative regulators of lipopolysaccharide-induced signaling. *J Exp Med*, 201, 333-9.

SHOEMAKER, B. A. & PANCHENKO, A. R. 2007. Deciphering protein-protein interactions. Part I. Experimental techniques and databases. *PLoS Comput Biol*, 3, e42.

SHOTORBANI, S. S., SU, Z. L. & XU, H. X. 2011. Toll-like receptors are potential therapeutic targets in rheumatoid arthritis. *World J Biol Chem*, 2, 167-72.

SIEDNIENKO, J., GAJANAYAKE, T., FITZGERALD, K. A., MOYNAGH, P. & MIGGIN, S. M. 2011. Absence of MyD88 results in enhanced TLR3-dependent phosphorylation of IRF3 and increased IFN-beta and RANTES production. *J Immunol*, 186, 2514-22.

SIPPL, C., BOSSERHOFF, A. K., FISCHER, D. & TAMM, E. R. 2011. Depletion of optineurin in RGC-5 cells derived from retinal neurons causes apoptosis and reduces the secretion of neurotrophins. *Exp Eye Res*, 93, 669-80.

SIREN, J., PIRHONEN, J., JULKUNEN, I. & MATIKAINEN, S. 2005. IFN-alpha regulates TLR-dependent gene expression of IFN-alpha, IFN-beta, IL-28, and IL-29. *J Immunol*, 174, 1932-7.

SMIETANA, K., MATEJA, A., KREZEL, A. & OTLEWSKI, J. 2011. PDZ domain from Dishevelled -- a specificity study. *Acta Biochim Pol*, 58, 243-9.

SO, E. Y. & OUCHI, T. 2010. The application of Toll like receptors for cancer therapy. *Int J Biol Sci*, 6, 675-81.

SODHI, C. P., SHI, X. H., RICHARDSON, W. M., GRANT, Z. S., SHAPIRO, R. A., PRINDLE, T., JR., BRANCA, M., RUSSO, A., GRIBAR, S. C., MA, C. & HACKAM, D. J. 2010. Toll-like receptor-4 inhibits enterocyte proliferation via impaired beta-catenin signaling in necrotizing enterocolitis. *Gastroenterology*, 138, 185-96.

SOLOMON, K. A., PESTI, N., WU, G. & NEWTON, R. C. 1999. Cutting edge: a dominant negative form of TNF-alpha converting enzyme inhibits proTNF and TNFRII secretion. *J Immunol*, 163, 4105-8.

SONG, H., LI, Y., LEE, J., SCHWARTZ, A. L. & BU, G. 2009. Low-density lipoprotein receptor-related protein 1 promotes cancer cell migration and invasion by

inducing the expression of matrix metalloproteinases 2 and 9. *Cancer Res*, 69, 879-86.

SOULAT, D., BURCKSTUMMER, T., WESTERMAYER, S., GONCALVES, A., BAUCH, A., STEFANOVIC, A., HANTSCHHEL, O., BENNETT, K. L., DECKER, T. & SUPERTI-FURGA, G. 2008. The DEAD-box helicase DDX3X is a critical component of the TANK-binding kinase 1-dependent innate immune response. *EMBO J*, 27, 2135-46.

STAAL, F. J., LUIS, T. C. & TIEMESSEN, M. M. 2008. WNT signalling in the immune system: WNT is spreading its wings. *Nat Rev Immunol*, 8, 581-93.

STAAL, F. J., WEERKAMP, F., BAERT, M. R., VAN DEN BURG, C. M., VAN NOORT, M., DE HAAS, E. F. & VAN DONGEN, J. J. 2004. Wnt target genes identified by DNA microarrays in immature CD34+ thymocytes regulate proliferation and cell adhesion. *J Immunol*, 172, 1099-108.

STACK, J., HAGA, I. R., SCHRODER, M., BARTLETT, N. W., MALONEY, G., READING, P. C., FITZGERALD, K. A., SMITH, G. L. & BOWIE, A. G. 2005. Vaccinia virus protein A46R targets multiple Toll-like-interleukin-1 receptor adaptors and contributes to virulence. *J Exp Med*, 201, 1007-18.

STEINER, T. S. 2007. How flagellin and toll-like receptor 5 contribute to enteric infection. *Infect Immun*, 75, 545-52.

SU, X., LI, S., MENG, M., QIAN, W., XIE, W., CHEN, D., ZHAI, Z. & SHU, H. B. 2006. TNF receptor-associated factor-1 (TRAF1) negatively regulates Toll/IL-1 receptor domain-containing adaptor inducing IFN-beta (TRIF)-mediated signaling. *Eur J Immunol*, 36, 199-206.

SUDHAKAR, C., NAGABHUSHANA, A., JAIN, N. & SWARUP, G. 2009. NF-kappaB mediates tumor necrosis factor alpha-induced expression of optineurin, a negative regulator of NF-kappaB. *PLoS One*, 4, e5114.

SUN, C., WU, M. H., GUO, M., DAY, M. L., LEE, E. S. & YUAN, S. Y. 2010. ADAM15 regulates endothelial permeability and neutrophil migration via Src/ERK1/2 signalling. *Cardiovasc Res*, 87, 348-55.

SUN, J., DUFFY, K. E., RANJITH-KUMAR, C. T., XIONG, J., LAMB, R. J., SANTOS, J., MASARAPU, H., CUNNINGHAM, M., HOLZENBURG, A., SARISKY, R. T., MBOW, M. L. & KAO, C. 2006. Structural and functional analyses of the human Toll-like receptor 3. Role of glycosylation. *J Biol Chem*, 281, 11144-51.

SUN, J., HOBERT, M. E., DUAN, Y., RAO, A. S., HE, T. C., CHANG, E. B. & MADARA, J. L. 2005. Crosstalk between NF-kappaB and beta-catenin pathways in

bacterial-colonized intestinal epithelial cells. *Am J Physiol Gastrointest Liver Physiol*, 289, G129-37.

SWANTEK, J. L., TSEN, M. F., COBB, M. H. & THOMAS, J. A. 2000. IL-1 receptor-associated kinase modulates host responsiveness to endotoxin. *J Immunol*, 164, 4301-6.

SWARUP, G. & NAGABHUSHANA, A. 2010. Optineurin, a multifunctional protein involved in glaucoma, amyotrophic lateral sclerosis and antiviral signalling. *J Biosci*, 35, 501-5.

TABETA, K., GEORGEL, P., JANSSEN, E., DU, X., HOEBE, K., CROZAT, K., MUDD, S., SHAMEL, L., SOVATH, S., GOODE, J., ALEXOPOULOU, L., FLAVELL, R. A. & BEUTLER, B. 2004. Toll-like receptors 9 and 3 as essential components of innate immune defense against mouse cytomegalovirus infection. *Proc Natl Acad Sci U S A*, 101, 3516-21.

TAKAGI, M. 2011. Toll-like receptor--a potent driving force behind rheumatoid arthritis. *J Clin Exp Hematop*, 51, 77-92.

TAKEDA, K. & AKIRA, S. 2004. TLR signaling pathways. *Semin Immunol*, 16, 3-9.

TAKEDA, K. & AKIRA, S. 2005. Toll-like receptors in innate immunity. *Int Immunol*, 17, 1-14.

TAKEUCHI, O. & AKIRA, S. 2010. Pattern recognition receptors and inflammation. *Cell*, 140, 805-20.

TAKEUCHI, O., HOSHINO, K., KAWAI, T., SANJO, H., TAKADA, H., OGAWA, T., TAKEDA, K. & AKIRA, S. 1999. Differential roles of TLR2 and TLR4 in recognition of gram-negative and gram-positive bacterial cell wall components. *Immunity*, 11, 443-51.

TAKEUCHI, O., KAWAI, T., MUHLRADT, P. F., MORR, M., RADOLF, J. D., ZYCHLINSKY, A., TAKEDA, K. & AKIRA, S. 2001. Discrimination of bacterial lipoproteins by Toll-like receptor 6. *Int Immunol*, 13, 933-40.

TAKEUCHI, O., SATO, S., HORIUCHI, T., HOSHINO, K., TAKEDA, K., DONG, Z., MODLIN, R. L. & AKIRA, S. 2002. Cutting edge: role of Toll-like receptor 1 in mediating immune response to microbial lipoproteins. *J Immunol*, 169, 10-4.

TAKEUCHI, O., TAKEDA, K., HOSHINO, K., ADACHI, O., OGAWA, T. & AKIRA, S. 2000. Cellular responses to bacterial cell wall components are mediated through MyD88-dependent signaling cascades. *Int Immunol*, 12, 113-7.

TAUSZIG-DELAMASURE, S., BILAK, H., CAPOVILLA, M., HOFFMANN, J. A. & IMLER, J. L. 2002. Drosophila MyD88 is required for the response to fungal and

Gram-positive bacterial infections. *Nat Immunol*, 3, 91-7.

THEISS, A. L., IDELL, R. D., SRINIVASAN, S., KLAPPROTH, J. M., JONES, D. P., MERLIN, D. & SITARAMAN, S. V. 2007. Prohibitin protects against oxidative stress in intestinal epithelial cells. *FASEB J*, 21, 197-206.

THOMAS, A., LAXTON, C., RODMAN, J., MYANGAR, N., HORSCROFT, N. & PARKINSON, T. 2007. Investigating Toll-like receptor agonists for potential to treat hepatitis C virus infection. *Antimicrob Agents Chemother*, 51, 2969-78.

UEMATSU, K., SEKI, N., SETO, T., ISOE, C., TSUKAMOTO, H., MIKAMI, I., YOU, L., HE, B., XU, Z., JABLONS, D. M. & EGUCHI, K. 2007. Targeting the Wnt signaling pathway with dishevelled and cisplatin synergistically suppresses mesothelioma cell growth. *Anticancer Res*, 27, 4239-42.

UEMATSU, S. & AKIRA, S. 2008. Toll-Like receptors (TLRs) and their ligands. *Handb Exp Pharmacol*, 1-20.

ULRICHTS, P. & TAVERNIER, J. 2008. MAPPIT analysis of early Toll-like receptor signalling events. *Immunol Lett*, 116, 141-8.

UMEMURA, N., ZHU, J., MBURU, Y. K., FORERO, A., HSIEH, P. N., MUTHUSWAMY, R., KALINSKI, P., FERRIS, R. L. & SARKAR, S. N. 2012. Defective NF-kappaB signaling in metastatic head and neck cancer cells leads to enhanced apoptosis by double-stranded RNA. *Cancer Res*, 72, 45-55.

UNGERER, C., DOBERSTEIN, K., BURGER, C., HARDT, K., BOEHNCKE, W. H., BOHM, B., PFEILSCHIFTER, J., DUMMER, R., MIHIC-PROBST, D. & GUTWEIN, P. 2010. ADAM15 expression is downregulated in melanoma metastasis compared to primary melanoma. *Biochem Biophys Res Commun*, 401, 363-9.

URCUQUI-INCHIMA, S., CASTANO, M. E., HERNANDEZ-VERDUN, D., ST-LAURENT, G., 3RD & KUMAR, A. 2006. Nuclear Factor 90, a cellular dsRNA binding protein inhibits the HIV Rev-export function. *Retrovirology*, 3, 83.

VAN DER HEIJDEN, I. M., WILBRINK, B., TCHETVERIKOV, I., SCHRIJVER, I. A., SCHOOLS, L. M., HAZENBERG, M. P., BREEDVELD, F. C. & TAK, P. P. 2000. Presence of bacterial DNA and bacterial peptidoglycans in joints of patients with rheumatoid arthritis and other arthritides. *Arthritis Rheum*, 43, 593-8.

VARON, R., VISSINGA, C., PLATZER, M., CEROSALETTI, K. M., CHRZANOWSKA, K. H., SAAR, K., BECKMANN, G., SEEMANOVA, E., COOPER, P. R., NOWAK, N. J., STUMM, M., WEEMAES, C. M., GATTI, R. A., WILSON, R. K., DIGWEED, M., ROSENTHAL, A., SPERLING, K., CONCANNON,

P. & REIS, A. 1998. Nibrin, a novel DNA double-strand break repair protein, is mutated in Nijmegen breakage syndrome. *Cell*, 93, 467-76.

VINCENT, I. E., ZANNETTI, C., LUCIFORA, J., NORDER, H., PROTZER, U., HAINAUT, P., ZOULIM, F., TOMMASINO, M., TREPO, C., HASAN, U. & CHEMIN, I. 2011. Hepatitis B virus impairs TLR9 expression and function in plasmacytoid dendritic cells. *PLoS One*, 6, e26315.

VISSE, R. & NAGASE, H. 2003. Matrix metalloproteinases and tissue inhibitors of metalloproteinases: structure, function, and biochemistry. *Circ Res*, 92, 827-39.

VOSS, A., GESCHER, K., HENSEL, A., NACKEN, W. & KERKHOFF, C. 2011. Double-stranded RNA induces MMP-9 gene expression in HaCaT keratinocytes by tumor necrosis factor-alpha. *Inflamm Allergy Drug Targets*, 10, 171-9.

WAHAMAA, H., SCHIERBECK, H., HREGGVIDSDOTTIR, H. S., PALMBLAD, K., AVEBERGER, A. C., ANDERSSON, U. & HARRIS, H. E. 2011. High mobility group box protein 1 in complex with lipopolysaccharide or IL-1 promotes an increased inflammatory phenotype in synovial fibroblasts. *Arthritis Res Ther*, 13, R136.

WANG, J., HU, Y., DENG, W. W. & SUN, B. 2009. Negative regulation of Toll-like receptor signaling pathway. *Microbes Infect*, 11, 321-7.

WANG, J., YING, G., JUNG, Y., LU, J., ZHU, J., PIANTA, K. J. & TAICHMAN, R. S. 2010. Characterization of phosphoglycerate kinase-1 expression of stromal cells derived from tumor microenvironment in prostate cancer progression. *Cancer Res*, 70, 471-80.

WANG, J. H., MANNING, B. J., WU, Q. D., BLANKSON, S., BOUCHIER-HAYES, D. & REDMOND, H. P. 2003. Endotoxin/lipopolysaccharide activates NF-kappa B and enhances tumor cell adhesion and invasion through a beta 1 integrin-dependent mechanism. *J Immunol*, 170, 795-804.

WANG, J. P., LIU, P., LATZ, E., GOLENBOCK, D. T., FINBERG, R. W. & LIBRATY, D. H. 2006. Flavivirus activation of plasmacytoid dendritic cells delineates key elements of TLR7 signaling beyond endosomal recognition. *J Immunol*, 177, 7114-21.

WANG, N., CHEN, X., HE, T., YANG, Y., ZHANG, G., WU, X., LI, P. & NIU, L. 2007. [The comparison of retention of different post and core systems]. *Sheng Wu Yi Xue Gong Cheng Xue Za Zhi*, 24, 133-5.

WANG, P., SONG, W., MOK, B. W., ZHAO, P., QIN, K., LAI, A., SMITH, G. J., ZHANG, J., LIN, T., GUAN, Y. & CHEN, H. 2009. Nuclear factor 90 negatively

regulates influenza virus replication by interacting with viral nucleoprotein. *J Virol*, 83, 7850-61.

WANG, T., TOWN, T., ALEXOPOULOU, L., ANDERSON, J. F., FIKRIG, E. & FLAVELL, R. A. 2004. Toll-like receptor 3 mediates West Nile virus entry into the brain causing lethal encephalitis. *Nat Med*, 10, 1366-73.

WANG, Y., KRIVTSOV, A. V., SINHA, A. U., NORTH, T. E., GOESSLING, W., FENG, Z., ZON, L. I. & ARMSTRONG, S. A. 2010. The Wnt/beta-catenin pathway is required for the development of leukemia stem cells in AML. *Science*, 327, 1650-3.

WEAVER, A. M. 2006. Invadopodia: specialized cell structures for cancer invasion. *Clin Exp Metastasis*, 23, 97-105.

WESCHE, H., HENZEL, W. J., SHILLINGLAW, W., LI, S. & CAO, Z. 1997. MyD88: an adapter that recruits IRAK to the IL-1 receptor complex. *Immunity*, 7, 837-47.

WOO, C. H., LIM, J. H. & KIM, J. H. 2004. Lipopolysaccharide induces matrix metalloproteinase-9 expression via a mitochondrial reactive oxygen species-p38 kinase-activator protein-1 pathway in Raw 264.7 cells. *J Immunol*, 173, 6973-80.

WU, B., CRAMPTON, S. P. & HUGHES, C. C. 2007. Wnt signaling induces matrix metalloproteinase expression and regulates T cell transmigration. *Immunity*, 26, 227-39.

XIA, X., CUI, J., WANG, H. Y., ZHU, L., MATSUEDA, S., WANG, Q., YANG, X., HONG, J., SONGYANG, Z., CHEN, Z. J. & WANG, R. F. 2011. NLRX1 negatively regulates TLR-induced NF-kappaB signaling by targeting TRAF6 and IKK. *Immunity*, 34, 843-53.

YAMAMOTO, M. & AKIRA, S. 2004. [TIR domain--containing adaptors regulate TLR-mediated signaling pathways]. *Nihon Rinsho*, 62, 2197-203.

YAMAMOTO, M., SATO, S., HEMMI, H., HOSHINO, K., KAISHO, T., SANJO, H., TAKEUCHI, O., SUGIYAMA, M., OKABE, M., TAKEDA, K. & AKIRA, S. 2003. Role of adaptor TRIF in the MyD88-independent toll-like receptor signaling pathway. *Science*, 301, 640-3.

YAMAMOTO, M., SATO, S., HEMMI, H., SANJO, H., UEMATSU, S., KAISHO, T., HOSHINO, K., TAKEUCHI, O., KOBAYASHI, M., FUJITA, T., TAKEDA, K. & AKIRA, S. 2002. Essential role for TIRAP in activation of the signalling cascade shared by TLR2 and TLR4. *Nature*, 420, 324-9.

YAMAMOTO, M., SATO, S., HEMMI, H., UEMATSU, S., HOSHINO, K., KAISHO, T., TAKEUCHI, O., TAKEDA, K. & AKIRA, S. 2003. TRAM is specifically involved in the Toll-like receptor 4-mediated MyD88-independent signaling pathway. *Nat*

*Immunol*, 4, 1144-50.

YAMAMOTO, M., SATO, S., MORI, K., HOSHINO, K., TAKEUCHI, O., TAKEDA, K. & AKIRA, S. 2002. Cutting edge: a novel Toll/IL-1 receptor domain-containing adapter that preferentially activates the IFN-beta promoter in the Toll-like receptor signaling. *J Immunol*, 169, 6668-72.

YAN, W. & CHEN, S. S. 2005. Mass spectrometry-based quantitative proteomic profiling. *Brief Funct Genomic Proteomic*, 4, 27-38.

YANG, L., ZHANG, H. & BRUCE, J. E. 2009. Optimizing the detergent concentration conditions for immunoprecipitation (IP) coupled with LC-MS/MS identification of interacting proteins. *Analyst*, 134, 755-62.

YAROVINSKY, F., ZHANG, D., ANDERSEN, J. F., BANNENBERG, G. L., SERHAN, C. N., HAYDEN, M. S., HIENY, S., SUTTERWALA, F. S., FLAVELL, R. A., GHOSH, S. & SHER, A. 2005. TLR11 activation of dendritic cells by a protozoan profilin-like protein. *Science*, 308, 1626-9.

YASMEEN, A., BISMAR, T. A. & AL MOUSTAFA, A. E. 2006. ErbB receptors and epithelial-cadherin-catenin complex in human carcinomas. *Future Oncol*, 2, 765-81.

YAZGAN, O. & PFARR, C. M. 2002. Regulation of two JunD isoforms by Jun N-terminal kinases. *J Biol Chem*, 277, 29710-8.

YI, H., PATEL, A. K., SODHI, C. P., HACKAM, D. J. & HACKAM, A. S. 2012. Novel role for the innate immune receptor Toll-like receptor 4 (TLR4) in the regulation of the Wnt signaling pathway and photoreceptor apoptosis. *PLoS One*, 7, e36560.

YONEDA, T., IMAIZUMI, K., OONO, K., YUI, D., GOMI, F., KATAYAMA, T. & TOHYAMA, M. 2001. Activation of caspase-12, an endoplasmic reticulum (ER) resident caspase, through tumor necrosis factor receptor-associated factor 2-dependent mechanism in response to the ER stress. *J Biol Chem*, 276, 13935-40.

YONEYAMA, M. & FUJITA, T. 2010. Recognition of viral nucleic acids in innate immunity. *Rev Med Virol*, 20, 4-22.

YONEYAMA, M., KIKUCHI, M., NATSUKAWA, T., SHINOBU, N., IMAIZUMI, T., MIYAGISHI, M., TAIRA, K., AKIRA, S. & FUJITA, T. 2004. The RNA helicase RIG-I has an essential function in double-stranded RNA-induced innate antiviral responses. *Nat Immunol*, 5, 730-7.

ZHANG, B., SHEN, M., XU, M., LIU, L. L., LUO, Y., XU, D. Q., WANG, Y. X., LIU, M. L., LIU, Y., DONG, H. Y., ZHAO, P. T. & LI, Z. C. 2012. Role of macrophage migration inhibitory factor in the proliferation of smooth muscle cell in pulmonary

hypertension. *Mediators Inflamm*, 2012, 840737.

ZHANG, Q., HUI, W., LITHERLAND, G. J., BARTER, M. J., DAVIDSON, R., DARRAH, C., DONELL, S. T., CLARK, I. M., CAWSTON, T. E., ROBINSON, J. H., ROWAN, A. D. & YOUNG, D. A. 2008. Differential Toll-like receptor-dependent collagenase expression in chondrocytes. *Ann Rheum Dis*, 67, 1633-41.

ZHANG, S. Y., JOUANGUY, E., UGOLINI, S., SMAHI, A., ELAIN, G., ROMERO, P., SEGAL, D., SANCHO-SHIMIZU, V., LORENZO, L., PUEL, A., PICARD, C., CHAPGIER, A., PLANCOULAIN, S., TITEUX, M., COGNET, C., VON BERNUTH, H., KU, C. L., CASROUGE, A., ZHANG, X. X., BARREIRO, L., LEONARD, J., HAMILTON, C., LEBON, P., HERON, B., VALLEE, L., QUINTANA-MURCI, L., HOVNANIAN, A., ROZENBERG, F., VIVIER, E., GEISSMANN, F., TARDIEU, M., ABEL, L. & CASANOVA, J. L. 2007. TLR3 deficiency in patients with herpes simplex encephalitis. *Science*, 317, 1522-7.

ZHANG, Y., NEO, S. Y., HAN, J. & LIN, S. C. 2000. Dimerization choices control the ability of axin and dishevelled to activate c-Jun N-terminal kinase/stress-activated protein kinase. *J Biol Chem*, 275, 25008-14.

ZHANG, Z., KIM, T., BAO, M., FACCHINETTI, V., JUNG, S. Y., GHAFARI, A. A., QIN, J., CHENG, G. & LIU, Y. J. 2011. DDX1, DDX21, and DHX36 helicases form a complex with the adaptor molecule TRIF to sense dsRNA in dendritic cells. *Immunity*, 34, 866-78.

ZHONG, J. L., POGHOSYAN, Z., PENNINGTON, C. J., SCOTT, X., HANDSLEY, M. M., WARN, A., GAVRILOVIC, J., HONERT, K., KRUGER, A., SPAN, P. N., SWEEP, F. C. & EDWARDS, D. R. 2008. Distinct functions of natural ADAM-15 cytoplasmic domain variants in human mammary carcinoma. *Mol Cancer Res*, 6, 383-94.

ZHOU, J., CHENG, P., YOUN, J. I., COTTER, M. J. & GABRILOVICH, D. I. 2009. Notch and wingless signaling cooperate in regulation of dendritic cell differentiation. *Immunity*, 30, 845-59.

ZHOU, M. & VEENSTRA, T. D. 2007. Proteomic analysis of protein complexes. *Proteomics*, 7, 2688-97.

ZHU, G., WU, C. J., ZHAO, Y. & ASHWELL, J. D. 2007. Optineurin negatively regulates TNFalpha- induced NF-kappaB activation by competing with NEMO for ubiquitinated RIP. *Curr Biol*, 17, 1438-43.

ZHU, L., LEE, P. K., LEE, W. M., ZHAO, Y., YU, D. & CHEN, Y. 2009. Rhinovirus-

induced major airway mucin production involves a novel TLR3-EGFR-dependent pathway. *Am J Respir Cell Mol Biol*, 40, 610-9.

ZIEGLER, S., ROHRS, S., TICKENBROCK, L., MOROY, T., KLEIN-HITPASS, L., VETTER, I. R. & MULLER, O. 2005. Novel target genes of the Wnt pathway and statistical insights into Wnt target promoter regulation. *FEBS J*, 272, 1600-15.

ZIGRINO, P., STEIGER, J., FOX, J. W., LOFFEK, S., SCHILD, A., NISCHT, R. & MAUCH, C. 2007. Role of ADAM-9 disintegrin-cysteine-rich domains in human keratinocyte migration. *J Biol Chem*, 282, 30785-93.

ZURHOVE, K., NAKAJIMA, C., HERZ, J., BOCK, H. H. & MAY, P. 2008. Gamma-secretase limits the inflammatory response through the processing of LRP1. *Sci Signal*, 1, ra15.

# **Appendix 1**

**Table 3.1 Poly(I:C)-independent TRIF interacting proteins**

HEK293-TLR3 were transfected with HA-TRIF, after 20 h cells were collected and IP of HA-TRIF was performed, followed by LC-MS analysed of the IP-complex. The MS spectra of the peptide ions were identified using the Mascot software programme.

Protein name	NCBI accession no	Mascot score	PI	MW	Peptide Match	Sequence Coverage %
AF4/FMR2 family member 4	7656879	51	9.33	127788	3	3
Ran-binding protein 17	12597633	55	6.02	125977	4	3
NIK and IKK beta binding protein	119612606	50	6.29	124293	2	2
EVH1 domain binding protein	7416993	33	6.48	90831	1	2
cAMP-specific 3',5'-cyclic phosphodiesterase	259906420	55	4.84	85189	1	1
Semaphorin-3C	5454048	58	8.96	86487	3	4
Nibrin	33356172	54	6.50	85602	2	3
Phosphatidylinositol-4,5-bis-phosphate 3-kinase catalytic subunit beta isoform	4826908	46	6.03	81837	1	2
Leucine rich repeat neuronal 4	20381181	40	6.82	80395	1	2
NF-kappa-B-repressing factor	33860178	59	8.74	78320	3	4
E3 ubiquitin-protein ligase RNF6	5174653	55	9.16	78451	2	3
Guanylate cyclase soluble subunit beta-2	14916977	42	8.84	70892	2	3
Structure of The Nalp1 Pyrin Domain	17380146	52	6.68	50486	1	11

F-box/LRR-repeat protein 20 isoform 1	27734755	38	7.65	50248	1	4
GA-binding protein subunit beta-1 isoform beta 1	8051593	50	4.77	44906	2	3
ribosome biogenesis protein BRX1 homolog	55770900	40	9.92	41990	1	2
cAMP-dependent protein kinase catalytic subunit alpha	4506055	52	8.84	40678	1	3
Mis18-binding protein 1 (p243)	5101770	44	8.74	27686	1	8
T-box transcription factor	5689744	37	9.23	23183	1	8

**Table 3.2 TRIF interactors following 20 min poly(I:C) stimulation**

HEK293-TLR3 were transfected with HA-TRIF, after 20 h cells were stimulated with 20 µg/ml poly(I:C) for 20 min. Then IP of HA-TRIF was performed and IP-complex was analysed by LC-MS. The MS spectra of the peptide ions were identified using the Mascot software programme.

Protein name	NCBI accession no	Mascot score	PI	MW	Peptide Match	Sequence Coverage %
Cardiomyopathy-associated protein 5	62241003	51	4.73	450792	4	1
sacsin	6907042	51	6.81	441744	3	1
Ubiquitin carboxyl-terminal hydrolase 32	22550104	54	6.01	183861	4	2
Bifunctional aminoacyl-tRNA synthetase	62241042	110	7.02	172107	4	4
Erythroid differentiation-related factor 1	321117522	50	5.93	139833	4	4
Cullin-associated NEDD8-dissociated protein 1	21361794	124	5.52	137999	3	3

Caspase recruitment domain-containing protein 11	157743265	54	5.78	134512	4	3
Vinculin	7669550	72	5.5	134962	1	1
Protein AF-17	215273929	57	8.93	119643	3	6
Exportin-2(cellular apoptosis susceptibility protein )	371502112	218	5.5	111145	4	6
Transportin-1	133925811	73	4.83	103797	2	2
Replication licensing factor MCM	33356547	49	5.34	102528	1	1
Plasminogen	38051823	51	6.89	93310	2	3
RUN and TBC1 domain containing 3	119580785	54	8.08	74953	3	2
Far upstream element-binding protein 2	154355000	104	6.84	73443	3	6
Plastin-3	7549809	103	5.41	71288	2	6
SUMO-activating enzyme subunit 2	4885649	74	5.15	71759	1	2
Calnexin	10716563	115	4.47	67990	3	5
Numb-like protein	10863899	47	9.1	65605	1	2
Fragile X mental retardation syndrome-related protein 1 isoform c	61835172	51	6.34	63280	3	4
Alpha adrenergic receptor subtype alpha	7690135	58	9.35	61305	2	4
T-complex protein 1 subunit theta	9988062	89	5.42	60153	3	6

Telomeric repeat-binding factor 2	21542277	53	9.22	55688	3	8
Secretogranin-3	19557645	61	4.94	52973	2	3
Serine/threonine-protein phosphatase 2A	4758954	58	5.82	52182	1	3
Ribonuclease inhibitor	62087972	66	4.71	51766	2	7
M-phase phosphoprotein 4	1770456	62	6.01	49148	3	12
Peptidase M20 domain-containing protein 2	58082085	51	5.56	48094	1	2
Lupus La protein	125985	71	6.68	46979	3	10
Phosphoglycerate kinase 1	52788229	146	8.30	44992	2	6
inactive caspase-12	300360580	51	5.63	39130	2	9
Poly(rC)-binding protein 2	14141168	147	6.33	38962	4	13
SUMO-activating enzyme subunit 1	4885585	125	5.17	38890	3	13
Serine/threonine-protein phosphatase PP1-alpha catalytic subunit	4506003	76	5.94	38242	1	5
Poly(rC)-binding protein 1	6754994	193	6.66	37987	4	12
TALDO1 protein	48257056	122	6.35	37556	4	12
Annexin A5	4502107	153	4.94	35972	3	12
Prohibitin-2	6005854	91	9.83	33276	2	20

Hyaluronan-binding protein 1/Mitochondrial matrix protein p32	4502491	209	4.74	31749	4	26
Myristoylated alanine-rich C-kinase substrate	153070260	94	4.74	31710	2	9
Prohibitin	4505773	197	5.57	29844	5	29
Proteasome activator complex subunit 3	47117724	90	5.69	29604	2	9
Replication protein A 32 kDa subunit	4506585	102	5.75	29344	2	14
Tropomyosin alpha-3 chain isoform 2 (TPMsk3)	19072649	95	4.72	28906	2	9
Acidic leucine-rich nuclear phosphoprotein 32	5453880	71	3.99	28684	2	10
Triosephosphate isomerase	4507645	258	6.45	26943	5	28
B-cell receptor associated protein	1673514	96	9.57	23621	3	28
Transgelin-2	4507357	124	8.41	22551	3	21
Ubiquitin-conjugating enzyme E2 K	4885417	64	5.33	22509	1	14
Peroxiredoxin-1	4505591	86	8.27	22328	3	16
Peroxiredoxin-2	32189392	141	5.66	22052	3	29
Ras-related protein Rap-1A	4506413	81	6.38	21322	1	6
Peptidyl-prolyl cis-trans isomerase A	10863927	113	5.06	20018	2	19
Macrophage myristoylated alanine-rich C kinase	13491174	47	4.68	19575	1	6
Nucleoside diphosphate kinase B	4505409	51	8.52	17403	3	23

**Table 3.3 TRIF interactors following 40 min poly(I:C) stimulation**

HEK293-TLR3 were transfected with HA-TRIF, after 20 h cells were stimulated with 20 µg/ml poly(I:C) for 40 min. Then IP of HA-TRIF was performed and IP-complex was analysed by LC-MS. The MS spectra of the peptide ions were identified using the Mascot software programme.

Protein name	NCBI accession no	Mascot score	PI	MW	Peptide Match	Sequence Coverage %
Trio	45439359	48	5.96	349815	3	1
zinc finger protein 462	114431236	62	7.53	289552	3	1
Ras GTPase-activating-like protein IQGAP1	4506787	55	6.08	189772	3	1
Nucleolar transcription factor 1	136652	46	5.63	89698	1	2
Serine/threonine-protein phosphatase 4 regulatory subunit 3B	39930397	50	4.70	87960	2	3
Nuclear autoantigenic sperm protein	23503077	46	4.26	85476	1	1
Glycyl-tRNA synthetase	116805340	51	6.61	83867	3	5
T-box transcription factor TBX3	28381401	54	8.30	79745	3	4
SEC14-like protein 5	150010661	56	6.08	79704	2	3
Mitogen-activated protein kinase 8 interacting protein 1	46249764	49	4.89		2	2
R3H domain containing 2	119617414	50	9.33	76607	2	5
DEAD/H (Asp-Glu-Ala-Asp/His) box polypeptide 3 variant	62087546	88	7.72	74939	1	1

vitamin D3 receptor interacting protein	4838129	50	6.71	73527	2	5
poly(ADP-ribose) polymerase	178152	113	8.34	64291	2	4
pyruvate kinase	33286418	188	7.69	58480	3	11
polypyrimidine tract-binding protein 1	14165466	60	9.21	57360	2	6
Lysosomal acid phosphatase	115502439	47	6.28	48719	1	2
alpha-enolase	119339	531	7.01	47487	8	26
HIV-1 Nef interacting protein	1800303	56	6.92	45611	1	5
phosphoglycerate kinase 1	4505763	72	8.03	44992	3	11
ELAV (embryonic lethal, abnormal vision, Drosophila)-like 4	119627246	53	9.44	44798	2	5
Fructose-bisphosphate aldolase A	4557305	109	8.30	39859	4	20
Inactive caspase-12	300360580	58	5.63	39130	2	11
Glyceraldehyde-3-phosphate dehydrogenase	7669492	68	8.57	36204	3	12
heterogeneous nuclear ribo-nucleoprotein C-like 1	61966711	54	3.94	32181	1	4

**Table 3.4 TRIF interactors following 60 min poly(I:C) stimulation**

HEK293-TLR3 were transfected with HA-TRIF, after 20 h cells were stimulated with 20 µg/ml poly(I:C) for 60 min. Then IP of HA-TRIF was performed and IP-complex was analysed by LC-MS. The MS spectra of the peptide ions were identified using the Mascot software. programme

Protein name	NCBI accession no	Mascot score	PI	MW	Peptide Match	Sequence Coverage %
Nucleoprotein TPR	114155142	87	4.97	267537	3	1
Ral GTPase-activating protein subunit alpha-2	118600961	49	5.74	213130	3	2
Ras GTPase-activating-like protein IQGAP1	4506787	50	6.08	189772	3	1
Kinesin-like protein KIF21B	59799772	53	7.94	184346	1	7
CAP-Gly domain-containing linker protein 1	261260059	58	5.29	162901	4	3
Microtubule-associated tumor suppressor candidate 2	259016371	48	6.23	150915	3	3
DEAH (Asp-Glu-Ala-His) box polypeptide 8	127797813	35	8.32	140070	3	2
AF4/FMR2 family member 4	7656879	52	9.33	127788	3	3
POTE ankyrin domain family member E	134133226	54	5.83	122910	2	2
Inositol 1,4,5-triphosphate receptor, type 1, isoform CRA	119584312	52	6.18	118754	2	2
proteasome activator 200 kDa iii	62467428	57	7.57	114882	2	2
Coatomer subunit beta	7705369	50	5.72	108234	2	2
Scaffold attachment factor B2	7661936	51	5.84	107930	3	3
GluR4	790538	58	8.43	101487	2	3

ADAM15 metargidin precursor	1235674	55	6.03	90367	2	2
Phosphatidylinositol 3-kinase regulatory subunit beta	317373311	55	6.03	81843	2	3
E3 ubiquitin-protein ligase RNF6	5174653	53	9.16	78451	2	5
Nucleophosmin-anaplastic lymphoma kinase fusion protein	609342	36	6.43	76136	1	3
Coagulation factor XII	145275213	50	8.04	70068	2	2
Menin	317373574	61	6.14	68387	2	3
CREB-regulated transcription coactivator 1	68565585	43	5.65	67374	1	2
Zinc finger with UFM1-specific peptidase domain protein	292494919	50	6.05	67192	2	2
Probable ATP-dependent RNA helicase DDX28	296434476	38	10.43	59777	2	3
Lysosomal acid phosphatase	4557010	49	6.28	48719	1	2
Heterogeneous nuclear ribo-nucleoprotein A1	288558857	84	9.17	38839	2	11

**Table 3.5 LPS-independent TRIF interacting proteins**

HEK293-TLR4 were transfected with HA-TRIF, after 20 h cells were collected and IP of HA-TRIF was performed, followed by LC-MS analysed of the IP-complex. The MS spectra of the peptide ions were identified using the Mascot software programme.

Protein name	NCBI acession no	Mascot score	PI	MW	Peptide Match	Sequence Coverage %
Human immunodeficiency virus type I enhancer binding protein 1	55662194	53	7.92	299186	3	1
Mitogen-activated protein kinase kinase kinase 1	218512139	49	7.93	166455	3	1
Collagen alpha-6(IV) chain	158264217	51	9.31	164922	2	1
Rho GTPase-activating protein SYDE2	149274655	58	8.83	143770	3	3
Transcriptional regulating factor 1	119624498	51	6.51	107114	2	2
protocadherin gamma subfamily A	62087936	51	4.94	103200	1	1
G protein-regulated inducer of neurite outgrowth 1	31418165	55	8.33	103148	3	3
26S proteasome non-ATPase regulatory subunit 2	6174930	44	5.08	100890	2	3
Disintegrin and metalloproteinase domain-containing protein 15	55960135	56	6.03	95683	2	2
intraflagellar transport 88 homolog	119628677	59	5.79	91852	4	7
Inactive carboxypeptidase-like protein X2	37182252	47	6.03	86454	3	1
Nexilin	148839339	42	5.31	80841	2	3
Protein DBF4 homolog A	5729734	43	8.03	77564	1	1
Zinc finger protein 37 homolog	4507963	52	9.26	73136	2	4
TANK-binding kinase 1-binding protein 1	171769798	39	5.62	68588	1	2

Menin	1945390	51	6.14	68387	1	2
Exoribonuclease 1	23271401	52	6.29	40502	2	5

**Table 3.6 TRIF interactors following 20 min LPS stimulation.** HEK293-TLR4 were transfected with HA-TRIF, after 20 h cells were stimulated with 1 µg/ml LPS for 20 min. Then IP of HA-TRIF was performed and IP-complex was analysed by LC-MS. The MS spectra of the peptide ions were identified using the Mascot software programme.

Protein name	NCBI accession no	Mascot score	PI	MW	Peptide Match	Sequence Coverage %
Serine/threonine-protein kinase ATR	157266317	48	7.17	304826	4	1
Nuclear mitotic apparatus protein 1	145559510	56	5.63	239217	2	1
Clathrin heavy chain 1	4758012	89	5.48	193291	2	2
Collagen alpha-6(IV)	148536823	51	9.31	164922	2	2
Leucine-rich PPR motif-containing protein	31621305	158	5.81	159023	5	6
Exportin-5	22748937	62	5.56	138368	1	1
Full-Length Vinculin	83753119	135	5.77	116498	4	5
Poly [ADP-ribose] polymerase 1	190167	137	8.99	113824	3	4
Next to BRCA1 gene 1 protein	296439290	55	5.03	108486	2	3
Tetrahydrofolate synthase, cytoplasmic	115206	85	6.89	102191	2	3

Polypeptide BM28	468704	53	7.72	100102	3	5
Importin subunit beta-1	19923142	176	4.68	98442	3	5
Protein zer-1 homolog	33589814	50	5.43	89505	3	1
Protein transport protein Sec23A	38202214	50	6.64	87033	2	3
Inactive carboxypeptidase-like protein X2	223005864	48	6.40	86484	2	1
Transmembrane protein 8A	157676334	63	7.67	86388	2	2
TNF receptor-associated protein 1	23272132	79	8.30	80350	2	2
Segment polarity protein dishevelled homolog DVL-3	2612833	64	6.18	78384	4	7
GRB2-associated-binding protein 3	18079323	57	6.79	66244	3	5
T-complex protein 1 subunit zeta	4502643	238	6.23	58452	4	15
Heterogeneous nuclear ribonucleoprotein	14110420	54	7.62	38584	2	9
Glyceraldehyde-3-phosphate dehydrogenase	7669492	231	8.57	36204	4	20
Myristoylated alanine-rich C-kinase substrate	153070260	119	4.47	31710	2	10
Prohibitin	4505773	124	5.57	29844	2	11
Proliferating cell nuclear antigen	4505641	82	4.57	29098	3	18
Phosphoglycerate mutase 1	4505753	220	6.67	28902	5	27

14-3-3 protein zeta/delta	4507953	293	4.73	27902	7	27
Triosephosphate isomerase	4507645	133	6.45	26943	3	15
Transgelin-2	586000	149	8.41	22551	2	18
Peroxioredoxin-2	32189392	161	5.66	22052	3	25
Ras-related protein Rap-1A	51338607	87	8.36	21316	1	8
Peptidyl-prolyl cis-trans isomerase	10863927	87	7.68	18233	3	19
Recognition particle 14 kDa protein	149999611	75	10.05	14677	1	10
Macrophage migration inhibitory factor	4505185	57	7.57	12647	1	7

**Table 3.7 TRIF interactors following 40 min LPS stimulation.** HEK293-TLR4 were transfected with HA-TRIF, after 20 h cells were stimulated with 1 µg/ml LPS for 40 min. Then IP of HA-TRIF was performed and IP-complex was analysed by LC-MS. The MS spectra of the peptide ions were identified using the Mascot software programme.

Protein name	NCBI accession no	Mascot score	PI	MW	PeptideMatch	Sequence Coverage %
Low-density lipoprotein receptor-related protein 2	126012573	55	4.89	540699	4	1

Nucleoprotein TPR	114155142	65	4.97	267537	2	1
Scribble	18032008	53	5.02	175809	3	1
MYB-binding protein 1A	157694492	58	9.34	149744	2	2
Cohesin subunit SA-1	62243696	47	5.40	145322	3	3
Insulin receptor substrate 4	4504733	67	8.72	134729	3	2
Transcription termination factor 2	130784	47	6.63	130784	2	2
Hypoxia up-regulated protein 1	5453832	118	5.16	111498	4	7
CAS cellular apoptosis susceptibility protein	62297557	300	5.51	111056	6	10
AP-2 complex subunit beta	4557469	59	5.22	105414	1	2
Adaptor-related protein complex 1 (AP1)	119580203	64	4.98	105111	1	2
Amyloid-like protein 1	4885065	56	5.54	72827	3	5
Apoptosis-inducing factor 1	13431764	76	9.04	67149	2	5
Dihydropyrimidinase-related protein 1	4503051	47	6.55	62493	3	5
T-complex protein 1 subunit zeta	4502643	81	6.23	58452	2	6
Tat binding protein 7	263099	63	5.52	51635	3	4
Forkhead box protein	166988458	57	5.25	50795	3	8

26S protease regulatory subunit 7	4506209	50	5.71	49009	1	3
Putative zinc finger CCHC domain-containing protein 18	300681209	52	7.02	45538	3	7
Glyceraldehyde-3-phosphate dehydrogenase	7669492	380	8.57	36204	10	40
Myristoylated alanine-rich C-kinase substrate	153070260	128	4.74	31710	3	9
Annexin A5	4502107	62	4.49	35972	1	4
Prohibitin2	6005854	53	9.83	33276	1	4
Prohibitin	4505773	81	5.57	29844	1	7
S-phase kinase-associated protein 1	52783797	43	4.40	18820	1	9

**Table 3.8 TRIF interactors following 60 min LPS stimulation.** HEK293-TLR4 were transfected with HA-TRIF, after 20 h cells were stimulated with 1 µg/ml LPS for 60 min. Then IP of HA-TRIF was performed and IP-complex was analysed by LC-MS. The MS spectra of the peptide ions were identified using the Mascot software programme.

Protein name	NCBI accession no	Mascot score	PI	MW	PeptideMatch	Sequence Coverage %
Apolipoprotein B-100	178730	56	6.58	516675	3	1
PI-3-kinase-related kinase SMG-1	14132744	52	6	343765	3	1

Histone-lysine N-methyltransferase ASH1L	7739725	52	9.46	336214	3	1
Cadherin EGF LAG seven-pass G-type receptor 1	7656967	56	5.59	334440	2	1
Probable E3 ubiquitin-protein ligase TRIP12	10863903	55	8.76	222268	3	2
Leucine-rich repeat-containing protein 53	212286191	38	11.8	142104	2	3
Nuclear protein SA-2	2204215	53	5.19	135176	4	6
SWI/SNF related, matrix associated	119604571	54	9.26	120442	3	3
POTE ankyrin domain family member F	215273934	47	5.83	123049	2	4
Discoidin domain-containing receptor 2	215273969	38	5.10	97602	1	1
Metabotropic glutamate receptor 6 protein	2231438	53		96652	4	5
Rho guanine nucleotide exchange factor 19	40255149	54	7.31	90012	3	3
Nucleolar transcription factor 1	136652	41	5.63	89698	1	2
U4/U6-associated RNA splicing factor	2853287	51	9.53	77530	3	7
HERV-K_3q12.3 provirus ancestral Gag polyprotein	50400656	33	9.26	74412	1	2
Mediator of RNA polymerase II transcription subunit 17	296437366	42	7.05	73367	2	5
Otolin-1	122937273	37	8.60	49971	1	2
Developmentally-regulated GTP-binding protein 1	6685390	35	9	45849	1	5

cul-3	3360457	53	9.56	39482	1	5
Absent in melanoma 2 (AIM2)	5902751	43	9.79	39045	1	3
alpha enolase	2661039	262	6.53	36634	4	18
Glyceraldehyde-3-phosphate dehydrogenase	31645	107	8.26	36205	4	14
Triosephosphate isomerase	4507645	69	6.45	26943	2	11
Dermcidin	148271059	36	6.08	11393	1	10

## **Appendix 2**

## 2.1 General Materials

### 2.1.1 Chemicals

Acetic acid glacial, 100 %. Cat. # 27221. Sigma-Aldrich.

Acetonitrile. Cat. # A/0620/PB17. Fisher Scientific.

Agar. Cat. # 05039. Fluka.

Ammonium bicarbonate. Cat. # 09830-500G. Sigma-Aldrich

Ammonium persulfate. Cat. # A3678-100G. Sigma-Aldrich.

Ammonium sulphate. Cat. # A/6440/65. Fisher Scientific.

Ampicillin salt. Cat. # A0166-5G. Sigma-Aldrich.

Bacto yeast extract. Cat. # 212750. B.D. Medical supplies.

Bacto Peptone. Cat. # 21677. B.D. Medical supplies.

$\beta$ -Mercaptoethanol. Cat. # M7522-100 ml. Sigma-Aldrich.

Bromphenol blue. Cat. # 11439-1. Sigma-Aldrich.

Albumin, from Bovine Serum (BSA) Cat. # A7906-100G. Sigma-Aldrich.

Dimethylsulfoxide (DMSO). Cat. # D2650. Sigma-Aldrich.

DL-Dithiothreitol, BioUltra, 99.5 % (DTT). Cat. # D9163-25G. Sigma-Aldrich.

Ethanol. Cat. # 02860-2.5L. Fluka.

Ethylene-diamin-tetraacetic acid-disodium salt (EDTA). Cat. # EG758-500G. Sigma-Aldrich.

Ethylene glycol tetraacetic acid (EGTA). Cat. # E3889-10G. Sigma-Aldrich.

Formalin. Cat. # F 8775-500 ml. Sigma-Aldrich.

Formic acid. Cat. # 1002640100. Merck.

Geneticin sulphate (G418). Cat. # BPE673-1. Fisher Scientific.

Glycerol. Cat. # BPE229-1. Fisher scientific.

Glycine. Cat. # G/0800/60. Fisher Scientific.

HEPES. Cat. # 54457-50G-F. Sigma-Aldrich.

Hydrochloric acid. Cat. # 30720-2.5L. Sigma-Aldrich.

Iodoacetamide. Cat # I1149-25G. Sigma-Aldrich.

Isopropanol. Cat. # 278475-1L. Sigma-Aldrich.

Methanol. Cat. # M/3900/17. Fisher Scientific.

NP-40. Cat. # I3021-100 ml. Sigma-Aldrich.

OPD (*o*-Phenylenediamine dihydrochloride) tablets. Cat. # P9187-50SET. Sigma-Aldrich.

Paraformaldehyde. Cat. # 158127-500G. Sigma-Aldrich.  
PBS Tablets. Cat. # P4417-100TAB. Sigma-Aldrich.  
Potassium ferricyanide. Cat. # 702587-250G. Sigma-Aldrich.  
Precision Plus Dual Colour Standards. Cat. # 161-0374. Bio-Rad.  
Complete protease inhibitor tablets. Cat. # 11836153001. Roche.  
Protogel (30 % (w/v) Acrylamide: 0.8% (w/v) bis Acrylamide). Cat. # EC-890. National Diagnostic.  
Silver Nitrate. Cat. # S/1280/46. Fisher Scientific.  
Sodium chlorid. Cat. # S/3160/63. Fisher Scientific.  
Sodium-dodecylsulfate (SDS). Cat. # L4390-1KG. Sigma-Aldrich.  
Sodium deoxycholate. Cat. # D6750-25G. Sigma-Aldrich.  
Sodium hydroxide pellet. Cat. # S/4920/60. Fisher Scientific.  
Sodiumorthovanadate. Cat. # 450243-10G. Sigma-Aldrich.  
Sodium potassium carbonate. Cat. # 86352-500G. Sigma-Aldrich.  
Sodium thiosulfate. Cat. # 72049-250G. Sigma-Aldrich.  
SYBR Safe DNA gel stain. Cat. # MP 33100. Invitrogen.  
Tetramethylethylenediamine (TEMED). Cat. # T9281-25 ml. Sigma-Aldrich.  
Tris Base. Cat. # BPE 152-1. Fisher Scientific.  
Triton X-100. Cat. # T8787-100 ml. Sigma-Aldrich.  
TRIZOL. Cat. # 15596026. Invitrogen.  
Trypsin. Cat. # V5111. Promega.  
West Dura Extended Duration Substrate. Cat. # 34075. Fisher Scientific.  
Tween-20. Cat. # 8221841000. Merck.  
Water (DNase, RNase, Protease free). Cat. # 4502. Sigma-Aldrich.

### **2.1.2 Kits**

#### **Plasmid purification:**

High speed Midi purification kit. Cat. # 12643. QIAGEN.

#### **Transfection:**

Lipofectamine 2000. Cat. # 11668019. Invitrogen.

DreamFect™ Gold Cat. # DG81000. OZ Bioscience.

#### **Luciferase reporter gene assay:**

Dual-Luciferase Reporter Assay System. Cat. # E194A. Promega.

Coelenterazine Native. Cat. # 10110-1. Biotim.

D-Luciferin. Cat. # L8200. Biosynth.

**ELISA:**

Human IL-6, ELISA Kit. Cat. # DY206. R&D systems.

Human TNF $\alpha$ , ELISA Kit. Cat. # 900-K25. Peprotech.

Human Rantes ELISA Kit. Cat. # 900-K33. Peprotech.

Human Pro-Inflammatory (7-plex) ELISA kit. Cat. # K11008B-1. Meso ScaleDiscovery.

Human MMP (3-plex) ELISA kit. Cat. # K11034C-1. Meso ScaleDiscovery.

Human Rantes (single-plex) ELISA kit. Cat. # K111BFB-1. Meso ScaleDiscovery.

Human IFN $\beta$  (single-plex) ELISA kit. Cat. # K111ADB-1. Meso ScaleDiscovery.

**2.1.3 Antibodies**

**Primary antibodies:**

Anti-HA tag Mouse monoclonal antibody. Cat. # MMS-101P. Covance.

Anti-V5 tag mouse monoclonal. Cat. # R960-25. Invitrogen.

Anti Myc tag mouse monoclonal antibody. Cat. # 2276. Cell signalling Technology.

Anti-DVL3 rabbit polyclonal antibody. Cat. #3218. Cell signalling Technology.

Anti-I $\kappa$ B $\alpha$  mouse monoclonal antibody. Cat. # 4814s. Cell signalling Technology.

Anti-phosph-IRF3 rabbit monoclonal antibody. Cat. # 4947s. Cell signalling Technology.

Anti-phosph-p65 rabbit monoclonal antibody. Cat. # 3033. Cell signalling Technology.

Anti-Phosph-P38 rabbit monoclonal antibody. Cat. # 9211s. Cell signalling Technology.

Anti-human ADAM15 goat monoclonal antibody. Cat. # AF935. R&D Systems.

Anti- $\beta$ -Actin mouse monoclonal antibody. Cat. #A1978. Sigma-Aldrich.

Anti-human TICAM-1 rabbit polyclonal antibody. Cat. # X1827P. Exalpa.

Anti-human TICAM-1 rabbit polyclonal antibody. Cat. # AL227. Alexis.

Anti-human TICAM-1 rabbit polyclonal antibody. Cat. # PAB0317. Abnova.

Anti-human Optineurin mouse monoclonal antibody. Cat. # SC-271549. Santa Cruz.

IgG from rabbit serum. Cat. #I5006. Sigma-Aldrich.

**Secondary antibodies:**

Anti-rabbit IgG HRP. Cat. # W401B. Promega.

Anti-mouse IgG HRP. Cat. # W402B. Promega.

Anti-goat IgG HRP. Cat. # V805A. Promega.

Goat anti-mouse IgG Alex fluor 488. Cat. # A-11001. Invitrogen.

Goat anti-mouse Alex fluor 568. Cat. # A-11011. Invitrogen.

#### **2.1.4 cDNA synthesis**

dNTPS. Cat. # N0447S. Biolabs.

M-MLV Reverse Transcriptase. Cat. # BPE3208-1. Fisher Scientific.

Random Hexamer Primers. Cat. # C118A. Promega.

Rnase Inhibitor. Cat. # FQ-EO0381. Fisher Scientific.

#### **2.1.5 Real-time RT-PCR**

##### **Primers sequence**

All primers were designed online using the Integrated DNA Technology software.

Access at: <http://eu.idtdna.com/Scitools/Applications/Primerquest/>.

Primers were purchased from, Euro fins MWG.

Human IFN- $\beta$ , forward 5'-AACTGCAACCTTTTCGAAGCC-3'.

Human IFN- $\beta$ , reverse 5'-TGTCGCCTACTACCTGTTGTGC-3'.

Human TNF- $\alpha$ , forward 5'-CACCACTTCGAAACCTGGGA-3'.

Human TNF- $\alpha$ , reverse 5'-CACTTCACTGTGCAGGCCAC-3'.

Human CCL5, forward, 5'-TGCCTGTTTCTGCTTGCTCTTGTC-3'.

Human CCL5, reverse, 5'-TGTGGTAGAATCTGGGCCCTTCAA-3'.

Human TRIF, forward, 5'-ACGCCATAGACCACTCAGCTTTCA-3'.

Human TRIF, reverse, 5'-AGGTTGCTCATCATGGCTTGGTTC-3'.

Human ADAM15, forward, 5'-TTCGCGAATCCAAGATCTCCACCT-3'.

Human ADAM15 reverse, 5'-TCACCAACTCCACAGTCTTGGTCT-3'.

Human MMP9, forward, 5'-TACCACCTCGAACTTTGACAGCGA-3'.

Human MMP9, reverse, 5'-GCCATTCACGTCGTCCTTATGCAA-3'.

Human MMP10, forward, 5'-AATGGATTGTGGCTCATTGGTGGG-3'.

Human MMP10, reverse, 5'-TGGAAGTGGTTTAGGAGGAGGCAA-3'.

Human GAPDH, forward, 5'-TTCGACAGTCAGCCGCATCTTCTT-3'.

Human GAPDH, reverse, 5'-GCCCAATACGACCAAATCCGTTGA-3'.

Murine DVL1, forward, 5'-ACAAAGGCCTATGCAGTAGTGGGT-3'.

Murine DVL1, reverse, 5'-GCAGCGCTGAAGACATTGGTTGAT-3'.

Murine DVL2, forward, 5'-ATGTGGCTCAAGATCACCATCCCA-3'.

Murine DVL2, reverse, 5'-TAATCTTGTGACGGTGTGCCGGA-3'.

Murine DVL3, forward, 5'-ACCATTCCCAATGCTTTCATCGGC-3'  
Murine DVL3, reverse, 5'-TGATCTTGTGACGGTATGGCGGA-3'  
Murine IFN- $\beta$ , forward, 5'-CTGGATGGTGGTCCGAGCAG-3'.  
Murine IFN- $\beta$ , reverse, 5'-CACTACCAGTCCCAGAGTCC-3'.  
Murine IFN- $\alpha$ , forward 5'-ACAGGATCACTGTGTACCTGAGA-3'.  
Murine IFN- $\alpha$ , reverse 5'-GGGCTCTCCAGACTTCTGCTCTG-3'.  
Murine TNF- $\alpha$ , forward, 5'-CATCTTCTCAAATTCGAGTGACAA-3'.

Murine TNF- $\alpha$ , reverse, 5'-TGGGAGTAGACAAGGTACAACCC-3'.  
Murine Rantes, forward, 5'-GGAGATGAGCTAGGATAGAGGG-3'.  
Murine Rantes, reverse, 5'-TGCCCATTTTCCCAGGACCG-3'.  
Murine IL-6, forward, 5'-GACAACCTTTGGCATTGTGG-3'.  
Murine IL-6, reverse, 5'-ATGCAGGGATGATGTTCTG-3'.  
Murine GAPDH, forward, 5'-GCACAGTCAAGGCCGAGAAT-3'.  
Murine GAPDH, reverse, 5'-GCCTTCTCCATGGTGGTGAA-3'.

Syber green Mater Mix. Cat. # QT650-05. Bioline.

Real time RT-PCR was performed using DNA Engine Opticon system; MJ Research.

## **2.1.6 Cell culture**

### **2.1.6.1 Cell lines**

Human embryonic kidney (HEK)293, HEK293-TLR3 and HEK293-TLR4 were a generous gift from Professor Kate Fitzgerald (University of Massachusetts Medical School USA). Human Astrocytoma cells U373-CD14 cells were a generous gift from Professor Paul Moynagh (Institute of Immunology, NUIM, Ireland). Immortalized cervical carcinoma cells (Hela) were a gift from Dr Martina Schröder, (Institute of Immunology, NUIM, Ireland). Wild-type immortalized murine bone-derived macrophages were a gift from Professor Douglas Golenbock, (University of Massachusetts Medical School USA).

### **2.1.6.2 Cell culture media and supplements**

HyClone DMEM. Cat. # HyC001113Q. Fisher Scientific.

RPMI Medium. Cat. # 61870-044. Invitrogen.

Sodium Pyruvate. Cat. # S8636. Sigma-Aldrich.

Penicillin/Streptomycin. Cat. # P0781-100 ml. Sigma-Aldrich.

Fungizone. Cat. # 15290-026. Invitrogen.  
Blasticidin. Cat. # A11139-03. Invitrogen.  
HygroGold. Cat. # ant-hg. Invivogen.  
FBS (Heat Inactivated). Cat. # 50867051810/500. BioSera.  
Dulbecco's Phosphate-Buffered Saline (PBS). Cat. # 14190-169. Invitrogen.  
Trypsin EDTA. Cat. # T4174. Sigma-Aldrich.  
5 ml pipette. Cat. # tkv-670-051R. Fisher Scientific.  
10 ml pipette. Cat. # tkv-670-071L. Fisher Scientific.  
25 ml pipette. Cat. # tkv-670-091F. Fisher Scientific.  
T175 flasks. Cat. # 83.1812.302. SARSTED.  
T75 flasks. Cat. # 83.1813.302. SARSTED.  
6 well plates. Cat. # tkt-520-030t. Fisher Scientific.  
96 well tissue culture plates. Cat. # 831835. SARSTED.  
Collagen coated Coverslip. Cat. # 354089. BD Biosciences.  
Cell Scrapers. Cat. # 83.1830. SARSTED.  
Cryotube Vials Nunc. Cat. # CRY-960-090S. Fisher Scientific.  
Cryo Canes. Cat. # CC-302. Tocris Bioscience.

### **2.1.7 Plasmids and bacteria**

The following plasmids were kindly provided by the following individuals.  
pCDNA3-HA-TRIF by Prof. Shizuo Akira, (Osaka University, Japan ).  
pCDNA4-V5-ADAM15 by Prof. Edwards Dylan (University of East Angelia, United Kingdom).  
pCDNA3-Myc-MyD88 by Prof. Luke O'Neill, (Trinity College Dublin, Ireland).  
pCDNA3-Myc-Optineurin by Prof. Swarup, (Centre for Cellular and Molecular Biology, India).  
pCDNA3- Myc DVL1, pCDNA3-Myc-DVL2, and pCDNA3-Myc-DVL3 by Prof. Hsien-Yu Wang, (Stony Brook University, NY, USA).  
pFOS-Flag-Aim2 by Dr. Kate Fitzgerald (University of Massachusetts, Medical School, USA).  
NFκB-Luc, p125-Luc, PRII-luc and PRDIII-luc by Prof. Luke O'Neill (Trinity College Dublin, Ireland).  
Rantes promoter-luc by Prof. Paul Moynagh (Institute of Immunology, NUIM, Ireland).

PCMV1-HA-Beta-catenin, and Lef-Luc by Prof. Li (Chinese Academy of Sciences, China).

DH5 $\alpha$  subcloning efficiency competent cells. Cat. # 18265-017. Invitrogen.

LB broth (10 g tryptone, 10 g NaCl, 5 g yeast extract (with 20 g Agar for plates; 1L) was used for bacterial transformation of plasmid

### **2.1.8 Equipment**

Analytical balance SI234. Denver Instrument.

Centrifuge 5804. Eppendorf.

CO<sub>2</sub> Incubater. Fisher Scientific.

Gryo Rocker SSL3. STUART.

Heat-stir SB162. STUART.

IKA Vortex. Genius.

Luminoscan. Fisher Scientific.

Magnetic stirrer. SM1 STUART.

Mastercycler. Eppendorf.

pH meter ultra-basic. Denver instrument.

Plate shaker PMS-1000 Grant-Bio.

Roller mixer SRT9. STUART.

ROTANTA 460R centrifuge. Lennox.

See saw rocker SSL4. STUART.

Spectrafuge 16M. Labnet.

Spectrometer ELX800. Bio-Tek.

### **2.1.9 TLR ligands**

Lipopolysaccharides (LPS) TLR grade. Cat. # 581-010-L002. Alexis.

Polyinosinic:polycytidylic acid (poly(I:C)). Cat. # tlr1-pic. Invivogen.

R848. Cat. # tlr1-r848-5. Invivogen.

### **2.1.10 esiRNAs, DVLs inhibitor and EGF**

esiRNA human ADAM15. Cat. #. EHU076821. Sigma-Aldrich.

esiRNA human Optineurin. Cat. #. EHU077201. Sigma-Aldrich.

esiRNA control. Cat. #. AM16106. Ambion.

DVL-PDZ Domain Inhibitor. Cat. #. 322338. Calbiochem

Recombinant human epidermal growth factor. Cat. #. 236 EG. R&D (generous gift from Dr Shirley O'Dea, Institute of Immunology, NUIM, Ireland).

**Table 2.2.1** 10 % resolving gel

Protogel (30 % (w/v) Acrylamide: 0.8 % (w/v) bis Acrylamide).	5 ml
1.5 M Tris-CL, pH 8.8	3.8 ml
H <sub>2</sub> O	5.9 ml
10 % SDS	150 µl
10 % SDS	150 µl
TEMED	6 µl

**Table 2.2.2** 5 % stacking gel

Protogel (30 % (w/v) Acrylamide: 0.8 % (w/v) bis Acrylamide).	1ml
0.5 M Tris-CL, pH 6.8	1.5 ml
H <sub>2</sub> O	3.35 ml
10 % SDS	60 µl
10 % SDS	60 µl
TEMED	6 µl

**Table 2.2.3** 10 x running buffer

25 mM Tris Base	30.3 g
192 mM glycine	144 g
0.1 % SDS	10 g
H <sub>2</sub> O	Fill to 1L

**Table 2.2.4** 1 x running buffer

10 x running buffer	100 ml
H <sub>2</sub> O	900 ml

**Table 2.2.5** 5 x loading buffer (50ml)

Glycerol	15 ml
10 % SDS	10 ml
0.5 M Tris-CL, pH 6.8	12.5 ml
Bromophenol blue	10 mg
H <sub>2</sub> O	12.5 ml

**Table 2.2.6** 10 x transfer buffer pH 8.5

25 mM Tris Base	30.3 g
192 mM glycine	144 g
H <sub>2</sub> O	Fill to 1L

**Table 2.2.7** 1 x transfer buffer

10 x Transfer buffer	100 ml
Methanol	200 ml
H <sub>2</sub> O	700 ml

**Table 2.2.8** 10 x TBS, pH 8

Tris Base	12.11g
Sodium chloride	87.6 g
H <sub>2</sub> O	Fill to 1L

**Table 2.2.9** 1 x TBST pH 8

10 x TBST	100 ml
H <sub>2</sub> O	900 ml
Tween-20	1 ml